

This document is confidential and is proprietary to the American Chemical Society and its authors. Do not copy or disclose without written permission. If you have received this item in error, notify the sender and delete all copies.

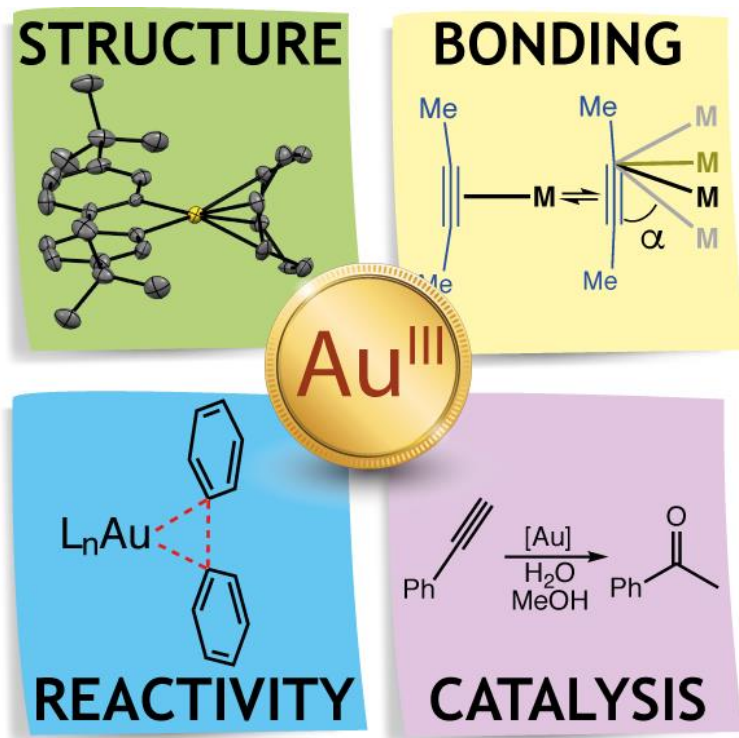
**Recent Advances in Gold(III) Chemistry: Structure, Bonding, Reactivity and Role in Homogeneous Catalysis**

Journal:	<i>Chemical Reviews</i>
Manuscript ID	cr-2020-00552a.R2
Manuscript Type:	Thematic Review
Date Submitted by the Author:	02-Sep-2020
Complete List of Authors:	Rocchigiani, Luca; University of East Anglia, Bochmann, Manfred; University of East Anglia, School of Chemistry

SCHOLARONE™  
Manuscripts

## TOC ENTRY:

Gold(III) complexes are becoming increasingly important in catalysis and synthetic methodology. This review summarizes the advances in the organometallic chemistry and mechanistic understanding of gold(III) over the last decade.



# Recent Advances in Gold(III) Chemistry: Structure, Bonding, Reactivity and Role in Homogeneous Catalysis

Luca Rocchigiani\* and Manfred Bochmann\*

School of Chemistry, University of East Anglia, Norwich Research Park, Norwich, NR47TJ, United Kingdom. E-mail [L.Rocchigiani@uea.ac.uk](mailto:L.Rocchigiani@uea.ac.uk), [m.bochmann@uea.ac.uk](mailto:m.bochmann@uea.ac.uk)

## Abstract

Over the last decade the organometallic chemistry of gold(III) has seen remarkable advances. This includes the synthesis of the first examples of several compound classes that have long been hypothesized as being part of catalytic cycles, such as gold(III) alkene, alkyne, CO and hydride complexes, and important catalysis-relevant reaction steps have at last been demonstrated for gold, such as migratory insertion and  $\beta$ -H elimination reactions. Also, reaction pathways that were already known, such as the generation of gold(III) intermediates by oxidative addition and their reductive elimination, are much better understood. A deeper understanding of fundamental organometallic reactivity of gold(III) has also revealed unexpected mechanistic avenues, which can open when the barriers for reactions that for other metals would be regarded as “standard” are too high. This review summarizes and evaluates these developments, together with applications of gold(III) in synthesis and catalysis, with emphasis on the mechanistic insight gained in these investigations.

## CONTENTS

1. Introduction
  - 1.1 Scope, Limitations and Organization of the Review
2. General Aspects of Gold(III) Coordination Chemistry
  - 2.1 *Trans*-Effect and *Trans*-Influence
  - 2.2 Gold(III) Complexes with  $\pi$ -Ligands
    - 2.2.1 Au(III)-CO Complexes
    - 2.2.2 Alkene Complexes
    - 2.2.3 Alkyne Complexes
    - 2.2.4 Arene  $\pi$ -Complexes
    - 2.2.5 Allyl Complexes
  - 2.3 Gold(III) Complexes with  $\sigma$ -Ligands
    - 2.3.1 Gold(III) Hydrides

- 1  
2  
3 2.3.2 Agostic Interactions and Gold(III)  $\sigma$ -Complexes  
4  
5 2.3.3 Gold(III) Hydroxides and Fluorides  
6  
7 3. Catalysis-Relevant Reaction Steps  
8  
9 3.1 Oxidative Addition Reactions  
10 3.1.1 Controlled Oxidation of Au(I) by Halogens and Sacrificial Oxidants  
11 3.1.2 Oxidative Addition of C–X, C–C and E–E Bonds  
12 3.1.3 Photo-Assisted Oxidative Additions  
13  
14  
15 3.2 Reductive Elimination Reactions  
16 3.2.1 C–Halide Reductive Eliminations  
17 3.2.2 Reductive C–E (E = P, N, S) Bond Formation  
18 3.2.3 C–C Reductive Elimination  
19  
20  
21  
22 3.3 Nucleophilic Addition to C–C Double and Triple Bonds  
23  
24 3.4 Insertion Reactions  
25 3.4.1 Insertions into Gold–Carbon Bonds  
26 3.4.2 Insertions into Gold–Hydrogen Bonds  
27 3.4.3 Insertions into Gold–Oxygen Bonds  
28  
29  
30 4. Gold(III) Complexes in Catalytic Applications  
31 4.1 Coupling Reactions  
32 4.1.1 Mechanistic Aspects  
33 4.1.2 Catalytic C–C Coupling Reactions  
34 4.1.3 Photo-Assisted Coupling Reactions  
35 4.1.4 C–E Coupling Reactions (E = Non-Carbon Element)  
36  
37  
38  
39 4.2 Lewis Acid catalysis by Au(III)  
40 4.2.1 Au(III) as a Carbophilic Lewis Acid  
41 4.2.2 Au(III) as Oxophilic Lewis Acid  
42  
43  
44 4.3 Au(III) as Photosensitizer  
45  
46  
47 5. Conclusions  
48  
49 Author Information  
50 Corresponding Authors  
51 Notes  
52 Biographies  
53  
54 Acknowledgments  
55  
56 References  
57  
58  
59 Note Added in Proof  
60

## 1. INTRODUCTION

Gold has remarkable properties that set it apart from other metals. The bulk metal is of course best known for its inert character and resistance to oxidation and chemical attack and has therefore long been regarded as unpromising for catalytic applications. Being the most electronegative of metallic elements (2.54 on the Pauling scale), almost identical to carbon, gold forms highly covalent, hydrolytically stable, Au–C bonds. This is also the reason why the exploration of its organometallic chemistry has so long lagged behind work on other noble metals.<sup>1</sup> This situation has now drastically changed.

The position of gold in the Periodic Table is unique: In the oxidation state +I, with a filled d-shell, gold behaves rather like a main group element and forms linear, two-coordinate complexes which show a marked reluctance to interact with donor ligands perpendicular to the molecular axis. Gold in the oxidation state +III, on the other hand, displays all the characteristics of a transition metal, adopts almost exclusively the square-planar coordination geometry that is so familiar from other heavy metal d<sup>8</sup> ions, and is distinctly different in terms of structure and reactivity from Au(I) compounds.

Steric factors permitting, gold(I) compounds have a pronounced tendency to interact with neighboring gold(I) centers or with other heavy metals to give multimetallic aggregates through “aurophilic” or, more generally, “metallophilic” interactions. More than any other element gold is subject to relativistic effects, which for electron-rich gold(I) lead to a contraction of the 6s and 6p orbitals and an expansion of the 5d shell. Aurophilic interactions are one consequence of this. The theoretical aspects and structural diversity of aurophilic interactions have been reviewed in detail.<sup>2-8</sup> Relativistic effects, as well as the lanthanide contraction, reduce the covalent radius of gold(I), which is significantly smaller than that of silver(I),<sup>9-11</sup> and its bonds to carbon are correspondingly stronger and highly covalent.

For gold(III) relativistic effects are much less pronounced; for example, where such comparisons are possible, it could be shown that unlike the Ag<sup>I</sup>/Au<sup>I</sup> pair, for Au(III) the relativistic Au–L bond length contraction is much diminished, and Ag(III) and Au(III) have closely similar covalent radii.<sup>12,13</sup> The covalent radius of Au(III) bonded to alkyl or aryl ligands is about 1.27 – 1.30 Å, while the ionic radius is taken as 0.85 Å, which enables accommodation in the plane of porphyrins.<sup>14</sup>

In line with the reduced influence of relativistic effects, in gold(III) complexes aurophilic interactions are essentially absent. In cases where structural studies indicated Au(III)⋯Au(III) contacts closer than the sum of the van der Waals radii, studies have shown possible Au⋯Au

1  
2  
3 interaction energies of the order of 2 to <1 kcal/mol,<sup>15-17</sup> and it is questionable whether compared to  
4 other attractive interactions ( $\pi$ -stacking, Au $\cdots$ Cl contacts) “aurophilic” interactions between Au(III)  
5 centers make an energetically meaningful contribution.  
6  
7

8 The reactivity of metal complexes is directed by the trend in metal-ligand bond energies. For  
9 gold, depending on the nature of the O-ligand, the sequence is Au-H > Au-O > Au-C or Au-H >  
10 Au-C > Au-O, whereas for other metals including its neighbor in the Periodic Table, platinum(II),  
11 the trend Pt-O > Pt-H > Pt-C is observed.<sup>18</sup> Oxygen and fluoride ligands tend to act as good leaving  
12 groups and are utilized with good effect in ligand substitution and catalytic reactions. The bond  
13 dissociation energies of gold(I) compounds tend to be larger than those of gold(III) but follow the  
14 same trend. However, whereas gold(I) species [LAu]<sup>+</sup> are known as carbophilic electrophiles and  
15 bind preferentially to “soft” atoms like P and S, gold(III) is a “hard” Lewis acid. This is reflected in  
16 the stability of their OH and F compounds: whereas the first isolable gold(I) hydroxide and fluoride  
17 complexes LAuX (X = OH<sup>19-21</sup>, F;<sup>22</sup> L = N-heterocyclic carbene NHC) were only reported since  
18 2005, examples of structurally characterized hydroxo<sup>23-25</sup> and fluoro<sup>26-29</sup> complexes of gold(III)  
19 have been known for several decades.  
20  
21  
22  
23  
24  
25  
26  
27  
28

29 Homogeneous gold catalysts (almost exclusively gold(I)) have often been considered in  
30 close comparison with platinum(II), particularly PtCl<sub>2</sub>,<sup>30-34</sup> which catalyzes very similar processes.  
31 Consequently, the mechanisms proposed for gold-mediated reactions tend to borrow heavily from  
32 the better-known mechanisms of platinum and palladium catalysts.<sup>35</sup> However, there are significant  
33 differences, not least in the redox potentials: under standard conditions the Au<sup>III</sup>/Au<sup>0</sup>, Au<sup>I</sup>/Au<sup>0</sup> and  
34 Au<sup>III</sup>/Au<sup>I</sup> potentials (1.52, 1.83 and 1.36 V, respectively) are very much more positive than Pd<sup>II</sup>/Pd<sup>0</sup>  
35 (0.91 V) and Pt<sup>II</sup>/Pt<sup>0</sup> (1.19 V).<sup>36</sup> Gold is therefore much more easily reduced than palladium or  
36 platinum, to either Au(I) or the metallic state, and it is often not at all easy to determine which of  
37 these forms and oxidation states is responsible for the observed catalysis. Comprehensive  
38 mechanistic and spectroelectrochemical studies have also shown that nucleophilic substitution and /  
39 or reduction of gold(III) halides, at least in aqueous media, is dependent on the solvent, pH, redox  
40 potential and nucleophilicity of the coordinated ligands.<sup>37</sup>  
41  
42  
43  
44  
45  
46  
47  
48  
49

50 Ligands, in particular chelating bi- and tridentate ligands, are of course capable of modifying  
51 the redox potentials, thus providing stability against reduction. For this reason, chelating and pincer  
52 ligands play a prominent role in gold(III) chemistry, as documented in several pertinent  
53 reviews.<sup>38-40</sup> For example, while the alkylation of gold(III) complexes with nucleophilic main group  
54 alkyls usually gives only low yields of the desired gold(III) alkyl product and is accompanied by  
55 extensive reduction to gold metal,<sup>41</sup> C<sup>^</sup>N chelated gold complexes (tpy)Au(OAc<sup>F</sup>)<sub>2</sub> (tpyH = 2-(*p*-  
56 tolyl)pyridine) react with lithium reagents to give (tpy)AuR<sub>2</sub> (R = Me, Ph) in near-quantitative  
57  
58  
59  
60

1  
2  
3 yields.<sup>41</sup> However, in several instances, even Au(III) complexes stabilized by C<sup>^</sup>N<sup>^</sup>C or N<sup>^</sup>N<sup>^</sup>N  
4 pincer ligands were found to be susceptible to reduction on reaction with nucleophiles.<sup>42,43</sup>  
5  
6 Photolysis of gold(III) halide complexes, and even exposure to diffuse daylight, can lead to  
7  
8 reductive elimination, including the reductive elimination of C-Cl bonds and of Cl<sub>2</sub>.<sup>44-47</sup>  
9

10 While platinum is similar to gold in being subject to relativistic effects, these are much less  
11 pronounced. The reactivity towards standard ligands can also be substantially different, as  
12 exemplified most clearly in the reaction towards CO: whereas CO adducts of PtCl<sub>2</sub> were the first  
13 metal carbonyl complexes ever to be isolated,<sup>48,49</sup> the analogous gold complex AuCl<sub>3</sub>(CO) is  
14 unknown, and as early as 1905 the treatment of AuCl<sub>3</sub> with CO was recommended as a convenient  
15 method for generating gold colloids.<sup>50</sup> While there are obvious formal similarities between the  
16 coordination chemistry and reactivity of square-planar Pt(II) and Au(III) compounds, these  
17 examples illustrate that there are also quite fundamental differences between these two isoelectronic  
18 metal centers, so that extrapolation of mechanistic intermediates from one to another should be  
19 treated with caution.  
20  
21  
22  
23  
24  
25  
26

27 There has been a spectacular rise in the application of soluble gold catalysts in synthesis. By  
28 far the most widely studied are complexes of gold(I). Their development has been the subject of  
29 several monographs<sup>51-53</sup> and numerous reviews,<sup>54-77</sup> as well as themed issues including *Chem. Rev.*  
30 **2008**,<sup>78-82</sup> *Chem. Soc. Rev.* **2008**,<sup>83-84</sup> *J. Organomet. Chem.* **2009**, 694,<sup>85</sup> *Beilstein J. Org. Chem.*  
31 **2011**, 7,<sup>86</sup> *Isr. J. Chem.* **2013**, 53,<sup>87</sup> *Acc. Chem. Res.* **2014**,<sup>88-93</sup> *Chem. Soc. Rev.* **2016**<sup>94-98</sup> and *Adv.*  
32 *Synth. Catal.* **2016**.<sup>99-101</sup>  
33  
34  
35  
36

37 Remarkably, even though the presumably first application of a soluble gold catalyst for  
38 organic transformation, the isomerization of bicyclo[1.1.0]butanes by gold triiodide,<sup>102</sup> involved a  
39 complex of gold(III), in subsequent studies gold(III) complexes have played a lesser role in  
40 homogeneous catalysis and synthetic applications. In many instances, although gold(III) precursors  
41 were used, the nature of the active species remains uncertain. A series of reviews include gold(III)  
42 complexes in their discussions, either as catalyst precursors or as intermediates generated *in-situ* as  
43 part of proposed catalytic cycles.<sup>103-111</sup> The need for more mechanistic information through detailed  
44 knowledge of the coordination chemical behavior of gold species during catalysis and identification  
45 of intermediates has been stressed repeatedly,<sup>112-114</sup> and with the growth in volume and diversity of  
46 gold catalysis this need has certainly not diminished.  
47  
48  
49  
50  
51  
52  
53  
54  
55

### 56 **1.1. Scope, Limitation, and Organization of the Review**

57 The role of gold(III) complexes in catalysis is now set to change, and in recent years much  
58 has been learned about the bonding and reactivity of gold(III) species. Progress in this area has led  
59  
60

1  
2  
3 to pertinent recent reviews covering key catalytic reaction steps<sup>115</sup> and the chemistry and  
4 photophysical aspects of cyclometallated Au(III) complexes.<sup>39,40</sup> A previous (and to our knowledge  
5 most recent) review devoted specifically to gold(III) catalysts by Schmidbaur and Schier in 2012  
6 concentrated predominantly on the use and reactions of gold(III) halides, although the authors point  
7 out the uncertainty that persists in many cases regarding the actual oxidation states, structures and  
8 mechanisms of such gold halide catalysts or catalyst precursors.<sup>116</sup>  
9  
10  
11  
12

13 This review aims to summarize the development of well-defined organometallic gold(III)  
14 complexes and catalysts over the last decade. While the large range of studies on gold(III)  
15 complexes with photophysical properties<sup>117,118</sup> and anti-tumour and biological application<sup>39,119</sup> is  
16 beyond the scope of this review, emphasis will be placed on new insights into coordination types  
17 and the chemistry and bonding in gold(III) compounds, followed by a discussion of catalytic  
18 applications, providing a rational link between the fundamental aspects described in Sections 2 and  
19 3 and catalytic reactivity.  
20  
21  
22  
23  
24

25 The review begins with a brief outline of general aspects. Section 2 covers major recent  
26 advances in the organometallic chemistry of gold(III) complexes and is structured according to  
27 complex type, with emphasis on isolated or at least spectroscopically characterized species of  
28 relevance to catalysis, such as complexes of alkenes, alkynes, and  $\pi$ - and  $\sigma$ -bonding interactions.  
29 Section 3 describes new insight into key reaction steps in catalytic cycles. Section 4 of the review  
30 will cover applications of gold(III) catalysts and reactions where Au(III) intermediates are invoked  
31 in the reaction mechanisms of organic transformations, including photo-assisted catalysis, with  
32 emphasis on investigations providing mechanistic insight.  
33  
34  
35  
36  
37  
38  
39  
40

## 41 **2. GENERAL ASPECTS OF GOLD(III) COORDINATION CHEMISTRY**

42 The reactivity, mechanistic pathways and consequently the catalytic activity of transition  
43 metal centers are determined by a number of factors that depend on the nature of metal-ligand  
44 interactions. For example, the tendency of a metal fragment to engage in elementary steps such as  
45 nucleophilic attack, migratory insertions, oxidative addition/reductive elimination is determined by  
46 its ability to (i) to undergo ligand exchange, (ii) to bind a substrate through electron acceptor and  
47 back-donation interactions or (iii) to induce dipoles in the coordinated substrates. In the following  
48 section, we will describe the advancements in the understanding of structure and bonding in well-  
49 defined Au(III) complexes that are catalytically relevant, focusing our attention on how metal-  
50 ligand interactions can trigger the reactivity towards the elementary steps described above.  
51  
52  
53  
54  
55  
56  
57  
58  
59  
60

### **2.1 *Trans*-Effect / *trans*-Influence**



1  
2  
3 The ligand reactivity in gold(I) and gold(III) complexes is subject to the influence of ligands  
4 in *trans* position: strongly electron-donating ligands weaken gold-*trans*-ligand bonds, ligands with a  
5 weak donor strength in the spectrochemical series, such as water, pyridine or fluoride, have the  
6 opposite effect. Quantitative studies on ligand substitution kinetics (*trans*-effect) in gold complexes  
7 are rare, those on gold(III) in particular. One such study on the ligand exchange kinetics of gold(III)  
8 complexes demonstrated the strong *trans*-effect exerted by  $\sigma$ -donating aryl anions, which facilitates  
9 the displacement of the chloride ligands *trans* to phenyl by methanol and its subsequent substitution  
10 by nucleophiles in the sequence  $\text{Nu} = \text{NO}_2 < \text{Cl} < \text{Br} < \text{N}_3 \approx \text{I} < \text{NCS}$ .<sup>120</sup> Recent years have seen a  
11 resurgence of interest in such ligand effects in gold(I) chemistry,<sup>121-125</sup> since they underpin the  
12 behavior of these complexes in catalysis, notably their propensity to undergo oxidative addition.<sup>126</sup>  
13 Ligands L that exert a strong ground state *trans*-influence in complexes of type *trans*-LAu(Y)<sub>2</sub>X  
14 lead to the elongation / weakening of the Au-X bond.<sup>127</sup>

15  
16  
17 Gold(III) complexes are frequently stabilized by chelating ligands, in particular by  
18 cyclometalated 2-phenylpyridine (ppy) derivatives, as in structures **1** to **5** (Figure 1).<sup>128-131</sup> The Au-  
19 N distances tend to be “soft” and particularly subject to the influence of *trans* ligands. As the Tilset  
20 group has shown,<sup>132-135</sup> Au-N(ppy) leads to a shortening (strengthening) of *trans*-Au-X bonds,  
21 while Au-C(ppy) has the opposite effect. The coordination site *trans* to Au-C(ppy) is therefore more  
22 labile than that opposite to Au-N(ppy); however, the primary substitution product can rearrange, so  
23 that insertion appears to have taken place *trans* to N rather than *trans* to C.

24  
25  
26 However, a recent computational study by Budzelaar, Bochmann and co-workers advised  
27 against relying solely on crystallographically determined bond distances when assessing the *trans*-  
28 influence, since such distances are determined by a number of factors of comparable magnitude.  
29 Using two series of compounds, (C<sup>^</sup>N)Au(Z)(OTf) (with Z *trans* to N) and (C<sup>^</sup>N)AuZ<sub>2</sub>, where Z =  
30 Me, aryl or halogen, three descriptors of the *trans*-influence were considered: (i) the Au-N bond  
31 length; (ii) the Au-N Wiberg Bond Index (WBI) and (iii) the NPA charge on the nitrogen atom  
32 (NPA = natural population analysis). All three showed fairly consistent trends, and on going from  
33 Me to F (a) the Au-N bond length decreases from 2.17 to 2.04 Å, (b) the Au-N WBI increases from  
34 0.29 to 0.45, and (c) the N atom becomes less negative, from -0.46 to -0.42 *e*-.<sup>136</sup>

35  
36  
37 The *trans*-influence in cyclometalated complexes leads to significant changes in ligands bond  
38 energies. As a comparison of the cationic complexes **6** and **7** (Figure 1) showed, the binding  
39 enthalpy *trans* to anionic C (as in **7**) is about 2/3 of the value for **6** *trans* to N. The latter ranges  
40 from 33 to 53 kcal/mol. For unsubstituted  $\pi$ -donors the weakening of the Au-L bond follows the  
41 trend  $\text{CO} > \text{CH}_2=\text{CH}_2 > \text{HC}\equiv\text{CH} > \text{OH}_2$ . For alkenes and alkynes binding enthalpies increase  
42  
43  
44  
45  
46  
47  
48  
49  
50  
51  
52  
53  
54  
55  
56  
57  
58  
59  
60

significantly with substitution, for example alkyne binding strengthens for  $\text{RC}\equiv\text{CR}$ ,  $\text{R} = \text{H} \ll \text{Me} < t\text{Bu}$ .

Anionic C-donors weaken the *trans*-Au-L bonds in all cases, although simple  $n$ -donors such as  $\text{H}_2\text{O}$  or ethers are less affected than  $\pi$ -donors. Ligands L which are  $\pi$ -donors but weak  $\pi$ -acceptors show an average binding enthalpy  $\Delta H_{\text{av}}(\text{C}^{\wedge}\text{C})$  of about 40-45% that of the  $\text{C}^{\wedge}\text{N}^{\wedge}\text{C}$  system (Table 1). This means for example that only bulky alkynes would be able to displace a water ligand from a  $[(\text{C}^{\wedge}\text{C})\text{Au}(\text{OH}_2)\text{L}]^+$  precursor ( $\text{C}^{\wedge}\text{C} = 1,1'$ -biphenyl-2,2'-diyl). The strongest *trans*-influence is experienced by the strong  $\pi$ -acceptor CO; its bond enthalpy in the  $\text{C}^{\wedge}\text{C}$  system falls to only 35% of that in the  $\text{C}^{\wedge}\text{N}^{\wedge}\text{C}$  complex.<sup>137</sup>

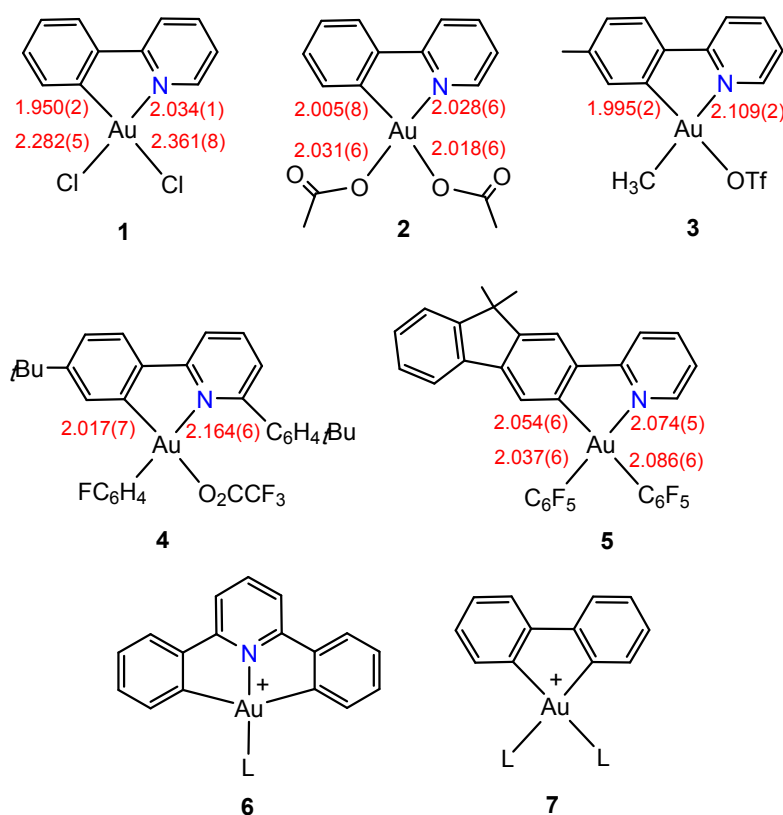


**Figure 1.** Structures and bond distances (Å) of selected gold(III) chelate complexes illustrating the structural *trans*-influence (data from refs. 128 (1, 2), 129 (3), 130 (4) and 131 (5)).

**Table 1.** Substrate binding enthalpies<sup>a</sup> (298 K, kcal/mol) of representative  $n$ - and  $\pi$ -donor ligands L to  $[(\text{C}^{\wedge}\text{N}^{\wedge}\text{C})\text{Au}]^+$  (6) and  $[(\text{C}^{\wedge}\text{C})\text{Au}]^+$  (7) fragments.

	$\text{C}^{\wedge}\text{N}^{\wedge}\text{C}$	$\text{C}^{\wedge}\text{C}$
<b>Substrate</b>	$\Delta H_{\text{tot}}^b$	av. $\Delta H$ per L
$\text{OH}_2$	-33.4	-19.1
$\text{OMe}_2$	-36.6	-20.9

OEt <sub>2</sub>	-38.1	-21.5
CO	-45.5	-16.0
HC≡CH	-35.5	-14.2
MeC≡CMe	-44.6	-21.8
CH <sub>2</sub> =CH <sub>2</sub>	-41.2	-16.9
MeCH=CH <sub>2</sub>	-43.3	-18.7

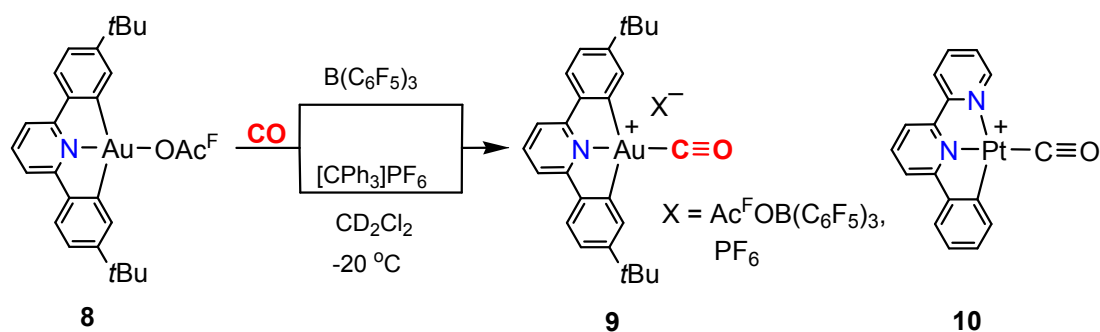
<sup>a</sup> TPSSH/cc-pVTZ/PCM(CH<sub>2</sub>Cl<sub>2</sub>)/B3LYP/SVP/PCM(CH<sub>2</sub>Cl<sub>2</sub>) with DFT-D3(zero damping) dispersion correction. <sup>b</sup> Enthalpy change for the reaction [(C<sup>^</sup>N<sup>^</sup>C)Au]<sup>+</sup> + L → [(C<sup>^</sup>N<sup>^</sup>C)Au(L)]<sup>+</sup>.

## 2.2. Gold(III) Complexes with π-Ligands

**2.2.1 Au(III)-CO Complexes.** As pointed out in the introduction, there are no CO adducts of simple gold(III) halides. In 2015 Roşca *et al.* reported the first example of an isolable gold(III)-CO complex.<sup>138</sup> This compound relies for stability on the C<sup>^</sup>N<sup>^</sup>C 2-6-diarylpyridine pincer ligand framework and was prepared by abstraction of a trifluoroacetate ligand from (C<sup>^</sup>N<sup>^</sup>C)AuOAc<sup>F</sup> (**8**) with B(C<sub>6</sub>F<sub>5</sub>)<sub>3</sub> in the presence of CO or <sup>13</sup>CO at -20 °C to give **9** (Scheme 1). The complex could be precipitated from dichloromethane / light petroleum as a yellow microcrystalline solid, although crystal suitable for X-ray diffraction could not be obtained. The same product is formed by exposing the ethylene complex [(C<sup>^</sup>N<sup>^</sup>C)Au(C<sub>2</sub>H<sub>4</sub>)]<sup>+</sup> to CO. The PF<sub>6</sub><sup>-</sup> salt was similarly prepared by treating **8** with [CPh<sub>3</sub>]PF<sub>6</sub> under a CO atmosphere. These CO complexes are thermally sensitive and decompose above -10 °C. The infrared spectrum of **9** in CH<sub>2</sub>Cl<sub>2</sub> shows the ν<sub>CO</sub> stretch at 2167 cm<sup>-1</sup>, 24 cm<sup>-1</sup> higher than that of free <sup>12</sup>CO. The value is fairly close to the one found for CO bound to Au<sup>3+</sup> centers in titania-supported heterogeneous gold CO oxidation catalysts (2158 cm<sup>-1</sup>).<sup>139</sup> The <sup>13</sup>C NMR signal of **9**(<sup>13</sup>C), appears at δ 167.6 (cf. δ 184 for free CO), within the range observed for “non-classical” gold(I) CO complexes [Au(CO)]<sup>+</sup> and [Au(CO)<sub>2</sub>]<sup>+</sup> (δ 158 - 172)<sup>140</sup> and is apparently little influenced by the metal d-electron configuration (d<sup>8</sup> vs d<sup>10</sup>). The IR ν<sub>CO</sub> signal of **9** recorded in cold dichloromethane solutions was always accompanied by a signal for <sup>12</sup>CO<sub>2</sub> / <sup>13</sup>CO<sub>2</sub>, indicating a facile attack by adventitious water on the coordinated CO, leading to water-gas shift (see Section 3.4.3).

The susceptibility towards nucleophilic attack and the high ν<sub>CO</sub> frequency would suggest a very low degree of back-bonding. This contrasts with the stability of the isostructural C<sup>^</sup>N<sup>^</sup>N platinum complex **10** (Scheme 1), which could be recrystallized from boiling methanol, shows a much lower CO stretch at 2094 cm<sup>-1</sup>, and has no water-gas shift reactivity.<sup>141,142</sup>

### Scheme 1. Gold(III) and Platinum(II) CO Complexes



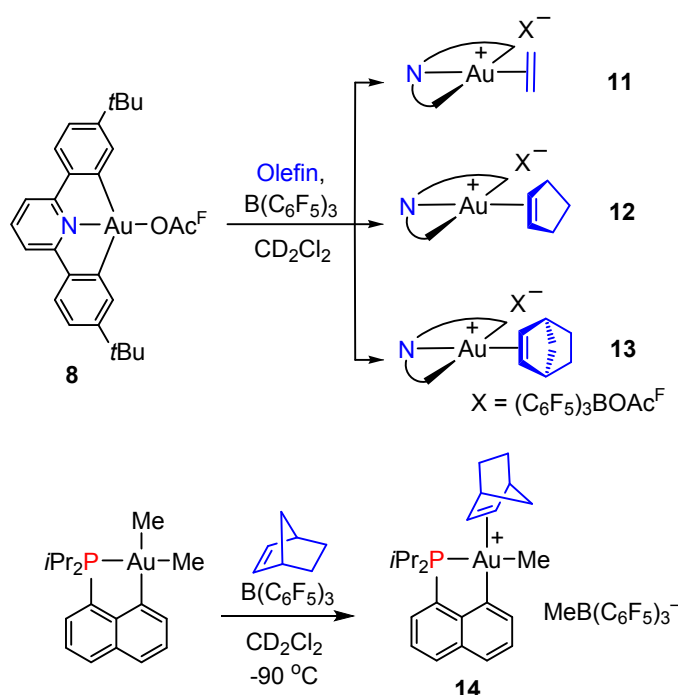
The bonding of CO has been the subject of several computational studies. None of the high-lying molecular orbitals, from HOMO-3 to HOMO, show any  $\pi$ -bonding contribution to the Au-CO bond. Charge decomposition analysis (CDA) for **9** gave a back-donation/donation (*b/d*) ratio of 0.44, compared to a value of 0.65 for the platinum analogue  $[(\text{N}^{\wedge}\text{N}^{\wedge}\text{C})\text{Pt}(\text{CO})]^+$  (**10**), in line with the significantly stronger back-bonding in Pt(II)-CO complexes.<sup>138</sup> Using the methods specified in Table 1, Budzelaar obtained M-CO bond enthalpies of -45.5 kcal/mol for Au, about 7 kcal/mol less stable than Pt-CO, with calculated  $\nu_{\text{CO}}$  frequencies Au-CO > Pt-CO close to the observed values.<sup>143</sup> These calculations also further illustrate the role of *trans*-influence and suggest that formation of complexes of the type  $[(\text{C}^{\wedge}\text{C})\text{Au}(\text{CO})_2]^+$  (**7**, L = CO), i.e. CO *trans* to anionic C, would be endothermic.<sup>137</sup> An alternative interpretation by Gaggioli *et al.*, based on charge displacement analysis, proposes that there is strong  $\sigma$ -donation but also strong  $\pi$ -back-donation, with net charge transfer  $\text{CT}^{\text{net}}$  made up of  $\text{CT}^{\sigma\text{-don}}$  of  $0.25 e^-$  and a large total  $\pi$  back-donation component  $\text{CT}^{\pi\text{-back}}$  of  $0.28 e^-$ , coupled with significant polarization of CO from O to the C atom, thus strengthening the CO bond. A  $\nu_{\text{CO}}$  value of  $2106 \text{ cm}^{-1}$  was calculated, rather lower than observed. In contrast to the bonding in **9**, the CT in the platinum complex **10** is much larger ( $\text{CT}^{\pi\text{-back}} = -0.40 e^-$ ). The polarization of the CO ligand in the gold complex is positive,  $0.03 e^-$ , whereas in Pt it is slightly negative. These differences are seen as responsible for the ability of gold to engage in water-gas shift, while the Pt-CO complex resists nucleophilic attack under such conditions.<sup>144,145</sup>

**2.2.2. Alkene Complexes.** A comprehensive 2010 review by Schmidbaur of  $\pi$ -complexes of gold stressed the surprising absence of gold(III) alkene and alkyne complexes.<sup>146</sup> This lack of gold(III)  $\pi$ -complexes is certainly surprising since an alkene complex of isoelectronic platinum(II), Zeise's salt  $\text{K}[\text{PtCl}_3(\text{C}_2\text{H}_4)]$ , was the first transition metal organometallic complex ever to be isolated.<sup>147-149</sup> This gap was filled by two independent reports in 2013, on gold(III) monoalkene adducts by Bochmann and on 1,5-cyclooctadiene complexes by Tilset. Some of these developments have been highlighted in recent summaries.<sup>18,150</sup>

In 2013 Savjani *et al.* reported the first examples of gold(III)  $\pi$ -alkene complexes: the pincer compounds  $[(\text{C}^{\wedge}\text{N}^{\wedge}\text{C})\text{Au}(\text{L})]^+$  (L = ethylene, cyclopentene and norbornene) **11** to **13**.<sup>151</sup> A

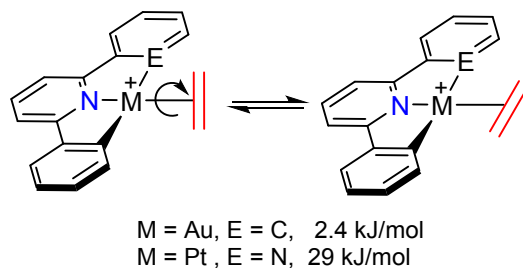
cyclometallated 2,6-diphenylpyridine C<sup>^</sup>N<sup>^</sup>C pincer ligand provided the necessary stability (Scheme 2). The alkene complexes were obtained in near-quantitative yields and isolated as yellow powders or needles. Alternatively, they could also be made by treating (C<sup>^</sup>N<sup>^</sup>C)AuOH with [H(OEt<sub>2</sub>)<sub>2</sub>]X [X = H<sub>2</sub>N{B(C<sub>6</sub>F<sub>5</sub>)<sub>3</sub>}<sub>2</sub> or B{3,5-C<sub>6</sub>H<sub>3</sub>(CF<sub>3</sub>)<sub>2</sub>}<sub>4</sub>] in the presence of olefins. Their isolation contrasts with the reactions of alkenes with common gold(III) starting materials like AuCl<sub>3</sub>, AuBr<sub>3</sub>, HAuCl<sub>4</sub> or NaAuCl<sub>4</sub>, which invariably lead to reduction to Au(I) or gold metal.<sup>146,152,153</sup>

### Scheme 2. Formation of Gold(III) Monoolefin Complexes



The norbornene (NBE) complex **13** is stable at room temperature, whereas the ethylene and cyclopentene complexes proved thermally labile in solution, although the solids are air-stable for hours at room temperature. The coordination of ethylene in **11** is indicated by a <sup>1</sup>H (<sup>13</sup>C{<sup>1</sup>H}) chemical shift change from δ 5.38 (δ 108.9) for free C<sub>2</sub>H<sub>4</sub> to δ 6.29 (δ 122.8) ppm in the complex. Coordination also caused an increase in the ethylene C-H coupling constant from 156 to 166 Hz.<sup>151</sup> The change in the <sup>13</sup>C NMR chemical shift is much smaller than that observed for Zeise's salt; this and the substitutional lability of **11** indicates the reduced back-bonding in Au(III) compared to Pt(II), as was also observed for the CO complexes. In agreement with this, the calculated barrier for ethylene rotation in **11** was only 0.6 kcal mol<sup>-1</sup>, less than a tenth of the value for [(C<sup>^</sup>N<sup>^</sup>N)Pt(C<sub>2</sub>H<sub>4</sub>)]<sup>+</sup> (Scheme 3), in agreement with the back-donation/donation ratio of 0.29 for Au(III)-C<sub>2</sub>H<sub>4</sub> compared to 0.59 for Pt(II)-C<sub>2</sub>H<sub>4</sub>.<sup>18</sup>

**Scheme 3 Rotational Barriers of Au(III) and Pt(II) Ethylene Complexes**



In solution the ethylene complex undergoes exchange with free ethylene. However, the methylene groups of the cyclopentene adduct were found to be diastereotopic, ruling out fast intermolecular exchange and flipping of the 5-ring from one  $\pi$ -face to the other.

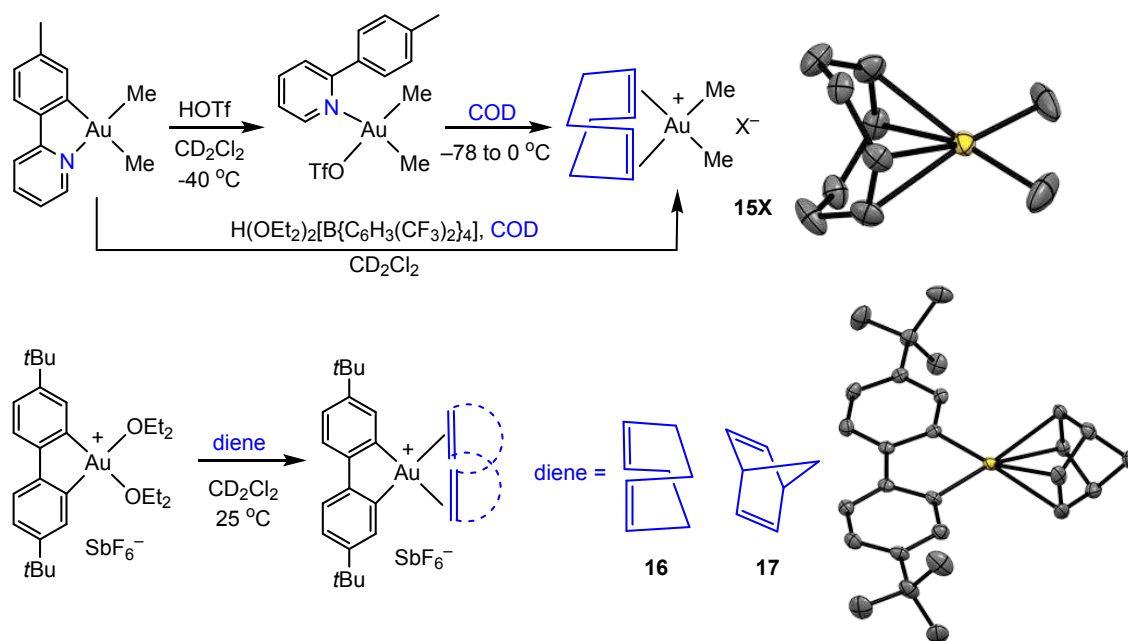
In contrast to isolable **13**, with NBE *trans* to pyridine, norbornene *trans* to aryl is much more labile. Bourissou and co-workers reported the identification of [(C<sup>^</sup>P)AuMe(NBE)] [MeB(C<sub>6</sub>F<sub>5</sub>)<sub>3</sub>] (**14**, Scheme 2) at -90 °C in CD<sub>2</sub>Cl<sub>2</sub>, alongside free NBE.<sup>154</sup> The compound disappeared rapidly on warming to -80 °C due to facile NBE insertion into the Au-Me bond (see Section 3.4.1). The four protons at the bridgehead and 5-positions of NBE are shifted upon coordination from  $\delta$  2.77 to  $\delta$  3.30 ppm and from  $\delta$  1.53 to  $\delta$  1.92 ppm, respectively. The =CH (<sup>13</sup>C) signal of the coordinated NBE is shifted from  $\delta$  5.90 (133.8) for the free olefin to  $\delta$  6.21 (119.0) ppm. Computational modelling gave a minimum for the isomer *trans* to naphthyl-C, which was more stable than the *cis* isomer by 3.3 kcal/mol. This structure was further confirmed by the computed  $J_{\text{CP}}$  coupling constants between P and the CH<sub>3</sub> ligands (*trans*:  $J_{\text{PC}} = 89 \text{ Hz}$ , vs. *cis* = 4.6 Hz), which agreed with experiment ( $^2J_{\text{PC}} = 76.2 \text{ Hz}$ ).

An alternative strategy was used by Langseth *et al.* to synthesize gold(III) 1,5-cyclooctadiene (COD) complexes. Starting with the cyclometallated phenylpyridine complex (C<sup>^</sup>N)AuMe<sub>2</sub>, the authors employed protodeauration with triflic acid at -40 °C in the presence of COD to strip off the C<sup>^</sup>N ligand and generate salts of the [Me<sub>2</sub>Au(COD)]<sup>+</sup> cation **15X** [X = OTf or BAR<sup>F</sup> = B{3,5-(CF<sub>3</sub>)<sub>2</sub>C<sub>6</sub>H<sub>3</sub>}<sub>4</sub>].<sup>155</sup> Because of the thermal instability of the product, the reactions were conducted -78 to 0 °C (Scheme 4). Dichloromethane solutions of **15OTf** decompose within hours at room temperature. The <sup>1</sup>H NMR spectrum the olefinic protons gave rise to a broad singlet at  $\delta$  6.39 ppm, high-frequency shifted by 0.8 ppm compared to free COD ( $\delta$  5.56 ppm). Protonation with [H(OEt<sub>2</sub>)<sub>2</sub>]BAR<sup>F</sup> gave the analogous BAR<sup>F</sup> salt which could be crystallized at -35 °C to allow the determination of the crystal structure. The COD ligand is twisted, and the cation exhibits two different Au-C distances to the olefinic C atoms, 2.362(4) and 2.406(4) Å. The asymmetry of COD ligation in **15** was replicated in the calculated gas-phase structure and is due to the conformational

1  
2  
3 preference of COD rather than crystal packing effects. The Au-C(olefin) distances are longer and  
4 the C=C distances of 1.348 and 1.364 Å significantly shorter than those in the analogous platinum  
5 complex, (COD)PtMe<sub>2</sub>, indicative of the reduced back-bonding in the gold complex compared to  
6 platinum.<sup>155</sup>  
7  
8  
9

10 Subsequently Chambrier *et al.* showed that thermally more stable gold(III) complexes with  
11 non-conjugated dienes are accessible by displacement of the ether ligands in [(C<sup>∧</sup>C)Au(OEt<sub>2</sub>)<sub>2</sub>]<sup>+</sup>  
12 (C<sup>∧</sup>C = 4,4'-di-*t*-butylbiphenyl-2,2'-diyl) with either COD or norbornadiene (NBD), to give **16** and  
13 **17**, respectively (Scheme 4).<sup>137</sup> The biphenyl ligand significantly stabilizes the products, which  
14 can be stored indefinitely at room temperature in solution and as solids. The NMR spectroscopic  
15 data of the COD complex are closely similar to those of [Me<sub>2</sub>Au(COD)]<sup>+</sup> (=CH δ<sub>H</sub> 6.87, Δδ -1.3  
16 ppm). The olefinic resonances of the NBD complex are found at δ 7.63 (Δδ -0.83 ppm). This  
17 compares with the olefinic resonance of (NBD)PtMe<sub>2</sub> at δ 5.0 ppm, yet another indication of the  
18 more electron-withdrawing character of the gold(III) cation.  
19  
20  
21  
22  
23  
24  
25  
26  
27

28 **Scheme 4. Formation of Gold(III) Diene Complexes and Crystal Structures of the Cations in**  
29 **15BAr<sup>f</sup> and 17**



The crystal structures of **16** and **17** were determined by X-ray diffraction. The COD complex shows asymmetric C=C bonding, similar to **15**. In contrast, the NBD coordination in **17** is symmetrical; the olefinic ligand lies astride the (C<sup>∧</sup>C)Au moiety, and differences in Au-C bond lengths are small (0.005–0.006 Å). The Au-C(olefin) bond lengths in the NBD complex (av. 2.022 Å) are noticeably shorter than in the COD analogue (av. 2.041 Å), a reflection of the reduced steric

1  
2  
3 interactions due to the smaller bite angle of NBD compared to COD (62 vs. 78°). The C=C bonds of  
4 the coordinated dienes experience a 1.4 – 1.8% elongation compared to the free ligands.

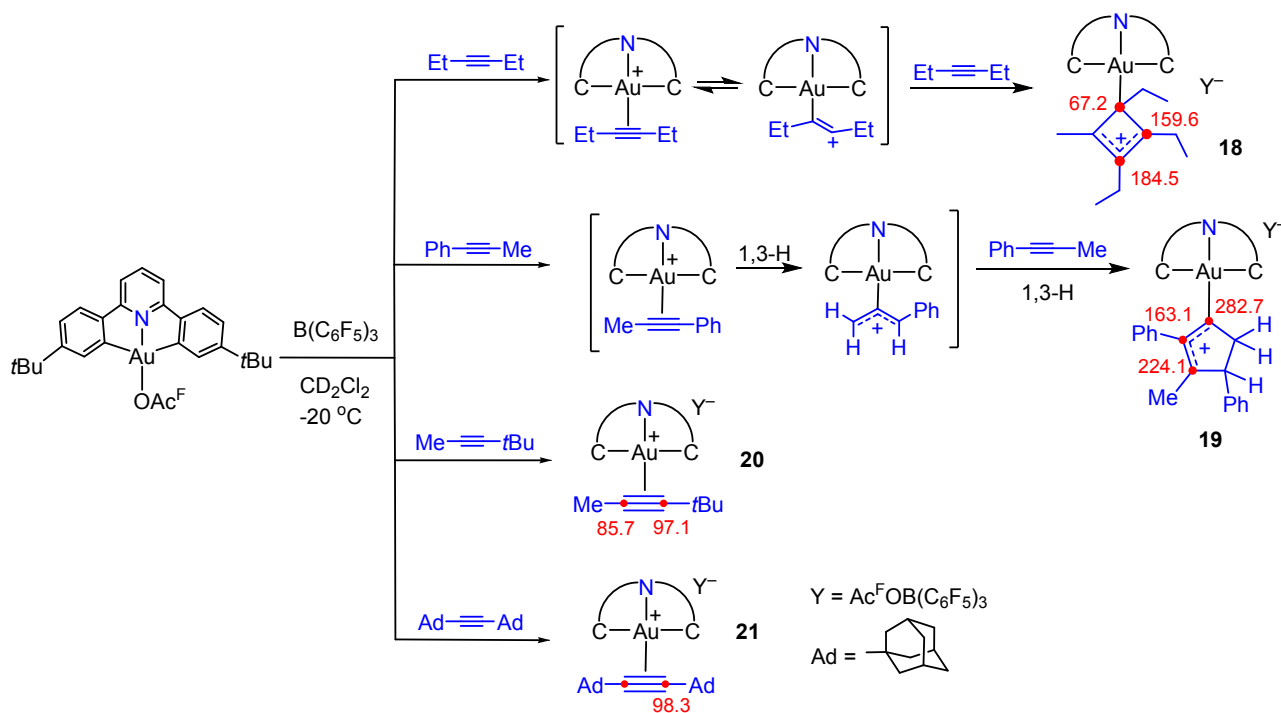
5  
6 Attempts to generate complexes  $[(C^{\wedge}C)AuL_2]^+$ , where L = non-chelating 1-alkene, were  
7 unsuccessful. DFT calculations showed that the formation of  $(C^{\wedge}C)Au$  alkene complexes is driven  
8 by the chelate effect. Relative to  $[(C^{\wedge}C)Au(OH_2)_2]^+$  alkene binding becomes favorable by -9.6  
9 kcal/mol for COD and -6.0 kcal/mol for NBD but is mildly endothermic for  $H_2C=CHR$  (R = H, Me,  
10 *t*Bu). The binding enthalpies of COD and NBD to metal fragments M decrease in the sequence M =  
11 PtMe<sub>2</sub> >  $(C^{\wedge}C)Au^+$  > Me<sub>2</sub>Au<sup>+</sup>. A charge analysis from natural population analysis suggested that  
12 the increased thermal stability of **16** and **17** may not least be due to the significantly higher  
13 accumulation of negative charge on  $C^{\wedge}C$  compared to methyl ligands.<sup>137</sup>

14  
15 **2.2.3 Alkyne Complexes.** Although many organic transformations are assumed to start with  
16 gold coordination to an alkyne moiety, identifiable complexes of gold(III) to alkynes have proved  
17 elusive.<sup>146,156</sup> By contrast, the first structurally characterized  $\eta^2$ -alkyne complex of platinum(II) was  
18 reported in 1959.<sup>157</sup> For gold(I), Widenhoefer could show that alkynes have comparable donor  
19 strength to alkenes,<sup>158</sup> and indeed gold catalysts have been described as “alkynophilic”.<sup>104</sup> During  
20 studies on the addition of water and methanol to alkynes mediated by gold(III)-C<sub>6</sub>F<sub>5</sub> complexes,  
21 Laguna and co-workers found that while treatment of  $[(C_6F_5)AuCl_2]_2$  with phenylacetylene at room  
22 temperature led within seconds to reduction to gold metal, at low temperatures NMR signals  
23 consistent with the formation of the alkyne complex  $[(C_6F_5)_2AuCl(PhC\equiv CH)]$  ( $\delta_H$  3.76 ppm,  $\equiv CH$ )  
24 were observed, although the assignment remained speculative.<sup>159</sup>

25  
26 However, in 2017 Rocchigiani *et al.* reported well-characterized gold(III) alkyne complexes,  
27 which could be obtained by abstraction of a trifluoroacetate ligand with B(C<sub>6</sub>F<sub>5</sub>)<sub>3</sub> from the pincer  
28 complex **8**, in analogy to the Au(III) 1-alkene compounds (Scheme 5).<sup>160</sup> Under these conditions,  
29 sterically undemanding alkynes react further and undergo carbocationic C-C bond formation to give  
30 **18** and **19**. These [2+2] cyclizations underline that the alkyne bound to gold(III) has pronounced  
31 vinyl cation character, which renders it susceptible to further reactions and C-C bond formation that  
32 typify gold-catalyzed alkyne reactions. Trimethylsilyl acetylenes undergo fast transmetalation to  
33 form the corresponding Au(III) acetylides. On the other hand, sterically more hindered alkynes  
34  $R^1C\equiv CR^2$  (R<sup>1</sup> = Me, R<sup>2</sup> = *t*Bu; R<sup>1</sup> = R<sup>2</sup> = 1-adamantyl) give simple  $\eta^2$ -alkyne adducts **20** and **21**.  
35 The cycloaddition products and alkyne complexes show diagnostic <sup>13</sup>C NMR chemical shifts  
36 (Scheme 5, red numbers). Alkyne  $\eta^2$ -coordination induces only modest <sup>13</sup>C NMR shifts, similar to  
37 the values observed for Au(I) complexes  $[(R_3P)Au(alkyne)]BF_4$ .<sup>161,162</sup> While **20** is thermally labile  
38 in solution, the more bulky adamantyl derivative **21** is stable for days at room temperature and was  
39 isolated as a yellow microcrystalline solid.



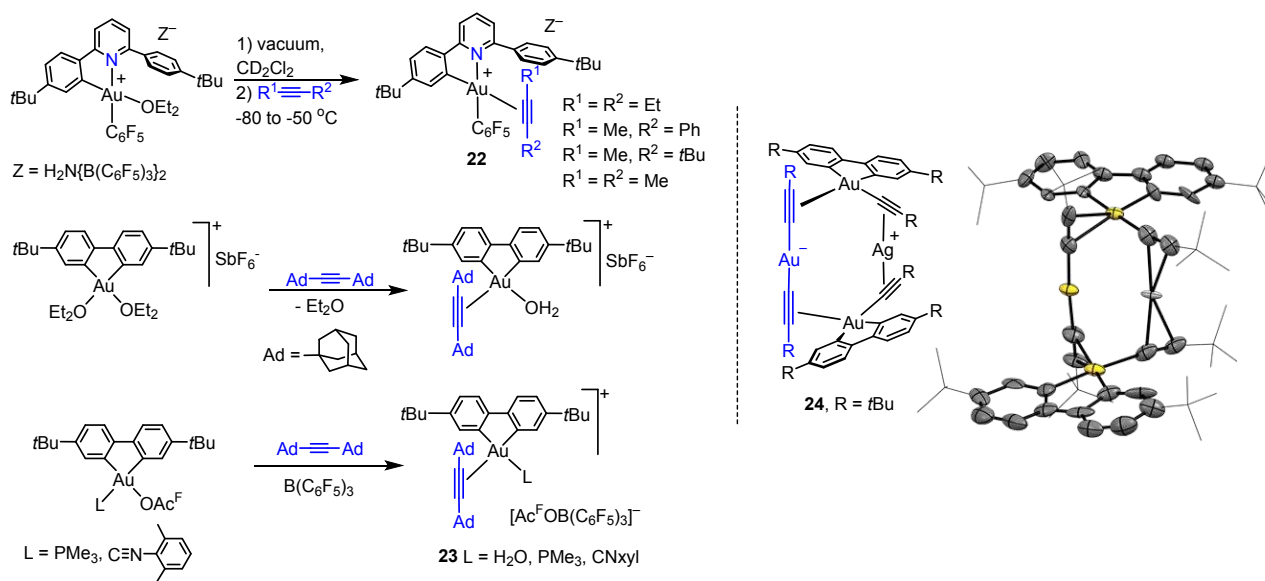
**Scheme 5. Synthesis and Reactions of Gold(III) Alkyne Complexes (Pertinent  $^{13}\text{C}$  NMR Data in Red).**



Further types of alkyne complexes could be obtained based on  $\text{C}^{\wedge}\text{N}$  chelate ligands (Scheme 6). Compounds of type **22** are thermally less stable since the alkyne ligands are *trans* to a strongly donating anionic carbon, which weakens the gold-alkyne interaction. The 3-hexyne complex exchanges in solution with free 3-hexyne by a dissociative mechanism.<sup>160</sup>

In 2018 Chambrier *et al.* found that, unlike the  $\text{C}^{\wedge}\text{N}$ -ligated complexes **22**, diadamantyl-acetylene complexes based on the biphenyl  $\text{C}^{\wedge}\text{C}$  ligand of type **23** are thermally stable at room temperature and could be isolated as bright-yellow microcrystalline powders (Scheme 6). DFT calculations indicated that the formation of the bis(alkyne) complex  $[(\text{C}^{\wedge}\text{C})\text{Au}(\text{AdC}\equiv\text{CAd})_2]^+$  was endergonic on steric grounds.<sup>137</sup> While these compounds failed to give crystals suitable for X-ray diffraction, the so far only example of a crystallographically characterized gold(III) alkyne adduct is complex **24**. The compound shows  $\eta^2$ -coordination of a bis(alkynyl)aurate(I) anion, which exhibits a  $\text{C}\equiv\text{C}$  bond length closely comparable to that calculated for  $[(\text{C}^{\wedge}\text{N}^{\wedge}\text{C})\text{Au}(\text{2-butynyl})]^+$ .<sup>160</sup>

**Scheme 6. Gold(III) Alkyne Complexes Based on  $\text{C}^{\wedge}\text{N}$  and  $\text{C}^{\wedge}\text{C}$  Chelate Ligands**



Alkyne bonding and the [2+2] cycloaddition pathway were explored by DFT calculations. Budzelaar, Bochmann and co-workers found that, surprisingly, the dissociation energies of Au(III) and Pt(II) with a pyridine donor *trans* to alkyne were remarkably similar, which suggests that the observed drastic differences in thermal stability and reactivity between Au and Pt are not due to thermodynamic effects. A charge-decomposition analysis suggested that back-donation is very small in all gold(III) alkyne complexes; for example, **20** shows a back-donation/donation (*b/d*) ratio of 0.43, much less than in structurally analogous  $[(\text{C}^{\wedge}\text{N}^{\wedge}\text{N})\text{Pt}^{\text{II}}(\text{3-hexyne})]^+$  (*b/d* = 0.77). Strong *trans* ligands reduce alkyne binding even further; a C-ligand *trans* to alkyne, as in **22**, reduces the binding energy by 30–40 kcal/mol, and the *b/d* ratio is reduced to 0.17. The stability of alkyne complexes therefore depends almost entirely on  $\pi$ -donation from the triple bond.

The lability of gold alkyne complexes is therefore the consequence of the reduced back-bonding capacity of Au(III), which makes alkyne slippage for Au(III) much easier than for Pt(II). This slippage leads to the accumulation of positive charge on one of the alkyne-C atoms, thus rendering it more susceptible to nucleophilic attack than Pt-bound alkyne (see Section 3.3).<sup>160</sup>

An in-depth theoretical study on gold(III)-alkyne binding by Gregori *et al.*, employing charge displacement (CD) analysis, comes to a similar conclusion: Alkyne binding to Au(III) involves a large total electron transfer to the metal, i.e. large  $\sigma$ -donation (of 0.24 – 0.44  $e^-$ ), coupled with a much smaller  $\pi$  back-donation. The resulting polarization of the  $\text{C}\equiv\text{C}$  bond was much larger for Au(III) than for Au(I) alkyne complexes. Nucleophilic attack by water was found to be very facile: Whereas the activation barrier for the gold(I) cation  $[(\text{NHC})\text{Au}(\text{2-butyn})]^+$  was 17.4 kcal/mol, the activation barriers for gold(III) complexes were much lower, to the point where nucleophilic attack may cease to be the rate-determining step in the reaction sequence.<sup>163</sup> Fully

relativistic *ab initio* calculations by Pernpointner and Hashmi on propyne complexes of AuCl<sub>3</sub> and, for comparison, PtCl<sub>2</sub>(H<sub>2</sub>O) came to similar conclusions: Strongly varying frontier orbital populations were considered as a major source of the differing catalytic activity of the two metals, leading to more difficult nucleophilic attack for Pt-alkyne than for the gold(III) analogue.<sup>164</sup>

**2.2.4 Arene  $\pi$ -Complexes.** Arene complexes of gold have long been postulated as intermediates in the electrophilic arylation of gold(III), ever since the first report on this topic by Kharasch in 1931,<sup>165,166</sup> and both  $\pi$ - and  $\sigma$ -arene complexes have been proposed in gold-catalyzed aryl C-H activation cycles.<sup>167,168</sup> While arene  $\pi$ -complexes of gold(I) are well-known,<sup>146</sup> evidence for identifiable gold(III) arene adducts have only recently come to light in two almost simultaneous reports by the groups of Bourissou<sup>169</sup> and Bochmann.<sup>170</sup> Compared to gold(I), the arene-Au(III) interactions are very weak. The (C<sup>^</sup>P)Au aryl compounds **25** (R = H, OMe) react with norbornene in the presence of AgSbF<sub>6</sub> as halide abstracting agent under alkene insertion into the Au-aryl bond to give the  $\beta$ -arylalkyl complexes **26** (Scheme 7). NMR spectroscopy shows that the rotation of the phenyl substituent (R = H) is hindered, with two different signals being observed for the *ortho*-C atoms and chemical shifts that suggest gold-aryl  $\pi$ -interaction. This was confirmed by the crystal structure of **26OMe**, which shows short Au-C<sub>*ipso*</sub> (2.416(2) Å) and Au-C<sub>*ortho*</sub> (2.593(3) Å) distances. The insertion of ethylene into the Au-Ph bond is even faster and proceeds below 0 °C. The final product **27** suggests that its formation involves an insertion –  $\beta$ -H elimination – reinsertion sequence to give the  $\alpha$ -phenylethyl derivative. Again, the NMR data are commensurate with gold(III)-phenyl  $\eta^2$ -coordination. However, whereas in **26** the alkyl ligand is *trans* to P, as judged from the large  $J_{PC}$  values, in **27** the alkyl is in *cis* position.<sup>169</sup>

An alternative route to complexes with  $\pi$ -arene interactions was employed by Rocchigiani *et al.* who used the strong Brønsted acid [H(OEt<sub>2</sub>)<sub>2</sub>][H<sub>2</sub>N{B(C<sub>6</sub>F<sub>5</sub>)<sub>3</sub>}<sub>2</sub>] to cleave one of the Au-C bonds in the pincer complexes (C<sup>^</sup>N<sup>^</sup>C)AuR (R = Cl, C<sub>6</sub>F<sub>5</sub>) to give **28**.<sup>170</sup> This complex is fluxional: the protodeauration is reversible, as long as an ether molecule is available to act as a proton-shuttle which transports H<sup>+</sup> from one side of the molecule to the other, with a barrier of  $\Delta G^\ddagger = 18.3$  kcal/mol. This appears to be the first demonstration of the role of such a weakly basic solvent as diethyl ether as protonolysis catalyst in gold-mediated C-H activation processes. There is a mechanistic resemblance to the “Concerted Metallation–Deprotonation” (CMD) process familiar from palladium catalysis.<sup>171</sup>

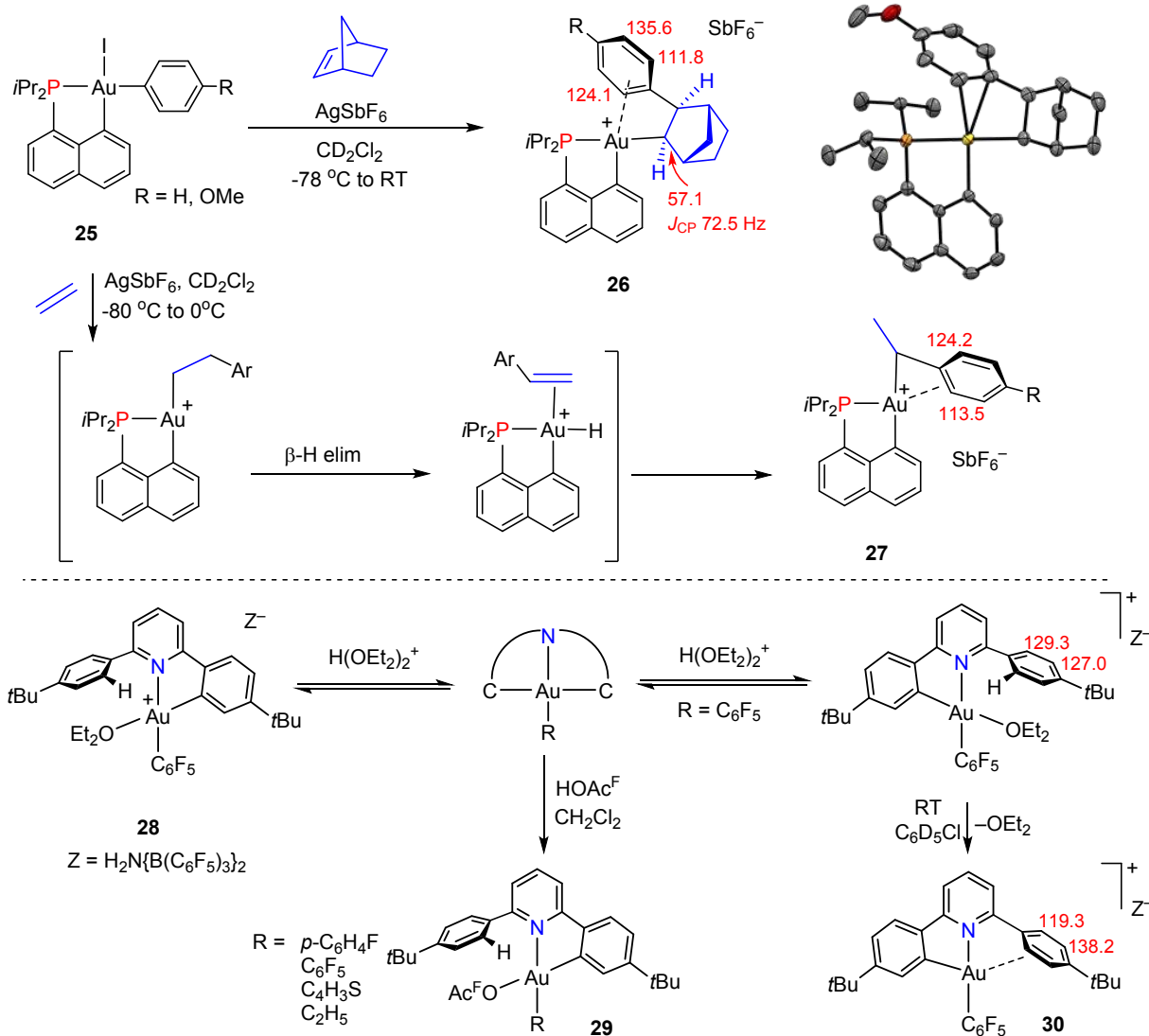
By contrast, Au-C cleavage with trifluoroacetic acid generates the non-fluxional alkyl and aryl complexes **29** (Scheme 7), whereas no cleavage was observed with acetic acid.<sup>130</sup>

Removing the ether from chlorobenzene solutions of **28** at room temperature stops the proton exchange process and generates the non-fluxional complex **30**. Its NMR data are consistent

1  
2  
3 with an interaction between the Au(III) center and the “dangling” aryl side-arm (Scheme 7;  $^{13}\text{C}$   
4 NMR chemical shifts given as red numbers). Since the C<sup>N</sup>-CH framework is too strained to allow  
5  $\eta^2$ -type  $\pi$ -coordination of the aryl to the metal centre, the C<sub>6</sub>H<sub>4</sub>*t*Bu moiety can only approach the  
6 metal by tilting by about 45° relative to the (C<sup>N</sup>)Au plane. Since the bilateral symmetry of  
7 C<sub>6</sub>H<sub>4</sub>*t*Bu is retained in the  $^1\text{H}$  NMR spectrum, there must be rapid oscillation between the two *ortho*  
8 positions, even on cooling to -85 °C.  
9

10  
11  
12  
13 The possible structure of **30** was interrogated by DFT methods. There was no evidence for  
14 Au···H-C(aryl) agostic bonding or for an  $\eta^2$ -arene  $\pi$ -complex. The optimized structure suggests  
15 rather long contacts with the metal, Au···C<sub>ortho</sub> 2.81 Å and Au···H-C<sub>aryl</sub> 2.61 Å. Calculations of the  
16  $^{13}\text{C}$  NMR chemical shifts confirmed the observed trends. According to Wiberg bond indices, the  
17 interaction of Au with the nearby *ortho*-C atom amounts to about 10% of a full covalent Au-C(aryl)  
18 bond.<sup>170</sup>  
19  
20  
21  
22  
23  
24

25 **Scheme 7. Gold(III) Arene Complexes and X-Ray Structure of the Cation of 26 (Pertinent  $^{13}\text{C}$  NMR**  
26 **Data in Red).**  
27  
28  
29  
30  
31  
32  
33  
34  
35  
36  
37  
38  
39  
40  
41  
42  
43  
44  
45  
46  
47  
48  
49  
50  
51  
52  
53  
54  
55  
56  
57  
58  
59  
60



### 2.2.5 Allyl Complexes. $\pi$ -Allyls are one of the most widespread ligand types in

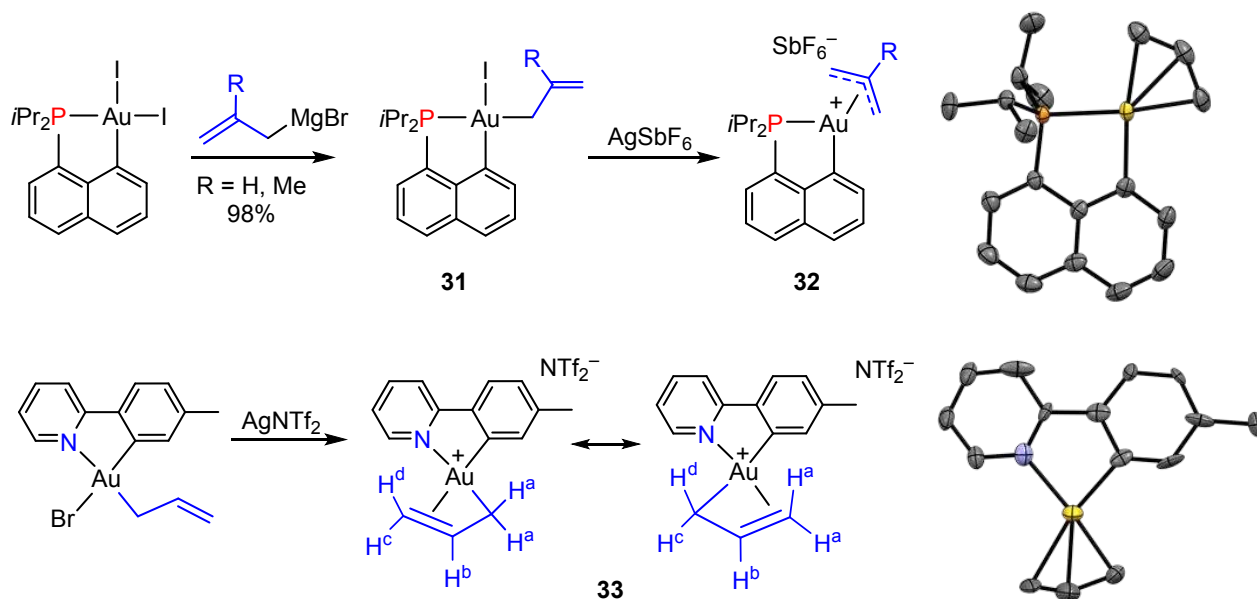
organometallic chemistry and catalysis. In stark contrast, well-characterized allyl complexes of gold(III) are rare. Gold(III)  $\eta^1$ -allyls have been known for some time, of the type  $\text{Me}_2\text{Au}(\text{allyl})(\text{PPh}_3)$ .<sup>172-174</sup>

Gold(III) complexes containing  $\pi$ -allyl ligands have only very recently been identified, in two simultaneous reports which demonstrate the remarkable sensitivity of the allyl bonding mode to the ligand environment (Scheme 8).<sup>175,176</sup> Taking advantage of the stabilization afforded by the  $\text{C}^{\text{P}}$  chelate framework, Bourissou *et al.* reacted  $(\text{C}^{\text{P}})\text{Au}_2$  with allyl Grignard reagents to give the  $\sigma$ -allyl products **31**, which on halide abstraction readily converted to the  $\eta^3$ -allyl complex **32** in quantitative yield. Both allyl and methallyl compounds are stable to air and storage at room temperature. The NMR data were consistent with an  $\eta^3$ -structure, and there was no temperature dependence in the range of  $-70$  to  $+110^\circ\text{C}$ . The crystal structures of **32H** and **32Me** confirmed the  $\pi$ -bonded nature, with metal-C(allyl) distances comparable to those found in palladium allyls. The

Au-C bond *trans* to P is shorter (2.195(12) Å for **32Me**) than the bond *trans* to C(naphthyl) (2.275(9) Å), as expected based on the strong *trans*-influence of the anionic C donor. The allylic C-C bond lengths, as well as computational analysis, confirmed the highly delocalized nature of the ligand. DFT studies showed also that alternative, coordinatively unsaturated  $\sigma$ -allyl structures are 20-30 kcal/mol less stable than the  $\pi$ -allyl state.<sup>175</sup>

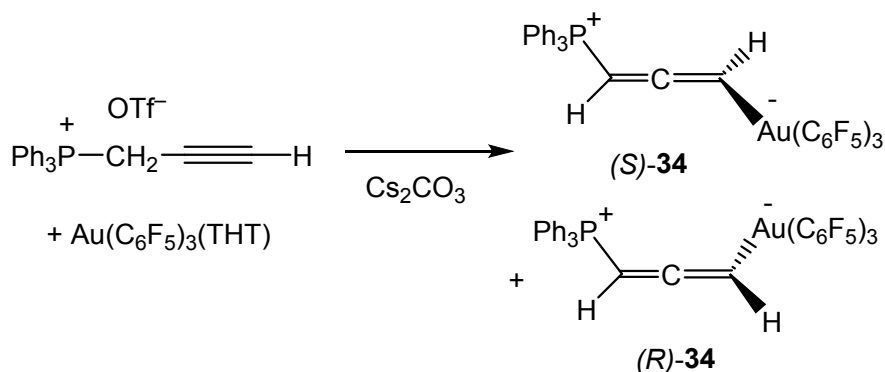
Tilset and co-workers used a similar halide-abstraction procedure to generate allyls stabilized by the 2-tolylpyridine C<sup>N</sup> chelate framework. The cation [(C<sup>N</sup>)Au(C<sub>3</sub>H<sub>5</sub>)]<sup>+</sup> (**33**) exists as two isomers in unequal proportions, with very asymmetrically bonded allyl ligands. The methylene-C retains its sp<sup>3</sup>-character, and there is exchange between the H<sup>a</sup> protons by decoordination of the  $\pi$ -bond *trans* to the tpy-C atom. The crystal structure of **33** shows two very unequal C-C bond lengths in the allyl ligand, 1.43(3) and 1.22(4) Å, so unlike the situation with allyls **32** in the softer C<sup>P</sup> system, here the  $\pi$ -system is not delocalized. The allyl in **33** is fluxional and there is an interchange between  $\eta^1$ - and  $\eta^3$ -structures.<sup>176</sup>

### Scheme 8. Gold(III) $\pi$ -Allyl Complexes



Also to be noted in this context is the synthesis by Gimeno and co-workers of the first examples of gold(III) allenyl complexes **34**, which were prepared from propargylic phosphonium salts by deprotonation with Cs<sub>2</sub>CO<sub>3</sub> in the presence of Au(C<sub>6</sub>F<sub>5</sub>)<sub>3</sub>(THT) as a racemic mixture (Scheme 9). The thermally stable compounds were characterized by X-ray diffraction. Enantiomer separation of these axially chiral complexes was not attempted.<sup>177</sup>

### Scheme 9. Formation of Axially Chiral Gold(III) Allenyl Complexes



### 2.3. Gold(III) Complexes with $\sigma$ -Ligands

While the chemistry of gold(III) hydrocarbyls is well established, the last decade has seen remarkable new insight into coordination modes of  $\sigma$ -ligands and the emergence of new compound classes, notably gold hydrides. Others, such as gold(I) and gold(III) hydroxides and fluorides, have proved their potential as synthetic reagents and catalyst precursors and are therefore included in the following sections.

**2.3.1 Gold(III) Hydrides.** Transition metal hydrides are an integral part of many catalytic cycles and involved in product release by  $\beta$ -H elimination or by M-C hydrogenolysis. Until quite recently, isolable or at least spectroscopically characterized gold hydride complexes were conspicuous by their absence in the chemical literature. The state of gold hydride chemistry up to July 2013, including  $\text{Au} \cdots \text{HE}$  hydrogen bonding and  $\text{Au} \cdots \text{H}$  polar interactions, has been covered in an in-depth review by Schmidbaur *et al.*,<sup>178</sup> and the structures and reactions of gold(I, III) hydrides were included in a 2015 Perspective article on gold chemistry.<sup>18</sup>

In pioneering work in 2000-2004, Andrews used the co-deposition of hydrogen with gold atoms in noble gas matrices at very low temperatures for the generation and spectroscopic identification of a number of gold(I) and gold(III) hydrides and  $\text{H}_2$  adducts.<sup>179-184</sup> These products were of course thermally extremely labile and may have given the impression that gold hydrides have only a fleeting existence. Phosphine-stabilized cationic  $[(\text{LAu}^{\text{I}})_2(\mu\text{-H})]^+$  species were identified in the gas phase.<sup>185</sup> In the course of studies on heterogenized gold(III) Schiff base complexes as hydrogenation catalysts by Corma *et al.*, computer models were developed that suggested the involvement of gold(III) hydrides of the type  $[(\text{O}^{\wedge}\text{N}^{\wedge}\text{N})\text{AuH}]^+$  and  $[(\text{O}^{\wedge}\text{N}^{\wedge}\text{N})\text{AuH}(\text{C}_2\text{H}_4)]^+$  as intermediates in alkene hydrogenation.<sup>186</sup> Gold(III) hydrides have on occasions been postulated as the products of  $\beta$ -H elimination from gold(III) alkyl intermediates, e.g.

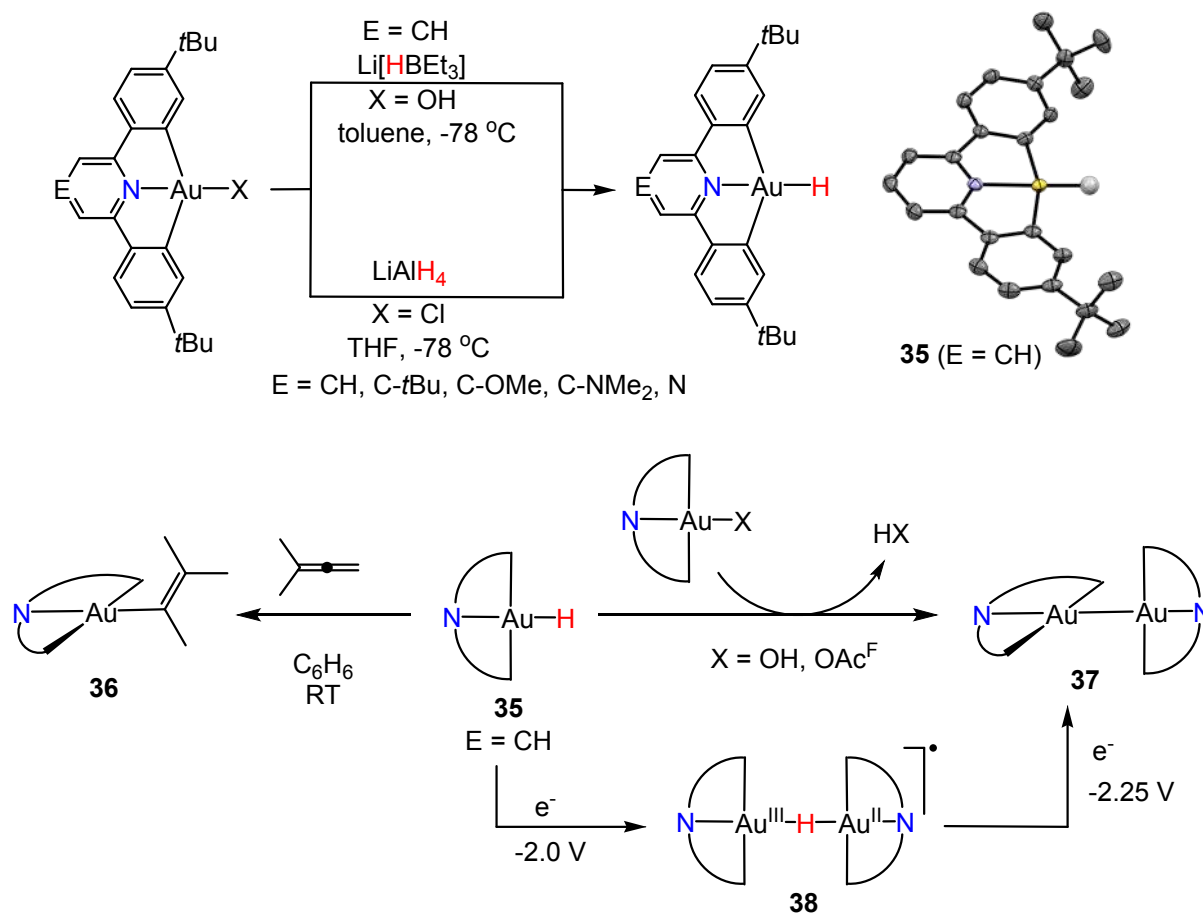
1  
2  
3 the elimination of “HAuCl<sub>2</sub>” to explain the formation of unsaturated organic products, although  
4 evidence for the formation of Au-H species, even fleetingly, was not strong.<sup>187,188</sup>

5  
6 This situation changed in 2008, when Sadighi and co-workers described the first stable,  
7 crystallographically characterized Au(I) hydride complexes of the type (IPr)AuH and  
8 [{(IPr)Au}<sub>2</sub>(μ-H)]<sup>+</sup> (IPr = 1,3-bis(2,6-diisopropylphenyl)imidazole-2-ylidene).<sup>189</sup> This was followed  
9 in 2012 by a report by Roşca *et al.* of the first isolable gold(III) hydride, (C<sup>^N^C</sup>)AuH (**35**).<sup>190,191</sup>  
10 The compound was originally made from (C<sup>^N^C</sup>)AuOH and LiHBET<sub>3</sub>; later it was shown that this  
11 as well as related hydrides are more easily accessible from (C<sup>^N^C</sup>)AuCl and LiAlH<sub>4</sub> (Scheme  
12 10).<sup>192</sup> Whereas the Au-H <sup>1</sup>H NMR signal of (IPr)AuH was observed at δ +5.11 (in C<sub>6</sub>D<sub>6</sub>; δ 3.38 in  
13 CD<sub>2</sub>Cl<sub>2</sub>), the signal for **37** (E = CH) was found at δ -6.51 in CD<sub>2</sub>Cl<sub>2</sub> and -5.73 in C<sub>6</sub>D<sub>6</sub>. The  
14 deuteride **35D** gave a <sup>2</sup>H NMR resonance at -6.58 (CH<sub>2</sub>Cl<sub>2</sub>). The IR spectrum shows a strong, sharp  
15 Au-H stretch at 2188 cm<sup>-1</sup>. The hydride is stable to air and moisture at room temperature, although  
16 solutions are light sensitive; for example, prolonged exposure of dichloromethane solutions to  
17 sunlight led to the formation of (C<sup>^N^C</sup>)AuCl. Whereas (IPr)AuH inserts dimethylacetylene  
18 dicarboxylate (DMAD)<sup>189</sup> and reacts with O<sub>2</sub> to give the gold(I) hydroperoxide,<sup>193</sup> no such Au-H  
19 insertion reactions were observed for **35**. However, the complex was found to readily hydroaurate  
20 allenes to give **36**, and to undergo condensation reactions with (C<sup>^N^C</sup>)AuX (X = OH or OAc<sup>F</sup>) to  
21 generate the gold(II) complex **37**. The latter is a rare example of a gold(II) complex with an  
22 unsupported Au<sup>II</sup>-Au<sup>II</sup> bond (**37**·CH<sub>2</sub>Cl<sub>2</sub>: 2.4941(4) Å;<sup>190</sup> **37**·C<sub>6</sub>H<sub>6</sub>: 2.5169(4) Å<sup>194</sup>). Like **35**,  
23 compound **37** is thermally stable; however, on exposure to light it disproportionates into Au(I) and  
24 Au(III) with Au-C bond cleavage.<sup>194</sup>

25  
26  
27  
28  
29  
30  
31  
32  
33  
34  
35  
36  
37  
38  
39  
40  
41  
42  
43  
44  
45  
46  
47  
48  
49  
50  
51  
52  
53  
54  
55  
56  
57  
58  
59  
60  
Hydride **35** is electrochemically reduced to give (C<sup>^N^C</sup>)Au<sup>II</sup> radicals. The process involves  
one-electron steps. A reduction wave at -2.25 V was assigned to the reduction of an H-bridged  
mixed-valence intermediate [(C<sup>^N^C</sup>)Au<sup>II</sup>-H-Au<sup>III</sup>(C<sup>^N^C</sup>)] **38**, formed from the reaction of **35**  
with a (C<sup>^N^C</sup>)Au<sup>II</sup> radical (Scheme 10). DFT calculations showed that the formation of this  
bridged species was exothermic by 11.7 kcal/mol. Further electron transfer led to dimerization of  
the Au<sup>II</sup> radicals to give **37**, with an estimated Au<sup>II</sup>-Au<sup>II</sup> bond enthalpy of 47.3 kcal/mol.<sup>195</sup>

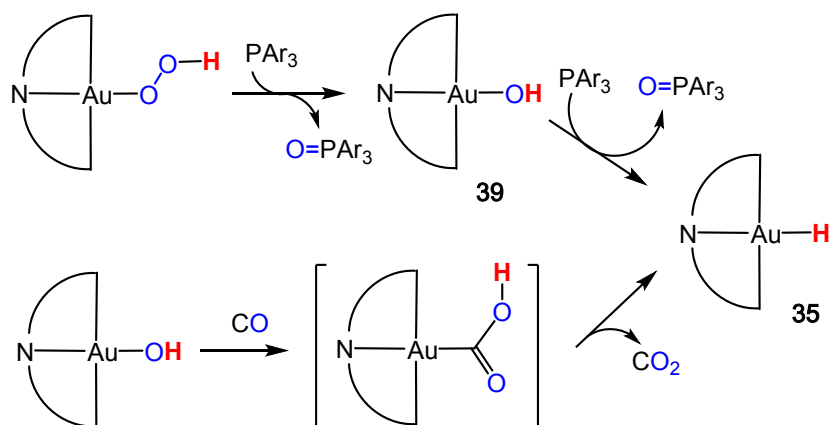
### Scheme 10 Synthesis and Reactions of (C<sup>^N^C</sup>) Gold(III) Hydride Complexes





Since the preparation of the stable hydride **35**, it has also been possible to detect the formation of this complex in other processes (Scheme 11). For example, Roşca *et al.* discovered that phosphines abstract O atoms from the gold(III) hydroperoxide ( $\text{C}^{\wedge}\text{N}^{\wedge}\text{C}$ )Au-OOH, leading stepwise first to ( $\text{C}^{\wedge}\text{N}^{\wedge}\text{C}$ )AuOH **39**, and then to the hydride **35**.<sup>196</sup> The driving force is the difference in bond energies, Au-H > Au-O. Applying the same reaction principle, Chambrier *et al.* were able deoxygenate ( $\text{C}^{\wedge}\text{N}^{\wedge}\text{C}$ )Au-OMe with tris(*p*-tolyl)phosphine to give ( $\text{C}^{\wedge}\text{N}^{\wedge}\text{C}$ )Au-Me, possibly via single-electron pathways with transfer of MeO radicals.<sup>197</sup> Similarly, Roşca *et al.* showed that the thermally unstable intermediate ( $\text{C}^{\wedge}\text{N}^{\wedge}\text{C}$ )Au-COOH eliminates CO<sub>2</sub> with formation of hydride **35**.<sup>138</sup>

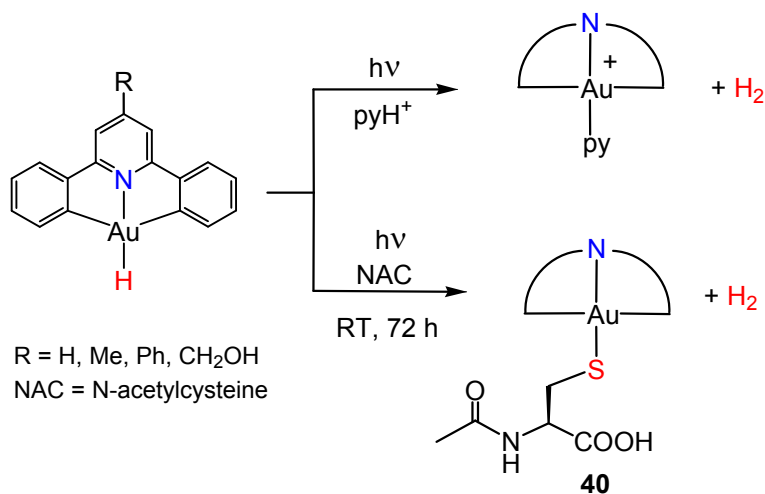
### Scheme 11. Formation of Gold(III) Hydride by Deoxygenation and $\beta$ -H Elimination



Fernandez-Cestau *et al.* reported that the pyrazine-derived hydride complex  $(\text{C}^{\wedge}\text{N}^{\text{pz}}\wedge\text{C})\text{AuH}$  (**35**,  $\text{E} = \text{N}$ ) shows photoemissions at 512 – 520 nm as a solid and in solution, and in a polymethyl methacrylate matrix gives a quantum yield of 10.3%. It could be shown that the emission energies of a series of pincer complexes  $(\text{C}^{\wedge}\text{N}^{\text{pz}}\wedge\text{C})\text{AuR}$  ( $\text{R} = \text{alkyl}, \text{H}$ ) depend linearly on the  $\text{p}K_{\text{a}}$  values of  $\text{H-R}$ .<sup>198</sup>

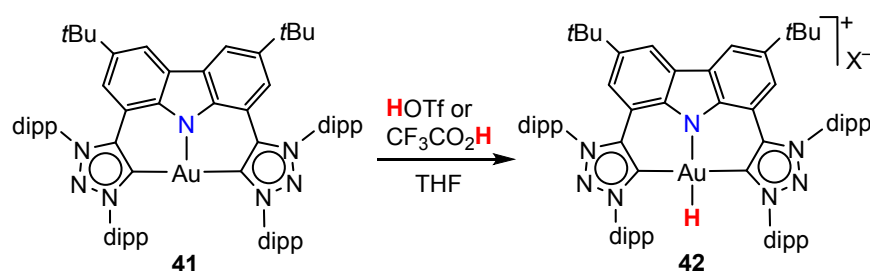
Luo *et al.* have recently employed the light sensitivity of pincer gold hydrides similar to **35**, but lacking in the *tert*-butyl substituents ( $\text{R} = \text{H}, \text{CH}_2\text{OH}, \text{Me}$  or  $\text{Ph}$ ), to generate light-activated anti-cancer agents. Whereas the hydrides themselves are not cytotoxic, irradiation ( $\lambda = 365 \text{ nm}$ ) leads to substitution of the hydride ligand, for example by pyridinium cations or by thiols. (Scheme 12). Upon reaction with *N*-acetylcystein (NAC) the thiolate **40** is formed, which showed good activity in TrxR (thioredoxin reductase) inhibition and induced apoptosis in a number of cancer cell lines.<sup>199</sup>

### Scheme 12. Photolytic $\text{H}_2$ generation from $(\text{C}^{\wedge}\text{N}^{\wedge}\text{C})\text{AuH}$ complexes



In recent years a number of alternative synthetic routes to gold(III) hydrides based on different structural motifs have been reported. Bezuidenhout and co-workers described the protonation of the T-shaped gold(I) complex **41** to give the air- and temperature stable cationic hydride **42** (Scheme 13). The complex was isolated in 35% yield. The hydride NMR signal appears at  $\delta -8.34$  ppm, low-frequency shifted with respect to the reported value for neutral **35**. The  $\nu(\text{Au-H})$  stretching mode was detected at  $2197\text{ cm}^{-1}$ , closely similar to the value for **35**. The complex is insensitive to acids but could be deprotonated slowly by NaH in THF over a period of days to regenerate **41**.<sup>200</sup>

### Scheme 13. Formation of a Gold(III) Hydride by Protonation of Au(I)

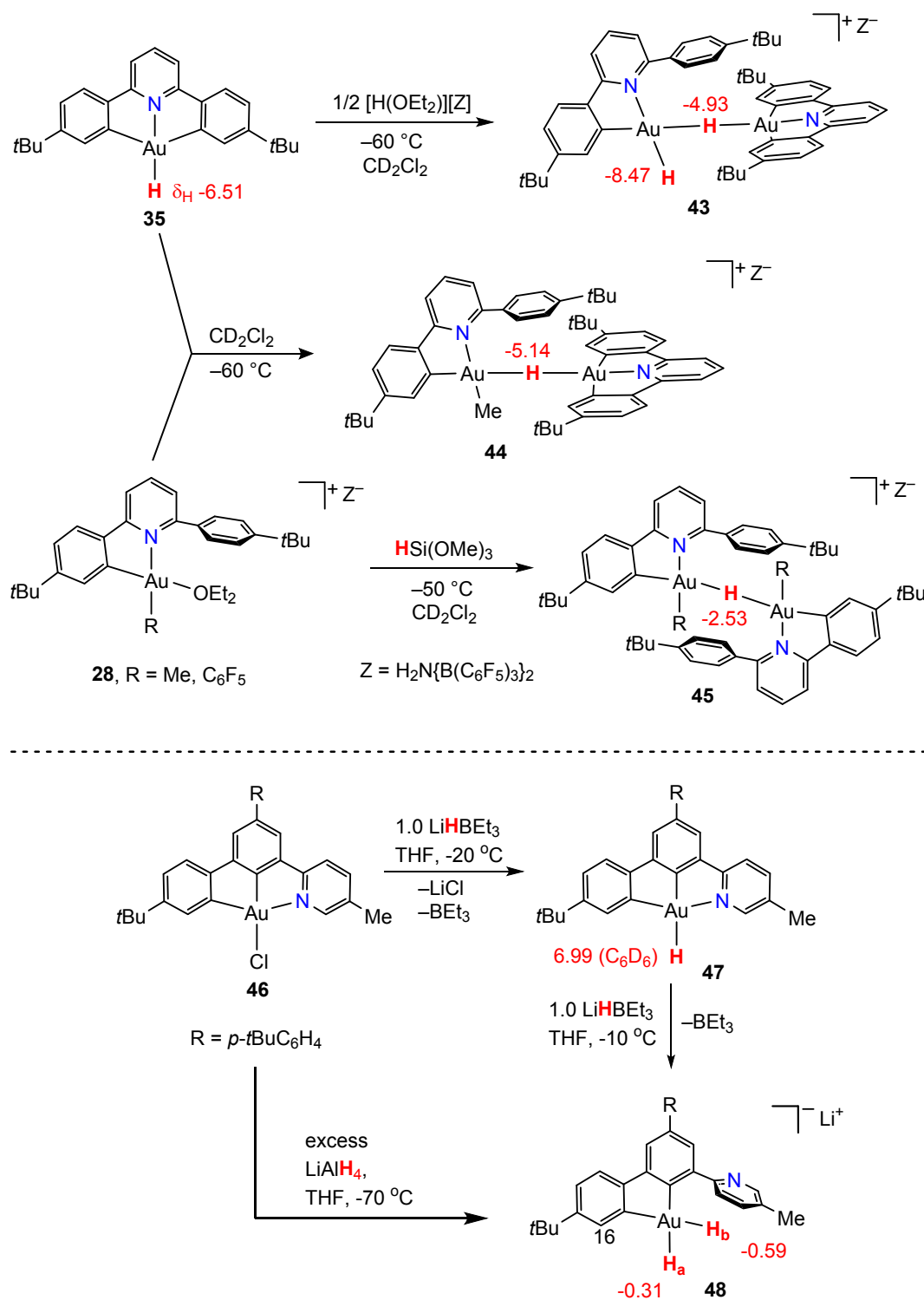


The structural variety of gold(III) hydrides was significantly increased in 2018 by Rocchigiani *et al.*, who reported the synthesis and characterization of a number of  $\text{C}^{\wedge}\text{N}$ ,  $\text{C}^{\wedge}\text{C}^{\wedge}\text{N}$  and  $\text{C}^{\wedge}\text{C}$ -ligated complexes with terminal and bridging hydride ligands.<sup>201</sup> These investigations extended the range of gold(III)-H  $^1\text{H}$  NMR chemical shifts from  $\delta -8.47$  to  $+6.99$  ppm. Protolytic cleavage of one of the pincer Au-C bonds in **35** leads to the generation of  $\text{C}^{\wedge}\text{N}$  bonded hydrides of types **43** - **45** (Scheme 14;  $^1\text{H}$  NMR resonances in red). These species are very temperature-sensitive and could only be identified in solution at or below  $-50\text{ }^{\circ}\text{C}$ . Complexes with H *trans* to N(py) show strongly negative  $^1\text{H}$  chemical shifts. By contrast the  $\text{C}^{\wedge}\text{C}^{\wedge}\text{N}$  bonded hydride **47**, a coordination isomer of **35** where the N and C positions are switched, shows a high-frequency  $^1\text{H}$  NMR shift of  $\delta +6.99$  ppm. This complex was generated from the corresponding chloride **46** by treatment with 1.0 equiv  $\text{LiHBEt}_3$ .  $(\text{C}^{\wedge}\text{C}^{\wedge}\text{N})\text{AuH}$  **47** is thermally labile and was identified in solution below  $-20\text{ }^{\circ}\text{C}$ . The low thermal stability is in striking contrast to  $(\text{C}^{\wedge}\text{N}^{\wedge}\text{C})\text{AuH}$  **35** and is evidently the result of the *trans*-influence exerted by the anionic aryl-C ligand. Hydride **47** had earlier been proposed as an intermediate in the  $\beta$ -H elimination of  $(\text{C}^{\wedge}\text{C}^{\wedge}\text{N})\text{Au}$  formate at  $100\text{ }^{\circ}\text{C}$ , which in the presence of  $\text{E-C}\equiv\text{C-E}$  gives  $\text{CO}_2$  and the *trans*-vinyl complex  $(\text{C}^{\wedge}\text{C}^{\wedge}\text{N})\text{Au-C(E)=CHE}$  ( $\text{E} = \text{COOtBu}$ ).<sup>202</sup>

When **46** is treated with 2 equiv of  $\text{LiHBEt}_3$ , the pyridyl arm of the  $\text{C}^{\wedge}\text{C}^{\wedge}\text{N}$  pincer is displaced, to give the anionic dihydride **48** (Scheme 14). The same product is also formed

quantitatively using an excess of  $\text{LiAlH}_4$ , with no sign of reduction.<sup>201</sup> In contrast to **47**, both the hydride signals of **48** are shielded and located at  $\delta$  -0.59 ( $\text{H}^a$ ) and -0.31 ppm ( $\text{H}^b$ ). In THF solution complex **48** is stable at room temperature for several days.

**Scheme 14. Gold(III) Hydrides with C<sup>^</sup>N and C<sup>^</sup>C<sup>^</sup>N Ligands (Hydride <sup>1</sup>H NMR Data in Red)**

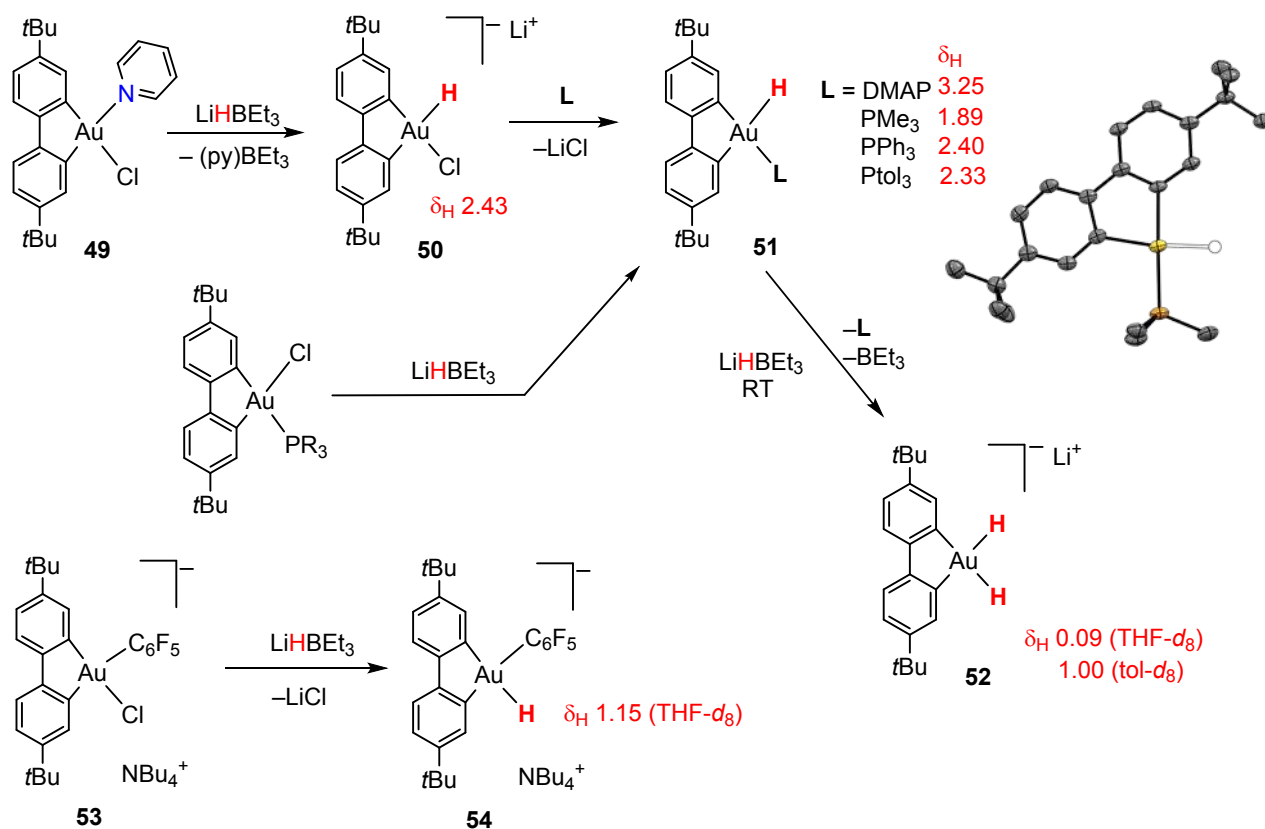


Rocchigiani *et al.* also developed another family of mostly thermally stable gold(III) hydrides based on the C<sup>^</sup>C chelate framework (Scheme 15). Starting with (C<sup>^</sup>C)AuCl(py) **49**,

displacement of the py ligand by  $\text{LiHBEt}_3$  gives the hydrido chloride intermediate **50**, which reacts further with  $\text{L} = N,N$ -dimethylaminopyridine (DMAP) or with phosphines  $\text{PR}_3$  ( $\text{R} = \text{Me}, \text{Ph}, p$ -tolyl) to give the stable adducts  $(\text{C}^{\wedge}\text{C})\text{AuH}(\text{L})$  **51**. These  $\text{PR}_3$  complexes represent the first examples of isolable (phosphine)gold hydrides. The  $\text{PMe}_3$  complex was crystallographically characterized. Adding further  $\text{LiHBEt}_3$  to the  $\text{PPh}_3$  complex led to substitution of the phosphine and formation of the dihydrido anion  $[(\text{C}^{\wedge}\text{C})\text{AuH}_2]^-$  **52**. This dihydride proved stable in THF solution at room temperature; however, attempts to remove the solvent led to reduction. Although for the neutral complex  $\text{AuH}(\text{Ph})\text{Cl}(\text{PPh}_3)$  a low barrier for reductive Ph-H elimination of 7.5 kcal/mol has been calculated,<sup>203</sup> the dihydrido aryls **48** and **52** are stabilized by the inability of the bis-aryl chelate to rotate into the conformation required for  $\text{C}\cdots\text{H}$  interaction.

A further example of a gold(III) aryl hydride resistant to reductive arene elimination was prepared from  $[\text{NBu}_4][(\text{C}^{\wedge}\text{C})\text{Au}(\text{Cl})\text{C}_6\text{F}_5]$  **53** and 1.2 equiv  $\text{LiHBEt}_3$  at room temperature, to give the hydrido-aryl complex **54**. While the formation of this complex was slow in THF, it was found to be instantaneous in toluene.

### Scheme 15. Formation of $\text{C}^{\wedge}\text{C}$ -Ligated Gold(III) Hydrides (Hydride $^1\text{H}$ NMR Data in Red) and X-ray Structure of **51PMe<sub>3</sub>**



1  
2  
3           Complexes **50** - **52** and **54** show hydride NMR shifts in the region of 0 – 3 ppm. Overall the  
4 scale of gold(III) hydride  $^1\text{H}$  NMR chemical shifts covers the range from about -9 to +7 ppm, from  
5 highly shielded to highly deshielded. There are systematic shifts relating to (a) the ligand *trans*-  
6 influence, and (b) bidentate *vs.* tridentate ligand structure (Figure 2). Relativistic DFT calculations  
7 at the two-component ZORA-SO level, including spin-orbit coupling, demonstrate a remarkably  
8 strong *trans* influence: weak ligands in the spectrochemical series placed in *trans* position lead to a  
9 large negative spin-orbit contribution to the chemical shift, while strong donor ligands have the  
10 opposite effect, on a scale from +5 to -15 ppm. The same ligands in *cis* position have a smaller (~6  
11 ppm scale) but opposite effect. The origin of this wide chemical shift variability lies in the ligand-  
12 dependent ordering and energy gap of gold-centered frontier orbitals, which are Au( $d_\pi$ )-based  
13 “shielding” for weak ligands, and  $\sigma(\text{Au-H})$ -type “deshielding” for strong donors.  
14  
15  
16  
17  
18  
19  
20  
21

22           The nature of frontier orbitals resulting from the ligand *trans*-influence has further  
23 consequences. The  $^1\text{H}$  NMR hydride shifts correlate linearly with the Au-H bond hydricity, as well  
24 as with the DFT-optimized Au-H distances (Figure 2).<sup>201</sup> Consequently, this correlation makes it  
25 possible to estimate Au-H distances from the hydride NMR chemical shifts.  
26  
27  
28

29           It is noted that both Au(III) and Au(I) hydrides fit on the same correlation curve, which  
30 suggest that the *trans*-influence in gold hydrides dominates over oxidation state and d-electron  
31 count.  
32  
33  
34  
35  
36  
37  
38  
39  
40  
41  
42  
43  
44  
45  
46  
47  
48  
49  
50  
51  
52  
53  
54  
55  
56  
57  
58  
59  
60

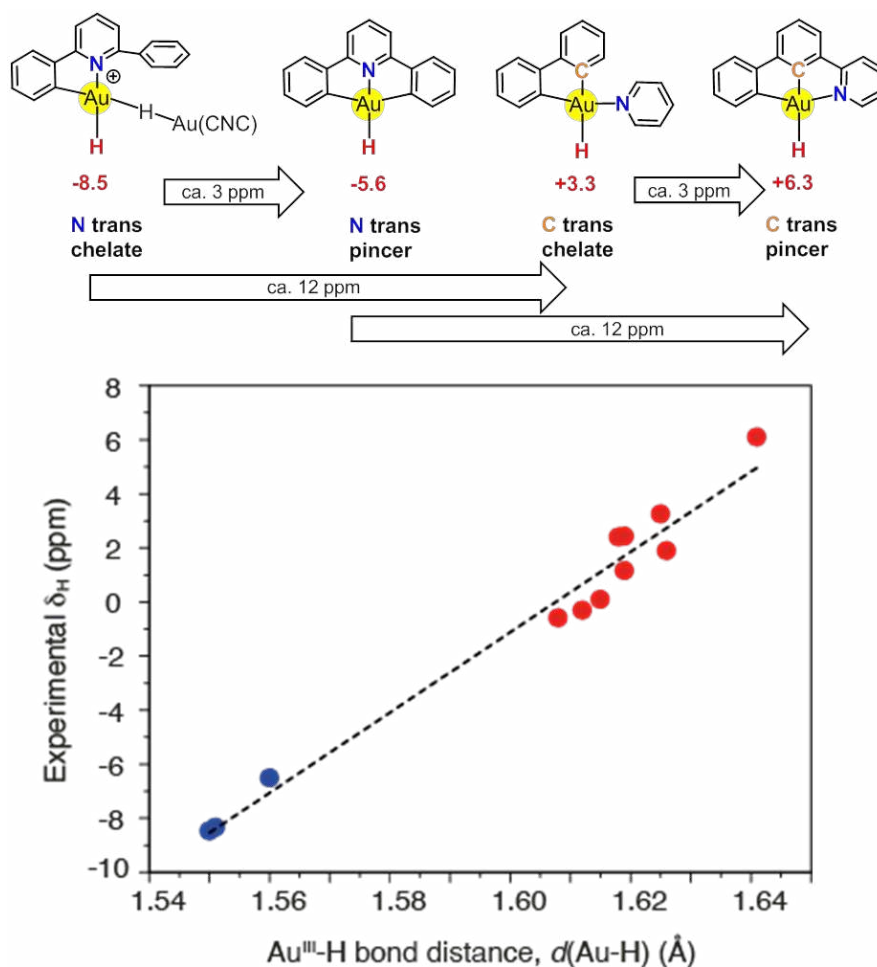


**Figure 2.** Systematic changes in Au-H <sup>1</sup>H NMR chemical shifts (red numbers) as a function of ligand structure (top) and correlation between chemical shift and calculated Au-H bond length (bottom). Red points: Gold hydrides **47** – **52** capable of undergoing single-electron transfer and reaction with O<sub>2</sub>; blue points: O<sub>2</sub>-stable gold hydrides of type **35**.

Since the observed chemical shifts also imply changes in the electronic characteristics of these complexes, they reflect chemical behavior. Complexes based on C<sup>^</sup>N<sup>^</sup>C pincer ligands, with short and less polar Au-H bonds, do not react with O<sub>2</sub> or DMAD (Figure 2, blue data points), whereas gold(III) hydrides with longer and more polar Au-H bonds (red data points) react with oxygen and also DMAD to give the *trans*-vinyl insertion product. As will be discussed in Section 3.4, the former undergo hydroauration with a wide range of alkynes, while the latter do not. There are therefore two distinct types of gold(III) hydrides, with rather different chemical behavior.

In spite of these reactivity differences, it is notable that the Au-H bonds in all these gold hydrides are highly covalent and, to the extent that this has been tested, do not undergo hydrogenations or hydroauration reactions by the classical coordination – migratory insertion mechanism. They are evidently very much less reactive than Au-H species generated on the surface

of gold nanoparticle hydrogenation catalysts. As Corma and co-workers have pointed out, the reactivity of heterogeneous gold catalysts based on nano-sized to sub-nanometre gold particles for various types of catalysis is highly sensitive to cluster size.<sup>204</sup> Gold-based homogeneous hydrogenation or hydrochlorination catalysts<sup>205,206</sup> based on identifiable hydride species have yet to be developed.

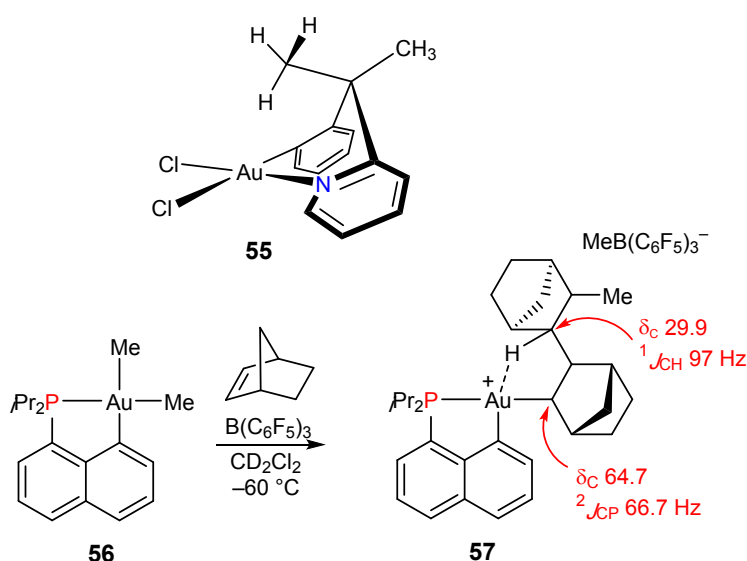
**2.3.2 Agostic Interactions and Gold(III)  $\sigma$ -Complexes.** Reactions such as C-H activation,  $\beta$ -H elimination and  $\sigma$ -bond metathesis are frequently part of catalytic cycles and involve the interaction of H-C or H-E bonds with metal centers (E = main group element). Many transition metals have been found to form identifiable intra- and inter-molecular  $\sigma$ -complexes. Intramolecular “agostic” M $\cdots$ H-E bonding involves 2-electron-3-center interactions in which the C-H bond is weakened, leading to a reduction in the  $J_{\text{CH}}$  coupling constant and M $\cdots$ H-E angles of 120° or less. The problematic nature of agostic bonding in the context of electron-rich metals such as gold has been discussed in detail in Schmidbaur’s recent review,<sup>178</sup> which concluded that in spite of several cases of close intra- or intermolecular H $\cdots$ Au contacts there was no unequivocal evidence for X-H $\cdots$ Au hydrogen bonding. For gold(I) complexes such as (IPr)AuEt,  $\beta$ -agostic interactions that may precede  $\beta$ -H elimination are ruled out on the basis of the very high (57 kcal/mol) activation barrier.<sup>207</sup> Regarding gold(III), it is telling that the first organometallic gold(III) compound was an ethyl complex, [Et<sub>2</sub>AuBr]<sub>2</sub>, which shows no tendency towards  $\beta$ -H elimination.<sup>208,209</sup> Recently Faza and co-workers have explored the barriers to  $\beta$ -H elimination computationally using the unified reaction valley (URV) approach. The authors found that the pre-chemical conformational changes required in EtAuCl<sub>2</sub> prior to C-H activation contributed about 78% to the overall activation barrier of ca. 34 kcal/mol. The final step of abstracting the  $\beta$ -H atom once the appropriate conformation had been achieved was comparatively small, 7.6 kcal/mol. The same process for the d<sup>10</sup> system EtAuCl is dominated by repulsive interactions. The barriers were however subject to significant changes due to ligand and substituent effects,<sup>210</sup> and recently both agostic interactions and  $\sigma$ -complexes of gold(III) have been unequivocally identified.

Studies on cyclometalated benzyl pyridine complexes (C<sup>^</sup>N)AuCl<sub>2</sub> **55**, with and without Me substituents in the bridge, concluded on the basis of quantum chemical calculations that in spite of short Au $\cdots$ HC contacts the ground state structures could be explained on the basis of simple conformation rules and that there was no evidence for Au(III) $\cdots$ H-C attractive interactions *perpendicular* to the coordination plane.<sup>211</sup> The story is different though for interactions with one of the coordination sites *within* the plane of square-planar Au(III). Bourissou and co-workers reacted (C<sup>^</sup>P)AuMe<sub>2</sub> **56** with B(C<sub>6</sub>F<sub>5</sub>)<sub>3</sub> in the presence of norbornene at -80 °C to trap the norbornene bis-insertion product **57** (Scheme 16). NMR spectroscopic analysis was consistent with a  $\gamma$ -agostic



interaction; in particular the  $^1J_{\text{CH}}$  coupling constant of the  $\gamma$  CH moiety decreased from the usual 135 Hz to 97 Hz, whereas the pyridine adduct shows a normal  $J_{\text{CH}}$  value of 130 Hz for this carbon atom. The large  $J_{\text{CP}}$  constant (66.7 Hz) of the Au-bound alkyl C-atom confirms that the norbornyl ligand is *trans* to P. The assignments were further confirmed by calculated NMR parameters and an optimized structure. Natural bond orbital (NBO) and quantum theory of atoms in molecules (QTAIM) analyses confirmed the  $\text{CH}\cdots\text{Au}$  interaction with a stabilizing energy  $\Delta E = 18.6$  kcal/mol.<sup>212</sup>

**Scheme 16. Gold(III) Systems With and Without Agostic Interactions (Pertinent NMR Data in Red).**

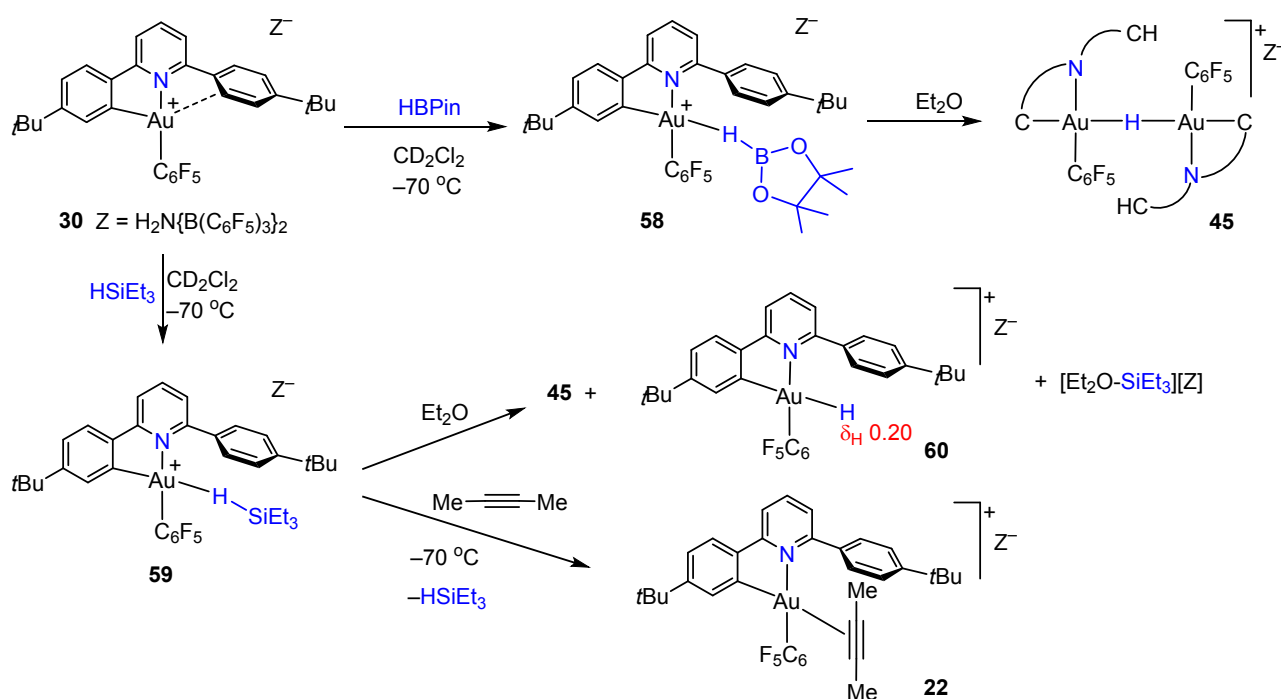


In 2019 Rocchigiani *et al.* provided the first examples of spectroscopically observable *intermolecular* gold(III)  $\sigma$ -complexes of main group hydrides by displacing the weakly bonded  $\pi$ -arene ligand in **30** with H-B and H-Si bonds to give **58** and **59**, respectively (Scheme 17).<sup>213</sup> On binding to Au(III) the H-Si  $^1\text{H}$  NMR signal shifts by 2.19 ppm with respect to free silane, to  $\delta$  1.27 ppm. Coordination of  $\text{HSiEt}_3$  is readily reversible; resonances are broad even at  $-70$  °C, and the  $^1\text{H}$  NOESY NMR spectrum confirmed chemical exchange between free and coordinated silane. The silane  $\sigma$ -complex is weak enough to be displaced by 2-butyne to give **22**, even at  $-70$  °C; hydrosilylation of the alkyne was not observed. While it was not possible on the basis of the NMR data to differentiate between side-on and end-on H-Si structures, DFT calculations indicated that end-on Au-H-Si bonding is preferred; this may not least be a reflection of the congested coordination pocket in this “Pacman”-like complex. The binding energies relative to **30** are  $-0.72$  and  $-5.28$  kcal/mol (at 253K) for the borane and the silane, respectively. The Wiberg Bond Index (WBI) changes from 0.9 (free  $\text{HSiMe}_3$  model) to 0.22 and 0.56 for the Au-H and H-Si bonds,

respectively, in the complex. The formation of silane complexes of gold(III) is in contrast with Au(I); as Joost *et al.* have pointed out, whereas copper(I) forms intramolecular  $\sigma$ -Si-H adducts, gold(I) does not.<sup>214</sup>

In the presence of diethyl ether, the borane and silane complexes give gold hydrides by heterolytic H-B and H-Si bond cleavage, to give **45**.<sup>213</sup> In the case of silane the mononuclear hydride **60** was observed, together with the  $[\text{Et}_2\text{O-SiEt}_3]^+$  cation (Scheme 17). Calculations showed that ether is essential for lowering the transition state energy. While formation of the mononuclear gold hydride is only mildly exothermic, capturing this as a binuclear  $[(\text{LAu})_2\text{H}]^+$  cation makes the process energetically substantially more favorable.

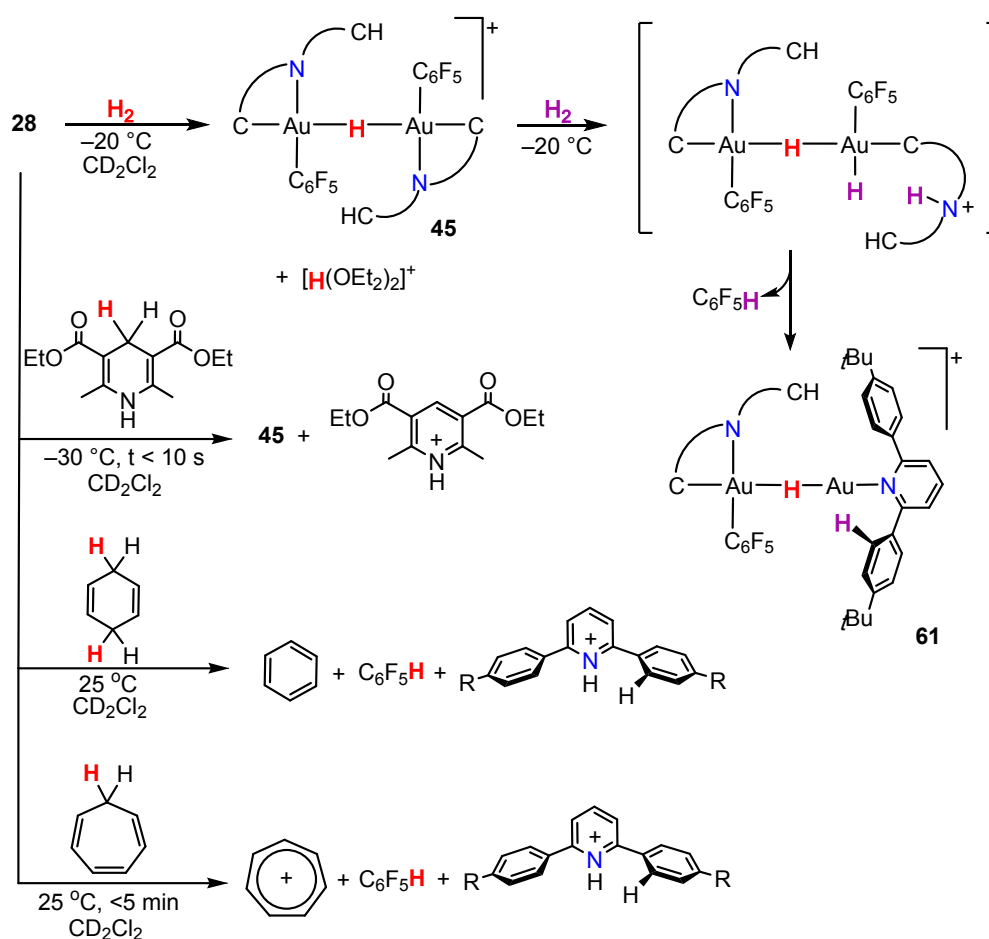
### Scheme 17. Formation and Reactions of Gold(III) Borane and Silane $\sigma$ -Complexes



The same heterolytic bond cleavage was observed in the reaction with  $\text{H}_2$  (Scheme 18). Dihydrogen binding to **30** is endergonic,  $+6.2$  kcal/mol by DFT, and the  $\text{H}_2$  complex cannot be observed. In agreement with this, no reaction occurred between  $\text{H}_2$  (1 bar,  $-10^\circ\text{C}$ ) and ether-free **30**. However, with the ether adduct **28** H-H cleavage takes place within a few hours at  $-20^\circ\text{C}$ , via an  $[\text{LAu}\cdots\text{H-H}\cdots\text{OR}_2]$  transition state of  $10.5$  kcal/mol, commensurate with the observed relatively slow  $\text{H}_2$  cleavage. This leads to the formation of  $[(\text{LAu})_2\text{H}]^+$  and  $[\text{H}(\text{OR}_2)_2]^+$  in a strongly exergonic process. In fact,  $\text{H}_2$  activation proved to be a two-stage process: the first sequence is followed by a slower, second step in which de-coordinated pyridine of the C^N ligand acts as base and reductive elimination of  $\text{C}_6\text{F}_5\text{H}$  leads to the Au(I,III) species **61**.

Similar heterolytic H-transfer processes also operate in the activation of C-H bonds. The Hantzsch ester reacts almost instantaneously under hydrogen transfer from C to Au, much faster than  $\text{H}_2$ , and does not require external  $\text{Et}_2\text{O}$  as base. 1,4-Cyclohexadiene and cycloheptatriene react more slowly at room temperature to give the corresponding dehydrogenated hydrocarbons. Since the resulting gold hydrides are not stable at  $25^\circ\text{C}$ , the reaction is accompanied by the reductive elimination products typical of Au(III)-H intermediates (Scheme 18).<sup>213</sup>

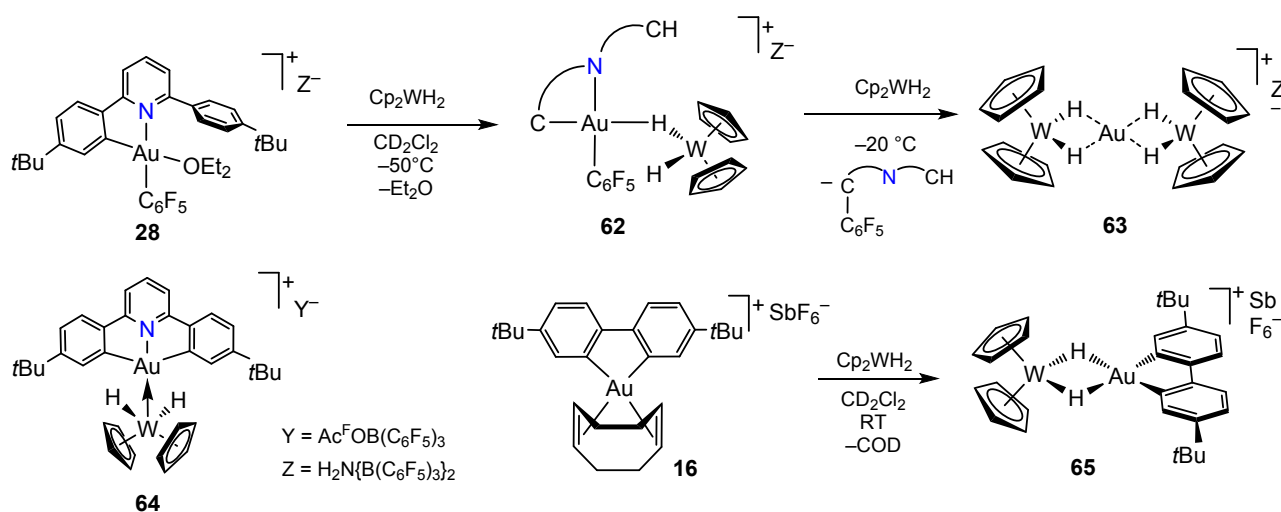
### Scheme 18. Gold(III) Mediated Heterolytic H-H and H-C Bond Activation



Gold(III)  $\sigma$ -complexes are also formed in the reaction of Lewis-acidic Au(III) compounds with transition metal hydrides. As Rocchigiani *et al.* showed, the reaction of **28** with  $\text{Cp}_2\text{ZrH}_2$  proceeds with immediate H-transfer, without any detectable intermediates, whereas  $\text{Cp}_2\text{WH}_2$ , on the other hand, gives identifiable adducts, although the W-H bond dissociation enthalpy is slightly lower than that of Zr-H ( $\text{Cp}^*_2\text{ZrH}_2$  81 kcal/mol;  $\text{Cp}_2\text{WH}_2$  74 kcal/mol).<sup>215</sup> Displacement of  $\text{OEt}_2$  in **28** at  $-50^\circ\text{C}$  generates the  $\sigma$ -adduct **62**, in which only one of the two hydrides is bonded to gold. The compound is thermally unstable and on warming to  $-20^\circ\text{C}$  gives the Au(I) adduct  $[\text{Au}(\text{H}_2\text{WCp}_2)_2]^+$  **63** (Scheme 19). Other interactions of gold(III) with  $\text{Cp}_2\text{WH}_2$  include an example

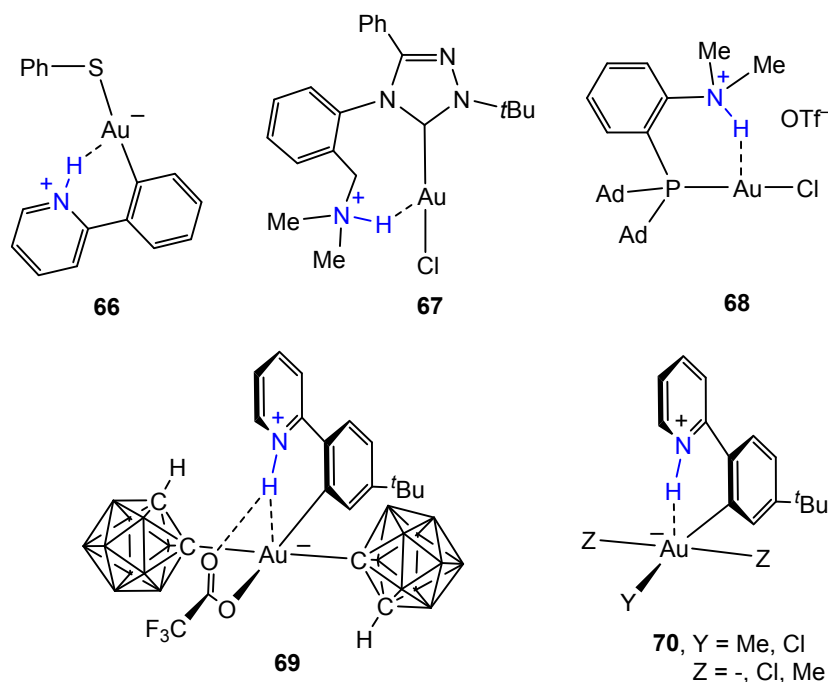
of a pure donor-acceptor interaction of the lone pair of W, without an Au...H bonding contribution, to give thermally labile **64**, as well as the thermally stable adduct **65** based on 2e-3c W-H-Au bonding. Compound **65** was conveniently prepared from the [(C<sup>∧</sup>C)Au(COD)]<sup>+</sup> complex **16** by alkene displacement with Cp<sub>2</sub>WH<sub>2</sub> and crystallographically characterized. Relativistic DFT calculations showed the presence of electron density along the Au-W vector of **64** and its absence in the case of **65**. The calculations also showed that in all these gold hydride complexes the W-H bond is polarized but remains present and strong, while true covalent Au-H bonds are not yet formed.<sup>216</sup>

### Scheme 19. Gold(III) Complexes of Cp<sub>2</sub>WH<sub>2</sub>



In addition to these  $\sigma$ -bonded species formed en-route to H-E bond activation, the question whether gold compounds are able to form hydrogen bonds of the type D-H<sup>(+)</sup>...M has attracted significant attention recently.<sup>217-222</sup> In such arrangements D is an electron-rich donor atom covalently bonded to H, and M possesses an electron pair capable of acting as proton acceptor, to give a 4-electron-3-center interaction. Many transition metals have been shown to be able to form such hydrogen bonds.<sup>223</sup> The ability of gold to participate in such interactions has been critically assessed,<sup>178,211</sup> but recent contributions have shown that for gold(I) compounds, for example **66** - **68** (Scheme 20), such interactions do exist.<sup>217-222</sup>

### Scheme 20. Compounds with Close Au...HN Interactions



The question whether gold(III) could entertain similar H-bonding interactions was probed following the isolation of complex **69**. DFT analysis of this and related gold(I) and gold(III) structures **70** established that while Au(I) analogues (without the carboranyl ligands) show a modest Wiberg bond index of  $\sim 0.15$ , corresponding to about 1/5 of a single Au-H bond, in **69** the WBI is reduced to  $\sim 0.02$ . This is significantly less than the WBI for the Au-H bond in the silane complex **59** (0.22).<sup>213</sup> Hydrogen bonding to Au(III) is therefore considerably weaker than to Au(I) and is not a structure-determining factor.<sup>136</sup>

**2.3.3. Gold(III) Hydroxides and Fluorides.** For the development of catalysts, as well as of synthetic methodology, the choice of the anion as leaving group is often critical. “Non-coordinating” anions<sup>224</sup> have long been used for the creation of highly reactive complexes and the active species in catalysis,<sup>59,60,225-227</sup> and their role in gold catalysis has been evaluated.<sup>59,60,228,229</sup> As described in Sections 2.2.1 – 2.3.2, the use of extremely weakly coordinating anions based on perfluorophenylborates was instrumental for the synthesis of a number of gold(III) complexes with highly labile ligands, such as alkenes, alkynes and arenes.

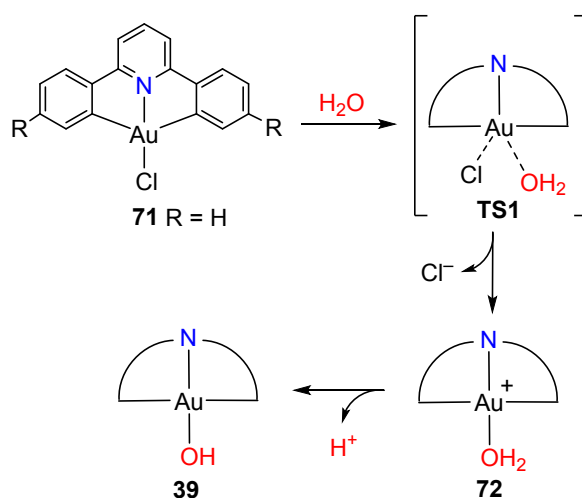
In addition, significant advances have been reported in the synthesis of neutral gold hydroxo, alkoxo and fluoro complexes, which exploit the lability of Au-O and Au-F bonds, notably for use in coupling reactions. Roesky *et al.* reviewed the chemistry of transition metal hydroxides in 2006,<sup>230</sup> and in 2017 Nelson and Nolan compiled a summary of the chemistry of (NHC)AuOH complexes.<sup>21</sup>

Organometallic gold(III) hydroxides were first reported in the late 1960s, when Tobias described the synthesis of  $[\text{Me}_2\text{Au}(\mu\text{-OH})]_n$  and the crystal structure of the tetramer.<sup>231</sup> This was

1  
2  
3 followed by reports by Vicente and Cinellu describing, respectively, Au(III)-OH aryl complexes  
4  $[\text{Ar}_2\text{Au}(\mu\text{-OH})]_2$  and the cationic bipy complexes  $[(\text{bipy})\text{AuCl}(\text{OH})]^+$  and  $[(\text{bipy})\text{Au}(\text{OH})_2]^+$ .<sup>232,233</sup>  
5  
6 The hydroxide  $[(\text{C}^{\wedge}\text{C})\text{Au}(\mu\text{-OH})]_n$  and the related crystallographically characterized water complex  
7  $[(\text{C}^{\wedge}\text{C})\text{Au}(\text{OH}_2)_2]^+$  are also known.<sup>137</sup> Recently Dutton and co-workers prepared and structurally  
8 characterized cationic pyridine complexes with terminal OH ligands, of the type  $[(\text{terpy})\text{AuOH}]^{2+}$   
9 and  $[(\text{bipy})\text{AuOH}(\text{DMAP})]^{2+}$  (see Section 3); these exchange with methanol to give the  
10 corresponding methoxides.<sup>234,235</sup> However, none of these species were used as synthetic reagents or  
11 catalysts.

12  
13  
14  
15  
16  
17 Whereas in most of these cases the hydroxide acts as bridging ligand, in 2012 Rořca *et al.*  
18 showed that the  $\text{C}^{\wedge}\text{N}^{\wedge}\text{C}$  pincer environment gives access to a thermally stable complex with a  
19 terminal OH ligand,  $(\text{C}^{\wedge}\text{N}^{\wedge}\text{C})\text{AuOH}$  **39**, which proved to be a useful starting material.<sup>236,237</sup> The  
20 substitution of the chloride ligand in square-planar  $(\text{C}^{\wedge}\text{N}^{\wedge}\text{C})\text{AuCl}$  **71**<sup>238,239</sup> by water has been  
21 studied computationally.<sup>43</sup> It is thought to follow a dissociative interchange mechanism, in which  
22 the elongation and breaking of the Au-Cl bond plays the primary role, via transition state **TS1**  
23 (Scheme 21). An activation barrier of  $\Delta G^\ddagger = 24.2$  kcal/mol was calculated. The resulting aquo  
24 complex **72** is strongly acidic (calculated  $\text{p}K_a$  1.7) and is easily deprotonated to give the hydroxide  
25 product. The calculated Au-OH distance of 1.978 Å compares quite well with the Au-O bond length  
26 of 2.010(2) Å determined for the *t*Bu-decorated analogue,  $(\text{C}^{\wedge}\text{N}^{\wedge}\text{C})\text{AuOH}\cdot\text{H}_2\text{O}$ .<sup>236</sup> However, the  
27 overall reaction was found to be endergonic ( $\Delta G_R = 26.1$  kcal/mol) and does not proceed under  
28 neutral conditions.

### 39 40 Scheme 21. Computational Model of $(\text{C}^{\wedge}\text{N}^{\wedge}\text{C})\text{AuCl}$ Hydrolysis

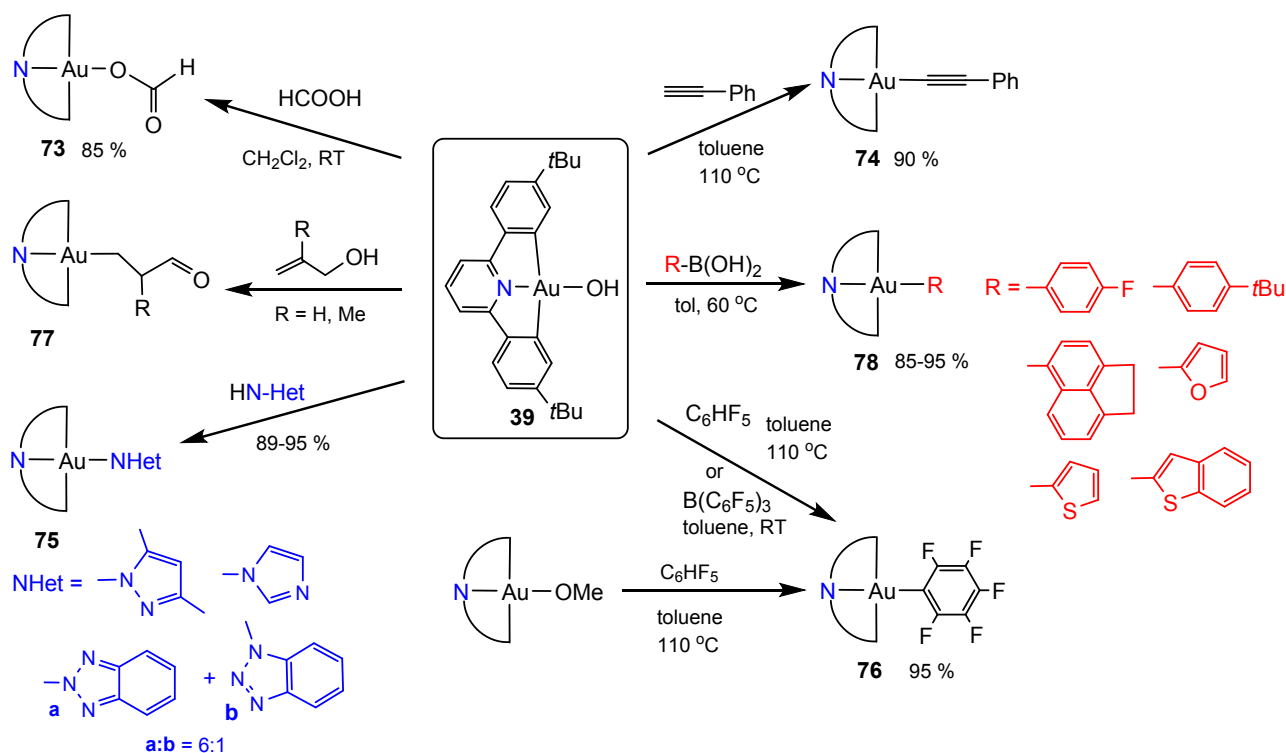


The hydroxide **39** can be isolated straightforwardly in high yield by treating  $(\text{C}^{\wedge}\text{N}^{\wedge}\text{C})\text{AuCl}$  with CsOH in a THF/toluene/water mixture at 60 °C. By contrast, attempts to remove the chloride

by reacting (C<sup>^</sup>N<sup>^</sup>C)AuCl with silver triflate led to decomposition and reduction to metallic gold. **39** undergoes acid/base reactions to give, for example, the formate **73**, alkynyls **74**, and heterocyclic complexes **75** (Scheme 22). The reaction of **39** with pentafluorobenzene in refluxing toluene generates the gold-C<sub>6</sub>F<sub>5</sub> complex **76** in near-quantitative yield. The same product can be made from C<sub>6</sub>F<sub>5</sub>H and the methoxide (C<sup>^</sup>N<sup>^</sup>C)AuOMe, or from **39** by aryl transfer with B(C<sub>6</sub>F<sub>5</sub>)<sub>3</sub>.<sup>236,237</sup> The reaction of allyl alcohols with hydroxide **39** involves rearrangement to Au-C bonded products, to give for example the 3-propanalyl complex **77**. This unexpected reaction is apparently driven by the difference in bond energies, Au-C > Au-O, and provides a convenient route to aldehyde-terminated gold alkyls.<sup>197</sup>

Possibly more interesting in view of the much-studied C-C coupling reactions based on aryl boronic acids is the facile reaction of **39** with aryl- and heteroarylboronic acids to give the corresponding gold(III) aryls **78** in near-quantitative yields. As Roşca *et al.* found, this reaction proceeds smoothly under neutral conditions in toluene at 60 °C without the need for added base or water and works for both electron-rich and electron-poor aryls.<sup>236</sup>

### Scheme 22. Reactions of the Terminal Hydroxide Complex (C<sup>^</sup>N<sup>^</sup>C)AuOH

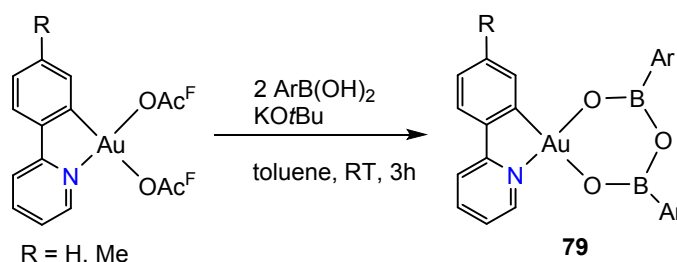


The smooth transmetalation of **39** with  $\text{ArB(OH)}_2$  under neutral conditions contrasts with the arylation of the gold(III) chlorides  $\text{Ph}_3\text{PAuCl}_2(\text{Ar}^1)$  with  $\text{Ar}^2\text{B(OH)}_2$ , which proceeds only if  $\text{Ar}^2$  is electron-poor, such as C<sub>6</sub>F<sub>5</sub>, and only under forcing conditions (1,2-dichloroethane, 150 °C).

Prolonged heating leads to the reductive elimination product, decafluorobiphenyl. There was no reaction with  $\text{PhB}(\text{OH})_2$ .<sup>240</sup> This lack of reactivity of  $\text{PhB}(\text{OH})_2$  with gold(III) chlorides was later confirmed by Gray *et al.* who found that the aryl transfer to  $(\text{C}^{\wedge}\text{N})\text{AuCl}_2$  proceeded only in the presence of a palladium catalyst and base. Of the various combinations of Pd complexes with phosphines and bases that were explored,  $\text{Pd}(\text{OAc})_2 + [\text{tBu}_3\text{PH}]\text{BF}_4 + \text{K}_3\text{PO}_4$  worked best (toluene, 25 °C) and gave the bis-arylation product  $(\text{C}^{\wedge}\text{N})\text{AuAr}_2$ . The authors proposed a mechanism which postulated an unusual  $(\text{C}^{\wedge}\text{N})\text{Au-Pd}$  intermediate, with a gold-palladium  $\sigma$ -bond; however, no experimental or computational evidence for such a species was provided.<sup>241</sup>

In this context it is interesting to note that the related reaction of  $(\text{C}^{\wedge}\text{N})\text{Au}(\text{OAc}^{\text{F}})_2$  with  $\text{ArB}(\text{OH})_2$  (Ar = aryl, 2-thiophenyl, ferrocenyl) in the presence of  $\text{KO}t\text{Bu}$  in toluene stopped at the formation of Au(III) boroxinato complexes **79** (Scheme 23).<sup>242,243</sup>

### Scheme 23. Arrested Transmetalation of Boronic Acids to Au(III)

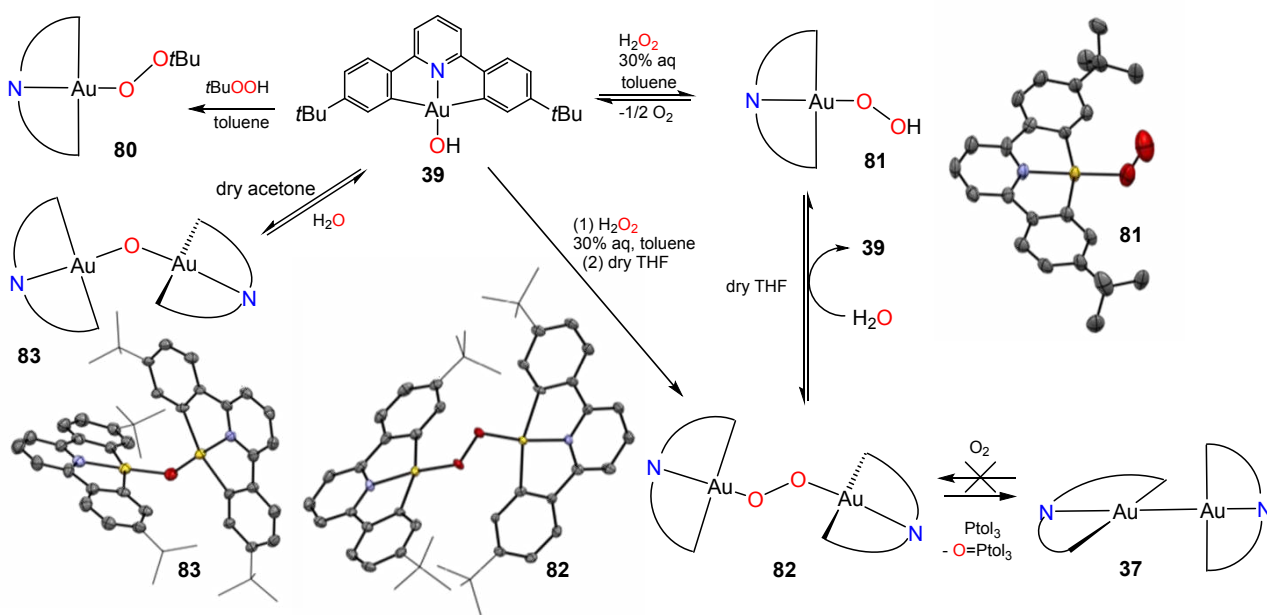


Treatment of **39** with peroxides gives a number of peroxy complexes (Scheme 24).<sup>196</sup> These, as well as superoxide surface species, have been postulated in computational studies as intermediates in oxidations catalyzed by heterogeneous gold-catalysts<sup>244-247</sup> but until now there were no isolable complexes of this type. The gold(III) complexes **80** – **83** were all characterized by X-ray diffraction. From the near-tetrahedral Au–O–Au angle of **83** it is evident that there is no  $\pi$ -bonding contribution to the  $\text{Au}^{\text{III}}\text{--O}$  bond; this agrees with findings by Hill and others that the previously claimed formation of an oxo-type  $\text{Au}=\text{O}$  double bond was an artefact.<sup>248</sup> The peroxide compounds do not act as oxidation catalysts, although the hydroperoxide is reduced by tris(*p*-tolyl)phosphine stepwise under O-atom transfer, first to the hydroxide **39**, and subsequently to the hydride **35** (Scheme 12).<sup>196</sup> Similarly, the peroxide **82** is slowly deoxygenated by phosphines to give the dimeric gold(II) complex **37**. There is however no reverse reaction, and **37** does not insert dioxygen to give either **82** or the oxide **83**. There was no evidence for the involvement of radicals in these O-abstraction reactions. Kinetic, isotopic labelling and computational studies suggested that the O-transfer from Au–OH to the phosphine proceeds by a concerted outer-sphere mechanism. A five-coordinate intermediate where the phosphine binds to gold prior to O-abstraction could be



ruled out; the Au(III) center remains strictly square-planar. The calculations also showed that the Au-O bond energy decreases steeply in the series LAuOH (67 kcal/mol) > LAuOOH (40) > LAuOOAuL (30).<sup>196</sup>

### Scheme 24. Formation, Interconversion and Crystal Structures of Gold(III) Oxo and Peroxo Complexes



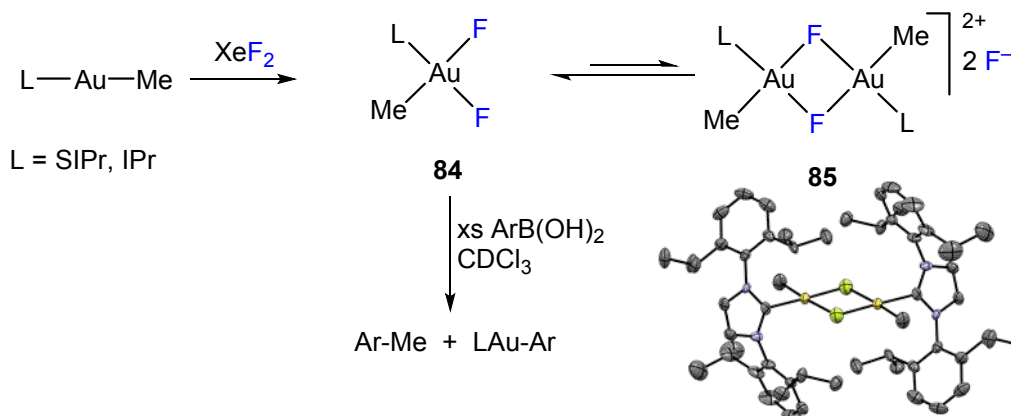
Like hydroxides, fluorides are good leaving groups in gold chemistry and are thought to be involved in reactions of gold(I) catalysts with Selectfluor as oxidant [Selectfluor = 1-chloromethyl-4-fluoro-1,4-diazoniabicyclo[2.2.2]octane-bis(tetrafluoroborate), also abbreviated “F<sup>+</sup>”]. Consequently, the reactivity of Au-F bonds has been widely exploited, particularly as coupling partners with arylboronic acids. The chemistry of fluorinated organic reagents and the generation of fluorinated products under the influence of homogeneous gold catalysts has recently been reviewed.<sup>68</sup>

The first organometallic gold(III) fluoride for such coupling reactions was reported by Mankad and Toste in 2010, who showed that gold(I) alkyls LAuR are oxidized by XeF<sub>2</sub> to give the expected Au(III) alkyl fluorides (Scheme 25; L = SIPr or IPr, R = Me, *t*Bu; SIPr = 1,3-bis(2,6-diisopropylphenyl)imidazolin-2-ylidene).<sup>249</sup> Monomeric *cis*-AuMeF<sub>2</sub>(L) (**84**) and dimeric [(L)AuMe(μ-F)]<sub>2</sub>[F]<sub>2</sub> (**85**) are in equilibrium, as indicated by two <sup>19</sup>F NMR signals for **84** and a singlet for **85**. Complex **85** was characterized by X-ray diffraction. The Au-F bond *trans* to Me (2.124(3) Å) is significantly longer than that *trans* to SIPr (2.034(3) Å). Spectroscopically pure *cis*-AuMeF<sub>2</sub>(IPr) was generated in solution but could not be isolated; it is closely related to reaction

intermediates of the type  $\text{LAu(R)(F)(halide)}$  that are thought to be involved in Au(I)/Au(III) catalytic cycles. **84** is stable to C-F reductive elimination; it contrasts therefore with  $\text{AuMe}_2(\text{IPr})$ , which eliminates  $\text{MeI}$  at room temperature and below (see Section 3).<sup>250</sup> This iodide complex also fails to give a coupling product with  $\text{PhB(OH)}_2$ , whereas **84** reacts with arylboronic acids  $\text{ArB(OH)}_2$  in chloroform at room temperature under  $\text{C(sp}^2\text{)}\text{-C(sp}^3\text{)}$  bond formation to give  $\text{Ar-Me}$  in yields of about 30-50%, with Ar ranging from electron-rich (*p*- $\text{MeOC}_6\text{H}_4$ ) to electron-poor ( $\text{C}_6\text{F}_5$ ).

On the other hand, steric pressure increases the propensity of *cis*- $\text{AuF}_2(\text{R})(\text{IPr})$  (R = 3- to 6-ring cycloalkyl,  $\text{CH}_2\text{Ad}$ ,  $\text{CH}_2\text{Ph}$  and others) to undergo reductive  $\text{C(sp}^3\text{)}\text{-F}$  elimination, with formation of the corresponding fluoroalkanes R-F (see Section 3.2).<sup>251</sup>

### Scheme 25. Formation and Reactions of Au(III)-F Complexes

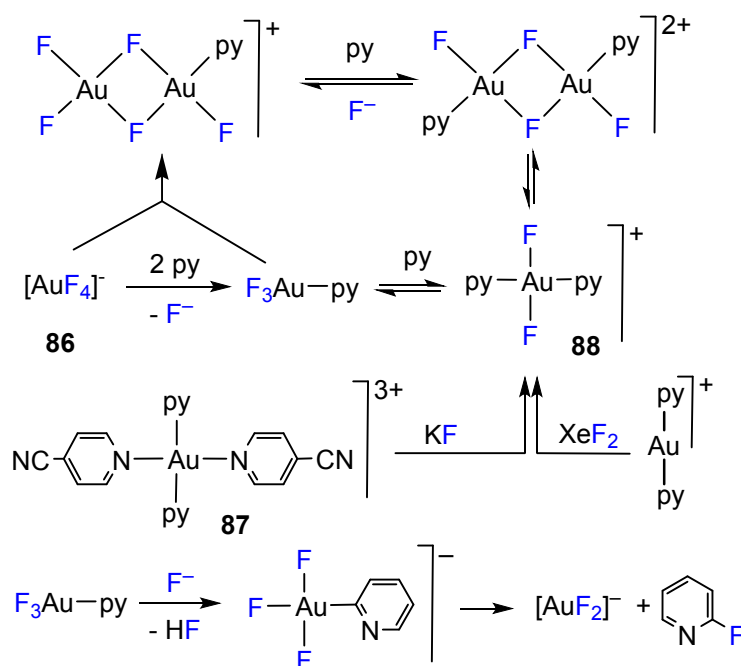


Methods for the synthesis of highly fluorinated gold(III) complexes are rare and inconvenient for general applications; others, such as the fluorination of  $[\text{Au(CN)}_4]^-$  with  $\text{ClF}$  to generate solutions of  $[\text{Au(CF}_3)_n\text{F}_{4-n}]^-$ , give mixtures of products.<sup>252</sup> However, a number of improved syntheses have recently been reported.

Riedel, Braun and co-workers reported the dissolution of gold metal in  $\text{BrF}_3$  at 60-70 °C under the effect of ultrasound to generate the adduct  $\text{F}_3\text{Au}\cdot\text{BrF}_3$ . The associated  $\text{BrF}_3$  can be removed by heating above 120 °C.  $\text{AuF}_3$  undergoes F/Cl exchange in chlorinated solvents but forms an acetonitrile adduct  $\text{AuF}_3(\text{NCMe})$  at -25 °C. Mixtures of gold,  $\text{BrF}_3$  and MF lead to stable salts  $\text{M[AuF}_4]$  (**86**, M = Cs,  $\text{NMe}_4$ ) which do not react with chlorocarbons. The crystallographically characterized  $\text{NMe}_4[\text{AuF}_4]$  salt is soluble in a wide range of organic solvents. It reacts with pyridine under  $\text{F}^-$  displacement in a series of equilibria affording bridging fluorides. The slow *ortho*-metalation of pyridine and formation of 2-fluoropyridine via reductive C-F elimination was also observed (Scheme 26).<sup>253</sup> Dutton and co-workers obtained structurally related gold(III) fluorides stabilized by pyridine ligands. These authors explored both the oxidation route of Au(I) precursors

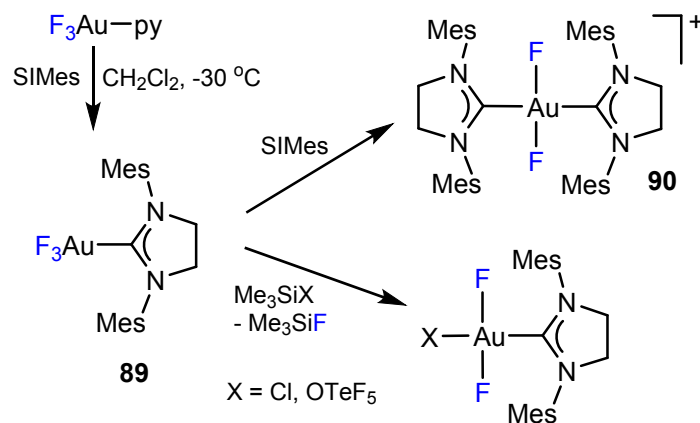
[Aupy<sub>2</sub>]<sup>+</sup> with XeF<sub>2</sub> and the displacement of *p*-cyanopyridine in the *trans*-[Aupy<sub>2</sub>(pyCN-4)<sub>2</sub>]<sup>3+</sup> cation **87** with KF, to generate *trans*-[AuF<sub>2</sub>(py)<sub>2</sub>]<sup>+</sup> **88**. The analogous complexes with methylimidazole as donor ligands were also obtained and structurally characterized. [AuF<sub>2</sub>(py)<sub>2</sub>]<sup>+</sup> undergoes pyridine/fluoride exchange with [PhI(py)<sub>2</sub>]<sup>2+</sup> to give [Aupy<sub>4</sub>]<sup>3+</sup> and PhIF<sub>2</sub>.<sup>254,255</sup>

### Scheme 26. Pyridine Complexes of Gold(III) Fluorides



The addition of SIMes to either NMe<sub>4</sub>[AuF<sub>4</sub>] at -30 °C or to AuF<sub>3</sub> at -80 °C to room temperature affords the carbene complex AuF<sub>3</sub>(SIMes) **89**, which was characterized by X-ray diffraction. The <sup>13</sup>C NMR signal of the carbene-carbon in **89** is observed at δ<sub>C</sub> 152.4 ppm, shifted upfield by ca. 20 ppm compared to AuCl<sub>3</sub>(SIMes), in line with the increased Lewis acidity of AuF<sub>3</sub>. **89** readily reacts with further SIMes to give the bis(carbene) cation *trans*-[AuF<sub>2</sub>(SIMes)<sub>2</sub>]<sup>+</sup> **90**; evidently the fluoride *trans* to C is labilized due to the *trans*-influence of the carbene.<sup>256</sup> This labilization also facilitates the selective substitution of F *trans* to C by other anions X = Cl or OTeF<sub>5</sub> (Scheme 27).<sup>257</sup>

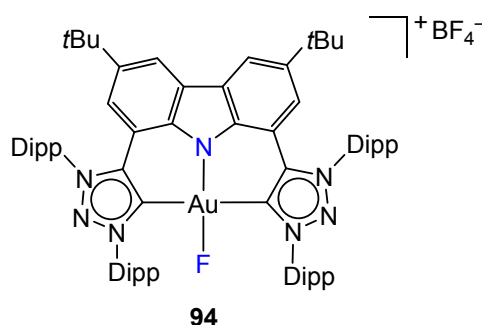
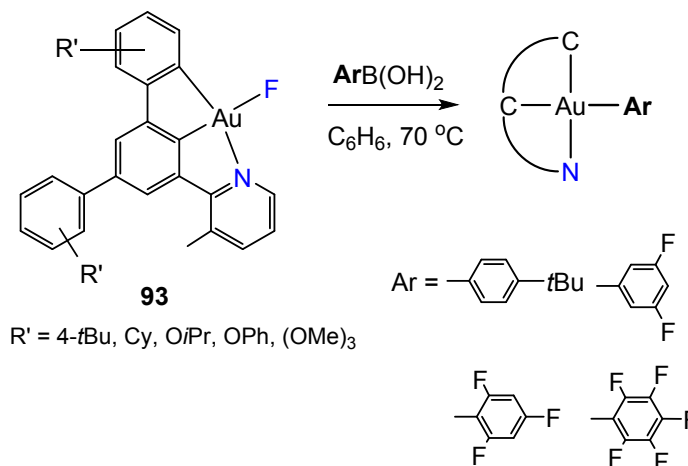
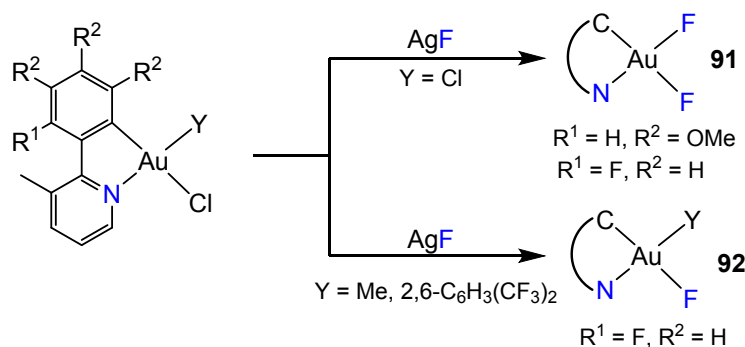
### Scheme 27. Reactions of AuF<sub>3</sub> with Carbene Ligands



The oxidation of  $\text{PPh}_4[\text{Au}(\text{CF}_3)_2]$  with  $\text{XeF}_2$  at  $0\text{ }^\circ\text{C}$  gives stereoselectively the *trans*-difluoride  $\text{PPh}_4[\text{AuF}_2(\text{CF}_3)_2]$ . The fluorides can be readily exchanged by  $\text{X} = \text{Cl, Br, I, CN}$  to give  $\text{PPh}_4[\text{AuX}_2(\text{CF}_3)_2]$ . The complex decomposes in the gas phase by  $\text{CF}_2$  extrusion.<sup>12</sup> Conversely,  $[\text{Au}(\text{CF}_3)_2]^-$  oxidatively adds  $\text{CF}_3\text{I}$  to generate  $[\text{AuI}(\text{CF}_3)_3]^-$ , by a radical mechanism that is induced by daylight. The iodide ligand can be exchanged with  $\text{AgF}$  or by treatment with  $\text{XeF}_2$  to give the fluoride  $\text{PPh}_4[\text{AuF}(\text{CF}_3)_3]$ .<sup>258</sup>

Organometallic gold(III) fluoro complexes are also accessible from the chlorides by ligand exchange with  $\text{AgF}$ . A series of  $\text{C}^{\wedge}\text{N}$  (**91**, **92**) and  $\text{C}^{\wedge}\text{C}^{\wedge}\text{N}$  (**93**) chelated complexes have been prepared.<sup>259,260</sup> The crystal structures of compounds **91** show, as expected, that the Au-F bonds *trans* to C are elongated compared to those *trans* to N. The complexes undergo transmetalation with arylboronic acids in dichloromethane or benzene under neutral conditions. Complexes of type **92** provided evidence that products due to inter- and intra-molecular reductive elimination can both be generated following transmetalation with boronic acids (see Section 4.1.1).<sup>259</sup> Complex **93** also reacts quantitatively with terminal acetylenes in dichloromethane at room temperature, without the addition of base.<sup>260</sup> Another pincer complex, the bis-carbene gold(III) fluoride **94**, was prepared by oxidation of the T-shaped bis-carbene ( $\text{C}^{\wedge}\text{N}^{\wedge}\text{C}$ )Au(I) precursor with Selectfluor; the complex is weakly photoemissive (Scheme 28).<sup>261</sup>

### Scheme 28. Cyclometalated Gold(III) Fluoride Complexes



### 3. CATALYSIS-RELEVANT REACTION STEPS

44  
45  
46  
47  
48  
49  
50  
51  
52  
53  
54  
55  
56  
57  
58  
59  
60

Catalytic cycles are composed of well-recognized reaction steps that have been realized for most transition metals, concerning the entry of a substrate into the cycle, its subsequent modification, and finally product release.<sup>262-264</sup> For gold, several of these steps have proved problematic, and some well-established mechanisms appeared to have no counterpart in gold chemistry. In Section 2 we have shown that ligand exchange and transmetalation steps can be probed by tuning the ancillary ligands on the metal, which also gives the opportunity to observe and isolate reaction intermediates. Section 3 discusses the factors controlling the making and breaking of chemical bonds in substrates and products, by means of (i) oxidative addition, (ii) reductive elimination, (iii) nucleophilic attack on unsaturated substrates, and (iv) insertion reactions.

### 3.1. Oxidative Addition Reactions

Oxidative addition of a substrate to a low-valent metal center is a key step in many catalytic coupling reactions. Particularly true for late transition metals, oxidative addition has been established for a broad spectrum of substrates featuring polarized or non-polar  $\sigma$  bonds, and mechanistic details have been widely rationalized.<sup>262-264</sup> In striking contrast with the isoelectronic Pt(0), studies on oxidative additions to Au(I) affording Au(III) complexes have remained quite rare until recently.

Oxidative addition of organic halides to Au(I) complexes has been known since the 1970s, when Schmidbaur,<sup>265</sup> Kochi,<sup>266,267</sup> and Puddephatt<sup>268</sup> reported the addition of methyl iodide to trimethylphosphine gold(I) methyl complexes, which afforded metastable Au(III) dimethyl species that were identified spectroscopically. The first examples of oxidative addition of  $sp^2$ -carbon atoms were reported in 1976 by Usón, who used Tl(III) derivatives such as  $BrTl(C_6F_5)_2$  to generate stable bis-pentafluorophenyl Au(III) salts.<sup>269</sup> However, since these early results, progress has been rather slow, as oxidative addition to Au(I) proved far from facile.

The past decade witnessed a great improvement in the understanding of oxidative addition to Au(I) and demonstrated the suitability of oxidized gold centers in cross-coupling catalysis. While this was achieved initially by using sacrificial oxidants, mainly iodine(III) or  $F^+$  reagents, to cycle between Au(I) and Au(III) (see Section 4), more recent organometallic studies have revealed that steric and electronic factors can play a key role in favoring direct oxidative addition of substrates such as aryl-halides to gold(I). This section highlights recent advances in the area, by focusing initially on progress in the controlled oxidation of gold(I) with halogens and sacrificial oxidants, before moving on to the direct oxidative addition of C–X, C–C and E–E bonds.

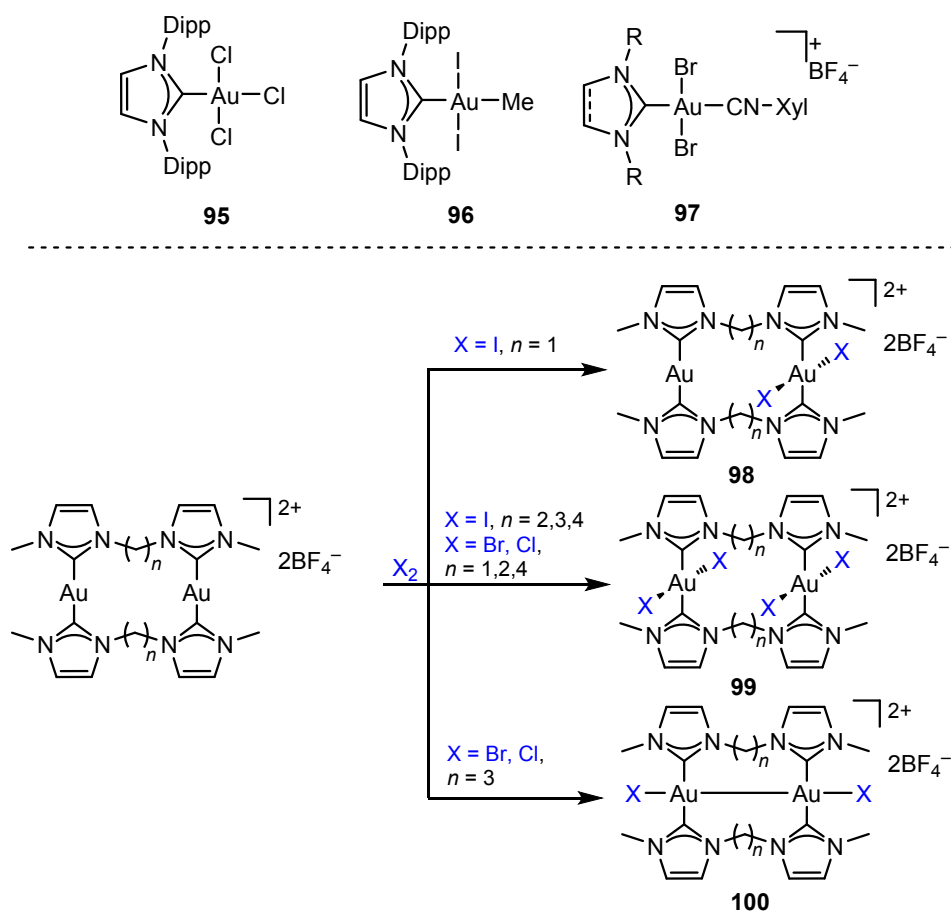
**3.1.1 Controlled Oxidation of Au(I) by Halogens and Sacrificial Oxidants.** Oxidative addition of halogens has been of interest for a long time in gold chemistry as a suitable method for the controlled oxidation of Au(I) complexes and the synthesis of novel Au(III) halides. These reactions have been widely investigated, particularly for phosphine gold(I) precursors, and the factors affecting stability and reactivity of the obtained Au(III) halides have been rationalized.<sup>270-275</sup> With the explosion of interest in N-heterocyclic carbenes as ligands for gold, halogenation of Au(I) precursor has been somehow rediscovered and a series of synthetic and mechanistic investigations has been reported over the past decade.

After the first successful results with  $Br_2$  in 2007,<sup>276</sup> Nolan and co-workers showed in 2010 that  $(IPr)AuCl$  can be cleanly oxidized by chlorine to give the  $(IPr)AuCl_3$  complex **95**.<sup>277,278</sup> Bercaw and co-workers showed that  $(IPr)AuMe$  can be oxidized with  $I_2$  to give the transient gold(III) complex **96**, which was crystallographically characterized but proved unstable and decomposed

with reductive elimination of MeI.<sup>250</sup> Other oxidants such as Cl<sub>2</sub> and Br<sub>2</sub> gave less clean reactions. Cationic NHC Au(I) complexes can also be oxidized to stable Au(III) intermediates. For example, Canovese *et al.* used Br<sub>2</sub> to synthesize cationic *trans* dibromides **97** stabilized by xylyl isocyanide ligands.<sup>279</sup>

Oxidative addition of halogens is viable also for cationic bis-carbene complexes.<sup>280</sup> Baron *et al.* have used dimeric bis-carbene gold(I) complexes in combination with halogens and found that complexes with different stoichiometry and oxidation state formed, depending on both the nature of the oxidant and the starting Au(I) complex.<sup>281</sup> When using dimeric carbene species with short spacers ( $n = 1$ ) in combination with I<sub>2</sub>, the mixed valence complex **98** selectively formed. Complexes with longer spacers ( $n = 2, 3$ , or 4) underwent double oxidative addition of I<sub>2</sub> to give the dimeric Au(III) species **99**. If Cl<sub>2</sub> or Br<sub>2</sub> were used instead, double oxidative addition to give **99** was observed also for the complex with the shorter bridge. An exception was provided by the complex with  $n = 3$ , for which the selective formation of the Au(II) dimer **100** was observed (Scheme 29).

### Scheme 29. Structures and Oxidation Reactions of Gold NHC Complexes With Halogens



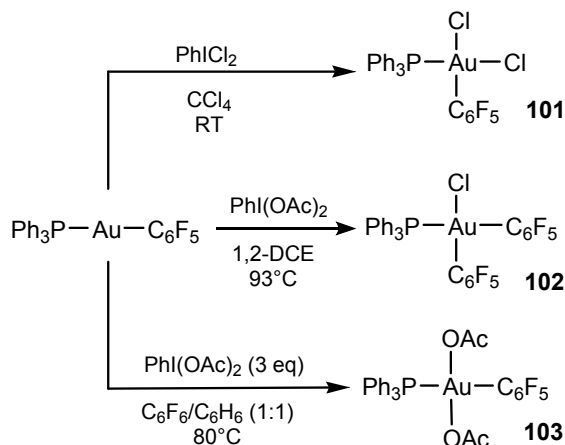
NHC gold complexes can also be oxidized by tribromide ions as shown by Monkowius, who used CsBr<sub>3</sub> as brominating agent for (IPr)AuBr.<sup>282</sup>

In 2013, Menjón and co-workers reported oxidative addition of Cl<sub>2</sub>, Br<sub>2</sub> and I<sub>2</sub> to anionic [Au(CF<sub>3</sub>)<sub>2</sub>]<sup>-</sup> complexes to give stable Au(III) bis-trifluoromethyl bis-halides. In the case of the chloride complex, a *trans* stereochemistry was attributed on the basis of IR spectroscopy. Bromides and iodides were suggested to possess the same stereochemistry.<sup>283</sup>

Together with halogens, strong oxidants, such as As(V) or Tl(III) salts, have long been known as viable reagents for the synthesis of high-valent Au(III) halides upon controlled oxidation. With the first report of gold-catalyzed C–C coupling by Tse *et al.* in 2008,<sup>284,285</sup> usage of such strong oxidants compatible with catalytic applications has skyrocketed in the subsequent decade. In particular, λ<sup>3</sup>-iodane reagents ArIX<sub>2</sub>, where X = OAc or OAc<sup>F</sup>, have found broad applications as they tolerate harsh conditions, as well as a wide range of functional groups, and can engage in proton transfer reactions (see Section 4).

Despite the growing interest in these reagents, spectroscopic studies on such oxidation reactions have remained limited. In 2009, Iglesias and Muñiz reported spectroscopic evidence for the oxidation of Ph<sub>3</sub>PAuMe with PhI(OAc)<sub>2</sub> but no clean product was isolated.<sup>286</sup> In 2012, Hofer *et al.* investigated the oxidation of Ph<sub>3</sub>PAuC<sub>6</sub>F<sub>5</sub> with PhICl<sub>2</sub> and PhI(OAc)<sub>2</sub> and found that, while PhICl<sub>2</sub> affords the known *cis*-Ph<sub>3</sub>PAu(C<sub>6</sub>F<sub>5</sub>)Cl<sub>2</sub> complex **101**, PhI(OAc)<sub>2</sub> produced *cis*-Ph<sub>3</sub>PAu(C<sub>6</sub>F<sub>5</sub>)<sub>2</sub>Cl **102** (Scheme 30).<sup>287</sup> The formation of the latter was suggested to arise from solvent activation and a series of ligand exchange or transmetalation steps between different intermediates. Similar outcomes were observed when using NHC as ancillary ligands.<sup>288</sup> Later on, the same authors reported a gold-catalyzed C–H arylation of arenes with electron-poor boronic acids, which exploits PhI(OAc)<sub>2</sub> as sacrificial oxidant.<sup>289</sup> By using different experimental conditions with respect to the previous study, the Au(III) bis acetate species **103** was isolated and characterized by X-Ray diffraction. Reactions of **103** with arenes revealed its ability to engage in C–H activation and C–C reductive elimination.

### Scheme 30. Oxidation Ph<sub>3</sub>PAu–C<sub>6</sub>F<sub>5</sub> with Iodine(III) Reagents



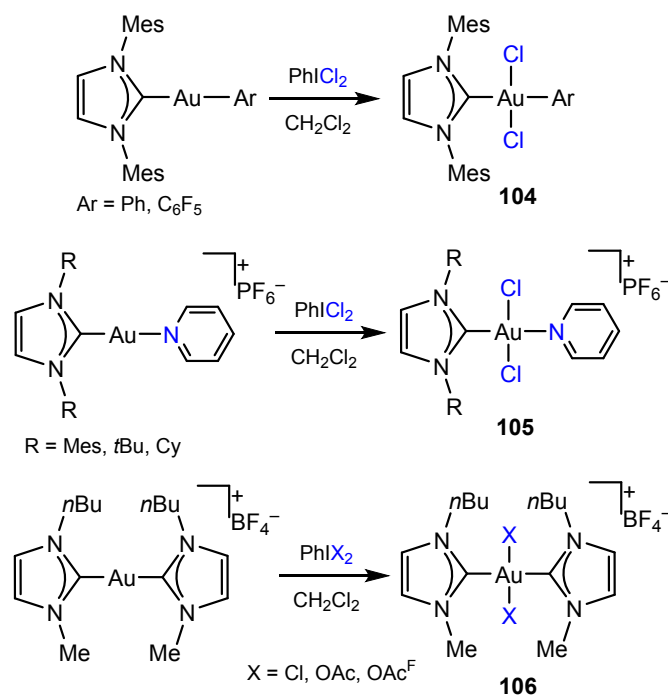


In the case of phosphine gold(I) acetylides, the same authors showed that oxidation with  $\text{PhI}(\text{OAc})_2$  is more difficult, even at high temperature, proving that the isolation of bis-acetato Au(III) acetylides is not achieved easily. On the other hand,  $\text{PhICl}_2$  affords the corresponding *cis*-dichlorogold(III) acetylides quantitatively at room temperature.<sup>290</sup>

In 2010, Nolan and co-workers reported the oxidation of (NHC)AuCl precursors with  $\text{PhICl}_2$  to give the corresponding trichlorides.<sup>277</sup> At the same time, Limbach and co-workers described the oxidation of (IMes)Au phenyl and pentafluorophenyl derivatives with  $\text{PhICl}_2$  to give the corresponding Au(III) dichlorides **104**, which were identified as the *trans* isomers by X-ray diffraction.<sup>291</sup> Subsequently, Ghidui *et al.* showed that while similar results can be obtained with (IPr)AuC<sub>6</sub>F<sub>5</sub>, matching the earlier findings by Hofer and Nevado,<sup>288</sup> no stable intermediate could be observed after reacting (IPr)AuC<sub>6</sub>H<sub>5</sub> and  $\text{PhICl}_2$ , suggesting that the nature of the ancillary ligand is fundamental in tuning the stability of the oxidation products.<sup>292</sup> Orbisaglia *et al.* reported in 2013 that also cationic NHC Au(I) pyridine adducts are oxidized by  $\text{PhICl}_2$ , affording the corresponding *trans*-Au(III) dichlorides **105**.<sup>293</sup>

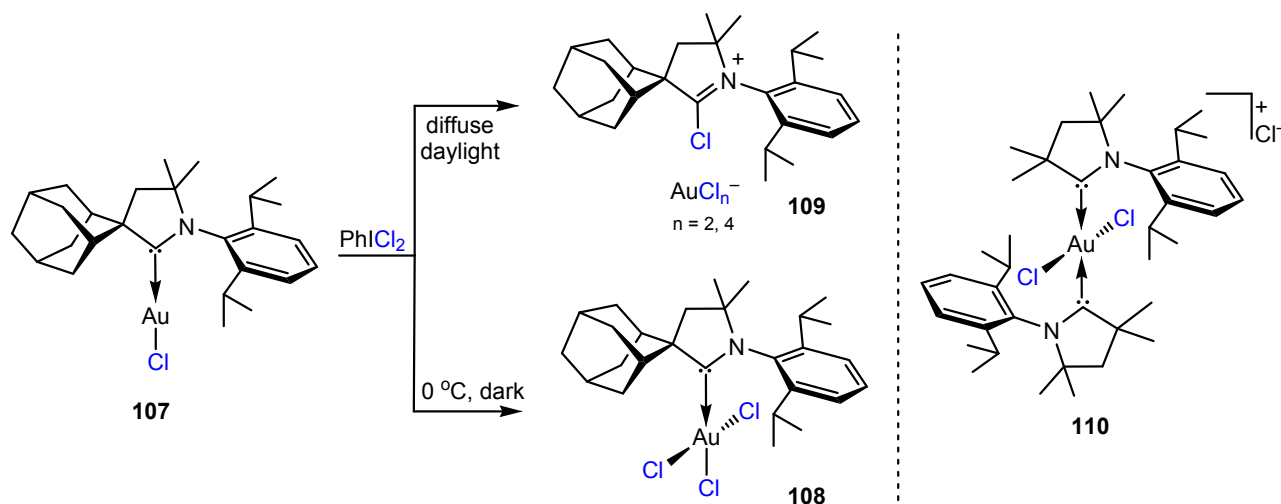
In 2016 Nolan and co-workers investigated extensively the oxidation of Au(I) bis-NHC complexes to Au(III) with hypervalent iodine(III) reagents.<sup>294</sup> Using a bis(1-butyl-3-methylimidazolium) derivative, the product of oxidation with  $\text{PhICl}_2$ ,  $\text{PhI}(\text{OAc})_2$  and  $\text{PhI}(\text{OAc}^F)$  **106** were isolated and structurally characterized (Scheme 31).

### Scheme 31 Oxidations of Gold NHC Complexes with Iodine(III) reagents



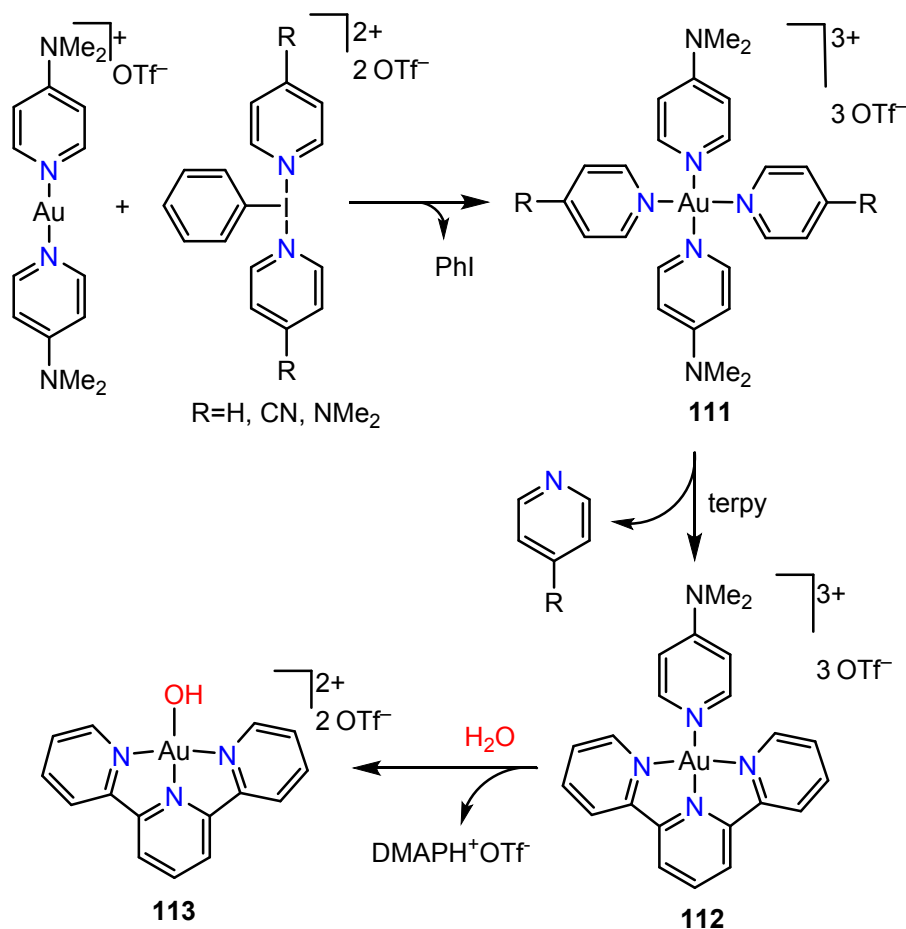
Cyclic (alkyl)(amino)carbene (CAAC) gold(I) complexes showed a quite different oxidation chemistry. Romanov and Bochmann reported in 2015 that in the absence of ambient light the oxidation of bulky (CAAC)AuCl complexes **107** with PhICl<sub>2</sub> at 0 °C proceeded quantitatively to afford the Au(III) trichloro species **108**. On the other hand, when the oxidations were carried out under laboratory light, quantitative formation of chloroimidazolium salts **109** was observed, as products of the photoinitiated reductive C-Cl elimination from **108**. Bis-carbene Au(I) species could be also oxidized under the same experimental conditions affording *trans*-[AuCl<sub>2</sub>(CAAC)<sub>2</sub>]<sup>+</sup> cations **110**. No clean oxidation was observed with CsBr<sub>3</sub> and I<sub>2</sub> (Scheme 32).<sup>47</sup>

**Scheme 32. Light-Dependent Oxidation of Gold CAAC Complexes**



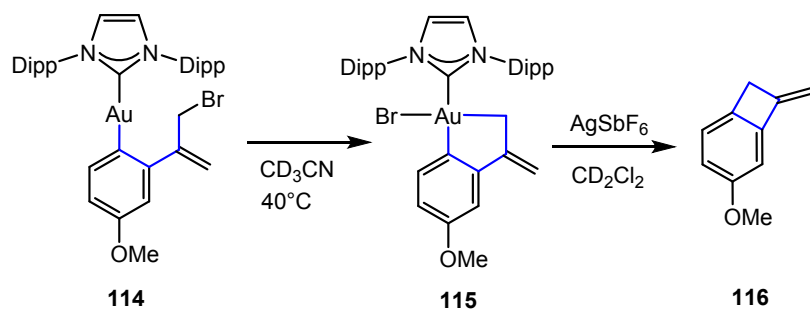
Dutton *et al.* showed that cationic hypervalent iodine reagents [PhI(py)<sub>2</sub>][X] (py = pyridine, 4-cyanopyridine, or 4-dimethylaminopyridine DMAP) can be used to oxidize Au(I) cations selectively to generate stable homoleptic Au(III) trications **111** (Scheme 33), offering an unprecedented synthetic route to halide-free high-valent gold. In addition to the fluoride chemistry described in section 2.3.3, these cations can also be used to prepare N<sup>^</sup>N<sup>^</sup>N pincer complexes **112** and to generate the Au(III) hydroxo species **113** by deprotonation of H<sub>2</sub>O.<sup>295</sup>

**Scheme 33. Formation of Gold(III) Pyridine and Terpyridyl Cations**



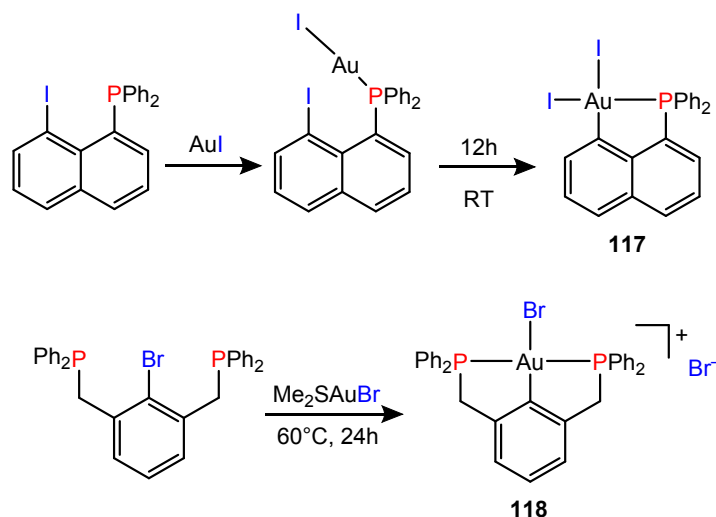
**3.1.2 Oxidative Addition of C–X, C–C and E–E Bonds.** In 2014, Levin and Toste reported the first example of redox-neutral  $\text{sp}^3$ - $\text{sp}^2$  C–C coupling between arylboronic acids and allyl bromides, catalyzed by the binuclear gold catalyst  $i\text{PrN}(\text{Ph}_2\text{PAuCl})_2$ .<sup>296</sup> Mechanistically, these reactions were suggested to start with the transmetalation of the boronic acid to Au(I), followed by the oxidative addition of the allyl bromide, which is the opposite of what is usually observed with Pd. The mechanistic speculations were corroborated by stoichiometric studies. The mononuclear complex **114** could be obtained upon transmetalation of the corresponding boronic ester and was used to trap the oxidative addition intermediate **115**, which was characterized by X-Ray crystallography. Upon reaction with silver salts, **115** undergoes fast and quantitative reductive elimination affording the corresponding cyclobutene **116** (Scheme 34).

**Scheme 34. Intramolecular Oxidative Addition/Reductive Elimination Reactions of Gold NHC Complexes**



15 Intramolecular oxidative additions of aryl halide C–Br and C–I bonds have been achieved by  
16 the group of Bourissou, by using halo-aryl phosphines in combination with simple Au(I) starting  
17 materials.<sup>297</sup> For example, 8-iodonaphthyl phosphine reacts fast and quantitatively with AuI to give  
18 the corresponding phosphine Au(I) iodide, which undergoes C–I oxidative addition over a period of  
19 12 h to give the (P<sup>^</sup>C)Au(III) chelate **117**. Similarly, 8-bromonaphthyl phosphine was found to  
20 react with (Me<sub>2</sub>S)AuBr giving C–Br oxidative addition, even though more forcing conditions were  
21 required (24 h at 130 °C). Chloronaphthyl phosphines proved unreactive, supporting the general  
22 conclusion that stronger C–X bonds disfavor oxidative addition. The same principle was applied to  
23 diphosphine ligands having a bromoarene spacer, which were successfully used to generate a new  
24 class of cationic (P<sup>^</sup>C<sup>^</sup>P)Au(III) complexes **118** (Scheme 35).  
25  
26  
27  
28  
29  
30  
31  
32  
33

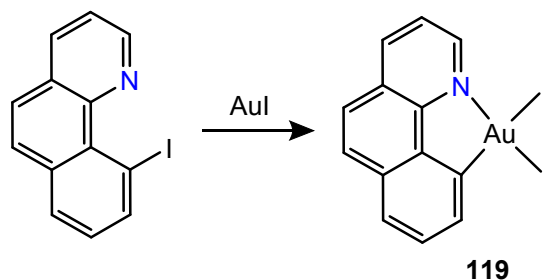
### Scheme 35. Formation of C<sup>P</sup> Chelate Complexes by Oxidative Addition of Haloaryl Phosphines



53 Steric and electronic effects have a remarkable impact on the ability of gold to undergo  
54 intramolecular oxidative addition. Livendahl *et al.* showed that replacing the haloarylphosphine  
55 with halobenzyl phosphines and phosphites shuts down the ability of Au(I) to be oxidized.<sup>298</sup> On the  
56 other hand, N-based donors such as iodoaryl-pyridines are able to oxidatively add to Au(I). Serra *et*  
57 *al.* have reported a catalytic C–N and C–O coupling of 2-(2-iodophenyl)pyridine with alkoxides and  
58 primary amines that does not require sacrificial oxidants.<sup>299</sup> The key step of the reaction is an  
59  
60

intramolecular oxidative addition of the C–I bond, which generates Au(III) chelates capable of reacting with nucleophiles *via* metathesis reactions and then give reductive elimination. The involvement of oxidative addition was demonstrated with 10-iodobenzo[h]quinolone, which reacts with AuI to afford the stable (C<sup>^</sup>N)Au(III) chelate **119** (Scheme 36) which was characterized crystallographically and used as stoichiometric probe to validate the mechanistic speculations.

### Scheme 36. Oxidative Addition of iodobenzoquinolone to AuI



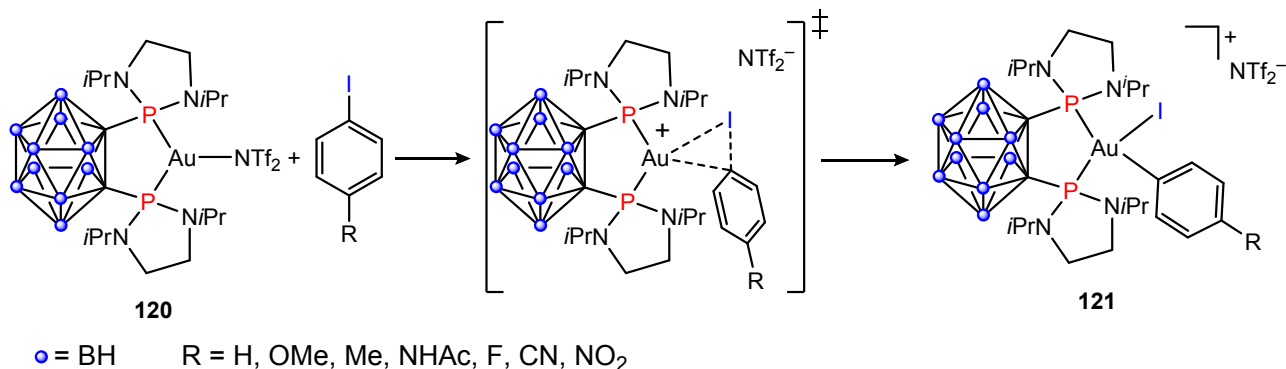
Despite enabling direct activation of C–X bonds and allowing cross-coupling in the absence of sacrificial oxidants, the scope and applications of *intramolecular* oxidative additions remain limited to substrates which are capable of acting as stabilizing ligands for Au(I) and Au(III). Strategies to enable *intermolecular* oxidative additions are therefore highly desirable.

Robinson *et al.* have studied the reaction between R<sub>3</sub>PAu<sup>+</sup> cations and iodobenzene in the gas phase and observed the formation of phenyl-phosphonium salts and Au<sup>I</sup> iodides, most likely as a consequence of a rapid oxidative addition/reductive elimination event. Diphosphine cations [R<sub>3</sub>PAuPR<sub>3</sub>]<sup>+</sup>, on the other hand, were unreactive.<sup>300</sup> While suggesting that gold cations can perform oxidative additions, the difficulties in achieving mono-coordination in solution poses a practical problem to the application of simple Au(I) salts in redox-neutral cross-couplings.

As suggested by Fernández *et al.* on the basis of DFT calculations, oxidative addition barriers are largely controlled by the energy required to deform the reactants to the geometries they adopt in the transition state.<sup>301</sup> Therefore a more general strategy to broaden the scope of such reactions is to favor intermolecular oxidative addition by destabilizing the linear coordination ground-state geometry of bis-ligated Au(I) species. This is relatively difficult as, in contrast to Pt(0), linear two-coordinate Au(I) complexes are remarkably stable and have a very low tendency to adopt higher coordination numbers.<sup>302</sup> Joost *et al.* have successfully used the low-bite angle diphosphine complex **120**, where the presence of the carboranyl skeleton favors the formation of a three-coordinate mononuclear environment over the more typical two-coordinate dinuclear arrangement.<sup>303</sup> This species reacts fast and quantitatively with a broad range of iodoarenes with different functional groups, to give the corresponding (P<sup>^</sup>P)Au(III) aryl derivatives **121**. Contrary to what is usually observed with Pd(0), the oxidative addition of electron-rich arenes occurs faster than

electron-poor ones, quite reasonably owing to the formation of an Au(I)  $\pi$  arene complex prior the oxidative event (Scheme 37).

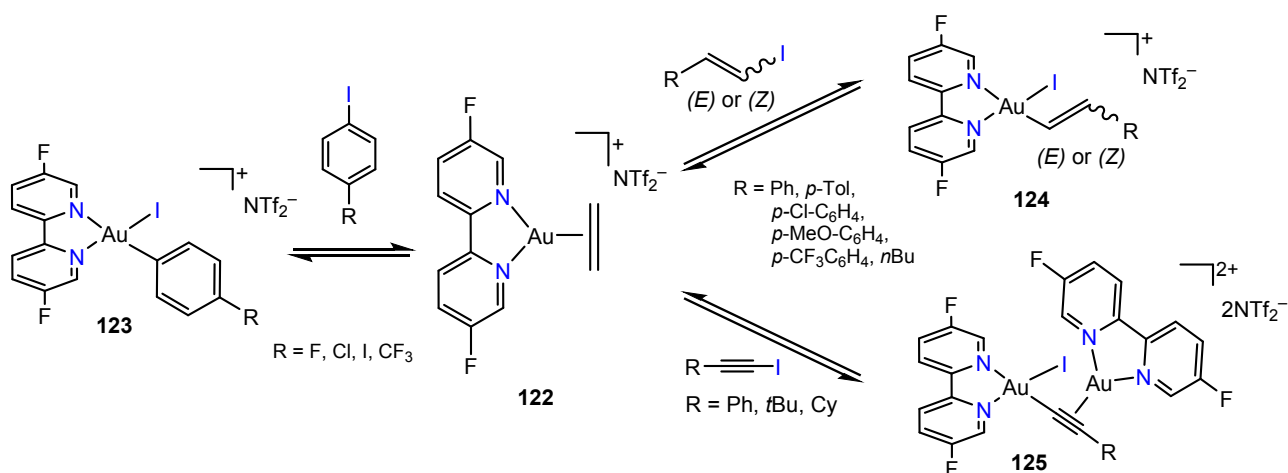
### Scheme 37. Oxidative Addition of Iodoarenes to (P<sup>^</sup>P)Au(I) Complexes



Harper *et al.* reported the oxidative addition of iodoarenes to a three-coordinated 2,2'-bipyridyl Au(I) ethylene adduct **122** (Scheme 38), showing that a successful distortion of the linear coordination of Au(I) can be achieved also with weaker donors. In line with the results reported by Joost *et al.*, oxidative addition of electron rich arenes was found to be significantly faster than electron poor ones, with good scope in functional groups.<sup>304</sup> As a reflection of facile Au(III)→Au(I) reduction, oxidative addition in these systems is reversible; exposure of the Au(III) aryls **123** to ethylene induced C–I reductive elimination and regeneration of the initial Au(I) complex **122**. The N<sup>^</sup>N ligand scaffold was used to investigate all the steps composing the catalytic coupling of arenes, including transmetalation with aryl-zinc reagents and C–C bond formation.

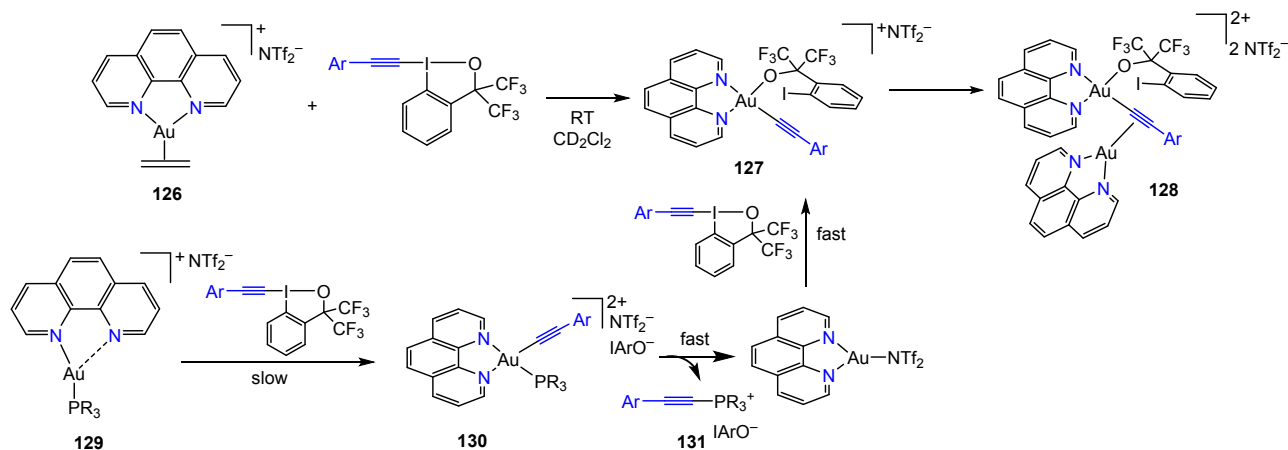
Cadge *et al.* showed very recently that this strategy can be further extended to vinyl and alkynyl iodides with equally satisfying scope (Scheme 38).<sup>305</sup> In particular, oxidative addition of iodostyrenes was reported to afford Au(III) vinyl complexes **124** in good yields, while alkyl derivatives were reluctant to react. Similar to iodoarenes, electron-rich substrates react faster than electron-poor ones. The oxidative addition of the iodovinyl moiety is stereospecific, so that the initial (*E*)- or (*Z*)-geometry of the substrates is retained in the Au(III) vinyl product. Alkynyl iodides oxidatively add reversibly to Au(I), affording the dinuclear Au(I)-Au(III) complex **125**, where an Au(I) center forms a  $\pi$ -complex with the Au(III) alkynyl cation. In contrast to iodovinyl substrates, both aryl and alkyl iodoalkynes oxidatively add in good yields.

### Scheme 38. Oxidative Addition of Iodo Compounds to (N<sup>^</sup>N)Au(I) Complexes



The application of bidentate N^N ligands in Au redox chemistry was also explored by Yang *et al.*, who have developed a catalytic alkylation of cyclopropenes mediated by a dual Au/Ag process.<sup>126,306</sup> In this process, phenanthroline Au(I) complexes oxidatively add alkynyl iodane reagents, to give (N^N)Au(III)alkynyl alkoxides that engage in transmetalation with silver-cyclopropenyl species. Stoichiometric mechanistic studies on [(phen)Au<sup>I</sup>(ethylene)]<sup>+</sup> **126** demonstrated the oxidative addition of the iodine(III) reagent to generate complex **127**, which was fully characterized by NMR spectroscopy (Scheme 39). Upon crystallization, the mixed valence Au(I)/Au(III) alkynyl complex **128** formed, as shown by Cadge *et al.* Oxidative addition reactivity was also observed when ethylene was replaced by phosphine ligands to give **129**. Phosphine ligation induces a considerable asymmetry in N^N coordination to Au(I).<sup>126</sup> Kinetic studies revealed that the reaction is accelerated by electron-poor phosphines and electron-rich iodane reagents. Mechanistically, the reaction is thought to follow a sequential mechanism, where the iodane oxidatively adds to the phosphine complex to give **130** and then reductively eliminates the phosphonium alkynyl **131**. This affords (phen)AuNTf<sub>2</sub>, which oxidatively adds a second equivalent of iodane. The kinetic effect of the nature of the phosphine suggests that the first oxidative addition is the rate limiting step. Remarkably, the same reactivity was also observed for linear bis(pyridine)gold(I) complexes, even though the obtained Au(III) alkynyls were somewhat less stable than the phenanthroline derivatives, supporting the idea that the formation of transient tri-coordinated species is a viable alternative to stimulate oxidative addition.<sup>126</sup>

### Scheme 39. Oxidative Addition of Alkynyliodine(III) Reagents

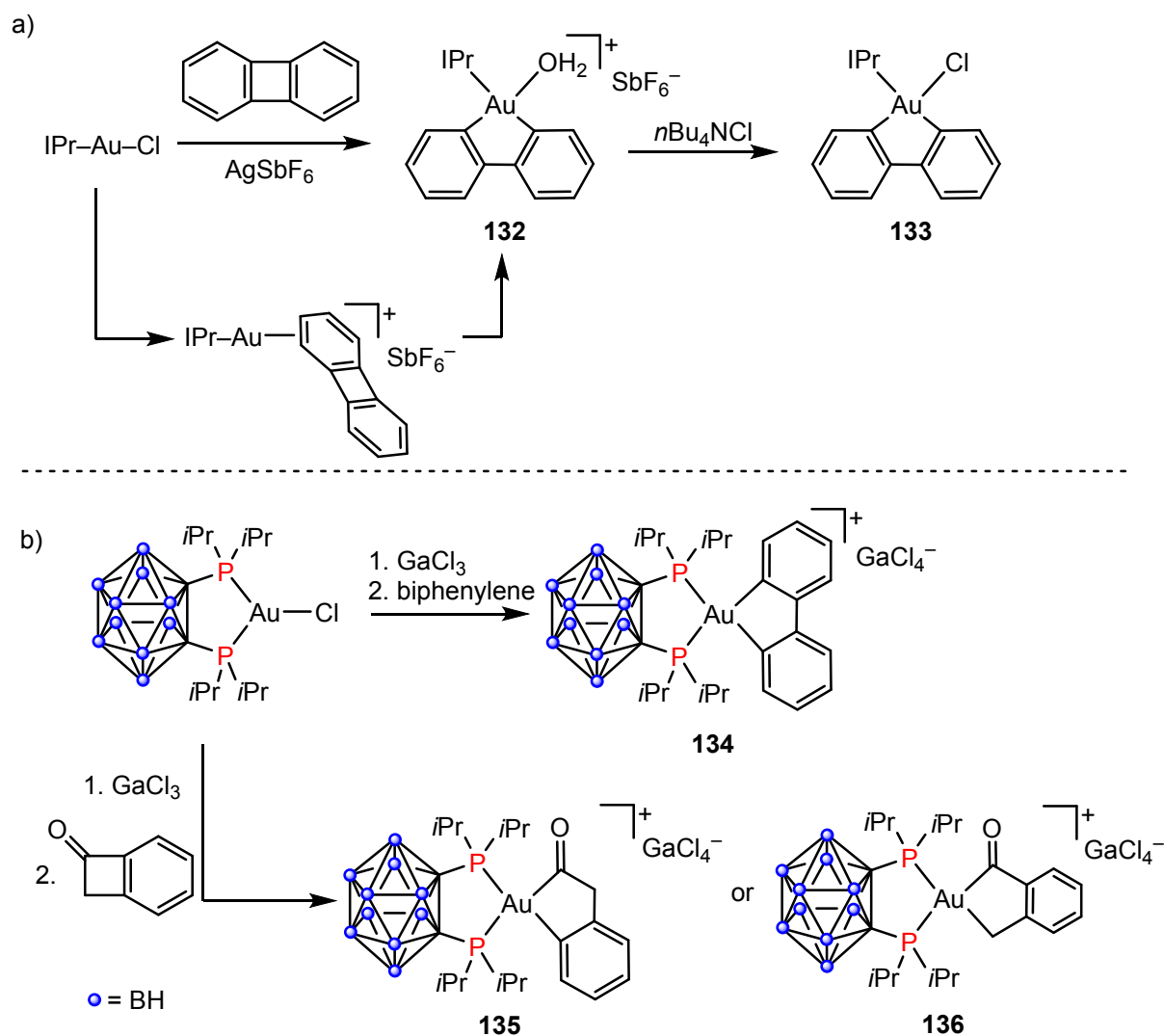


Substrates with strained C–C bonds are able to oxidatively add intermolecularly to Au(I). In 2015 Bourissou<sup>307</sup> as well as Toste and co-workers<sup>308</sup> demonstrated that the strained C–C bond of biphenylene can oxidatively add to Au(I) precursors to generate C<sup>∧</sup>C chelated Au(III) compounds, such as the IPr-stabilized **132** (Scheme 40a). The reaction occurs in two distinct steps, starting with a π-biphenylene Au(I) complex, which is formed immediately upon chloride abstraction, and proceeding with a slower C–C bond cleavage, which takes place in about 1.5 hours at RT. Adventitious water was found to be helpful in stabilizing the square-planar geometry of the resultant [(C<sup>∧</sup>C)Au(IPr)]<sup>+</sup> cation. The water can be easily displaced by *n*Bu<sub>4</sub>NCl to afford the more stable chloride complex **133**. The chelate **132** was found to be a competent Lewis acid catalyst, for example in the 1,4-Mukaiyama Michael addition of silyl ketene acetals to α,β-unsaturated aldehydes (See Section 4).<sup>308</sup>

Taking advantage of the increased reactivity of three-coordinate Au(I), Bourissou showed that carboranyldiphosphine gold complexes undergo oxidative addition of biphenylene and benzocyclobutenone (Scheme 40b). In the case of biphenylene, the reaction is believed to proceed as in the formation of **132**, even though it requires more forcing conditions and affords the corresponding Au(III) chelate **134** after 3h at 120 °C. Benzocyclobutenone was also found to be capable of adding to Au(I), to generate the chelates **135** and **136** as the first well-authenticated examples of Au(III) acyl complexes. These products arise from the cleavage of the C(sp<sup>2</sup>)–C(O) and the C(sp<sup>3</sup>)–C(O) bonds, respectively. The reaction outcome can be controlled selectively by adjusting the reaction conditions: **135** (kinetic product) can be obtained after 1h at 60°C, while **136** (thermodynamic product) is obtained by heating the same reaction mixture for 3h at 120 °C.<sup>307</sup>

#### Scheme 40. Oxidative Addition of C–C Bonds to NHC Au(I) Complexes (a) and Diphosphine Au(I) Complexes (b)



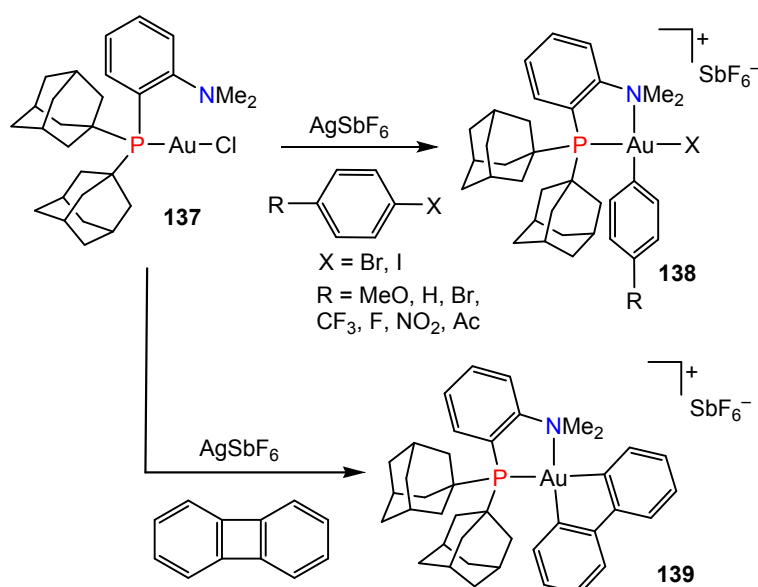


Taking the use of bidentate ligands one step further, hemilabile ligands are attractive since they can modify their denticity and stabilize reaction products after the formation of transient tricoordinated species.<sup>152</sup> As Zeineddine *et al.* have shown, the linear Au(I) complex **137** derived from the hemilabile MeDalPhos ligand engages in the oxidative addition of aryl bromides, aryl iodides and biphenylene to give the corresponding (P<sup>^</sup>N)Au(III) aryl derivatives **138** and **139** (Scheme 41).<sup>309</sup> The presence of the NMe<sub>2</sub> side group is fundamental for the stabilization of the square-planar geometry of Au(III) and prevents the non-productive reductive elimination of aryl-X. Oxidative addition to **137** tolerates a broad range of functional groups, including heteroatoms or polyarenes, and was found to proceed faster than with the previously employed bis-phosphine derivatives, to the point that most reactions went to completion upon mixing the reactants. Reactions are slower if more coordinating anions such as NTf<sub>2</sub><sup>-</sup> are used, indicating that the limiting step is likely the formation of a  $\pi$ -complex or iodine adduct prior oxidative addition. This finding

served as a basis for the development of a catalytic C–H arylation cycle (see Section 4.1.2, Scheme 102).

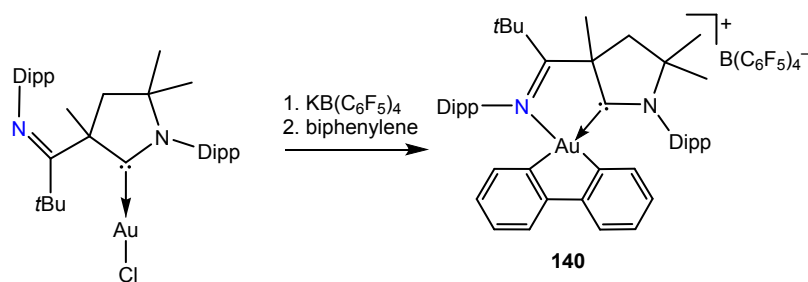
In a follow-up study, this reactivity was investigated in more detail by kinetic experiments and DFT calculations.<sup>310</sup> Hammett correlation and competition experiments corroborated the finding that electron-rich arenes react much faster than electron-poor ones. It was demonstrated that the highly electrophilic nature of the gold fragment induces a significant charge transfer from the iodonarene to the metal, which explains the preference for electron-rich arenes. This is in sharp contrast with the reactivity seen for palladium, where backbonding prevails and electron poor arenes are more reactive.

### Scheme 41. Oxidative Addition to Au(I) Complexes with Hemilabile P<sup>^</sup>N Ligands



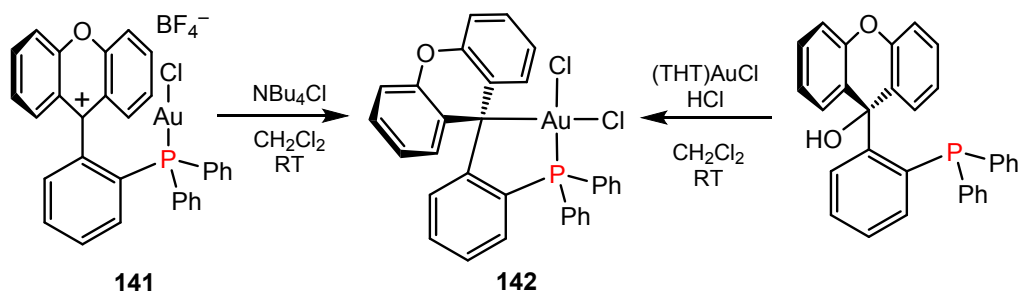
Chu *et al.* reported that cyclic (alkyl)(amino)carbenes with a pendant imine moiety, which are monodentate donor ligands for Au(I), react with biphenylene forming the (C<sup>^</sup>C)Au(III) chelate **140**, where the imino-functionalized carbene acts as bidentate ligand (Scheme 42). While the potentially hemilabile imino-CAAC complex undergoes quantitative C–C oxidative addition in 12h at room temperature, the correspondent CAAC complex without the N-substituent was found to be totally unreactive towards biphenylene.<sup>311</sup>

### Scheme 42. C–C Oxidative Addition to Complexes with Hemilabile CAAC Ligands



Another intriguing concept to induce oxidation of Au(I) and form a gold-carbon bond at the same time is to use carbocationic ligands that are able to accept electron density from Au(I), acting as latent Z-type ligands. This approach was exemplified by Wilkins *et al.* who showed that xanthene-based phosphine Au(I) complexes **141** react with alkylammonium salts to form the (P<sup>+</sup>C)Au chelate **142** (Scheme 43). The same complex was obtained starting from the corresponding triphenylcarbinol and (THT)AuCl in the presence of HCl.<sup>312</sup>

#### Scheme 43. Oxidative Au-C Bond Formation Via Carbocations

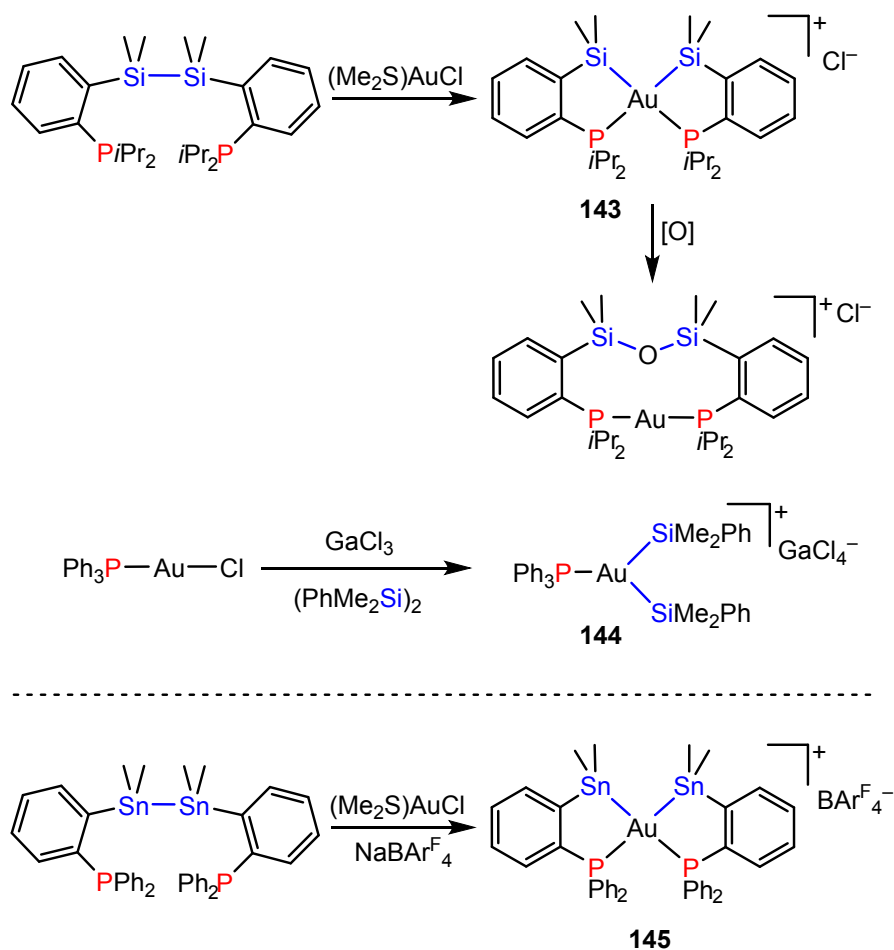


Non-carbon compounds with apolar E–E bonds were also found to oxidatively add to Au(I). The reversible oxidative addition of aryl disulfides to colourless [Au(SAr)<sub>2</sub>]<sup>+</sup> to give red [Au(SAr)<sub>4</sub>]<sup>+</sup> anions (Ar = C<sub>6</sub>F<sub>5</sub>, C<sub>6</sub>H<sub>4</sub>) was described by Bachman *et al.* in 2008; all three reagents are in equilibrium.<sup>313</sup> Gualco *et al.* reported in 2011 the first example of intramolecular oxidative addition of a Si–Si bond to Au(I), using diphosphine disilanes as ligating substrates (Scheme 44).<sup>314</sup> In 2012, the same authors showed that the obtained Au(III) bis-silyl complex **143** can react with adventitious H<sub>2</sub>O or O<sub>2</sub> under oxygen insertion and elimination of a Si–O–Si unit, by following an unprecedented Au(I)/Au(III) redox sequence.<sup>315</sup> In 2014, Joost *et al.* could show that oxidative addition of Si–Si bonds can occur also intermolecularly on triphenylphosphine Au(I) cations (Scheme 44).<sup>316</sup> Low-temperature NMR studies indicated that mixtures of Ph<sub>3</sub>PAuCl and GaCl<sub>3</sub> react with the disilane PhMe<sub>2</sub>Si–SiMe<sub>2</sub>Ph to give the Au(III) disilyl complex **144**. Calculations showed that the three-coordinate salt **144** was just slightly (3 kcal/mol) more stable than a square

complex with an associated  $\text{GaCl}_4^-$  anion. However, this compound is not thermally stable and decomposes above  $-60^\circ\text{C}$ .

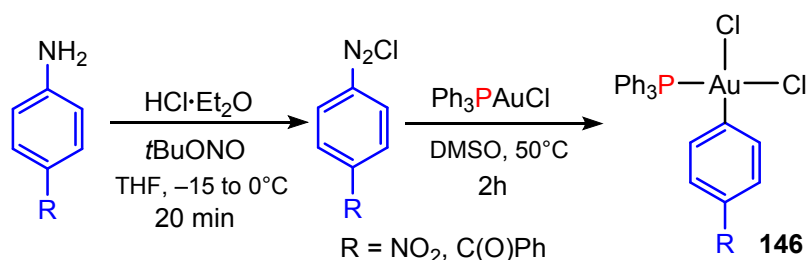
By using the same strategy shown for **143**, oxidative addition of an Sn–Sn bond has been achieved by Lassauque et al. to produce the Au(III) derivative **145**.<sup>317</sup> This reactivity was exploited later to develop a gold-catalyzed catalytic bis-stannylation of propiolates.<sup>318</sup>

#### Scheme 44. Oxidative Addition of Si–Si and Sn–Sn Bonds



Porcel and co-workers showed that aryldiazonium chloride salts oxidatively add to Au(I) precursors when heated.<sup>319</sup> Indeed, *para*-nitro and *para* benzoyl benzene diazonium chlorides afford the corresponding Au(III) aryl dichloro complexes **146** when stirred with  $\text{Ph}_3\text{PAuCl}$  at  $50^\circ\text{C}$  for 2h (Scheme 45). The thermally stable complexes **146** were characterized by X-Ray crystallography. This method was used in combination with silver acetylides to develop a stoichiometric  $\text{C}(\text{sp}^2)$ – $\text{C}(\text{sp})$  coupling reaction.

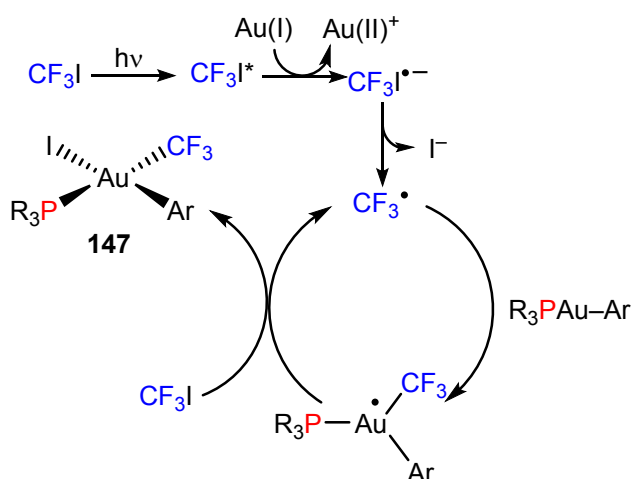
#### Scheme 45. Oxidative Addition of aryldiazonium chloride salts to Au(I)



A follow-up study revealed that oxidative addition of aryldiazonium chloride salts to Me<sub>2</sub>SAuCl or Ph<sub>3</sub>PAuCl can be catalyzed by substoichiometric amounts of ascorbic acid as a radical initiator.<sup>320</sup> This strategy was used to develop a stoichiometric arylation of indoles under mild conditions, with a good tolerance of functional groups on both indole and diazonium salt. EPR, DFT and electrochemical studies supported a mechanistic scenario where the oxidative addition occurs through a double one-electron oxidation pathway, where initially the Au(I) precursor is oxidized by an aryl radical to an Au<sup>II</sup>-aryl species, which then reacts with further diazonium salt to generate the Au<sup>III</sup> aryl dichloride.

**3.1.3 Photo-Assisted Oxidative Addition Reactions.** The application of radicals as oxidants in gold catalysis has emerged as a powerful strategy for realizing cross-coupling reactions without using sacrificial oxidants (See section 4.1.2). Several studies showed that clean oxidative addition to Au(I) can be achieved under photo-assisted conditions, either photo-initiated or requiring constant irradiation. One of the most important cases is the formation of gold trifluoromethyl complexes, which find potential application in trifluoromethylation catalysis. CF<sub>3</sub>-substituted compounds play an important role as pharmaceuticals.<sup>174</sup> Their formation, structures and reactivity has been reviewed, including their formation by oxidative addition.<sup>321</sup> Trifluoromethyl halides are suitable substrates for oxidative addition to Au(I), as originally reported by Puddephatt in the 1970s, who suggested the contribution of an odd-electron pathway involving CF<sub>3</sub> radicals.<sup>267</sup> In 2014, Winston *et al.* reinvestigated this chemistry and found that phosphine Au(I) aryl derivatives undergo oxidative addition of CF<sub>3</sub>I when exposed to UV light.<sup>322</sup> This affords stable Au(III) (trifluoromethyl)(aryl) complexes **147**, which have been characterized spectroscopically and structurally (Scheme 46). Mechanistic investigations suggest that photochemical generation of CF<sub>3</sub> radicals initiates a chain reaction composed of two distinct single electron oxidations. In the first step Au(I) is oxidized to Au(II), which reacts with further CF<sub>3</sub>I to give **147** and restarts the chain. A similar mechanism was proposed by Gil-Rubio and co-workers for the oxidative addition of perfluoroalkyl iodides to LAuR complexes (L = PPh<sub>3</sub>, IPr; R = Me, Mes, alkynyl) under irradiation at 402 nm.<sup>323</sup>

**Scheme 46. Oxidative Addition of CF<sub>3</sub>I by a Photoinitiated Radical Pathway**

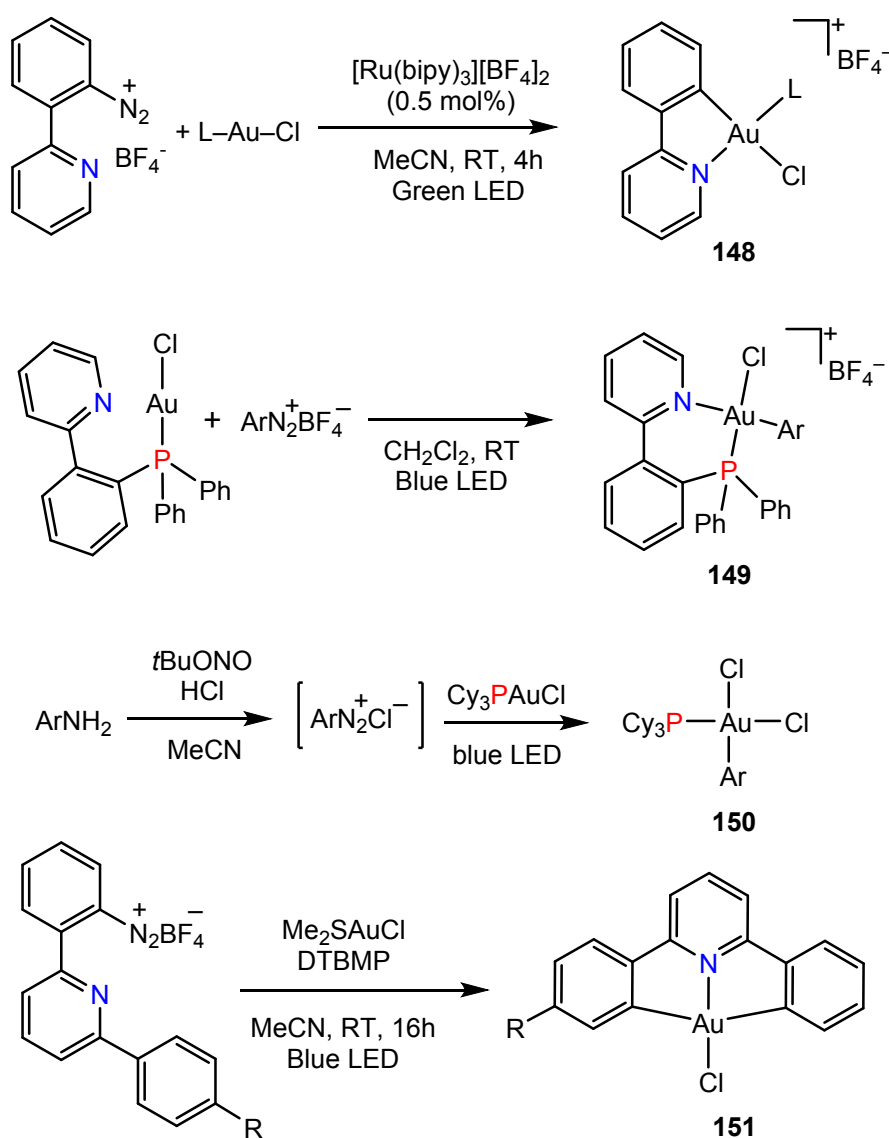


After the seminal work by the groups of Glorius and Toste (see Section 4), the oxidative addition of diazonium salts to linear Au(I) complexes has emerged as a powerful strategy to generate high-valent Au intermediates containing a metal-carbon bond that can participate in both stoichiometric and catalytic reactions. The same principle has been applied for developing new synthetic routes to stable Au(III) chelates, by following different approaches. Glorius *et al.* reported the oxidative addition of 2-(pyridin-2-yl)phenyldiazonium salts to a series of Au(I) chloride complexes having phosphine or NHC ligands, to generate stable (C<sup>^</sup>N)Au(III) chelates **148**.<sup>324</sup> In this particular case, oxidative addition is triggered by photoredox catalysis with [Ru(bipy)<sub>3</sub>][BF<sub>4</sub>]<sub>2</sub> under visible light irradiation ( $\lambda_{\text{max}} = 525 \text{ nm}$ ). Mechanistically, the reaction is thought to proceed by two distinct single-electron transfer (SET) steps: First, an aryl radical, generated by the reaction of the diazonium salt and the excited state of the photocatalyst, oxidizes the Au(I) precursor to give a (C<sup>^</sup>N)Au(II) transient. This Au(II) species then reacts with further equivalents of the diazonium salts generating a chain reaction to give a Au(III) phenylpyridyl complex and more aryl radicals (Scheme 47). Alternatively, the oxidized form of the photocatalyst can oxidise Au(II) to Au(III) and regenerate the original Ru(II) species.<sup>324</sup>

Concurrently, Hashmi and co-workers reacted pre-formed Au(I) complexes of potentially hemilabile phosphino-pyridine or phosphino-quinoline ligands with aryldiazonium salts to generate a broad range of (P<sup>^</sup>N)Au(III) aryl complexes **149** (Scheme 47).<sup>325</sup> These reactions proceeded smoothly under blue light irradiation and in the absence of a photocatalyst. The method proved to be very general and was extended to aryldiazonium salts prepared *in situ* from the corresponding anilines. By using aryldiazonium salts having a coordinating counterion, such as Cl<sup>-</sup>, the interception of thermally stable non-chelate Au(III) aryl complexes **150** was achieved by using Cy<sub>3</sub>PAuCl as starting material. The *cis*-configuration of the two Cl ligands was confirmed by X-Ray crystallography.

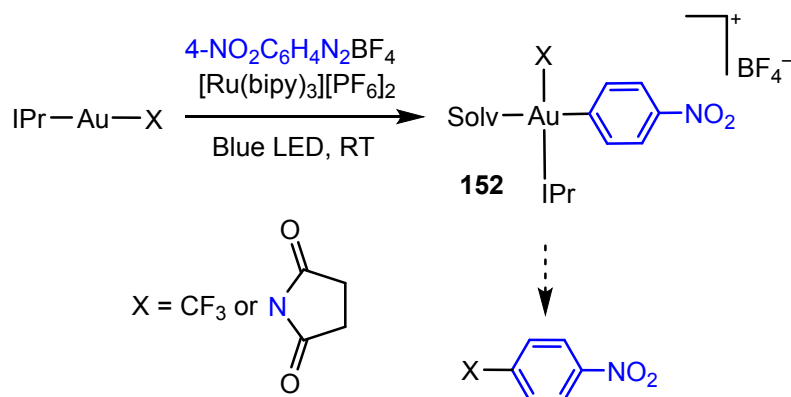
Very recently, Hashmi and co-workers have used aryldiazonium salts to generate (C<sup>^</sup>N<sup>^</sup>C)Au(III) pincer complexes **151**, offering a synthetic route that is alternative to the traditional mercuration/transmetalation strategy.<sup>239</sup> Similarly to the previous cases, the diazonium salt reacts under direct irradiation with blue light and does not require a photosensitizer to be activated. The oxidation of Au(I) generates a (C<sup>^</sup>N)Au(III) intermediate, where the C–H activation of the pendant aryl is triggered by a strong base such as 2,6-di-*tert*-butyl-4-methylpyridine (DTBMP) (Scheme 47), in line with previous reports on Au(III)-C bond formation by Rocchigiani *et al.*<sup>170</sup>

### Scheme 47. Generation of Au(III) Complexes by Oxidative Addition of Diazonium Cations under Photoassisted Conditions



The mechanism suggested by Glorius was also proposed by Kim and Toste, who have investigated the photoredox-initiated C–C and C–N coupling with Au(I) precursors. By using IPr-based Au(I) trifluoromethyl and succinimide complexes, it proved possible to trap Au(III) intermediates **152** as H<sub>2</sub>O or CH<sub>3</sub>CN solvates and to characterize them by X ray diffraction (Scheme 48).<sup>326</sup>

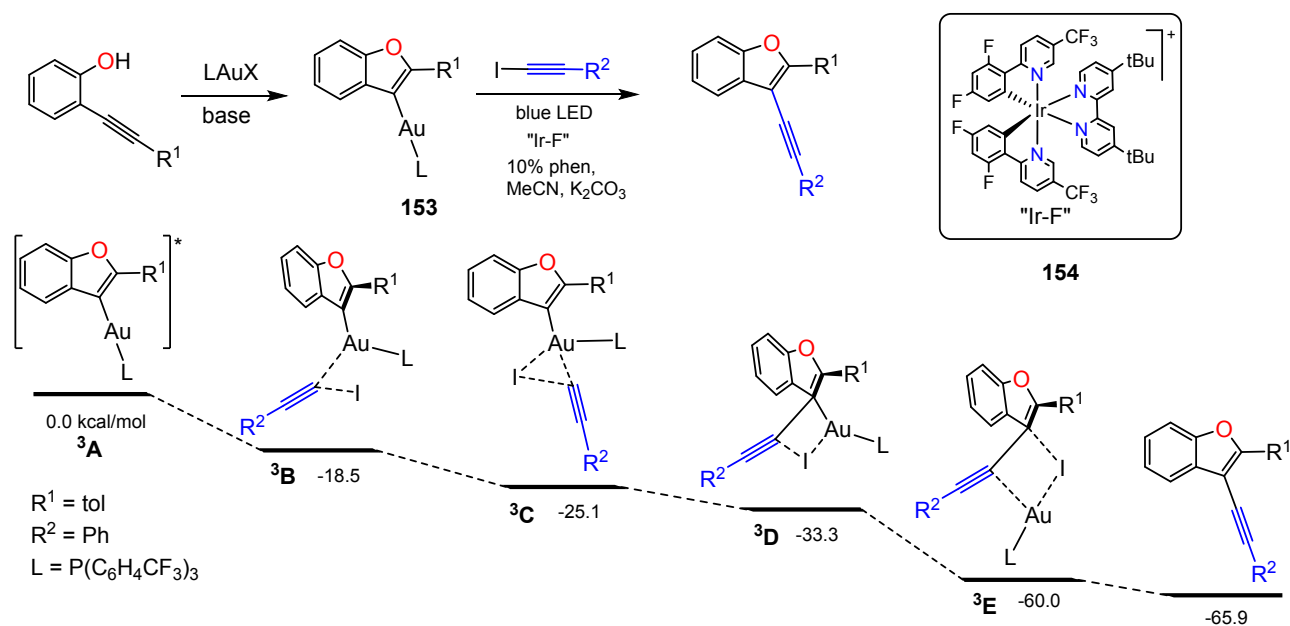
#### Scheme 48. Photocatalytic Formation of Stable Au(III) Aryl Intermediates



Whereas the previous mechanisms have always assumed an oxidation of the gold center to Au(III) under photocatalytic conditions, in 2019 Fensterbank and co-workers were able to show that this may not necessarily be so, and that alternative pathways and geometries may prevail in photoexcited states.<sup>327</sup> Investigating the possibility of oxidative addition of 1-iodoalkynes to the vinyl gold(I) precursor **153** under blue LED excitation, they obtained best results with an iridium(III) sensitizer, [Ir{dF(CF<sub>3</sub>)ppy}<sub>2</sub>(dtbbpy)]PF<sub>6</sub> (“Ir-F”, **154**), which, unlike [Ru(bipy)<sub>3</sub>]<sup>2+/3+</sup>, is not redox-active. Instead, on irradiation the Ir complex is promoted to the triplet state, followed by fast energy transfer to the gold complex to give <sup>3</sup>[LAuCl], i.e. the gold complex acts as luminescence quencher of Ir. In fact the triplet Au complex thus generated appears to function as relay for the energy transfer to the alkyne, generating <sup>3</sup>[I-C≡CAr]. This excited alkyne adopts a bent geometry, which facilitates C–C bond formation and iodine transfer to gold. Exploring the triplet energy surface computationally ruled out ground-state oxidative addition of the iodoalkyne to form a gold(III) alkynyl complex. Instead, a lower-energy pathway exists where the alkynyl ligand slips into position prior to formation of the C–C bond in the final coupling step. The transition state energies between these structures are all quite low and the process is energetically downhill (Scheme 49). Intermediate <sup>3</sup>C, with the two organic ligands in *trans* position, comes close to an Au(III) state. The yield is increased by the presence of 10 mol-% of 1,10-phenanthroline, although its function is not clear.<sup>327</sup>



### Scheme 49. C-C Bond Formation Via a Photoexcitation Triplet-State Cascade



## 3.2 Reductive Elimination Reactions

Reductive elimination, the reverse of oxidative addition, is the product-forming step of many metal-catalyzed cycles. Generally, reductive elimination is assumed to be extremely efficient for  $d^8$  complexes of groups 10-11 and  $d^6$  configuration of groups 9-10, for which various mechanisms are available.<sup>262-264</sup> Au(III) fits well into this family and its ability to engage in reductive decomposition processes has been known for more than 80 years.<sup>328</sup> In the 1970s, pioneering work by Kochi and Tobias started to address mechanistic aspects of reductive elimination from Au(III) di- and tri-methyl complexes, which produced ethane upon warming.<sup>329-331</sup> Further work by Komiya extended the investigation to other alkyl and aryl derivatives, providing the basis of the first rationale for C–C reductive elimination from Au(III).<sup>332</sup>

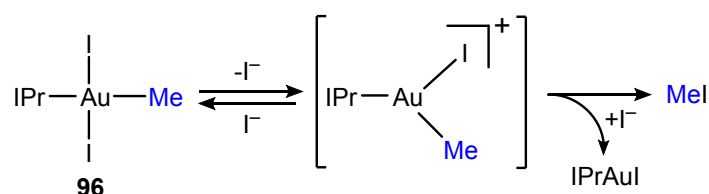
With the extensive development of redox gold catalysis, reductive elimination from high-valent gold centres has attracted growing interest. This section provides a description of recent advances in the understanding of reductive eliminations from well-defined Au(III) complexes, leading to C–heteroatom and C–C bond formation, and of their potential for catalytic applications.

**3.2.1 C–Halide Reductive Eliminations.** Carbon-halide reductive elimination is usually considered as a side-reaction that deactivates coupling catalysts and has not attracted as much attention as reductive C–C bond formation. In an early example, Aresta and Vasapollo showed that *trans*  $\text{Ph}_3\text{PAu}(\text{Br})_2(\text{Ar})$  complexes decompose with reductive C–Br elimination to give bromoarenes.<sup>333</sup> C–X elimination is of course important as a method of forming C–F bonds and in

the mechanistic understanding of catalyst deactivation, and a number of studies has been reported recently.

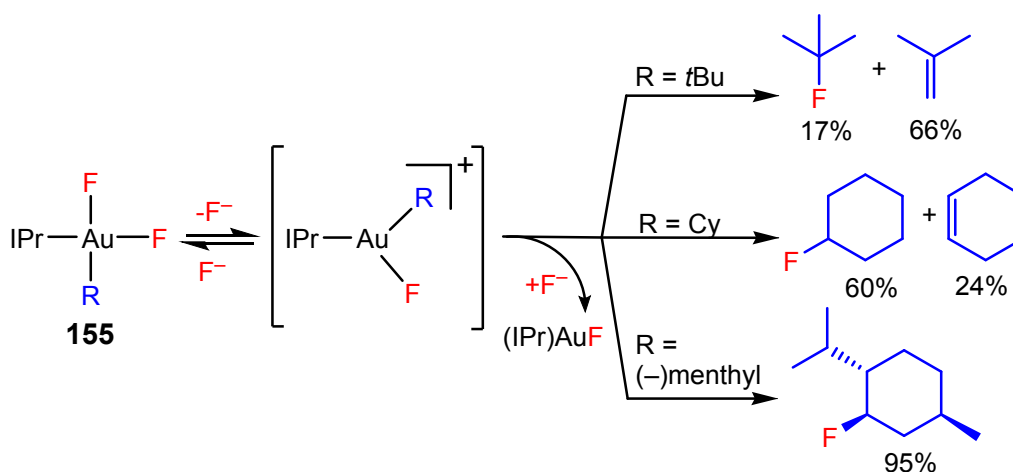
A detailed study on C(sp<sup>3</sup>)-I coupling was carried out by Scott *et al.* on complex **96** (see Section 3.1.1), which was found to release readily MeI in solution immediately after its formation.<sup>250</sup> The mechanism of this reaction was proposed to involve loss of iodide from **96** to form a 3-coordinate species, which then decomposes by intramolecular reductive MeI elimination (Scheme 50). Consistent with this, the addition of external iodide salts was found to slow down the decomposition rate of **96**.

#### Scheme 50. Reductive Elimination of MeI



Following up on their previous work on the oxidation of NHC gold(I) species with XeF<sub>2</sub>,<sup>249</sup> Mankad and Toste investigated the reductive decomposition of *cis*-Au(III) difluoro alkyls **155**.<sup>251</sup> These species readily decompose with reductive C-F elimination to give the expected fluoroalkanes. However, the fluorination of the sp<sup>3</sup> carbon was found to be competitive with the formation of olefins due to β-H elimination of the alkyl groups. The outcome of the reaction was controlled by the steric bulk of the alkyl group, and higher fluorination yields were obtained when cyclohexyl or menthyl derivatives were employed (Scheme 51). Systems lacking in β-H atoms undergo competitive carbocationic rearrangements, still competitive with C-F bond formation. In line with the previous results by Scott *et al.*,<sup>250</sup> C-I reductive elimination was found to be much easier after oxidation of (IPr)Au alkyl derivatives with I<sub>2</sub> and outperformed β-H elimination and carbocationic rearrangements. Mechanistically, both C-F reductive elimination and side-reactions were thought to occur via a 3-coordinated intermediate, formed upon dissociation of one F<sup>-</sup> ion from Au.

#### Scheme 51. Reaction Pathways in Reductive C-F Eliminations



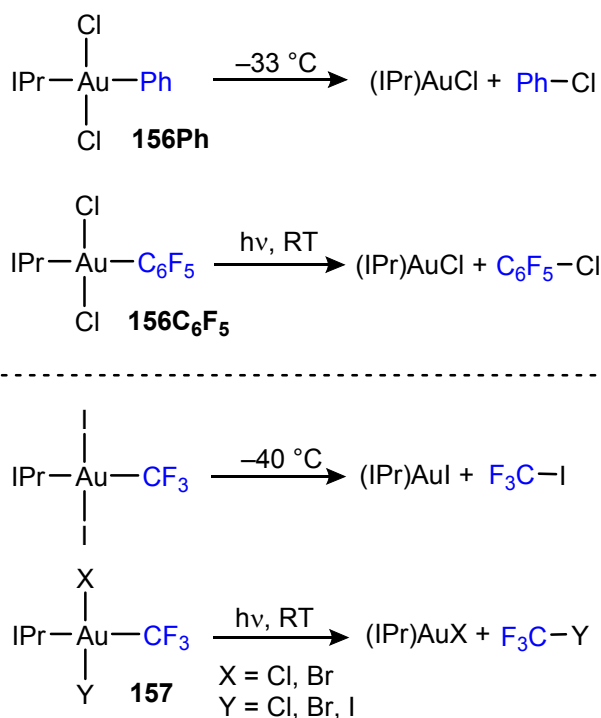
Ghidiu *et al.* investigated C–Cl bond formation from  $(\text{IPr})\text{AuCl}_2\text{Ar}$  complexes **156** ( $\text{R} = \text{Ph}$ ,  $\text{C}_6\text{F}_5$ ) and concluded that the nature of the aryl group dictates the mechanistic course of the reductive elimination.<sup>292</sup> In the case of the phenyl derivative, C–Cl reductive elimination is fast and follows a thermal pathway. In the case of the pentafluorophenyl complex **156C<sub>6</sub>F<sub>5</sub>**, no reductive elimination occurred at high temperatures; formation of  $\text{C}_6\text{F}_5\text{Cl}$  and  $(\text{IPr})\text{AuCl}$  was however observed upon UV irradiation, thus suggesting a photochemical route to reductive elimination. This striking difference between phenyl and pentafluorophenyl was ascribed to the increased electrostatic interaction between the chlorides and the metal in **156C<sub>6</sub>F<sub>5</sub>**, which, in turn, increases the reductive elimination barrier. This assumption agrees with the electrochemical data, which showed a strong increase in the redox potential of the  $\text{Au}^{\text{I}}/\text{Au}^{\text{III}}$  couple, from 1.77V for  $(\text{IPr})\text{AuPh}$  to 1.93V for  $(\text{IPr})\text{AuC}_6\text{F}_5$ .

Similar results were reported by Blaya *et al.*, who investigated the reactions of  $(\text{IPr})\text{AuCF}_3$  with different oxidants such as  $\text{PhICl}_2$ ,  $\text{Br}_2$ ,  $\text{ICl}$  and  $\text{I}_2$  and found that the stability towards reduction is notably affected by the halide.<sup>334</sup> Oxidation with  $\text{I}_2$  gave the Au(III) *trans*-diiodide which was stable only at very low temperatures and underwent thermal reductive elimination of  $\text{CF}_3\text{I}$ . In the case of the other halides, *trans*-dihalide Au(III) trifluoromethyl complexes **157** are thermally stable but reductively eliminate  $\text{CF}_3\text{Br}$  and  $\text{CF}_3\text{Cl}$  when exposed to UV light (Scheme 52).

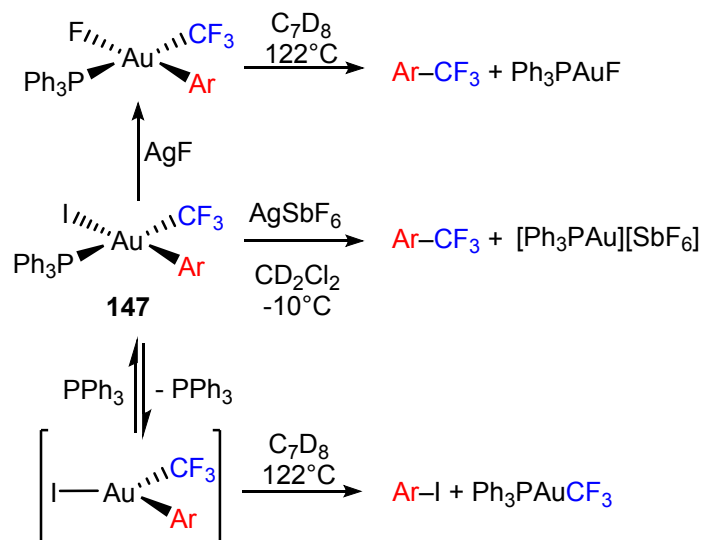
Photoinitiated reductive elimination from perfluoroalkyl Au(III) complexes was investigated by Portuguès *et al.*<sup>323</sup> In line with the previous results on trifluoromethyl derivatives, perfluoroalkyl iodides were found to oxidatively add to  $\text{LAuR}$  complexes ( $\text{L} = \text{PPh}_3$ ,  $\text{IPr}$ ;  $\text{R} = \text{Me}$ ,  $\text{Mes}$ , alkynyl) under irradiation at 402 nm and afforded Au(III) complexes with variable stability. In the case of  $\text{L} = \text{PPh}_3$  and  $\text{R} = \text{Mes}$ , Au(III) perfluoroalkyl complexes were isolated and characterized by X-Ray crystallography. However, it was found that they decompose under irradiation at  $\lambda = 402$  nm affording complex mixtures containing Au(I) iodide and perfluoroalkyl, mesitylene and  $\text{MeSI}$ .

Irradiation in the presence of radical traps revealed that the decomposition follows a radical mechanism, in analogy to what was proposed for the photoinitiated oxidative addition (see Section 3.1.3). Reductive elimination from alkynyl and methyl complexes occurred faster and no stable Au(III) complex could be isolated.<sup>323</sup>

### Scheme 52. Reductive C-Halide Eliminations



Winston *et al.* investigated the reductive decomposition of Au(III) trifluoromethyl aryl halides **147** formed upon photochemical oxidative addition of  $\text{CF}_3\text{I}$ .<sup>322</sup> For these species, two distinct reductive elimination events were observed, depending on the experimental conditions. Upon halide abstraction, fast and quantitative C–C reductive elimination to give trifluoromethyl arenes was observed. In contrast, heating **147** to 110 °C in toluene led to C–I reductive elimination, generating iodoarenes and  $\text{Ph}_3\text{PAuCF}_3$ . A systematic study on the halide effect revealed that moving from iodide to fluoride increased the rate of C–C reductive elimination versus C–X, to the point that, when X = F, trifluoromethyl arenes are the only products observed.<sup>335</sup> This seemed to indicate a correlation between Au–X bond strength and the preference for C– $\text{CF}_3$  reductive elimination. Reductive elimination from **147** was suggested to follow  $\text{PPh}_3$  dissociation, to give a reactive 3-coordinate transient intermediate which has a low barrier towards reductive elimination (Scheme 53). In the case of X = Br or Cl, it was proposed that  $\text{Ph}_3\text{PAuCF}_3$  formed *in situ* could reversibly coordinate to the latter intermediate and give rise to an autocatalytic accelerated reductive elimination mechanism.

Scheme 53. C-Halide Versus C-CF<sub>3</sub> Elimination

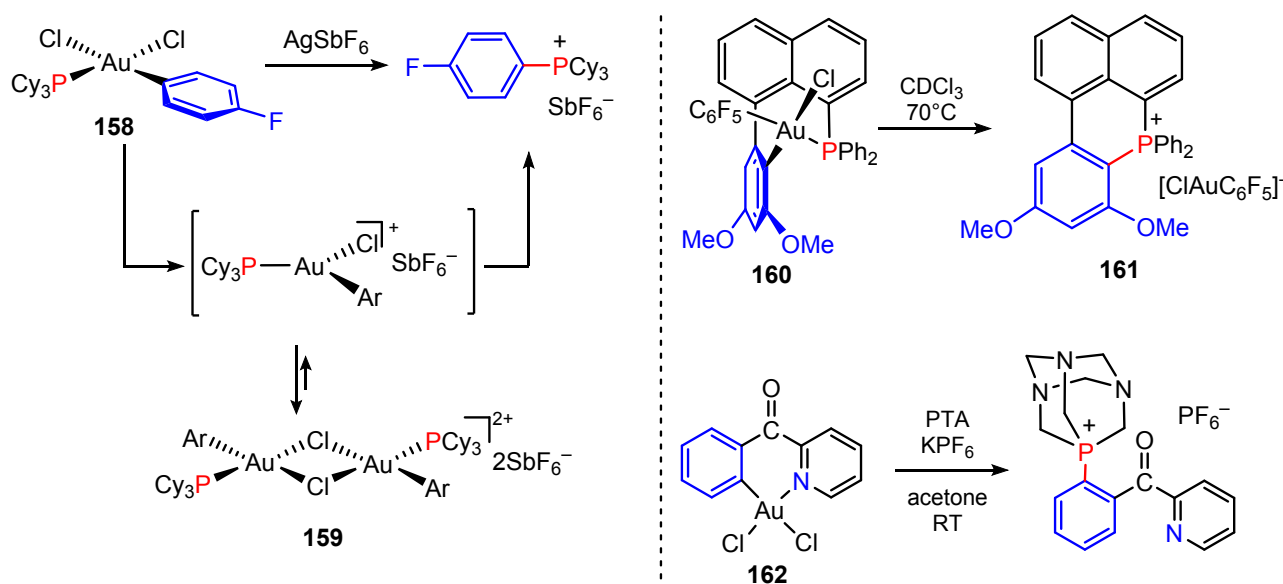
C-X vs. C-CF<sub>3</sub> elimination was addressed in detail by theoretical work by Datta and co-workers.<sup>336</sup> In the absence of autocatalytic effects, aryl-CF<sub>3</sub> reductive elimination from Ph<sub>3</sub>PAuCF<sub>3</sub>(X)(Aryl) complexes of type **147** (X = F, Cl, Br, I) showed the lowest reductive elimination barrier for all the halides. On the other hand, the autocatalytic pathway showed an increasing preference for C-CF<sub>3</sub> on moving from X = I to X = F, thus confirming that product selectivity is dictated by the ability of Au(III) intermediates to establish bridging halide interactions.

**3.2.2 Reductive C-E (E = P, N, S) Bond Formation.** The examples of C-halide reductive elimination discussed above indicate that the choice of ancillary ligands acting as good leaving groups is key for lowering the reaction barrier and tweak the selectivity. Generally, it appears that ligands which interact more strongly with the metal have a higher tendency to be reductively eliminated. Surprisingly, this was also the case for neutral L ligands such as phosphines.

Kawai *et al.* reported that phosphine Au(III) aryl derivatives can indeed undergo P-C reductive elimination.<sup>337</sup> The stable tricyclohexylphosphine complex **158**, obtained upon oxidation of the corresponding Au(I) salt with PhICl<sub>2</sub>, reacts with silver salts to give gold nanoparticles together with arylphosphonium salts as the only reaction products (Scheme 54). The reaction is thought to proceed, once again, through a 3-coordinate intermediate, which was too unstable to be isolated. Low-temperature NMR and trapping experiments provided evidence for the formation of a reaction intermediate immediately after halide abstraction, to which the dimeric structure **159** was assigned. In the case of the neutral complex **160** P-C reductive elimination occurred intramolecularly, to give ion pair **161** containing a cyclic phosphonium cation. Interestingly, this reaction was found to accelerate when coordinating solvents or PPh<sub>3</sub> were added to the reaction

1  
2  
3 mixtures. This was tentatively associated with the formation of a 5-coordinate intermediate, even  
4 though no structural information about the latter could be obtained. P–C reductive elimination of  
5 phosphines has been used extensively in catalytic studies to prove the intermediacy of Au(III)  
6 species in redox protocols (see Section 4.1.2).  
7  
8  
9

### 10 11 12 Scheme 54. Reductive C–P Eliminations

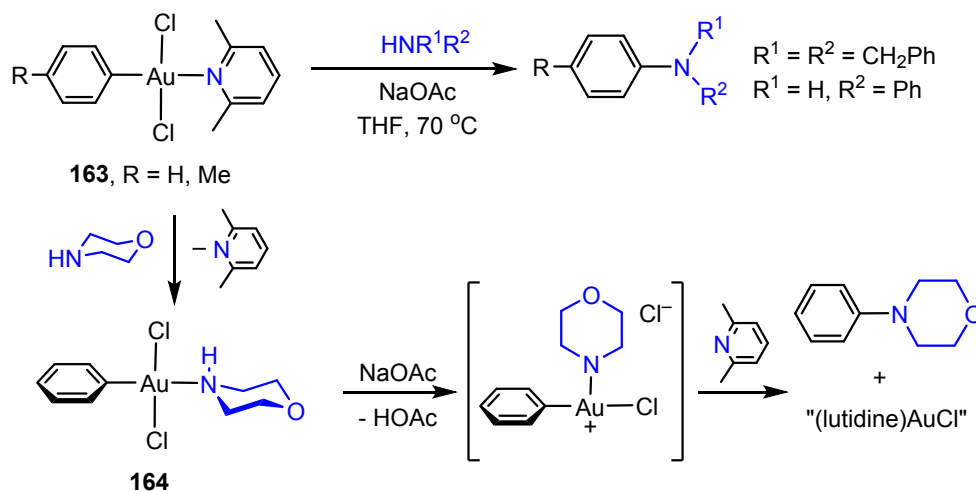


Another example of P–C reductive elimination was described by Bonsignore *et al.*, as the product of the reaction of the benzoyl-pyridine gold complex **162** with 1,3,5-triaza-7-phosphaadamantane (PTA) in the presence of KPF<sub>6</sub> (Scheme 54).<sup>338</sup> The reaction requires excess PTA (3 equiv) to achieve full conversion, likely because the cationic (C<sup>+</sup>N)AuCl(PTA) complex forms as a first intermediate and then further PTA can displace the pyridine ligand and initiate C–P bond formation, affording the corresponding phosphonium salt.

Catalytic C–N coupling reactions by gold(III) have emerged over the past 15 years as efficient system for the synthesis of functionalized amines. Earlier examples used gold(III) as a Lewis acid to catalyse nitrene insertion-type reactions,<sup>285,339</sup> while C–N reductive elimination processes appeared later in the literature. In 2010, Limbach and co-workers prepared complexes **163** from ArH and AuCl<sub>3</sub>, followed by capturing the product as the lutidine adduct. These are stable in refluxing THF in the absence of base but on addition of amines HNR<sup>1</sup>R<sup>2</sup> in the presence of acetate the reductive elimination products Ar–NR<sup>1</sup>R<sup>2</sup> are formed in high yield. Mechanistic studies showed that the amine displaces lutidine; the formation of the morpholine adduct, *trans*-PhAuCl<sub>2</sub>{HN(C<sub>2</sub>H<sub>4</sub>)<sub>2</sub>O} (**164**) was confirmed by X-ray diffraction. Heating this complex in the presence of acetate gives *N*-phenylmorpholine and gold(I) products. The acetate is likely to

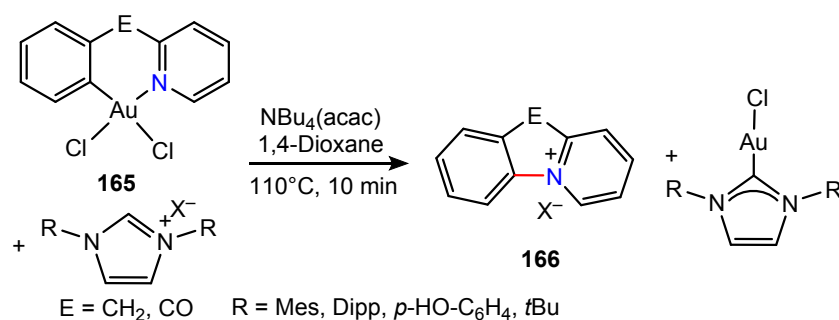
deprotonate the coordinated amine to give a putative T-shaped *cis*-(aryl)(amido) intermediate, with the required stereochemistry for reductive elimination (Scheme 55). No evidence for acetate coordination to gold was found.<sup>340</sup>

### Scheme 55. Reductive C-N Eliminations



More recently, Kim *et al.* reported another example of intramolecular C–N reductive elimination from the benzyl- or benzoyl-pyridine (C<sup>^</sup>N) chelates **165**, which were found to react with imidazolium salts at high temperature affording (NHC)AuCl and cyclic pyridinium salts **166** (Scheme 56).<sup>341</sup> The same result was obtained by reacting **165** with chelating diphosphines. The reaction was proposed to be initiated by the coordination of the carbene generated *in situ* from the imidazolium salt. This would afford an unstable cationic (C<sup>^</sup>N)Au(III)NHC adduct, from which fast intramolecular C–N reductive elimination takes places. Kinetic analysis of the reaction profile suggested a rate determining step with a rather low activation enthalpy ( $\Delta H^\ddagger = 6.3$  kcal/mol) and a negative activation entropy ( $\Delta S^\ddagger = -44$  e.u.), supporting the associative mechanism.

### Scheme 56. Reductive Elimination of Pyridinium Salts



1  
2  
3 In 2014 the first example of a C–S reductive elimination from Au(III) was described by  
4 Kung *et al.*, who reacted Au(III) C<sup>^</sup>N chelates **167** with N-acetyl-cysteine to give the thioether **168**  
5 (Scheme 57).<sup>342</sup> The efficiency of C–S bond formation was found to depend on the cyclometalated  
6 ligand: 6-membered auracycles **167** reacted readily, while the 5-membered auracycle derived from  
7 2-phenyl pyridine did not undergo reductive elimination. This agrees with the general concept that  
8 more rigid cyclometalated 5-ring structures are more stable towards reductive elimination. This  
9 stoichiometric C–S coupling was further extended to polypeptides and proteins containing thiol  
10 units, thus unlocking a new method for the selective modification of important biomolecules.  
11  
12  
13  
14  
15  
16

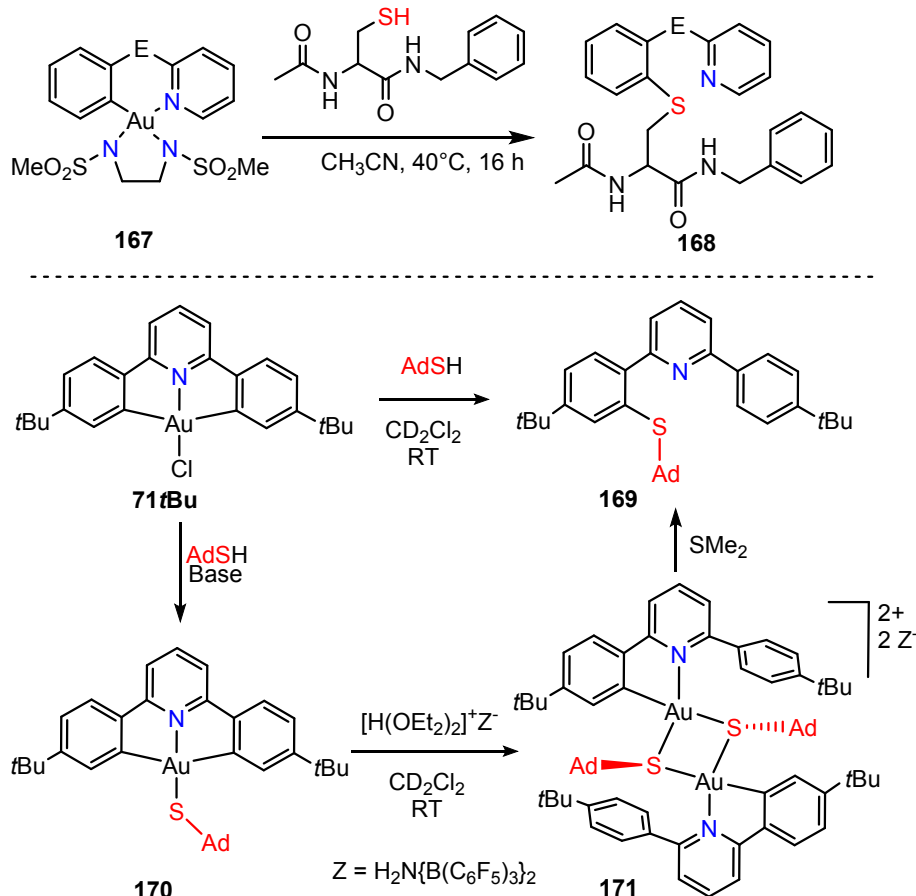
17 In 2018, Currie *et al.* reported that reaction of (C<sup>^</sup>N<sup>^</sup>C) pincer Au(III) chloride complexes  
18 **71tBu** with adamantane thiol led to the formation of the C–S elimination product **169**.<sup>343</sup> This is in  
19 striking contrast with previous results obtained by the same authors, who showed that the same  
20 reactions performed in the presence of a base led to the formation of thermally stable Au(III)  
21 thiolates **170**.<sup>344</sup> The reaction mechanism was probed extensively by kinetic experiments. The  
22 reaction starts with the protodeauration of one Au–C bond to generate a C<sup>^</sup>N chelate, followed by  
23 the displacement of the N donor by a second equivalent of thiol, which then triggers the C–S  
24 reductive elimination. The same reactivity was observed in a stepwise manner, starting from the  
25 neutral thiolate complex **170**. Upon reacting **170** with the strong acid [H(OEt<sub>2</sub>)<sub>2</sub>][H<sub>2</sub>N{B(C<sub>6</sub>F<sub>5</sub>)<sub>3</sub>}<sub>2</sub>],  
26 the bridged thiolate complex **171** could be isolated and characterized by X-Ray diffraction. The  
27 addition of SME<sub>2</sub> to this complex triggered reductive elimination to give **169** (Scheme 57).  
28  
29  
30  
31  
32  
33  
34  
35

36 Further mechanistic studies on this system revealed that C–S reductive elimination was  
37 feasible only starting with (C<sup>^</sup>N<sup>^</sup>C)AuX complexes, where X = Cl or SR. When using pincer  
38 complexes X = Me, aryl or acetylidyde, the addition of thiols triggered C–C rather than C–S reductive  
39 elimination, thus validating the hypothesis that ligands able to establish stronger bonds with Au(III)  
40 are more susceptible of being reductively eliminated.<sup>343</sup>  
41  
42  
43  
44  
45

#### 46 **Scheme 57. Reductive C-S Elimination**

47  
48  
49  
50  
51  
52  
53  
54  
55  
56  
57  
58  
59  
60



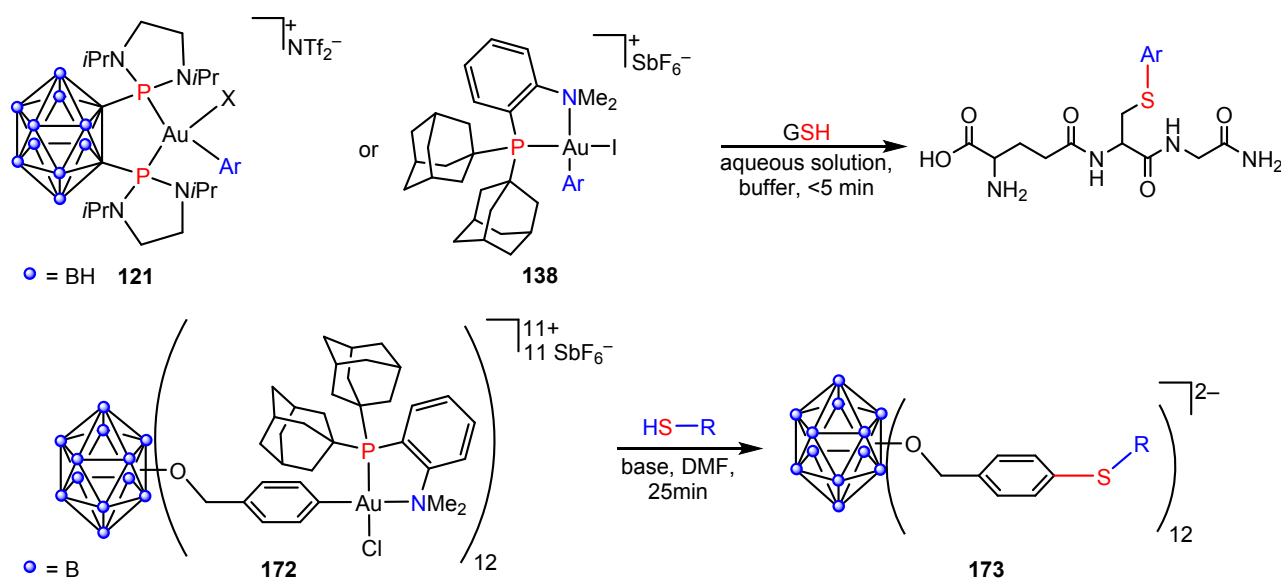


In 2018 Messina *et al.*<sup>345</sup> investigated cysteine bioconjugation of several peptides and proteins using the chelates **121** and **138** developed by Amgoune and Bourissou<sup>303,309</sup> (Scheme 58). These cationic Au(III) aryl derivatives were found to react very fast with glutathione (<5 min) and tolerated a broad range of pH conditions, thus broadening the bioconjugation scope with respect to the previous species reported by Kung *et al.*<sup>342</sup> The possibility to synthesize a broad library of stable Au(III) aryl derivatives from iodoarenes gave the opportunity to tag complex proteins with fluorescent dyes, drugs and other biologically relevant fragments.<sup>345</sup> The reaction was modelled computationally by Zhang and Dong, who calculated the energy profile for a two-step mechanism involving (i) the formation of an Au(III) thiolate upon elimination of HCl and (ii) reductive C–S elimination from the 4-coordinate thiolate intermediate. The latter was suggested to be the rate limiting step. The high selectivity of S-arylation versus N- and O-arylation, was explained by the interplay between the acidity of the SH group and the thiophilicity of Au.<sup>346</sup>

Arylation of polypeptides by C–S coupling was also exploited by Wenzel *et al.*, who showed that (C<sup>^</sup>N)Au(III) chelates can be used for arylating cysteine fragments in zinc finger protein domains.<sup>347</sup> The peptide fragment bearing the cysteine is thought to displace the N donor in C<sup>^</sup>N chelates, affording Au(III) bis(thiolato) aryls, which then undergo fast C–S bond formation.

Very recently, Stauber *et al.* showed that C–S reductive elimination from Au(III) can also be exploited to precisely functionalize dodecaborane clusters decorated with (P<sup>^</sup>N)Au(III) complexes **172** (Scheme 58). These clusters were obtained by oxidative addition of iodoaryl-modified dodecaborane onto the Au(I) precursor. Reaction with thiols triggered C–S reductive elimination, to give the thioether-capped cluster **173**. This procedure tolerates a broad range of functional groups, ranging from aryl to alkyl and heterocyclic functionalities, and was used to generate a large library of clusters, including carbohydrate-tagged species.<sup>348</sup>

### Scheme 58. Reductive C-S Elimination from Au(III) Cations for Functionalization of Peptides or Polyboranes

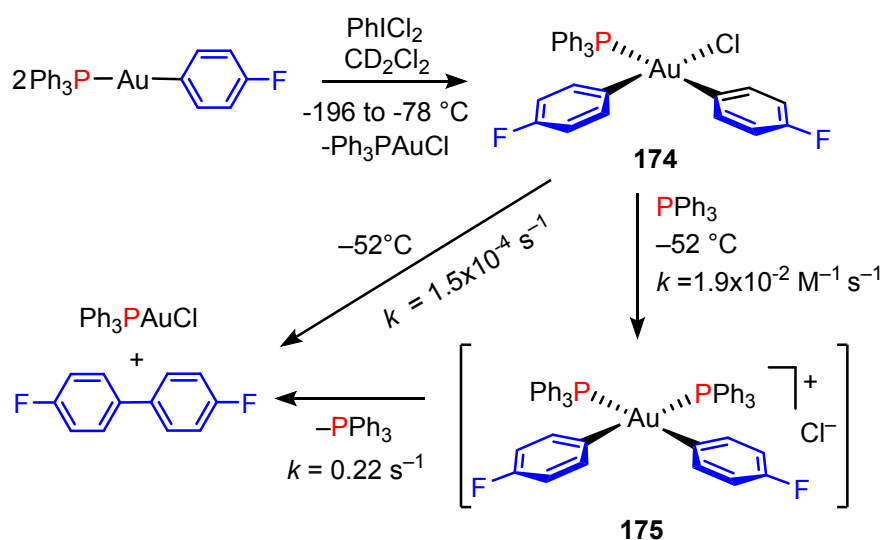


**3.2.3 C–C Reductive Elimination.** The ability of gold to reductively eliminate C–C bonds from Au(III) alkyl complexes has been known since the pioneering work by Tobias, Kochi and Schmidbaur.<sup>265,266,329-331</sup> These reactions were found to have significant barriers and required high temperatures to go to completion, thus competing with isomerization and ligand rearrangement processes. These elimination reactions were found to be inhibited by the addition of external phosphine ligands, indicative of a dissociative mechanism, in analogy with most of the cases presented before for C–X bond formation. Similarly, C(sp<sup>3</sup>)–C(sp<sup>2</sup>) couplings<sup>349</sup> were found to be rather slow and required high temperatures. C(sp<sup>2</sup>)–C(sp<sup>2</sup>) were shown to be faster.<sup>350</sup> However, the mechanistic details of these reactions received little attention for more than two decades.

In 2014, Toste and co-workers reported the generation of neutral *cis*-diarylgold(III) complexes **174** by partial oxidation of Ph<sub>3</sub>PAuAr with PhICl<sub>2</sub>, followed by fast transmetalation from residual starting material. Complex **174** was found to be thermally unstable and decomposed

readily to  $\text{Ph}_3\text{PAuCl}$  and 4,4'-difluorobiphenyl upon fast reductive elimination. Kinetic studies monitored by  $^{19}\text{F}$  NMR spectroscopy at  $-52^\circ\text{C}$  showed that the reaction was considerably accelerated by the addition of external triphenylphosphine, while it was not affected by the addition of chloride salts. This indicates that in the case of **174** reductive elimination takes place from a 4-coordinated square-planar species, in contrast with Kochi's finding on dimethyl Au(III) complexes. The addition of excess  $\text{PPh}_3$  to **174** was suggested to generate a spectroscopically not-observable cationic intermediate, *cis*- $[(\text{Ph}_3\text{P})_2\text{AuAr}_2]^+$  (**175**), from which reductive elimination takes place significantly faster than from neutral **174** (Scheme 59).<sup>351</sup> This exceptionally fast reductive elimination remains the highest C–C coupling rate measured so far for any metal.

### Scheme 59. Fast Reductive *p*-Fluorophenyl Elimination from Au(III)

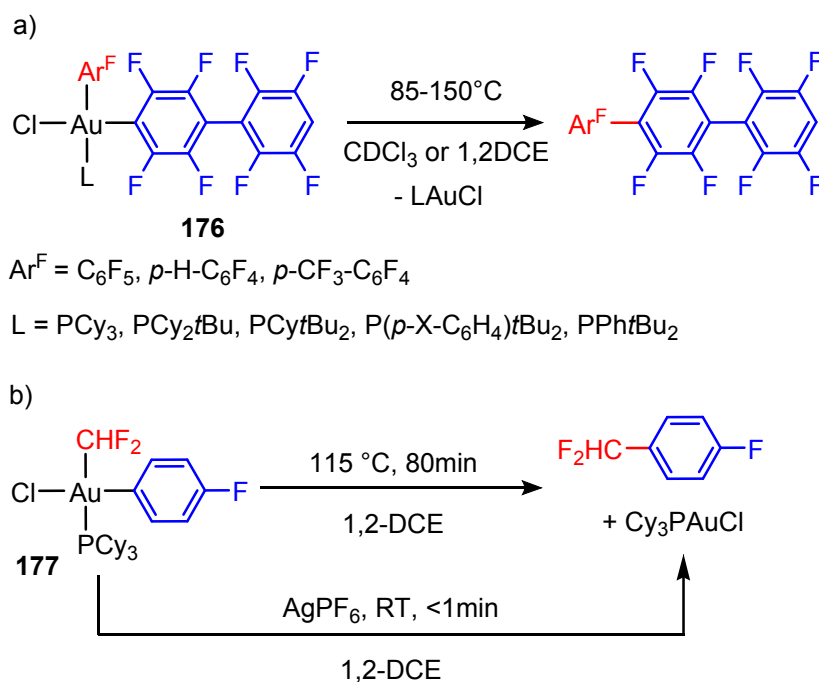


Kang *et al.* performed a systematic study on C–C reductive elimination from well-defined phosphine bis(fluoroaryl) Au(III) complexes **176** (Scheme 60a).<sup>352</sup> As already shown by Usón,<sup>269</sup> perfluorinated aryls are excellent for stabilizing Au(III), and a broad range of thermally stable bis-aryl complexes were isolated and crystallographically characterized. Thermolysis of **176** affords perfluorinated tris-arenes and phosphine Au(I) chloride. In agreement with the suggestions by Toste and co-workers,<sup>351</sup> reductive elimination of biaryls is thought to take place from a 4-coordinated intermediate, where the steric hindrance of the phosphine ligands plays a much more important role than electronic effects. On the other hand, electron-withdrawing aryl groups are eliminated more slowly than more electron-donating ones.

The same approach was then extended to aryl-difluoromethyl C–C coupling reactions from the neutral complex **177** (Scheme 60b).<sup>353</sup> The latter is stable at room temperature and, as in the case of **176**, undergoes C–C reductive elimination at high temperatures. By contrast,

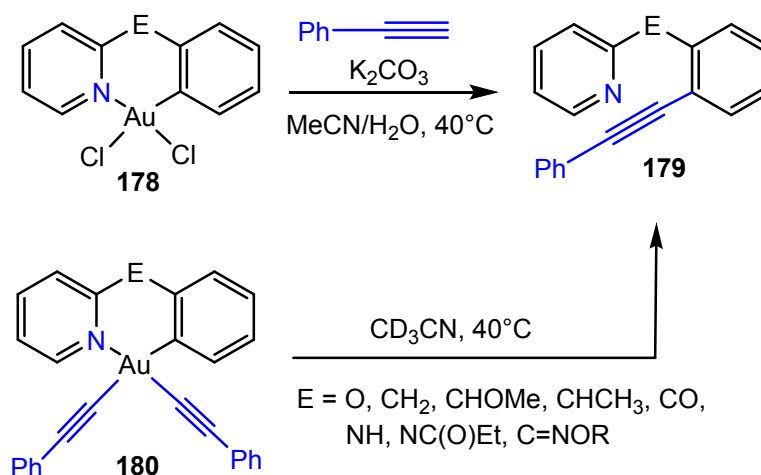
difluoromethylation is fast and quantitative at room temperature when a silver salt is used to abstract the chloride ligand from **177**. Contrary to what was observed by Toste and co-workers for the reductive aryl trifluoromethylation,<sup>335</sup> the rate of elimination from **177** is slightly accelerated by the addition of 1 equivalent of PCy<sub>3</sub>. This implies that there is no phosphine ligand dissociation to generate a 3-coordinated intermediate, which is in line with expectation given the presence of electron-withdrawing alkyl and aryl ligands on Au(III). Similarly, addition of *n*Bu<sub>4</sub>NCl does not inhibit the reaction, and chloride dissociation is therefore unlikely as well.

### Scheme 60. Reductive Elimination of (a) Fluoroaryls, and (b) Reductive Ar-CHF<sub>2</sub> Elimination



Wong and co-workers explored the reductive C(sp<sup>2</sup>)-C(sp) elimination from (C<sup>N</sup>)Au(III) chelates for applications in bioconjugation of alkynyl-linked peptides. Neutral (C<sup>N</sup>)gold(III) dichloride complexes **178** were found to react with phenylacetylene in the presence of a base, affording the reductive elimination product **179** in high yields (Scheme 61). This reactivity was shown to be general for 6-membered C<sup>N</sup> chelates, while 5-membered ones were unreactive, as the same authors showed for a similar C-S reductive elimination protocol.<sup>342</sup> Similarly, bis alkynyl Au(III) complexes **180** underwent C(sp<sup>2</sup>)-C(sp) reductive elimination only for 6-membered chelates and were proposed as intermediates in the reductive transformations.<sup>354</sup> Evidently C(sp<sup>2</sup>)-C(sp) coupling outcompetes the alternative C(sp)-C(sp) process.

### Scheme 61. Aryl-alkynyl reductive elimination from Au(III) C<sup>N</sup> chelates

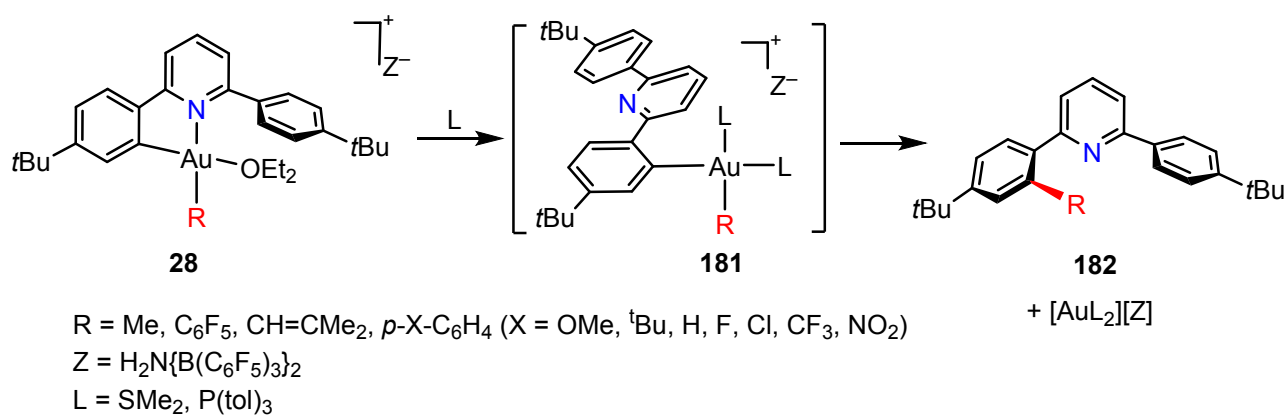


Rocchigiani *et al.* have investigated C–C reductive elimination from a range of (C<sup>^</sup>N)Au(III) cations of type **28** (cf. Scheme 7) obtained by protodeauration of (C<sup>^</sup>N<sup>^</sup>C)Au pincer complexes with the strong acid [H(OEt<sub>2</sub>)<sub>2</sub>][H<sub>2</sub>N{B(C<sub>6</sub>F<sub>5</sub>)<sub>3</sub>}<sub>2</sub>].<sup>355</sup> In agreement with earlier observations by Vicente *et al.*,<sup>356,357</sup> conformational flexibility was found to play a key role in the stability of Au(III) aryl complexes. Indeed, while C<sup>^</sup>N adducts **28** are thermally stable in solution for a prolonged time, they undergo reductive C–C elimination when treated with donor ligands such as SMe<sub>2</sub> or tri(*p*-tolyl) phosphine. This reaction is thought to involve pyridine displacement and formation of intermediates **181**, en-route to the coupling products **182** (Scheme 62). The rate of C–C reductive coupling was found to be dependent on the nature of the R group in the order  $k(\text{vinyl}) > k(\text{aryl}) \gg k(\text{C}_6\text{F}_5) > k(\text{Me})$  and required, at least, two equivalents of L per Au to go to completion. The elimination step is thought to depend on the formation of a 4-coordinated intermediate, where the pyridine N-donor is displaced by a second equivalent of L, thus allowing the metalated aryl group to rotate into a conformation that minimizes the barrier to reductive elimination. Hints for the formation of such an intermediate were obtained in the case of R = Me and L = P(tol)<sub>3</sub>, for which two non-equivalent <sup>31</sup>P NMR signals were observed, together with selective NOE interactions supporting the *cis*-arrangement. Consistent with this scheme, C–C reductive eliminations were found to be orders of magnitude faster for L = P(tol)<sub>3</sub> than for L = SMe<sub>2</sub>, most likely owing to the stronger coordination and increased steric demand of the phosphine in the tetracoordinate *cis* intermediate.<sup>355</sup>

Most recently Genoux *et al.* showed that reductive aryl-cyanide coupling can be induced by heating gold(III) CN complexes *trans*-Au(CN)<sub>2</sub>(C<sub>6</sub>H<sub>5-n</sub>F<sub>n</sub>)(PPh<sub>3</sub>) (n = 2 – 5) to 100 °C in 1,4-dioxane. The reaction is retarded by electron-withdrawing aryl substituents. The coupling follows an asynchronous mechanism in which the aryl acts as nucleophile and the cyanide as the

1  
2  
3 electrophile, which is not unexpected given the very different electronic characteristics of the aryl  
4 and CN ligands.<sup>358</sup> This process closely resembles the mechanism described earlier by Klinkenberg  
5 and Hartwig for the reductive aryl-CN coupling in palladium complexes (phosphine)<sub>2</sub>Pd-  
6 (CN)(aryl).<sup>359</sup>  
7  
8  
9

10  
11  
12 **Scheme 62. Donor-Ligand Induced Reductive Ar-R Elimination in Cyclometalated Complexes**

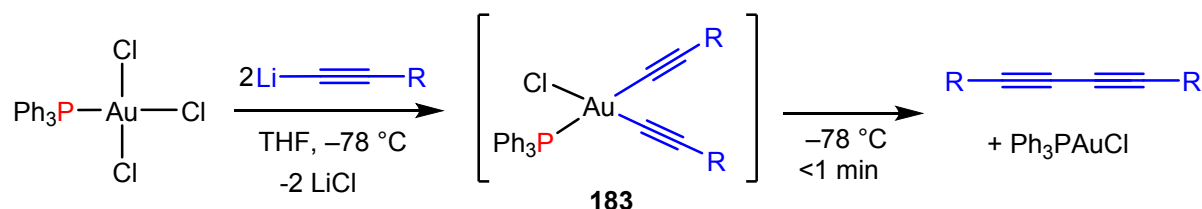


30  
31  
32  
33  
34  
35  
36  
37  
38  
39  
40  
41  
42  
43  
44  
45  
46  
47  
48

C(sp)–C(sp) bond formation has gained increasing interest in catalytic alkyne coupling (see Section 4.1). In 2014 Corma and co-workers reported a catalytic homocoupling of alkynes catalyzed by Au(I) phosphine complexes under basic conditions in the presence of Selectfluor as sacrificial oxidant.<sup>360</sup> Stoichiometric reactions revealed that reductive elimination from bis-alkynyl intermediates is extremely fast and goes to completion in less than 1 min at –78 °C. Similar homocoupling reactions were observed when one equivalent of (Ph<sub>3</sub>P)Au-alkynyl was combined with (Ph<sub>3</sub>P)AuCl<sub>3</sub>, although with a much slower kinetics. This seemed to suggest that C(sp)–C(sp) reductive elimination from neutral Au(III) bis-alkynyl complexes of type **183** (Scheme 63) is as efficient as C(sp<sup>2</sup>)–C(sp<sup>2</sup>) coupling.

49  
50  
51  
52  
53  
54  
55  
56  
57  
58  
59  
60

**Scheme 63. Alkynyl Coupling by C(sp)–C(sp) reductive elimination**



Computational studies by Datta and co-workers on *cis*-AuR<sub>1</sub>R<sub>2</sub>(PPh<sub>3</sub>)Cl complexes provided a theoretical rationale for the factors that impact on reductive elimination barriers. The authors

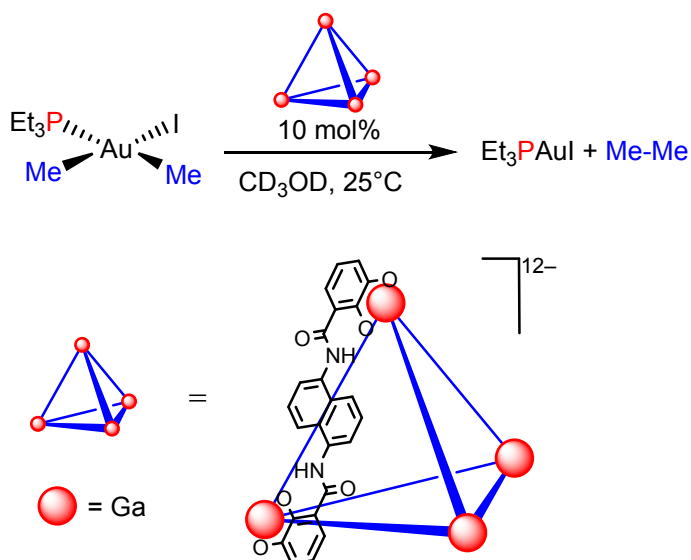
1  
2  
3 found that the activation enthalpies  $\Delta H^\ddagger$  (kcal/mol) of reductive eliminations follow the trend H, Ph  
4 (7.5) < H, Me (11.1) < vinyl, vinyl (15.1) < Ph, Ph (16.1) < H, H (17.1) < Ph, Me (24.9) < Me, Me  
5 (35.7).<sup>203</sup> The considerably higher barriers for reductive elimination of  $sp^3$ -C atoms was attributed  
6 to the directionality and lower s-character of their hybridized orbitals; consistent with the decrease  
7 of the elimination barriers with increasing s-character of the fragment that is to be eliminated. In  
8 line with experimental results, cationic bis(phosphine) complexes were calculated to eliminate  
9 much faster than the corresponding neutral chloride complexes.

10  
11 For the reasons described above, methyl-methyl couplings are difficult to achieve. However,  
12 Kaphan *et al.* showed that C( $sp^3$ )-C( $sp^3$ ) coupling from Au(III) can be accelerated if the complex is  
13 placed within the steric confines of a supramolecular cage.<sup>361</sup> In the presence of catalytic amounts  
14 of the anionic cage  $Ga_4L_6^{12-}$  (L = N,N'-bis(2,3-dihydroxybenzoyl)-1,5-diaminonaphthalene) the  
15 rate of C–C reductive elimination from *cis*-(L)AuMe<sub>2</sub>I (L = PEt<sub>3</sub>) increased by about 7 orders of  
16 magnitude, with a turnover number of 300 (Scheme 64). The reaction follows Michaelis-Menten  
17 kinetics; dissociation of iodide generates a cationic species that is encapsulated by the Ga<sub>4</sub>L<sub>6</sub> cage,  
18 where C–C reductive elimination is triggered by steric constraints and depends on the bulk of the  
19 ligands attached to the metal. The rate to ethane elimination thus increases with ligand size, L =  
20 PMe<sub>3</sub> < PEt<sub>3</sub>, provided the complex still fits into the cage cavity; therefore the triphenylphosphine  
21 derivative was not reactive at all. Similarly, reductive elimination of butane from *cis*-(Me<sub>3</sub>P)AuEt<sub>2</sub>I  
22 was found to be catalysed by the supramolecular cage.<sup>362</sup>

23  
24 Recent theoretical studies by Ujaque and co-workers showed that the difference in reductive  
25 elimination rate between encapsulated Et<sub>3</sub>PAuMe<sub>2</sub>I and Me<sub>3</sub>PAuMe<sub>2</sub>I arises predominantly from  
26 solvent inclusion effects. In the case of the smaller PMe<sub>3</sub> complex, there is sufficient space in the  
27 cage for hosting an extra MeOH molecule, together with the cationic intermediate  
28 [Me<sub>3</sub>PAu(HOMe)Me<sub>2</sub>]<sup>+</sup>, while for the larger ethyl derivative there is no such possibility. The extra  
29 encapsulated MeOH molecule was found to increase the barrier of reductive elimination, thus  
30 showing that the kinetic effects observed experimentally are not only simply related to  
31 encapsulation, but also to microsolvation effects that can occur inside the cage.<sup>363,364</sup> In a series of  
32 similar studies, Head-Gordon and co-workers have also shown the importance of electrostatic  
33 effects generated by the encapsulation of Au(III) alkyl cations. Here, the inclusion of a single water  
34 molecule in the cage was found to play a very important role in accelerating the rate of C-C bond  
35 formation in the cage, as it generates dipole forces that seem to stabilize the transition state.<sup>365,366</sup>

#### 58 **Scheme 64. Alkyl-Alkyl Elimination Catalyzed by Supramolecular Encapsulation**

59  
60

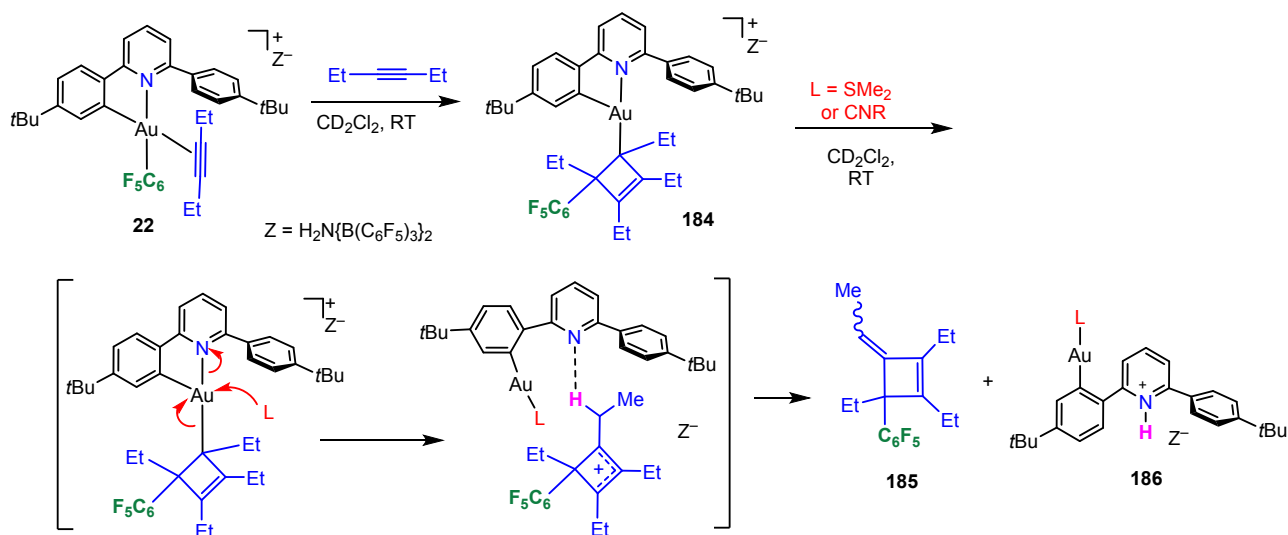


23 An alternative pathway to product release via C-C reductive elimination was discovered by  
24 Rocchigiani *et al.* during their studies on Au(III) alkyne complexes. This process involves reductive  
25 deprotonation (as distinct from reductive C-H elimination) from the gold alkyl **184**, which had been  
26 formed by a [2+2] cycloaddition–C<sub>6</sub>F<sub>5</sub> insertion cascade.<sup>160</sup> Despite the presence of a coordination  
27 vacancy and of β-hydrogen atoms on the ethyl substituent of the cyclobutenyl, **184** was found to be  
28 thermally stable. However, when a Lewis base such as SMe<sub>2</sub> or xylisocyanide was added to **184**,  
29 fast and quantitative formation of the diene **185** and the pyridinium salt **186** was observed (Scheme  
30 65). With the help of DFT calculations the classic path for β-H elimination was ruled out. Instead,  
31 the reaction is thought to originate from the dissociation of **184** to give an Au(I) species and a  
32 cyclobutenyl cation, followed by deprotonation of the latter by the pyridine ligand to generate the  
33 olefinic product **185** as an *E/Z* mixture. The external base (SMe<sub>2</sub>, isocyanide) serves to stabilize the  
34 Au(I) end product.

45 **Scheme 65. Product Release by a C-C Coupling - Reductive Deprotonation Sequence**

46  
47  
48  
49  
50  
51  
52  
53  
54  
55  
56  
57  
58  
59  
60





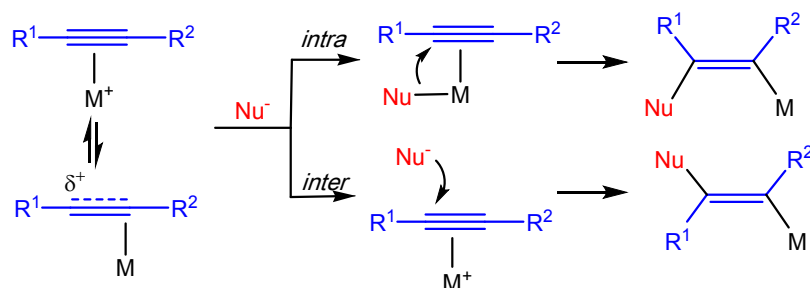
### 3.3 Nucleophilic Addition to C-C Double and Triple Bonds

23  
24  
25  
26  
27  
28  
29  
30  
31  
32  
33  
34  
35  
36  
37  
38  
39  
40  
41  
42  
43  
44  
45

This section deals with mechanistic aspects and stoichiometric reactions. Catalytic applications involving nucleophilic attack on C-C double and triple bonds and cascade reactions are summarized in Section 4.2. Nucleophilic attack on alkynes mediated by gold catalysts has been reviewed.<sup>367</sup>

The nucleophilic attack on unsaturated C-C bonds can occur by intra- or inter-molecular pathways, leading to products of different stereochemistries (Scheme 66). Early fully relativistic *ab-initio* calculations on propyne complexes of  $AuCl_3$  and  $PtCl_2(H_2O)$  explain the higher catalytic activity of gold by the strongly varying orbital populations and significant structural and energy differences of the frontier orbitals between Au and Pt.<sup>164</sup> On the other hand, the ease of ligand slippage is also important and was found to be more facile for Au(III) than for Pt(II) (Figure 3),<sup>160</sup> which explains the pronounced vinylcarbocation-type reactivity of gold-alkyne complexes.

#### Scheme 66. Pathways of Nucleophilic Attack on Alkyne Ligands



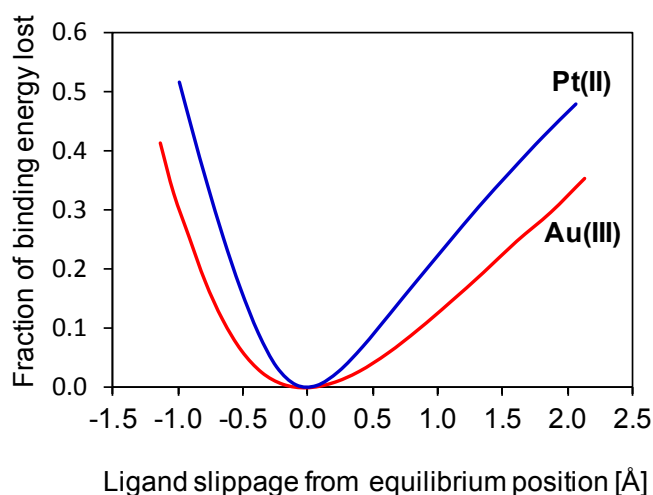


**Figure 3.** Energy potentials of 2-butyne slippage in  $\text{AuCl}_3$  and  $\text{PtCl}_2(\text{H}_2\text{O})$  adducts.

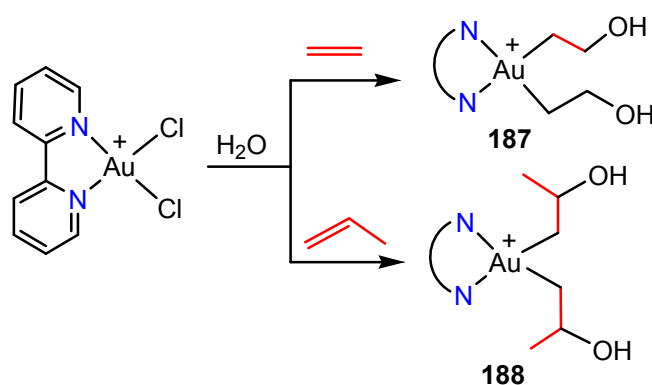
The hydration of propyne to acetone catalyzed by  $\text{AuCl}_3$  has been the subject of computational modelling at various levels. The reaction follows an intermolecular pathway with cooperative hydrogen bonding. The involvement of a second water molecule was found to reduce the activation energy by over 20 kcal/mol. Both relativistic effects and the inclusion of the solvent have a major effect on the reaction energy profile.<sup>368</sup> Later theoretical studies on the phenylacetylene hydration effected by dithiocarbamate  $\text{AuCl}_2(\text{S}_2\text{CNR}_2)$  catalyst,<sup>369</sup> and on the 2-butyne hydration by a series of  $(\text{C}^{\wedge}\text{N}^{\wedge}\text{C})$ ,  $\text{O}^{\wedge}\text{N}^{\wedge}\text{N}^{\wedge}\text{O}$ ,  $\text{C}^{\wedge}\text{N}$  and  $\text{C}^{\wedge}\text{C}$  ligated gold(III) complexes<sup>163</sup> confirm the importance of substrate polarization through alkyne ligand slippage, and of hydrogen-bonding to more than one solvent molecule during the intermolecular attack by external water. Earlier experimental work by Laguna and co-workers had identified  $[\text{BzPPh}_3][\text{Au}(\text{mes})\text{Cl}_3]$  as a particularly effective catalyst for the hydration of phenylacetylene.<sup>159</sup>

A series of stoichiometric reactions involving nucleophilic attack on coordinated alkenes has been reported. Atwood *et al.* studied the hydration of ethylene catalyzed by  $\text{HAuCl}_4$ ,  $\text{AuCl}_3(\text{TPPTS})$  ( $\text{TPPTS} = \text{P}(m\text{-C}_6\text{H}_4\text{SO}_3\text{Na})_3$ ) and  $[(\text{bipy})\text{AuCl}_2]^+$ .  $\text{HAuCl}_4$  is least selective and at room temperature gives a mixture of  $\text{L}_n\text{Au-CH}_2\text{CH}_2\text{OH}$ ,  $\text{HOCH}_2\text{CH}_2\text{OH}$  and  $\text{ClCH}_2\text{CH}_2\text{OH}$ . The formation of ethylene glycol is accompanied by reduction to gold metal.  $\text{AuCl}_3(\text{TPPTS})$  at 12 °C and  $[(\text{bipy})\text{AuCl}_2]^+$  at 50 °C were selective for the quantitative formation of Au(III)  $\beta$ -hydroxyethyl species, while there was no reaction with  $[(\text{terpy})\text{AuCl}]^+$ . With  $[(\text{bipy})\text{AuCl}_2]^+$ , the bis-alkyl intermediate  $[(\text{bipy})\text{Au}(\text{C}_2\text{H}_4\text{OH})_2]^+$  **187** was identified by mass spectrometry, while no evidence was found for the mono-alkyl. These gold alkyls proved to be insensitive to protonolysis or treatment with aqueous base. In prolonged reactions the formation of acetaldehyde was also seen, thought to arise from  $\beta$ -H elimination.

The analogous hydration of propene resulted in the formation of a mixture of isopropanol and acetone, via the Markovnikov product Au-CH<sub>2</sub>CH(OH)CH<sub>3</sub> **188** (Scheme 67). Acetone was the dominant product with AuCl<sub>3</sub>(TPPTS).

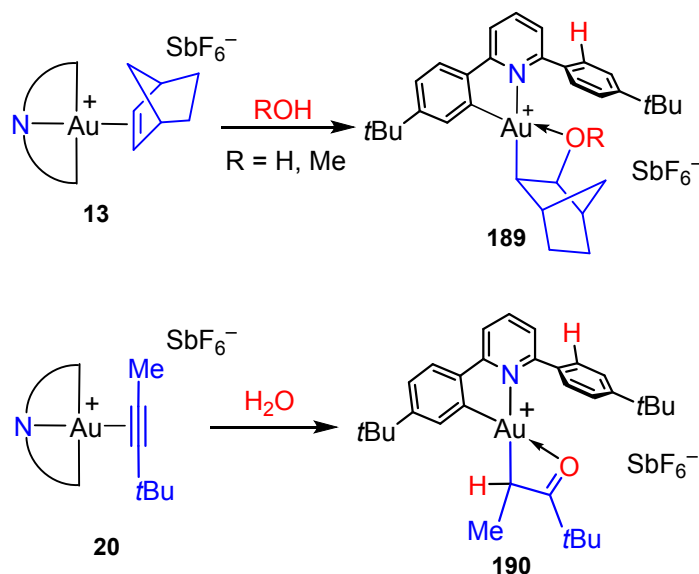
The authors also noted that these gold complexes in the presence of water were very sensitive to metal objects (syringe needles, metal spatula) which induced formation of gold nanoparticles, an important observation perhaps when handling Au(III) chloride catalysts.<sup>370</sup>

### Scheme 67. Intermediates in Au(III)-Mediated Alkene Hydration



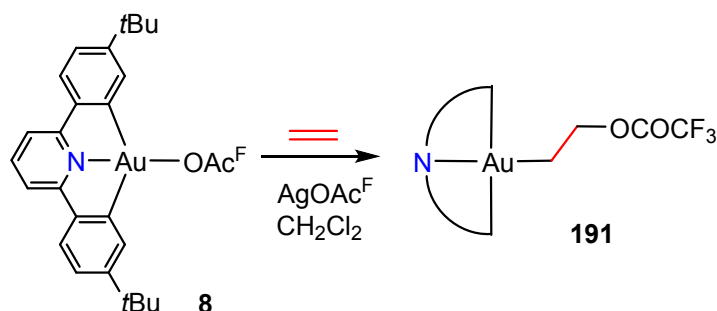
The ease of nucleophilic attack to alkyne and alkene coordinated to Au(III) was demonstrated on well-defined complexes based on the (C<sup>^</sup>N<sup>^</sup>C) pincer ligand (Scheme 68). The olefin adduct **13** was found to react with water or methanol to give the bidentate hydrolysis product **189**, which was crystallographically characterized.<sup>151</sup> Similarly, the alkyne adduct **20** reacted with a stoichiometric amount of H<sub>2</sub>O to give the isolated ketonyl complex **190**.<sup>160</sup>

### Scheme 68. Hydrolysis of (C<sup>^</sup>N<sup>^</sup>C)Au alkene and alkyne complexes



Attack by trifluoroacetate on coordinated ethylene was observed in the reaction of  $(C^{\wedge}N^{\wedge}C)AuOAc^F$  **8** in  $CH_2Cl_2$  in the presence of  $AgOAc^F$  with an ethylene atmosphere at room temperature over the course of 14–72 h, in the absence of  $B(C_6F_5)_3$  (Scheme 69). Formation of the 2-acetoxyethyl complex **191** was quantitative; this product was crystallographically characterized. The process assumes dissociation of  $Ac^FO^-$ , likely aided by Lewis-acidic  $Ag^+$ , and acetate attack on the  $\pi$ -ethylene intermediate.<sup>151</sup>

### Scheme 69. Ethylene Insertion Into a Gold-OAc<sup>F</sup> Bond

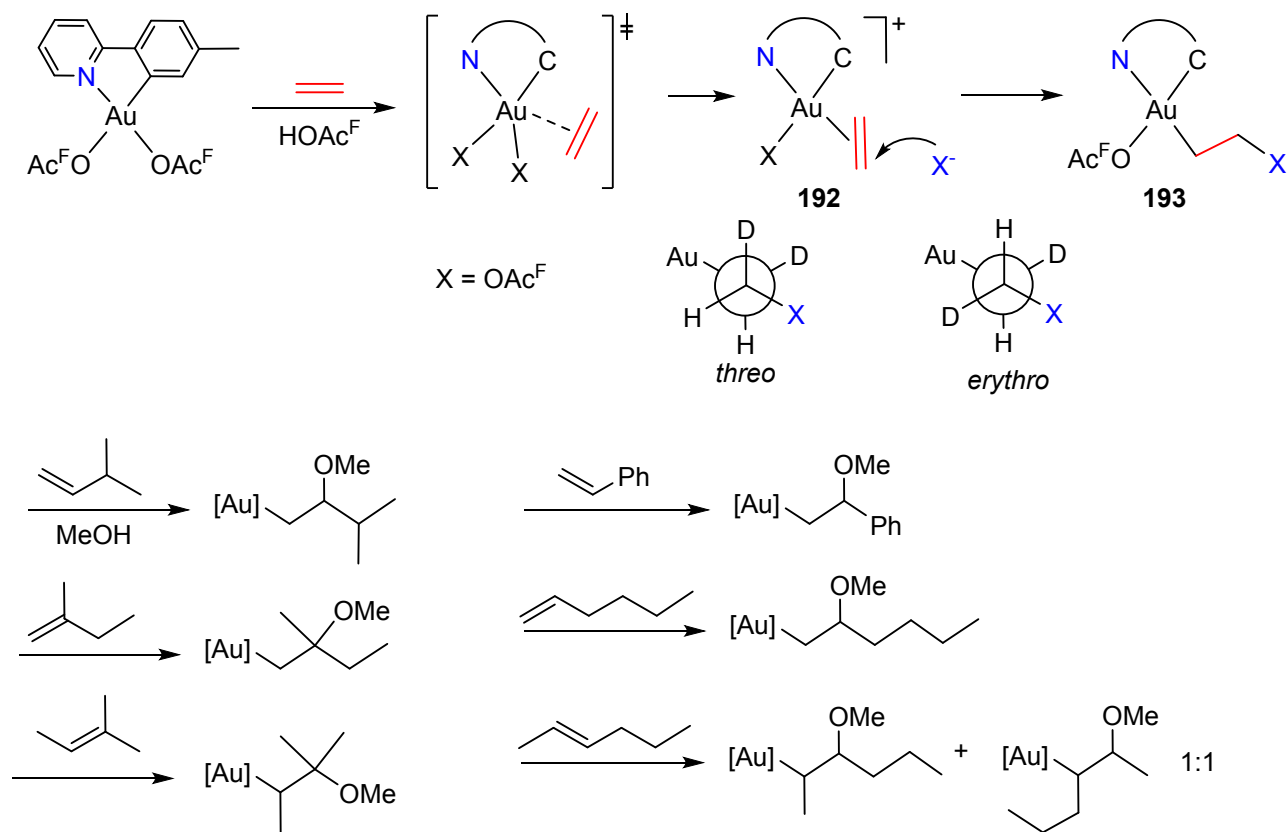


Tilset *et al.* observed the similar reaction of ethylene with  $(C^{\wedge}N)Au(OAc^F)_2$  to give exclusively a monoalkyl product **193** with the alkyl ligand *trans* to N (Scheme 70).<sup>132,133</sup> While this reaction, too, was slow in dichloromethane, in trifluoroacetic acid as solvent the reaction times were reduced to minutes. The presence of two coordination sites in  $(C^{\wedge}N)Au(OAc^F)_2$  implies that both *intra*- and *intermolecular* pathways can be envisaged. This was addressed using selectively deuterated *cis*-C<sub>2</sub>H<sub>2</sub>D<sub>2</sub>. Inter- and intra-molecular pathways should lead to the *threo* and *erythro* isomers, respectively. Only the former was found, consistent with *anti* attack by acetate. DFT modelling supported a rate-limiting, strongly solvent-dependent, associative substitution transition state, leading to the substitution of OAc<sup>F</sup> *trans* to N, as in intermediate **192**, followed by an intermolecular attack on C=C by the external nucleophile. Trifluoroethanol as the solvent led to the analogous product **193** (X = OCH<sub>2</sub>CF<sub>3</sub>). A low-barrier associative interchange pathway for ethylene exchange in  $[(C^{\wedge}N)Au(X)(C_2H_4)]^+$  between *trans*-C and *trans*-N sites has also been identified. Although kinetically substitution of X by ethylene *trans* to C is associated with a lower barrier, the overall thermodynamic preferences for alkyl *trans* to N results in the exclusive formation of **193**.<sup>132,133</sup>

This system was subsequently extended to other olefins and different alcohols as nucleophiles (Scheme 70). In all cases the Markovnikov products were formed. There was no ethylene exchange when an Au-C<sub>2</sub>H<sub>4</sub>OMe complex was treated with C<sub>2</sub>D<sub>4</sub>. In none of these

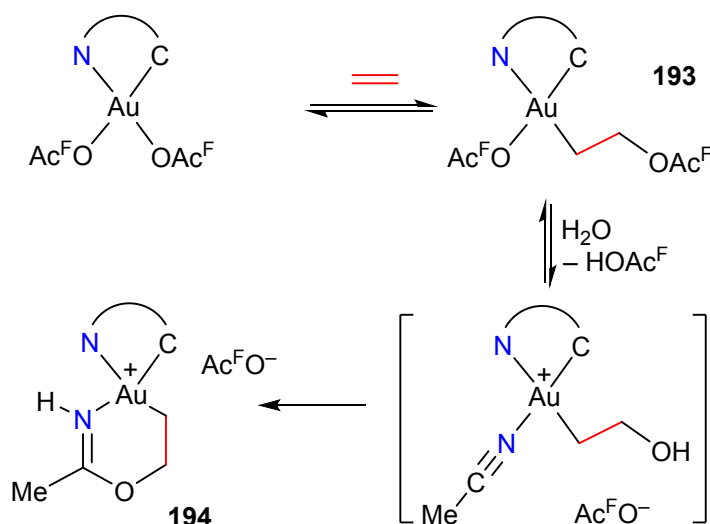
reactions was there substitution of the  $\text{OAc}^{\text{F}}$  ligand *trans* to C.<sup>371</sup> The Au(III) alkyl trifluoroacetate complex of type **193** can be converted into the corresponding gold(III) halide complexes by treatment with aqua regia, without cleavage of the Au-C bond.<sup>372</sup>

### Scheme 70. Mechanism and Products of Alkene Insertions in the $(\text{C}^{\wedge}\text{N})\text{AuX}_2$ System



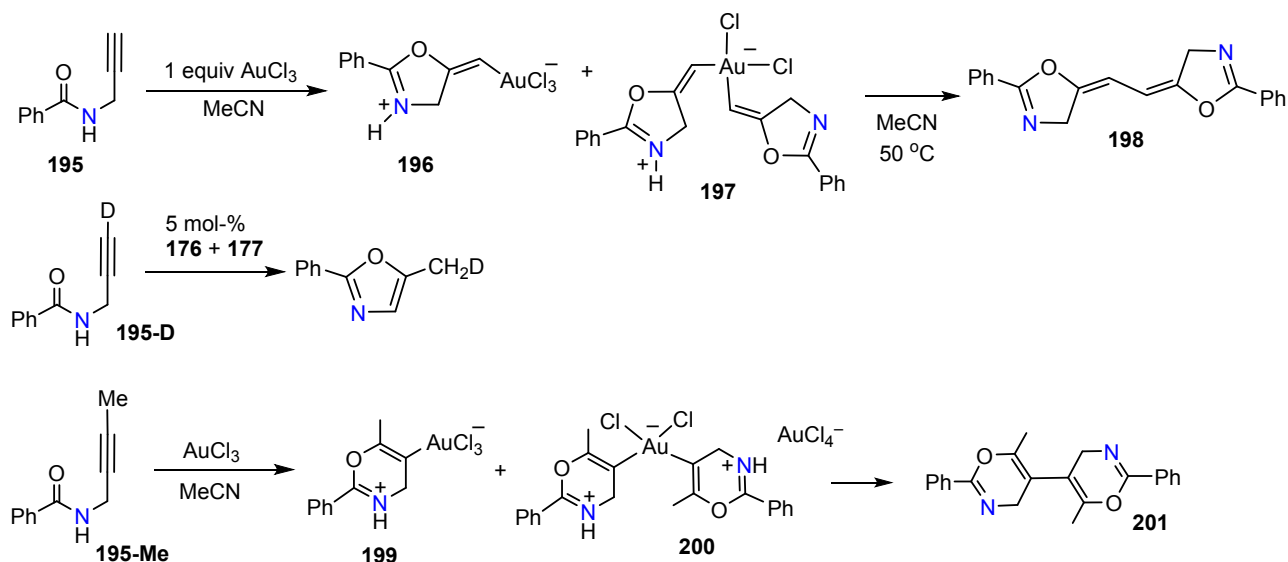
In the presence of water and acetonitrile the reaction of  $(\text{C}^{\wedge}\text{N})\text{Au}(\text{OAc}^{\text{F}})_2$  with ethylene leads to the crystallographically characterized Au(III) heterocycle **194** (Scheme 71). The same product is also obtained from **193** and acetamide in the presence of water. DFT modelling supports an acetonitrile adduct as intermediate.<sup>133</sup>

### Scheme 71. Au(III) Metallacycle from Ethylene, Acetonitrile and Water

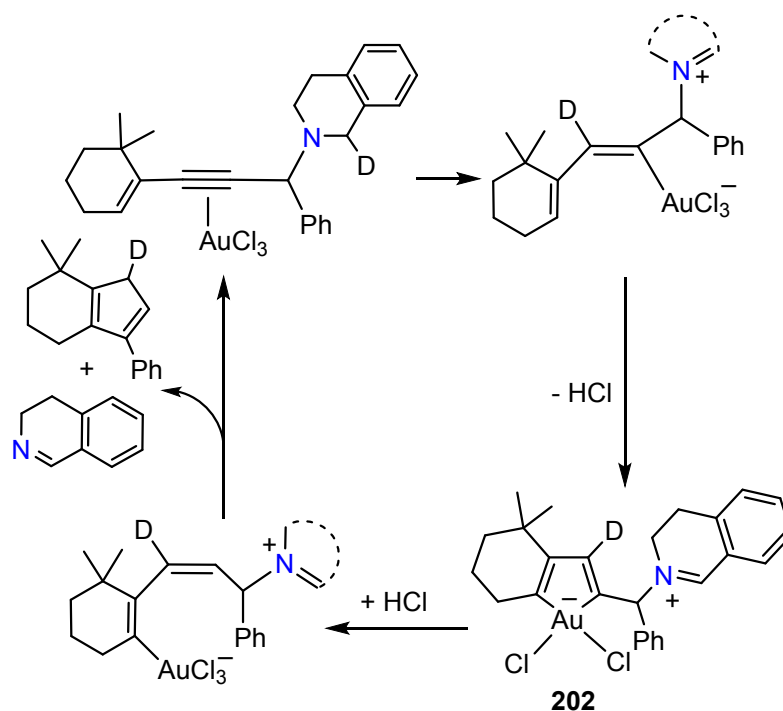


Important insight into the heterocyclization of propargylic amides was provided by Ahn and co-workers, who isolated and crystallographically characterized a number of vinylgold(III) intermediates (Scheme 72).<sup>373</sup> Reaction of **195** with AuCl<sub>3</sub> led to *anti*-attack on C≡C and formation of a mixture of the gold(III) vinyl complexes **196** and **197**. Heating to 50 °C gave the reductive elimination product **198**. The crystal structures of **196** and **198** were determined. Mixtures of **196/197** (5 mol-%) catalyze the cyclization of **195-D**; the substrate facilitates the protodeauration under these conditions. The internal alkyne **195-Me** in the presence of AuCl<sub>3</sub> in MeCN cyclizes to 6-ring vinyl products **199** and **200**, both of which were crystallographically characterized, as was the reductive elimination product **201**. Another gold(III) vinyl species, the auracyclopentadiene **202**, was crystallographically characterized as part of a mechanistic study on the conversion of enyne-amines to cyclopentadienes (Scheme 73).<sup>374</sup> These reactions are the first demonstration of the nature of Au(III) vinyl species in such heterocyclization sequences and support the notion that AuCl<sub>3</sub> can successfully generate gold-vinyl intermediates without reduction.

### Scheme 72. Gold(III) Vinyl Complexes in Alkyne Heterocyclizations



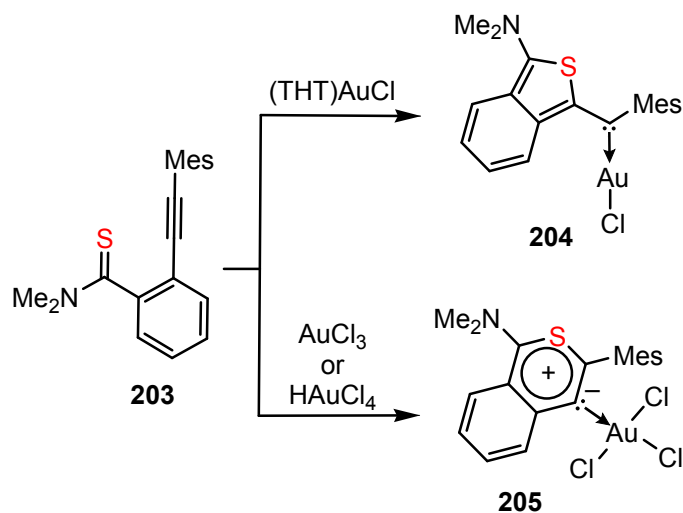
**Scheme 73. Au(III) Dienyl Intermediates in Alkyne to Cyclopentadiene Conversion**



Intramolecular cyclization through nucleophilic attack to an alkyne moiety is commonplace in gold catalysis (see Section 4) and the difference in oxidation states between Au(I) and Au(III) can lead to different reaction outcomes. This has been demonstrated also in stoichiometric reactions, e.g. by Bertrand and co-workers who synthesized the benzothioamido alkyne **203** and subjected it to reactions with Au(I) and Au(III) precursors (Scheme 74). When treated with (THT)AuCl, initially a thioamide adduct was formed which converted into the heteroaryl arylcarbene **204** upon *5-exo-dig* cyclization. On the other hand, when AuCl<sub>3</sub> or HAuCl<sub>4</sub> were used

as catalysts, a *6-endo-dig* cyclization took place, leading to the formation of the Au(III) mesoionic carbene complex **205**.<sup>375</sup>

#### Scheme 74. Intramolecular Alkyne Heterocyclization of Benzothioamides by Au(I) and Au(III)



### 3.4 Insertion Reactions

Insertions of unsaturated substrates into M-X bonds (X = C, H) are a key feature of transition metal catalysts. These reactions involve typically the binding of the substrate to a vacant coordination site *cis* to X, followed by migration of X to the substrate. For gold, however, these reactions are conspicuous by their absence. For example, although gold acyl complexes LAu-C(O)R are known,<sup>307,376,377</sup> these cannot be generated by CO insertion into the Au-R bond.<sup>378</sup> Gold(I), compounds L-Au-X, with their linear coordination geometry and low Lewis acidity, give only weak associations with substrates perpendicular to the molecular axis, which disfavors intramolecular migratory insertion pathways, and for gold(III) systems with suitable vacant coordination sites that enable such a process have only recently been developed. It has however become apparent that both gold(I) and gold(III) can overcome the barriers to insertion by adopting alternative mechanisms, including single-electron pathways.

**3.4.1 Insertions into Gold-Carbon Bonds.** There are a few early reports of formal insertions into Au(I)-methyl bonds. These involve strong electrophilic reagents, such as tetrafluoroethylene and hexafluoro-2-butyne; reactions are observed only under photolytic conditions and are thought to involve a radical mechanism.<sup>379</sup> The insertion of SO<sub>2</sub> into Au-Me and Au-Ar bonds has also been described; the former lead to thermally unstable gold sulfinato compounds including *cis*-AuMe<sub>2</sub>(SO<sub>2</sub>Me)(PMe<sub>2</sub>Ph).<sup>333,380</sup> In this pioneering work Puddephatt also observed the formation of gold vinyl complexes by the insertion of DMAD into Au(I)-Me bonds, including the



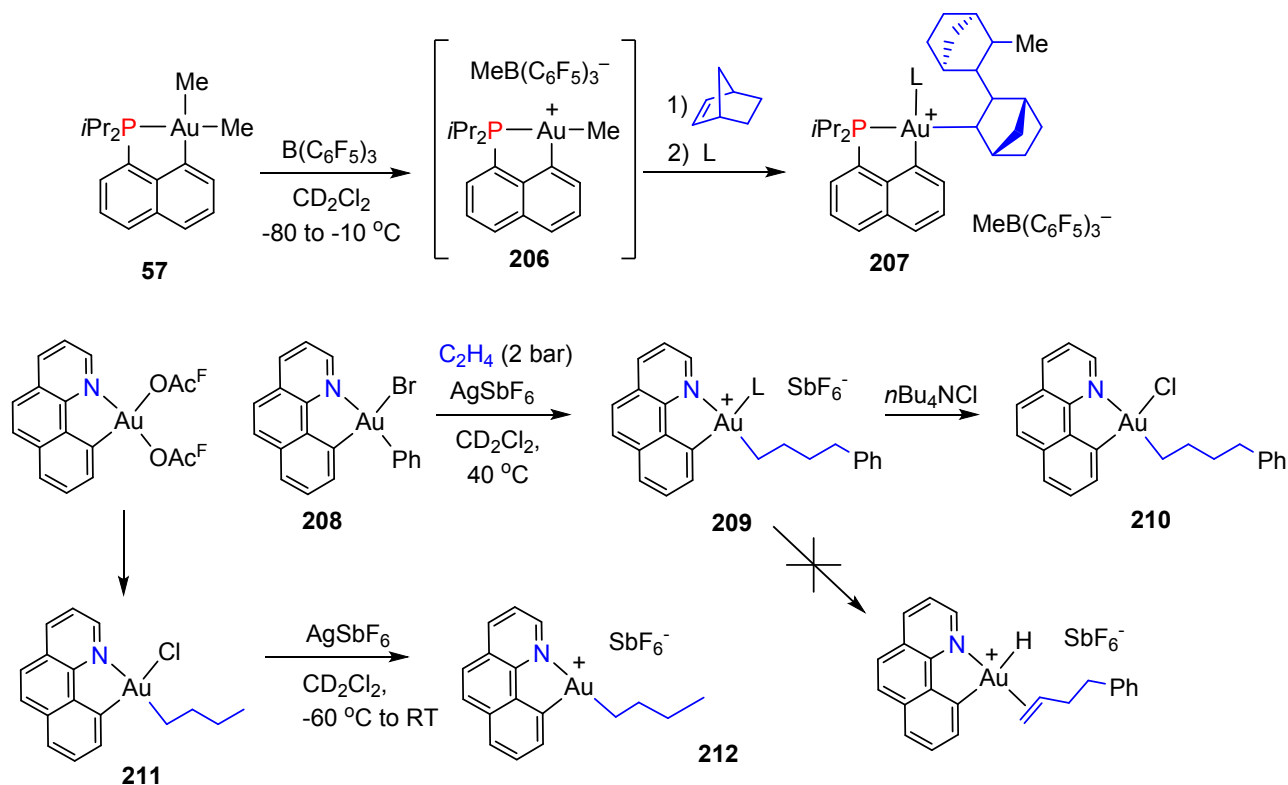
1  
2  
3 formation of the gold(III) product *cis*-AuMe<sub>2</sub>(C(CO<sub>2</sub>Me)=C(CO<sub>2</sub>Me)Me}(PMe<sub>3</sub>) together with  
4 metallic gold, due to subsequent redox reactions. The insertion mechanism was not established.<sup>380</sup>

5  
6 The insertion of unactivated alkenes into Au-C bonds by a coordination-migratory insertion  
7 mechanism was an unknown reaction in gold chemistry until quite recently. As mentioned in  
8 Section 2.3.2, Bourissou *et al.* demonstrated that norbornene is able to insert into the Au-Me bond  
9 of *in-situ* generated [(C<sup>^</sup>P)AuMe][MeB(C<sub>6</sub>F<sub>5</sub>)<sub>3</sub>] (**206**) (Scheme 75). The proposed 14-electron  
10 cation [(C<sup>^</sup>P)AuMe]<sup>+</sup> is unstable, and in the absence of alkene substrate reacts with the borate anion  
11 under C<sub>6</sub>F<sub>5</sub> transfer. While there was no insertion of ethylene or styrene, norbornene forms **207**, a  
12 product of double insertion which was trapped by the addition of L = pyridine, lutidine or  
13 chloride.<sup>381</sup> In the absence of L at temperatures below -30 °C this norbornene insertion product is  
14 stabilized by a  $\gamma$ -agostic interaction<sup>212</sup> (Section 2.3.2, Scheme 16). The precursor complex **206**  
15 could be identified spectroscopically below -10 °C. Calculations indicated anion binding via a close  
16 Au...H-CH<sub>2</sub>-B contact. The barrier to 1,2-insertion of the first norbornene into the Au-Me bond  
17 was found to be 18.7 kcal/mol. The second insertion has a slightly lower barrier, and the agostic  
18 interaction in the final product makes the overall process exergonic,  $\Delta G = -20.9$  kcal/mol relative to  
19 **206**.<sup>154</sup>

20  
21 While there was no reaction of **206** with ethylene or styrene, both ethylene and norbornene  
22 insert into Au-aryl bonds of [(C<sup>^</sup>P)Au-Ar]<sup>+</sup> as discussed in Section 2.2.4 and shown in Scheme 7, to  
23 give the corresponding 2-arylalkyl complexes **26** and **27**. Calculations show that the activation  
24 barrier for the migratory ethylene insertion is low ( $\Delta G^\ddagger = 9.5$  kcal/mol), as is the barrier for  $\beta$ -H  
25 elimination ( $\Delta G^\ddagger = 4.8$  kcal/mol).<sup>169</sup>

## 41 **Scheme 75. Alkene Insertions into Au-C Bonds**

42  
43  
44  
45  
46  
47  
48  
49  
50  
51  
52  
53  
54  
55  
56  
57  
58  
59  
60

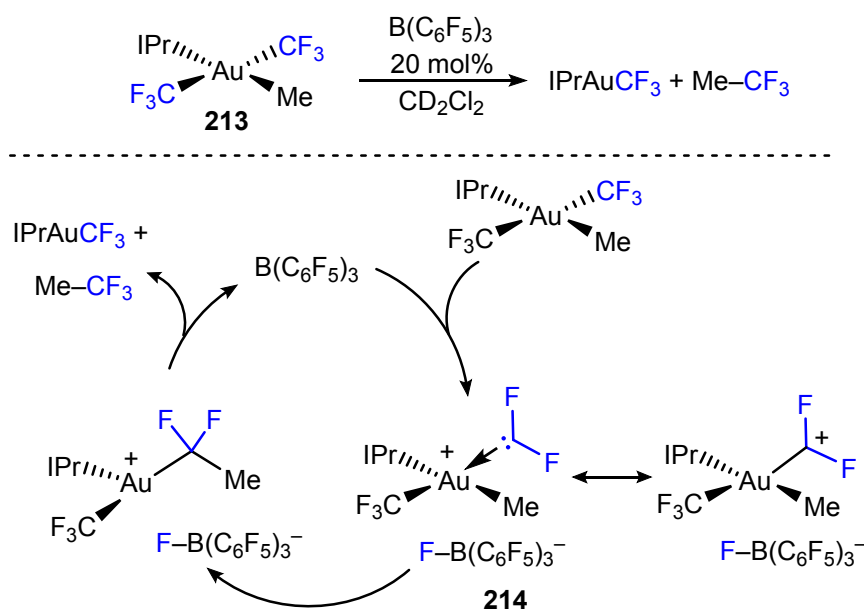


The difference between the C and the heteroatom donors is more pronounced in C<sup>^</sup>N than C<sup>^</sup>P chelates, as for example demonstrated by the very different bonding modes of the corresponding Au(III) allyl complexes (Scheme 8). The consequences of this difference as far as alkene insertions are concerned were probed in reactions between the benzoquinolinato complex (C<sup>^</sup>N)AuBr(Ph) **208** with ethylene (Scheme 75).<sup>382</sup> Whereas treating **208** with AgSbF<sub>6</sub> under ethylene (2 bar) at room temperature led to no insertion, at 40 °C double ethylene insertion was observed over a period of 18 hours, to give **209**. On addition of *n*Bu<sub>4</sub>NCl the more stable chloride **210** was obtained. Both **209** (L = H<sub>2</sub>O) and **210** were characterized by X-ray diffraction. Repeating the reaction with *trans*-CHD=CHD gave the analogous Au(CHD-CHD)<sub>2</sub>Ph complex, without evidence for H/D scrambling that might be expected to arise from β-H elimination / reinsertion sequences. The possibility of agostic interactions and the propensity towards β-H elimination was also probed by preparing (C<sup>^</sup>N)AuCl(*n*Bu) **211**, which could be converted into the cation [(C<sup>^</sup>N)Au<sup>+</sup>(*n*Bu)]<sup>+</sup> **212**, which proved to be stable in CD<sub>2</sub>Cl<sub>2</sub> at room temperature. None of these complexes showed evidence for agostic interactions or β-H elimination. DFT calculations showed that while such processes had quite low barriers, the extended alkyl structure was slightly more stable (by ca. 2.5 kcal/mol) than the γ-CH agostic form. Although the activation barrier for β-H elimination from the cation [(C<sup>^</sup>N)Au-(CH<sub>2</sub>)<sub>4</sub>Ph]<sup>+</sup> was found not to be prohibitively high (19.0 kcal/mol), the formation of the corresponding hydride was strongly endergonic (Δ*G* = 18.5

kcal/mol) due to the unfavorable H *trans* to C arrangement of the product. The behavior of these C<sup>^</sup>N chelate alkyl complexes is therefore distinctly different from the C<sup>^</sup>P analogues, where both β-H elimination and alkene insertions are very facile (see Section 3.4.2, Scheme 78).

Another type of insertion was found in investigations regarding the mechanism of what appeared to be a CH<sub>3</sub>-CF<sub>3</sub> reductive elimination from *trans*-(L)Au(CF<sub>3</sub>)<sub>2</sub>Me complexes **213** (L = IPr or PCy<sub>3</sub>) under very smooth conditions,<sup>174</sup> even though reductive eliminations of gold C(sp<sup>3</sup>)-CF<sub>3</sub> are usually not facile processes.<sup>203</sup> Levin *et al.* reported in 2017 that treating **213** with catalytic amounts of B(C<sub>6</sub>F<sub>5</sub>)<sub>3</sub> leads to the clean production of trifluoroethane and (IPr)AuCF<sub>3</sub> (room temperature, < 5 min). The authors showed that the reactivity originated from an initial fluoride abstraction by the borane, which afforded a transient cationic difluorocarbene complex **214**. The coordinated CF<sub>2</sub> is then able to undergo migratory insertion into the Au–Me bond, followed by C–F reductive elimination to give MeCF<sub>3</sub> (Scheme 76). This fluoride rebound mechanism was exploited for the incorporation of <sup>18</sup>F labels into drug molecules for applications as radiotracers in positron emission tomography.<sup>174</sup>

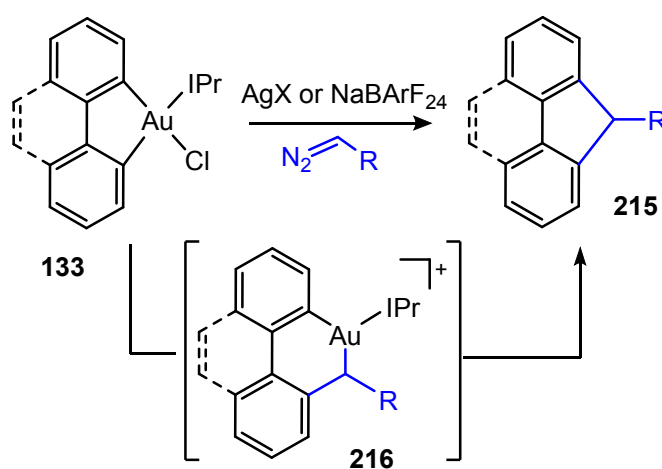
#### Scheme 76. CF<sub>2</sub> Insertion via a B(C<sub>6</sub>F<sub>5</sub>)<sub>3</sub> Catalyzed F-Rebound Mechanism



Carbene insertion was also observed by Zhukhovitskiy *et al.* upon reacting Au(III) chelates with diazoalkenes (Scheme 77). When the neutral (C<sup>^</sup>C)Au(IPr)Cl complexes of type **133** were reacted with chloride abstracting agents in the presence of different diazoalkenes, fluorene derivatives **215** formed as the major product in solution. The reaction is assumed to proceed through a migratory insertion of the carbene generated from the diazo-compound into the Au(III)–C bond of the chelate, which affords the strained intermediate **216**, which undergoes fast C(sp<sup>2</sup>)–

C(sp<sup>3</sup>) reductive elimination. The insertion reactivity was found to compete with C–C reductive elimination of biphenylene or biphenyl-alkyls and yields notably depended on the experimental conditions. In particular, the water content was found to be key, as the formation of aquo complexes stabilizes cationic species prior carbene insertion. However, excessive water content led to protodeauration side reactions, reducing the fluorene yields. By using a phenanthryl ligand, decomposition pathways could be minimized and the reaction was studied kinetically. The observed first-order kinetics was used to suggest a mechanistic scenario where N<sub>2</sub> elimination/insertion is unimolecular.<sup>383</sup>

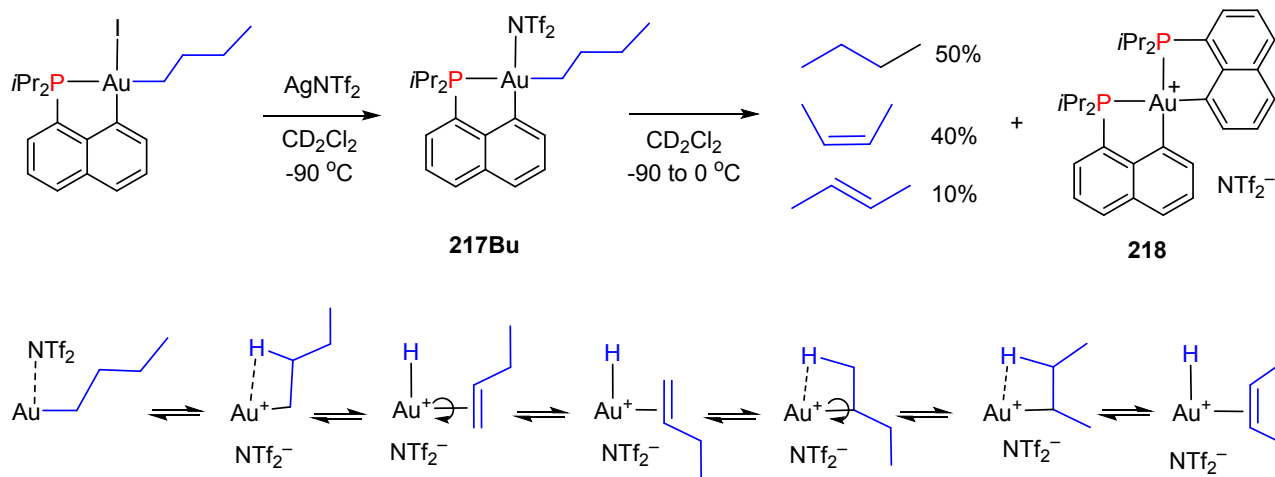
### Scheme 77. Carbene Insertion Into Au-C Bonds of (C<sup>^</sup>C)Au(III) Chelates



**3.4.2 Insertions into Gold-Hydrogen Bonds.** In contrast to other transition metals, in gold chemistry  $\beta$ -H elimination<sup>207,384</sup> and its reverse, the insertion of alkenes into M-H bonds by a migratory mechanism, was unknown until recently. Exploiting the particular geometric and bonding characteristics of the (C<sup>^</sup>P)Au system, Bourissou and co-workers were however able to demonstrate that both these processes can operate in cationic, 14-electron Au(III) alkyls. Substitution of the iodide ligand in the propyl complex (C<sup>^</sup>P)AuI(*n*Pr) by triflimidate NTf<sub>2</sub><sup>-</sup> in dichloromethane at -90 °C afforded (C<sup>^</sup>P)Au(NTf<sub>2</sub>)(R) (**217Pr**; R = *n*-propyl,) which, on warming to 0 °C, decomposed to a mixture of propane and propene, together with the bis-cyclometalated Au(III) complex **218**. Similarly, the *n*-butyl complex **217Bu** decomposed to **218** and a mixture of butane and *cis*- and *trans*-2-butene. The primary product of  $\beta$ -H elimination, 1-butene, was not detected. The process demonstrated that very facile  $\beta$ -H elimination from gold alkyls is possible, provided there is a suitable vacant coordination site, leading to a fast chain-walking sequence via alkene coordination, rotation and reinsertion into the Au-H intermediate (Scheme 78).<sup>385</sup> DFT modelling of this sequence

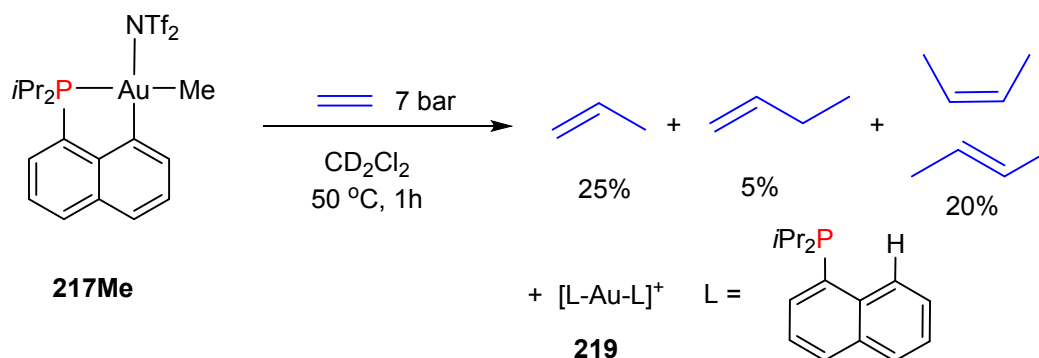
showed low barriers for all relevant steps leading to the *cis*-butene product. The same sequence leading to *trans*-2-butene followed the same pathway but with larger barriers.

### Scheme 78. $\beta$ -H Elimination, Alkene Insertions and Chain Walking Pathways



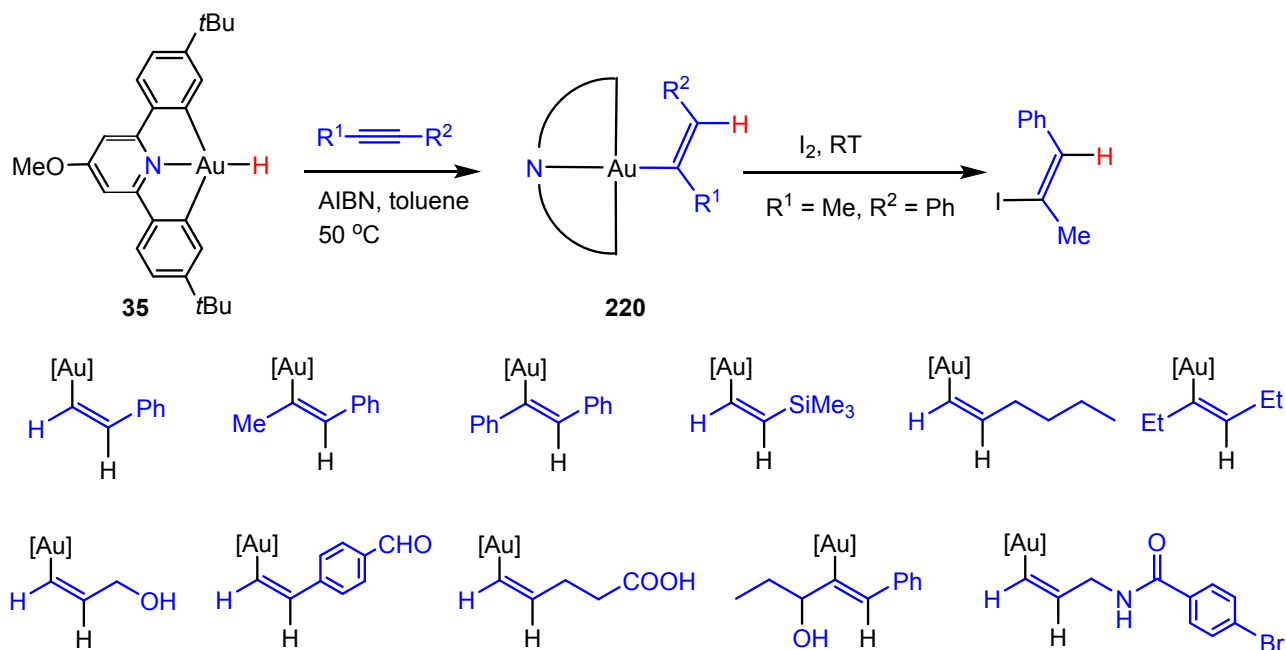
Exposing the (C<sup>^</sup>P)AuMe(NTf<sub>2</sub>) complex **217Me** to 7 bar ethylene pressure at 50 °C enabled the observation of ethylene insertion into an Au-Me bond (Scheme 79). The product mixture consisted of propene, as well as 1-butene and *cis* and *trans* 2-butene. Clearly the C<sub>4</sub> products arose from double ethylene insertion into a gold-H bond, associated with  $\beta$ -elimination / chain walking sequences. Modelling this reaction showed a higher insertion barrier, ( $\Delta G^\ddagger = 30.5$  kcal/mol), commensurate with the more forcing conditions required, but thermally certainly accessible. Insertion into Au-Et is more facile than into Au-Me, although the low barriers for  $\beta$ -H elimination prevent this reaction from generating ethylene oligomers or polymers. The by-product is a gold(I) bis-phosphine complex **219** arising from reductive Aryl-H elimination of the [(C<sup>^</sup>P)AuH]<sup>+</sup> intermediate.<sup>385</sup>

### Scheme 79. Ethylene Insertions into Au-Alkyl bonds



The gold hydride intermediate postulated in  $\beta$ -H eliminations shown in Scheme 78 is apparently highly reactive and was not detected. On the other hand, stable gold(III) hydrides like  $(C^{\wedge}N^{\wedge}C)AuH$  **35** do not react with olefins, and initial reports found that while they underwent insertion reactions with allenes, they did not react with 3-hexyne, phenylacetylene or dimethyl acetylenedicarboxylate (DMAD).<sup>190</sup> In subsequent investigations Bochmann and co-workers showed however that there was a very slow but highly stereoselective reaction with terminal and internal alkynes to give gold vinyl complexes **220** (Scheme 80). In the presence of radical sources like AIBN the reaction time was reduced from days to minutes. In all cases the alkyne insertion proceeded with almost quantitative stereo- and regioselectivity. A wide variety of functional groups was tolerated. N-propargyl carboxamides, which typically cycloisomerize to oxazoles in the presence of gold catalysts or protons, also form exclusively the corresponding gold vinyl product without cyclization. Release of the vinyl ligand was exemplified by treating the  $LAu-C(Me)=CHPh$  product with iodine; the reaction proceeds with retention of stereochemistry.<sup>192</sup>

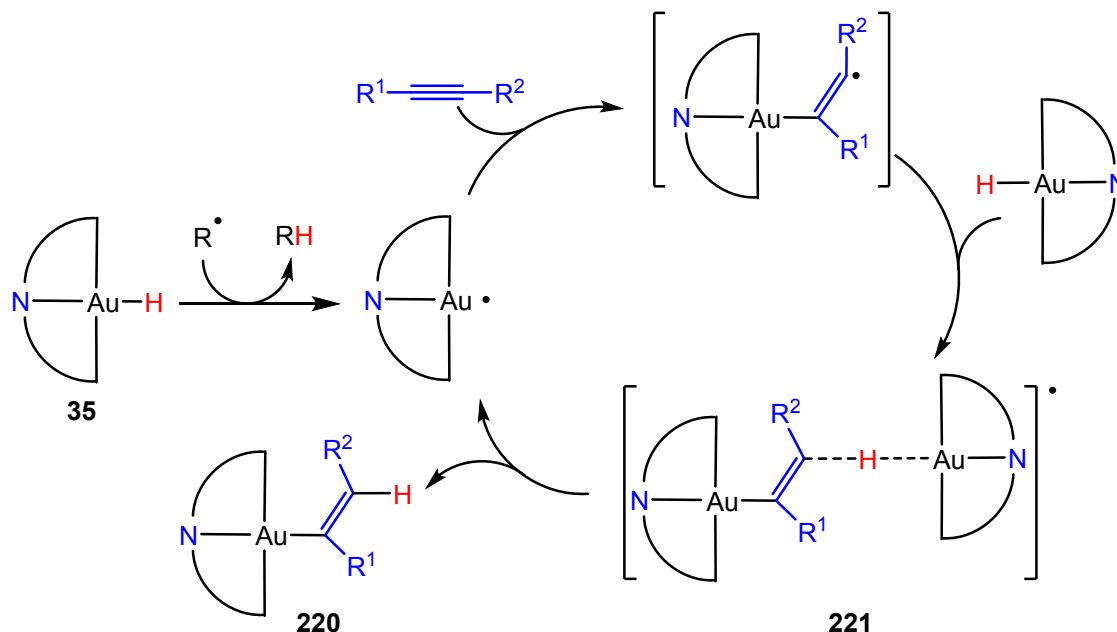
### Scheme 80. Stereoselective Alkyne Hydroaurations with $(C^{\wedge}N^{\wedge}C)AuH$



Gold(III) hydrides supported by pincer ligands are coordinatively saturated, and the Au-H bond is covalent and hardly polar. There is therefore no coordination site available for substrate binding, and efforts to search computationally for the possibility of 5-coordinate adducts as reaction intermediates were unsuccessful. A coordination-migratory insertion pathway was therefore ruled

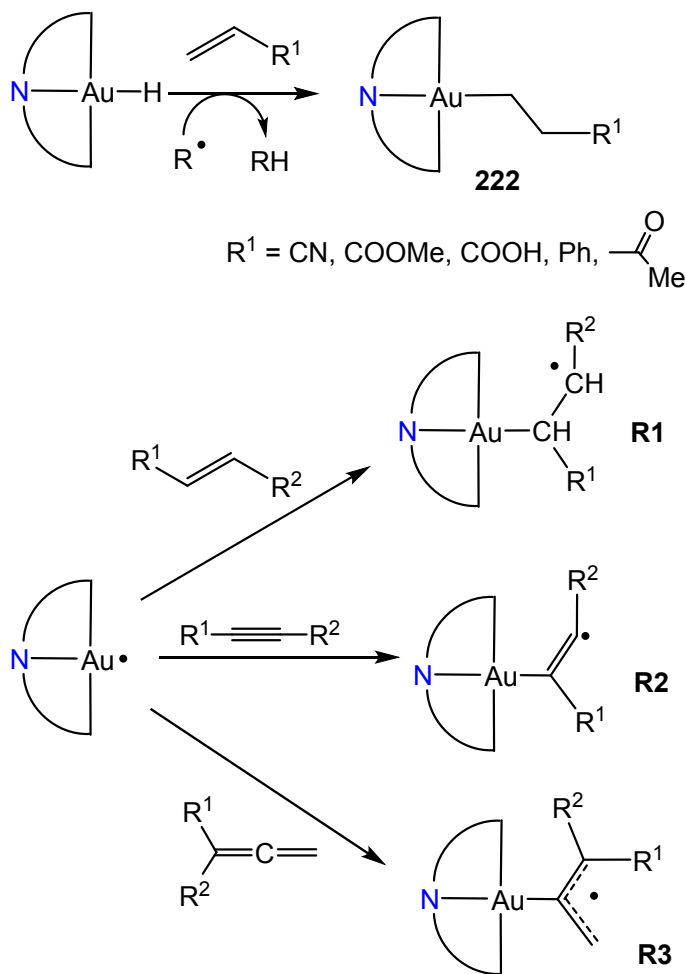
out; it would in any case lead to alkyne *cis*-hydroauration, whereas in all reactions the *trans*-(*Z*)-vinyl **220** was found. However, a bimolecular pathway involving (C<sup>^</sup>N<sup>^</sup>C)Au<sup>II</sup> radicals and H-transfer via a binuclear intermediate **221** overcomes the reactivity restrictions and was supported by DFT calculations. This bimolecular mechanism also smoothly explains the observed *trans*-hydroauration stereochemistry (Scheme 81).<sup>192</sup>

### Scheme 81. Bimolecular Hydroauration Mechanism via Au(II) Radicals



Subsequently Pintus and Bochmann found that the same radical pathway enables the insertion of 1-alkenes H<sub>2</sub>C=CHR (R = Ph, CN, COOMe, COOH or C(O)Me) into Au-H bonds, to give the gold alkyls (C<sup>^</sup>N<sup>^</sup>C)AuCH<sub>2</sub>CHR **222** (Scheme 82). Unfunctionalized alkenes and allyl derivatives (R = *n*Pr, *n*Bu, CH<sub>2</sub>OH, CH<sub>2</sub>NH<sub>2</sub>, CH<sub>2</sub>COOH) gave mixtures, while internal alkenes proved unreactive. Calculations showed that this behavior was a function of the exergonic or endergonic character of alkyl radical formation, driven by spin delocalization over the unsaturated substituents. The calculations also showed the increase in radical stability in the order **R1** < **R2** << **R3** (Scheme 82), which explains the facile insertion of allenes.<sup>386</sup>

### Scheme 82. Insertion of 1-Alkenes Into Au-H by a Radical Pathway

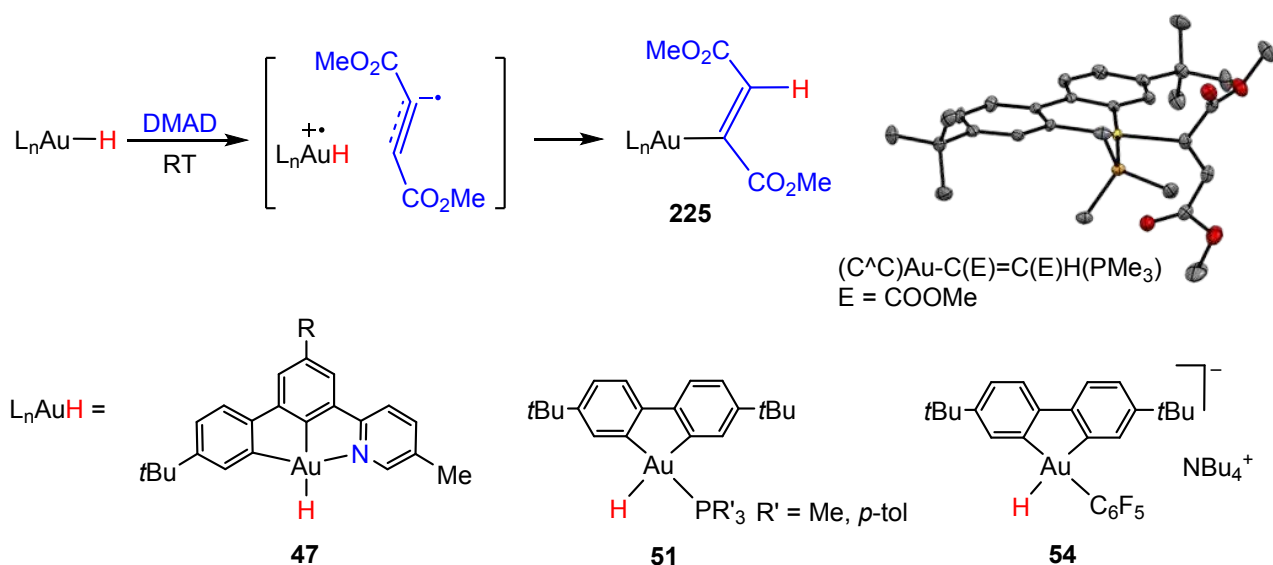


36  
37  
38  
39  
40  
41  
42  
43  
44  
45  
46  
47  
48  
49  
50  
51  
52  
53  
54  
55  
56  
57  
58  
59  
60

Whereas the previously described bimolecular reaction pathway via Au(II) radicals led to 1,2-insertion products, the hydroauration of arylisocyanides is a 1,1-insertion process. Fernandez-Cestau *et al.* reported the first example of such an insertion, to give the gold(III) iminoformyl complex  $(\text{C}^{\wedge}\text{N}^{\wedge}\text{C})\text{Au}-\text{CH}=\text{NAr}$  (**223**).<sup>387</sup> The xylyl complex ( $\text{Ar} = 2,6\text{-Me}_2\text{C}_6\text{H}_3$ ) was characterized by X-ray diffraction. Complex **223** ( $\text{Ar} = p\text{-MeOC}_6\text{H}_4$ ) exists as a mixture of *E* and *Z* isomers. Protonation gives the formimmonium salt **224** (Scheme 83); neither protolytic cleavage nor reductive C-C coupling induced by  $\text{SMe}_2$  addition could be observed. Calculations showed that the coordination of  $\text{ArN}\equiv\text{C}$  to the  $(\text{C}^{\wedge}\text{N}^{\wedge}\text{C})\text{Au}(\text{II})$  radical is barrierless. By contrast, the hydroauration of nitriles  $\text{ArC}\equiv\text{N}$  is energetically unfavorable. The isocyanide insertion process is almost thermoneutral and is driven forward by an excess of  $\text{ArN}\equiv\text{C}$ . The process is ligand dependent: whereas the barrier to H-transfer from  $(\text{C}^{\wedge}\text{N}^{\wedge}\text{C})\text{AuH}$  **35** is only 7.8 kcal/mol, for the  $\text{C}^{\wedge}\text{C}^{\wedge}\text{N}$  coordination isomer **47** (*C trans* to H) it is much higher (13.1 kcal/mol). There are also significant differences in spin delocalization between the two ligand systems, with a greater spin accumulation on the isocyanide-C atom in  $(\text{C}^{\wedge}\text{N}^{\wedge}\text{C})\text{Au}^{\text{II}}-\text{CNAr}$ , which favors H-transfer to C.<sup>387</sup> In contrast to







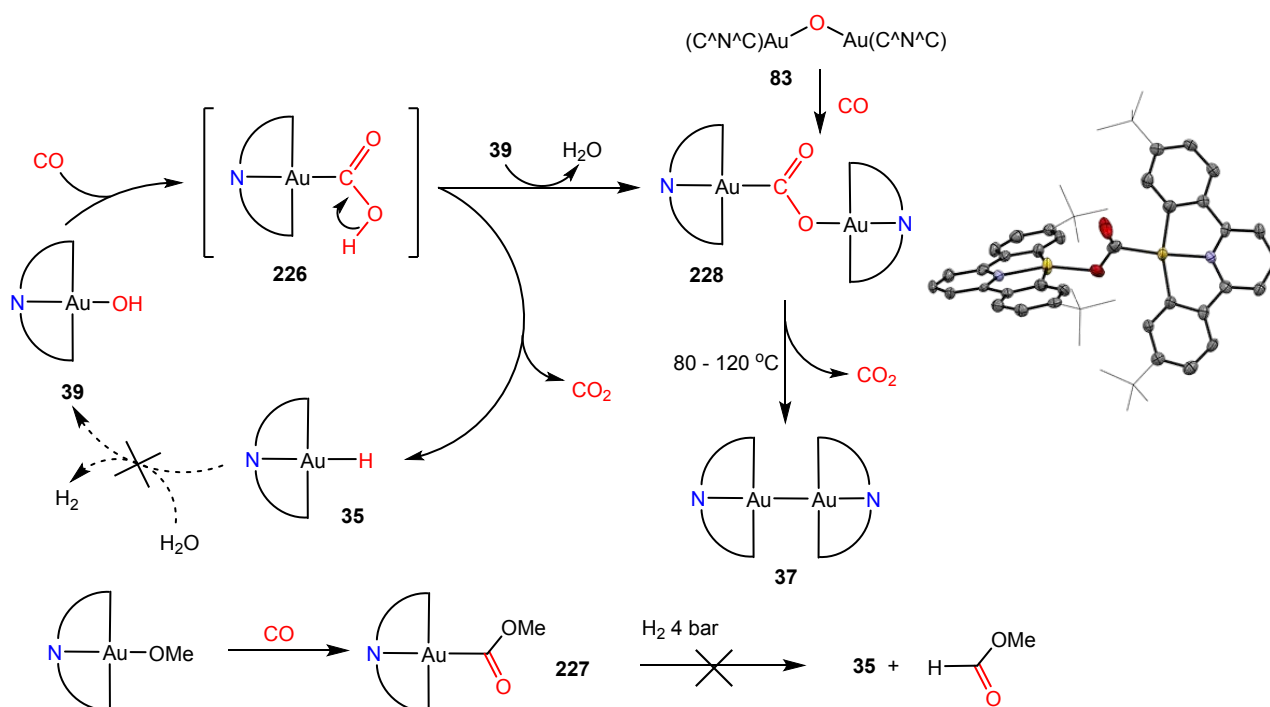
**3.4.3 Insertions into Gold-Oxygen Bonds.** CO insertions are central to many transition metal catalyzed reactions. The insertion of CO into an M-OH bond is a key step in the water-gas shift (WGS) reaction. Heterogeneous gold catalysts show higher WGS activity than platinum at lower temperatures.<sup>391</sup> Examples of CO insertions into Au-OH bonds have only recently been discovered; they demonstrate key steps of the WGS cycle.

In 2015 Roşca *et al.* demonstrated that the gold(III) hydroxide **39** reacts with CO in benzene at room temperature to give CO<sub>2</sub> and the spectroscopically detected hydride (C<sup>N</sup>C)AuH (**35**) (Scheme 85). The formation of (C<sup>N</sup>C)Au-COOH (**226**) as intermediate was supported by DFT calculations. The insertion of CO into the methoxide (C<sup>N</sup>C)AuOMe gives (C<sup>N</sup>C)Au-COOMe **227**, which was isolated as a thermally stable microcrystalline solid.<sup>138</sup> The formal insertion of CO into Au(III)-OMe bonds to generate Au-COOMe complexes has precedent, although the mechanism (insertion versus nucleophilic attack by external MeO<sup>-</sup>) was not unequivocally established.<sup>392,393</sup> Calculations showed that the CO insertion into to Au-OH bond of **39** is exothermic,  $\Delta H = -33.7$  kcal/mol and substantially more favorable for gold than for platinum. The CO<sub>2</sub> elimination and formation of the hydride is also exothermic ( $\Delta H = -6.7$  kcal/mol), although the stability of the hydride prevents the closure of the catalytic cycle by hydrolysis under neutral conditions. Overall this reaction sequence lends support for the carboxylate mechanism of WGS, as opposed to the formate hypothesis.<sup>394</sup>

(C<sup>N</sup>C)Au-COOH **226** undergoes condensation with excess **39** with water elimination, to give the Au<sub>2</sub>(μ-CO<sub>2</sub>) complex **228**, which was crystallographically characterized. **228** represents the first example of a CO<sub>2</sub> complex in gold chemistry. The same product was obtained by exposure of the gold oxide **83** to CO; here the CO insertion takes place even in the solid state. Attempts to

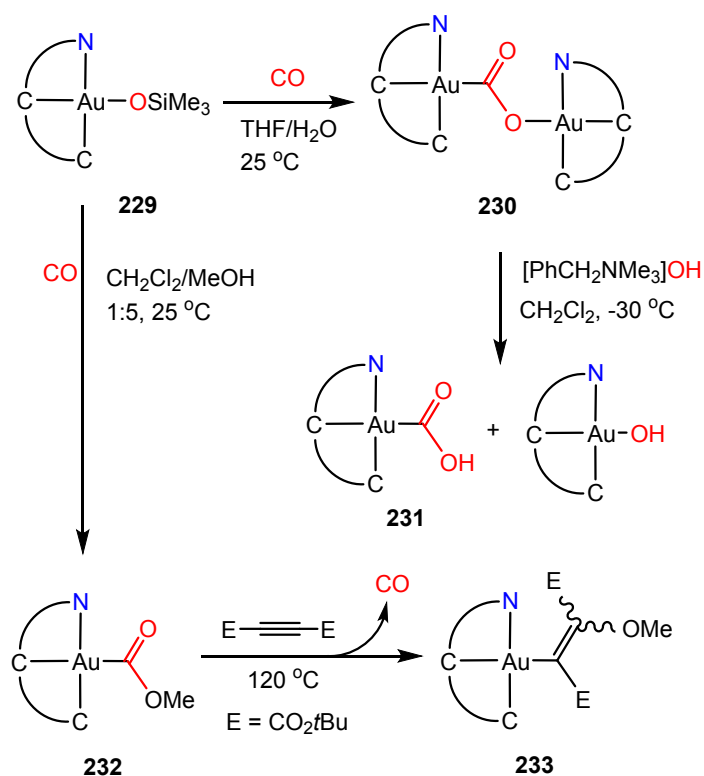
hydrogenolyze **228** under 4 bar of H<sub>2</sub> to generate formic acid failed; similarly, there was no hydrogenolysis of **227** to methyl formate. On the other hand, heating **228** to 80 – 120 °C led to the clean extrusion of CO<sub>2</sub> and the formation of the thermally stable Au(II) dimer **37**.<sup>138</sup>

### Scheme 85. Reaction of CO with Au-OH Bonds



More recently Nevado and co-workers reported closely similar reactions for the C<sup>^</sup>C<sup>^</sup>N-chelated Au(III) system. Treatment of the chloride **46** with KOH generated the hydroxide (C<sup>^</sup>C<sup>^</sup>N)AuOH. Reaction of this complex with CO at 25 °C led to decomposition, in line with the instability of the hydride intermediate **47**. More stable CO insertion products were however obtained starting from (C<sup>^</sup>C<sup>^</sup>N)AuOSiMe<sub>3</sub> **229**, which reacts with CO to give the μ-CO<sub>2</sub> complex **230**, the C<sup>^</sup>C<sup>^</sup>N analogue of **228** (Scheme 86). **230** was characterized by X-ray diffraction. Treatment of **230** in dichloromethane with a slight excess of [PhCH<sub>2</sub>NMe<sub>3</sub>]OH at -78 to -30 °C led to the metalcarboxylic acid, (C<sup>^</sup>C<sup>^</sup>N)Au-COOH **231**, together with (C<sup>^</sup>C<sup>^</sup>N)AuOH. Compound **231** is thermally unstable and was identified spectroscopically at -30 °C. Its methyl ester **232** was made by treating **229** with CO in CH<sub>2</sub>Cl<sub>2</sub>/methanol. Heating **232** with *t*-butyl acetylenedicarboxylate at 120 °C led to decarbonylation and formation of the methoxyvinyl complex **233**, as a 1:1 *E/Z* mixture.<sup>395</sup>

### Scheme 86. Reactions of (C<sup>^</sup>C<sup>^</sup>N)Au complexes with CO.



#### 4. GOLD(III) COMPLEXES IN CATALYTIC APPLICATIONS

Catalysis by gold(III) falls into two main categories. The first type involves changes in oxidation state. Although in these cases gold(I) complexes are usually employed as the entry to the catalytic cycle, the involvement of Au(III) species as reaction intermediates is either proven or hypothesized. These redox processes emulate palladium catalysis; however, for gold chemistry this is a comparatively new area which comprises the large field of C-C and C-E bond forming reactions (E = heteroatom). A potentially very important new development is the discovery that gold complexes under photoexcitation to triplet states may behave differently from complexes in the ground state, so that the high reactivity of open-shell species can be exploited (cf. Section 3.1.3).

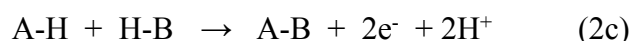
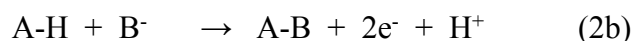
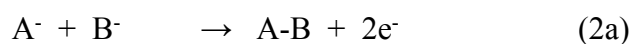
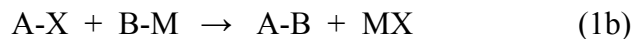
The second type of Au(III) catalysis involves its application as a Lewis acid. Here the carbophilicity of gold and the resistance (in many instances but not necessarily) of the active species to hydrolysis, and tolerance of functional groups offer distinct advantages.

The following section takes account of these different modes of action, starting with C-C and C-E bond forming reactions. Emphasis is placed on mechanistic insight rather than the breadth of synthetic applications.

##### 4.1 Coupling Reactions

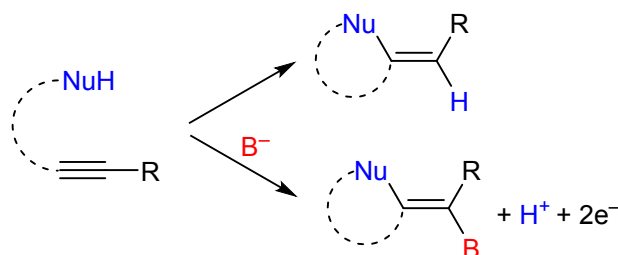
C-C coupling reactions and C-H activations leading to new C-C bond formation based on gold(I, III) catalysts have been the subject of several reviews.<sup>105,106,396,397</sup> In 2016 Kramer surveyed C-C and C-E bond formations by gold-catalyzed arene C-H activations,<sup>398</sup> and in 2020 Anilkumar and co-workers reviewed the role of gold(I) and gold(III) as catalyst in C-H activations and their synthetic applications, in more detail than can be included here.<sup>399</sup> While this manuscript was in preparation, further excellent reviews appeared, by Nijamudheen and Datta<sup>400</sup> on the mechanisms and applications of homogeneous and heterogeneous gold catalysts for C-C coupling reactions, and by Kramer on gold catalyzed aryl-aryl coupling reactions.<sup>401</sup>

**4.1.1 Mechanistic Aspects.** C-C cross-coupling reactions can be categorized broadly into two mechanistic types: Firstly, reactions where bonds are formed between an electrophile and a nucleophile under redox-neutral conditions (eqs. 1a, b); in these reactions the electrophile is typically an organic halide or halide-equivalent A-X (X = Cl, Br, I or N<sub>2</sub><sup>+</sup>) and the nucleophile B-M is a carbanion equivalent (A, B = hydrocarbyl, M = main group element). Secondly, reactions between two nucleophiles, in which electrons are consumed by sacrificial oxidants (eq. 2a). These reactions may include the activation of C-H bonds (e.g. if A-H and B-H are different or identical arenes) (eq. 2b, c).



Reactions of eq. (1) require a gold(I) precatalyst capable of oxidative addition which can react with either aryl halides or arenediazonium salts. Reactions of eq (2) involve instead a catalyst system combined with an external stoichiometric oxidant. Often these coupling reactions are part of a reaction sequence and are commonly preceded by nucleophilic attack on an unsaturated substrate, as in alkene or alkyne heteroarylations. A redox process is only required if a C-B bond is formed (Scheme 87).

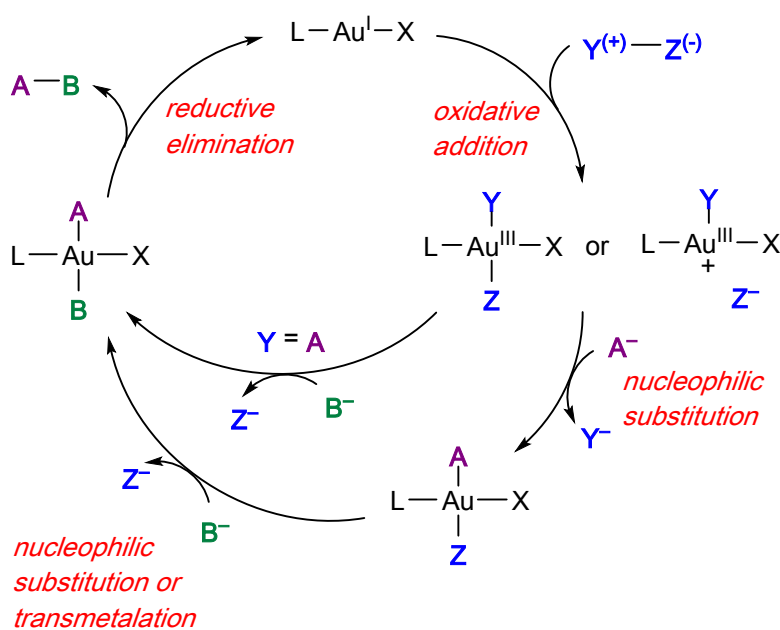
### Scheme 87. Alkyne Heterofunctionalization and Cross-Coupling



Whereas for palladium-based C-C coupling catalysts dioxygen under pressure or Cu-cocatalyzed O<sub>2</sub> oxidation have proved highly effective,<sup>402,403</sup> for soluble gold catalysts protocols with stronger oxidants have been developed, using Selectfluor or iodine(III) derivatives.<sup>284,404</sup> Catalytic cycles are based on Au(I, III) redox reactions; a general case is shown in Scheme 88. There is scope for mechanistic variation; for example, it is *a-priori* not self-evident whether the oxidative step should precede or follow the transmetalation event, and oxidants Y-Z may be external and not be part of the final product and hence be “sacrificial”, or they may be one of the reagent substrates. Also, the range of oxidation states of gold may not necessarily be limited to I and III, and the catalyst system may involve more than one gold center.

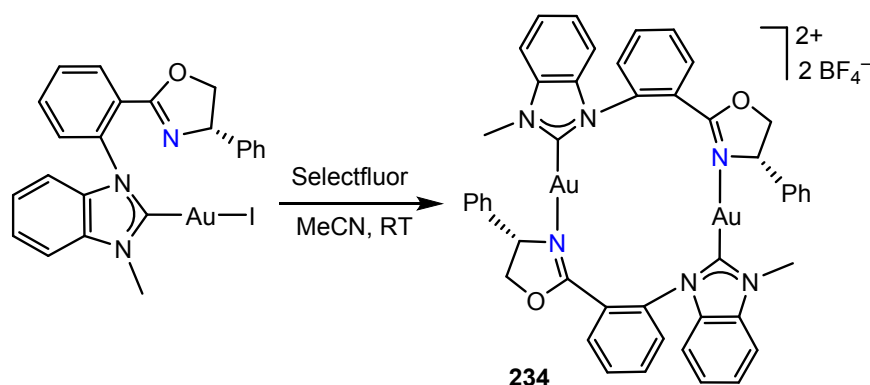
An added complication was the suggestion that C-C coupling reactions ascribed to gold catalysts, such as the Sonogashira cross-coupling, were actually catalyzed by trace impurities of palladium.<sup>405,406</sup> This appears to have been refuted, at least for supported gold nanoparticle catalysts,<sup>407</sup> but highlights the difficulty of unequivocally establishing the nature of the active species. In that context, it is also worth noting that while Au(III) complexes stabilized by suitable donor or chelating ligands do indeed most probably act as homogeneous catalysts as formulated, other commonly used Au(III) precursors such as HAuCl<sub>4</sub> can readily generate traces of nanoparticle reduction products during handling,<sup>369</sup> which may be the actual catalysts.<sup>408</sup>

### Scheme 88. General Catalytic Cycle for Gold Catalyzed Cross-Coupling Reactions



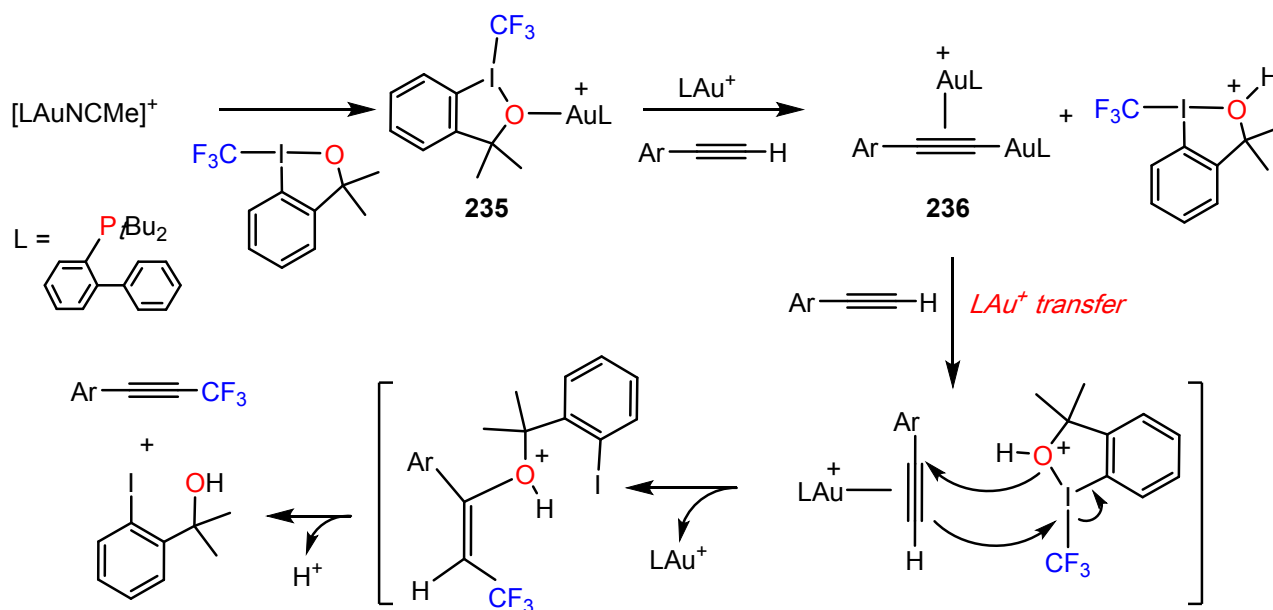
Many gold(III) catalyzed reactions rely on external oxidants in order to overcome the difficulty of cycling gold species between oxidation states +I and +III. However, before entering into detailed discussions on oxidative coupling processes, it may be useful to mention cases which show that reactions with these oxidants do not necessarily proceed as straightforwardly as envisaged (see also Section 3). For example, the reaction of Selectfluor with gold(I) iodide complexes LAuI, where L = potentially bidentate oxazoline-substituted NHC ligand, led not to an Au(III) species but to the oxidation of the iodide ligand and formation of the gold(I) chelate complex **234**; this then acts as the catalyst (in this case for the coupling of enynes with alkenes to give naphthalene derivatives), using air as oxidant (Scheme 89).<sup>409</sup>

**Scheme 89. Non-Oxidative Selectfluor Reaction With Au(I)**



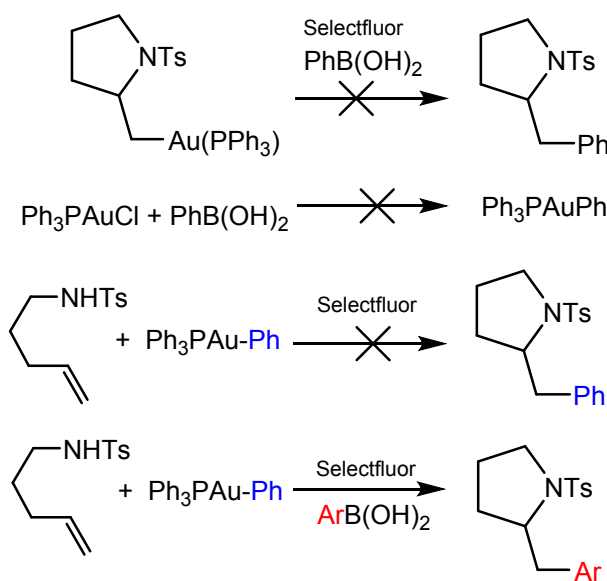
Another example is the reaction of (Ph<sub>3</sub>P)AuC<sub>6</sub>F<sub>5</sub> with either iodine(III) reagents or Selectfluor; although in this case there was the expected oxidation to Au(III), the process was accompanied by extensive ligand scrambling.<sup>287</sup> Furthermore, iodine(III) compounds may act as ligands rather than oxidants; for example, Siah and Fiksdahl proposed a mechanism for the trifluoromethylation of terminal alkynes with a combination of LAu<sup>+</sup> and an iodine(III) reagent (here Togni's reagent) which involves coordination of Au(I) to the iodine reagent without oxidation, based on spectroscopic investigations and the isolation and crystallographic characterization of complex **235** and the digold intermediate **236** (Scheme 90). There are no oxidative addition / reductive elimination steps. Neither Au(I)-alkynyl nor Au(III)(CF<sub>3</sub>)(alkynyl) species were detected.<sup>410</sup> It must also be noted that computational explorations of various possible catalytic cycles of oxidative C-O formations with Selectfluor have shown that in the energetically preferred pathway Selectfluor functions as an electrophilic fluorinating reagent, not as an external oxidant, and the reactions are therefore catalyzed by Au(I) species.<sup>411</sup>

**Scheme 90. Proposed Au(I) / Iodine(III) Based Alkyne Trifluoromethylation**



The mechanism of oxidative C-C coupling involving boronic acids, and the mode of interaction of arylboronic acids with the gold species, has been the subject of much debate. In principle, two possible catalytic sequences exist for C-C coupling reactions: oxidation of Au(I) to Au(III) followed by transmetalation, or transmetalation to Au(I) followed by oxidation. However, as Toste has highlighted,<sup>412</sup> the oxidative coupling of gold reagents with boronic acids often do not proceed as envisaged; as indicated in a number of attempted couplings using Selectfluor (Scheme 91).

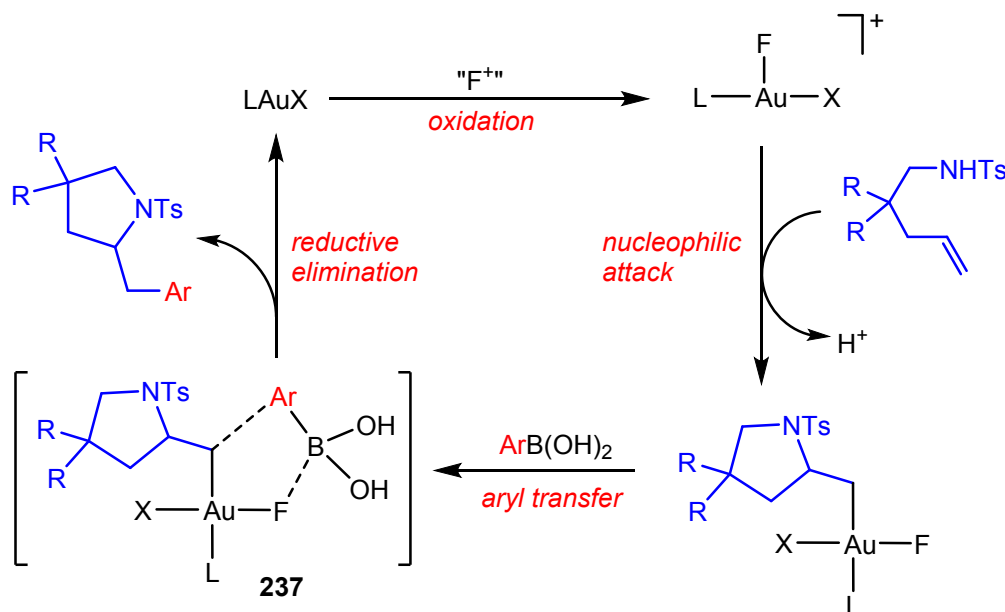
#### Scheme 91. Mechanistic Information Gained from Attempted C-C Coupling Reactions





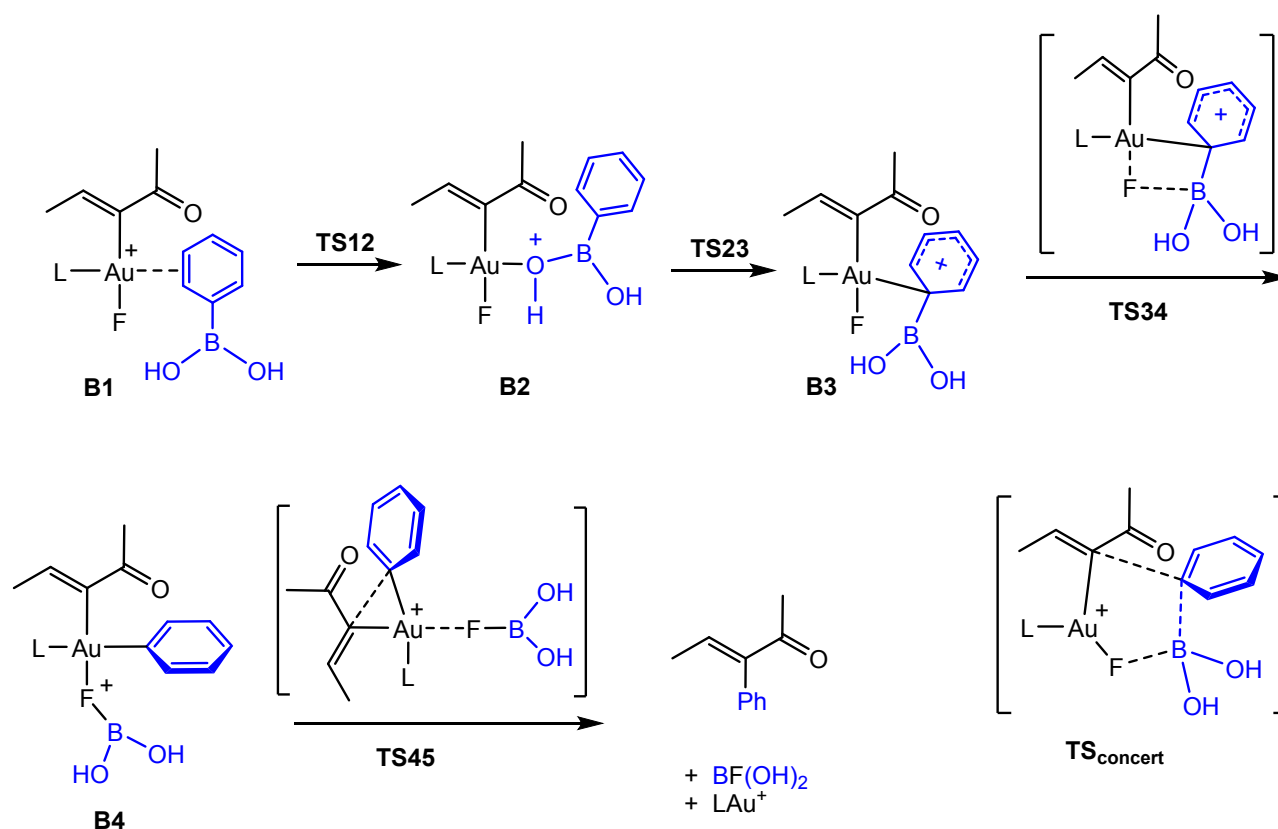
Oxidation of Au(I) must therefore precede nucleophilic attack on C=C, followed by aryl transfer from the boronic acid. Any aryl group bound to Au(III) initially is not involved, and a concerted bimolecular aryl exchange from boron to the organic moiety has been proposed, as in intermediate **237** (Scheme 92), avoiding a separate B→Au aryl transfer step.<sup>105,249,413</sup>

### Scheme 92. Proposed Catalytic Cycle for Nucleophilic Addition–Oxidative Arylation Cascade Via Au(III) Intermediates



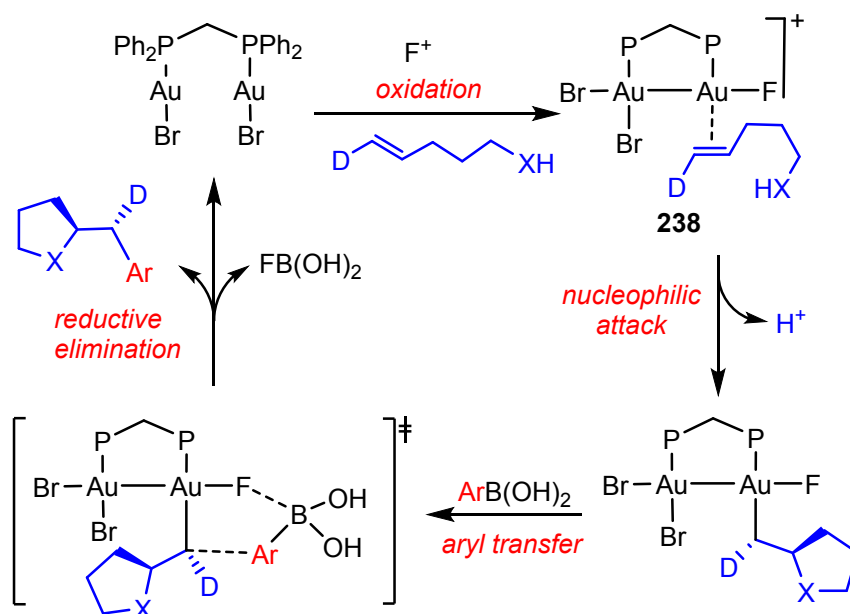
On the other hand, DFT studies by Faza and Lopez for a similar C–C arylation reaction favored a transmetalation prior to reductive C–C bond formation (Scheme 93).<sup>414</sup> Starting from the phenylboronic adduct **B1**, for most ligands L transition state **TS23** leading to **B3** is rate limiting. Intermediate **B3** shows a weak  $B \cdots F$  interaction and an aryl bond to Au, which is fully formed in **B4**. The calculations show the importance of fluoride in this reaction, which favors the process by B–F bond formation, fully established in **B4**. The final step leading to **TS45** has only a low barrier, from which the products are formed in an almost barrierless step. A concerted transition state with a 5-membered ring structure,  $TS_{concert}$ , was found to be about 6 kcal/mol higher, although with different hydrocarbyl and donor ligands that picture may change.

### Scheme 93. Computational Model of C–C Cross-Coupling Mechanism Via Transmetalation



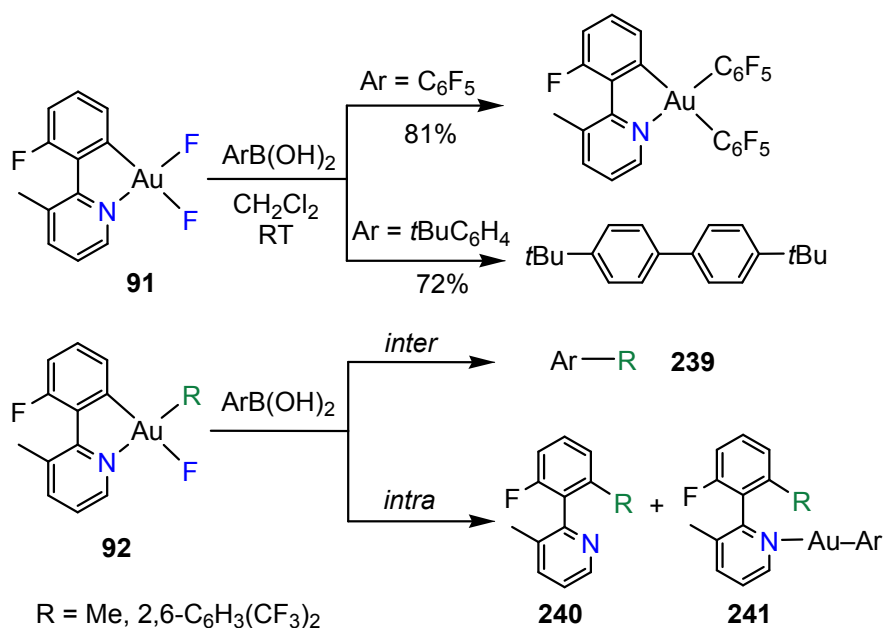
Based on the superior performance of  $(\text{dppm})(\text{AuBr})_2$  compared to  $\text{Ph}_3\text{PAuBr}$ , in a combined experimental and computational study on alkene aminoarylations Toste suggested a catalytic cycle involving the binuclear Au(II) intermediate **238**, as well as a bimolecular F/aryl exchange with boronic acid to generate the new C-C bond (Scheme 94). It was also shown that the transmetalation of alkylboronic acids  $\text{R}^*\text{B(OH)}_2$  [ $\text{R}^* = \text{syn-}t\text{BuCHDCHD-}$ ] with  $(\text{IPr})\text{AuOH}$  proceeds with inversion of stereochemistry to give *anti*- $\text{R}^*\text{Au}(\text{IPr})$ , whereas the C-C coupling step between *anti*- $\text{R}^*\text{AuF}_2(\text{IPr})$  and  $\text{PhB(OH)}_2$  involves retention, to give *anti*- $\text{R}^*\text{-Ph}$ . The slightly stronger *trans*-influence of Br compared to Cl was thought to assist the arylation by labilizing the Au-F bond, thus facilitating F transfer to B, and explains the superior performance of the bromide catalyst.<sup>412</sup>

#### Scheme 94. Toste's Bimolecular Aryl Transfer Mechanism via Au(II) Intermediates



In heteroarylations of alkenes as depicted in Schemes 92 and 94 the aryl-C bond formation is thought to involve a concerted aryl transfer from the boronic acid to the C-ligand, without a gold(III) aryl intermediate. On the other hand, the ability of well-defined Au(III) bis-aryl complexes to undergo reductive aryl-aryl coupling had been demonstrated by Vicente nearly 30 years ago.<sup>356,357</sup> Rather more recently, and using the isolated gold(III) fluorides **91** and **92**, Nevado showed that transmetalation with arylboronic acids in dichloromethane at room temperature under neutral conditions was facile. With  $\text{Ar} = \text{C}_6\text{F}_5$  the aryl complex  $(\text{C}^{\wedge}\text{N})\text{Au}(\text{C}_6\text{F}_5)_2$  was obtained, whereas with  $\text{Ar} = p\text{-}t\text{BuC}_6\text{H}_4$  only the aryl homo-coupling product  $\text{Ar-Ar}$  was produced (Scheme 95). The reactions of arylboronic acids with the monofluoride **91** gave either products of type  $\text{Ar-R}$  (**239**), which can arise from *intermolecular* aryl transfer (bimolecular mechanism), or products of types **240** and **241** (depending on the nature of R and Ar) which can evidently only arise from *intramolecular* reductive elimination following transmetalation from boron to gold. The results therefore provide evidence for a  $\text{B} \rightarrow \text{Au}$  transmetalation step prior to C-C coupling.<sup>259</sup>

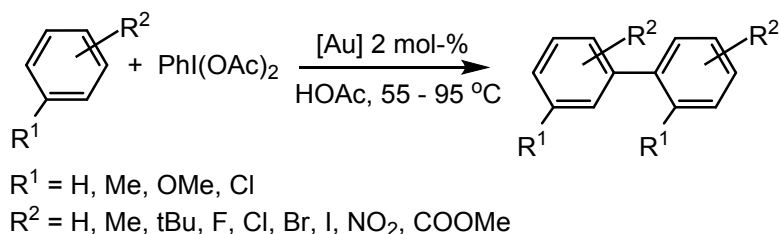
#### Scheme 95. Evidence for Transmetalation and Intramolecular Aryl Coupling



**4.1.2 Catalytic C-C Coupling Reactions.** This section will cover examples of C-C bond formations *via* Au(III) in the absence of photochemical assistance, ordered according to coupling partners, with emphasis on contributions with mechanistic evidence. Several of these reaction pathways involve C-H activation/ metalation reactions.

**Arene-Arene Coupling.** As mentioned in Section 3.1.1, the ability of gold catalysts to oxidatively couple a range of unactivated arenes using  $\text{PhI(OAc)}_2$  as stoichiometric oxidant was first demonstrated by Tse and co-workers. Good yields were obtained under comparatively mild conditions (Scheme 96).<sup>284,285</sup> Mixtures of two different arenes gave both homo- and hetero-coupling products. A range of gold complexes was tested, and  $\text{HAuCl}_4$  and  $\text{Ph}_3\text{PAuCl}$  performed about equally well, indicating that the phosphine ligand was not a requirement, although in the electrophilic amination of xylene the Au(I) complex proved inactive.<sup>285</sup>

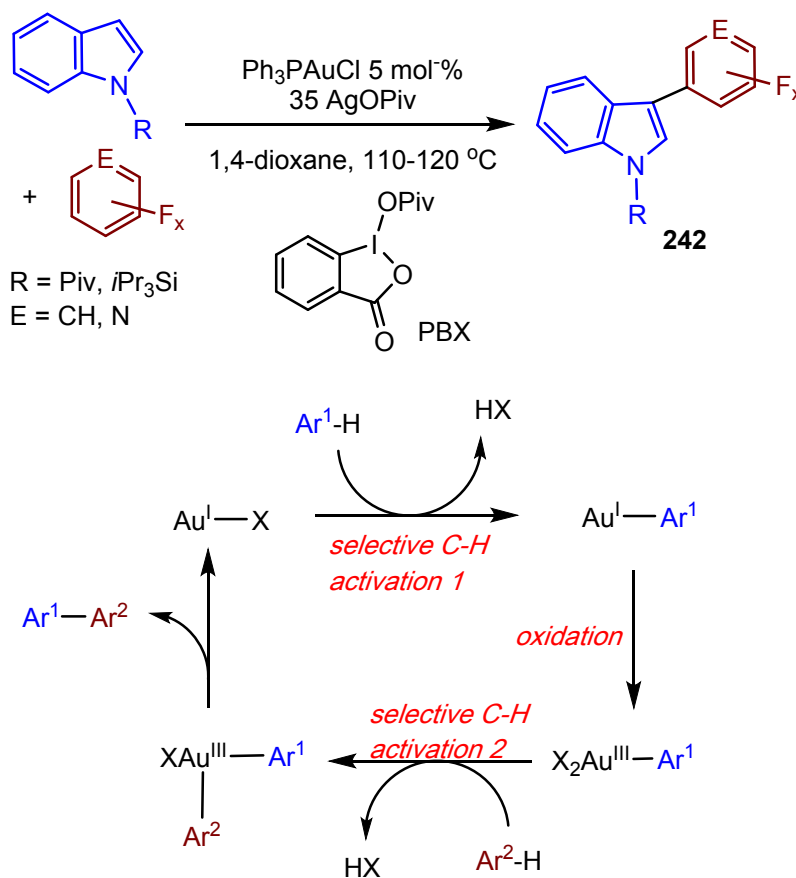
#### Scheme 96. Tse's Oxidative Homocoupling of Arenes



In 2010 Larrosa showed that electron-poor fluorinated arenes  $\text{Ar}^{\text{F}}\text{H}$  undergo C-H activation by gold(I) complexes in an acid/base reaction to give  $\text{LAu-Ar}^{\text{F}}$ .<sup>415</sup> Realizing that C-H activation of electron-rich arenes would require oxidation to Au(III), these authors provided an entry into the

selective synthesis of hetero-biaryl compounds by coupling electron-poor with electron-rich arenes. The success of this reaction was however strongly dependent on the choice of oxidant: Selectfluor and XeF<sub>2</sub> were very poor, PhI(OAc)<sub>2</sub> gave modest results, while almost quantitative yields were obtained using PhI(OH)(OTf). Test reactions showed that while LAuCl<sub>2</sub>(C<sub>6</sub>F<sub>5</sub>) was incapable of C-H activating 1,3-dimethoxybenzene, C-C coupling did proceed on addition of silver pivaloate and gave high yields, suggesting that chloride substitution by OPiv<sup>-</sup> was required to generate a sufficiently electrophilic gold(III) species. This method enabled the synthesis of a wide range of biaryls Ar<sup>1</sup>-Ar<sup>2</sup>, albeit on the basis of stoichiometric use of gold.<sup>416</sup> Further mechanistic studies showed that silver was required for catalysis and a catalytic method could be developed, based on two selective arene C-H activation steps before and after oxidation to Au(III) (Scheme 97), using Ph<sub>3</sub>PAuCl as catalyst precursor in the presence of an excess of AgOPiv and PBX as oxidant. This enabled the synthesis of a wide range of 3-arylated indoles **242**, as well as methoxy-substituted benzenes and 5-ring heterocycles.<sup>417</sup>

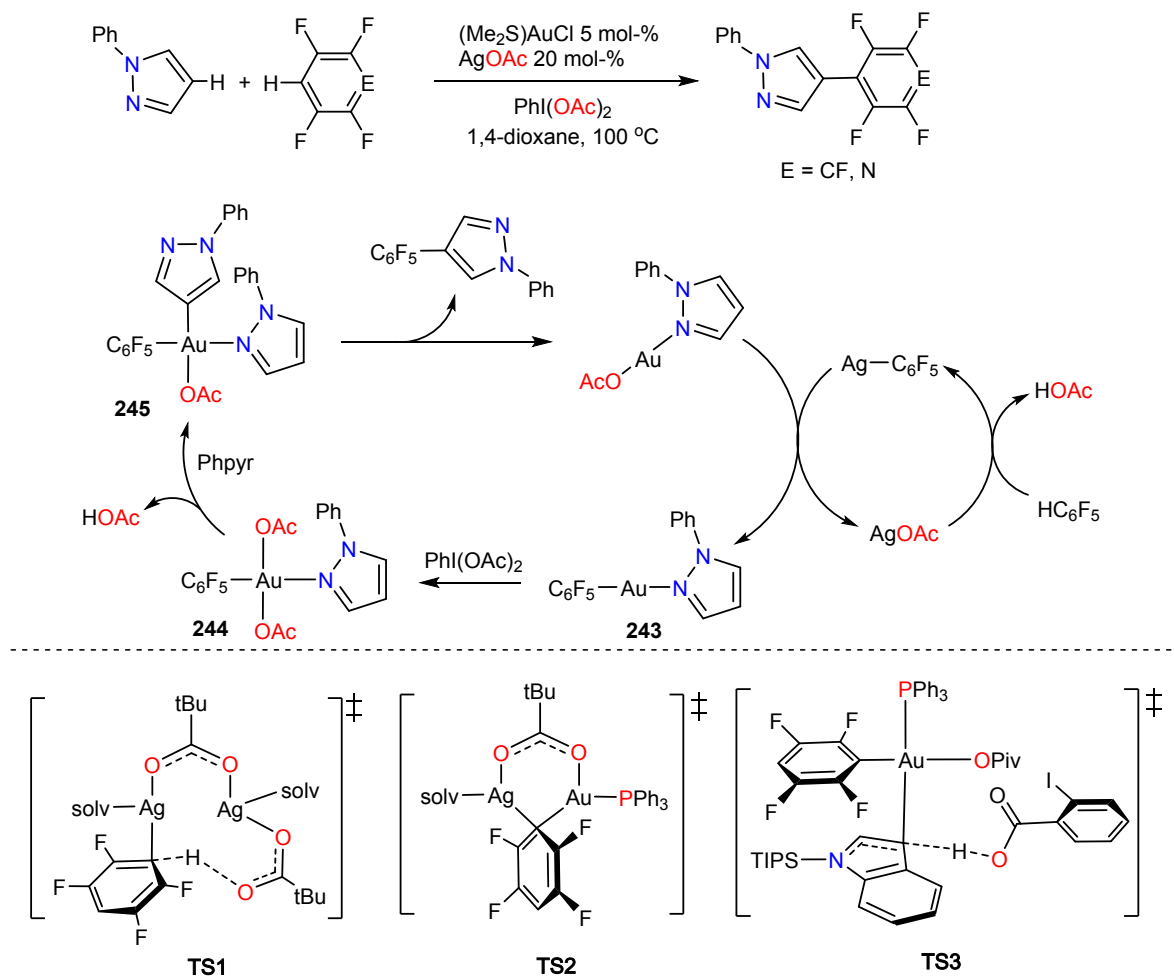
### Scheme 97. Synthesis of Biaryls by Selective Double C-H Activation



More recently Zhu and co-workers showed that highly selective double C-H activation and coupling between electron-rich and electron-poor arenes can be achieved using an Au/Ag bimetallic

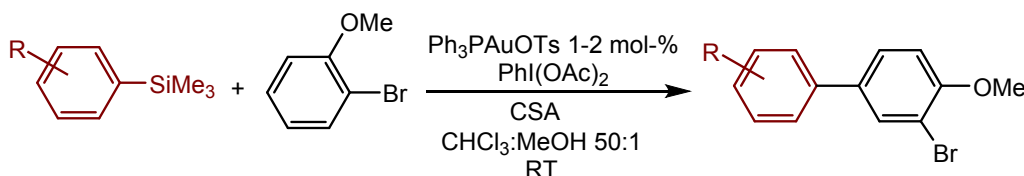
catalyst system,  $\text{Me}_2\text{SAuCl}$  /  $\text{AgOAc}$  /  $\text{PhI}(\text{OAc})_2$ . In a combined experimental and DFT study the authors demonstrated that silver acetate was an essential component capable of metalating pentafluorobenzene and tetrafluoropyridine by a concerted metalation-deprotonation (CMD) pathway, where acetate acts as base. This  $\text{Ag}^+$ -mediated process wins kinetically because it has a lower barrier than the C-H activation by Au(I). The fluoroaryl is then transferred to a pyrazole-ligated Au(I) complex **243**. Following oxidation to Au(III) aryl **244** this species then metalates the coordinated pyrrole by an  $\text{S}_{\text{E}}\text{Ar}$  mechanism to generate a bis-aryl complex **245** suitable for reductive C-C coupling (Scheme 98). The pyrazole is selectively arylated in the 4-position.<sup>418</sup> The mechanism of the related selective cross-coupling between 1,2,4,5-tetrafluorobenzene and *N*-TIPS-indole with a bimetallic  $\text{Ph}_3\text{PAuCl}$  /  $\text{AgOPiv}$  / PBX catalyst system was studied using DFT calculations. The reaction follows the mechanism outlined in Scheme 98: an  $\text{Ag}^+$ -catalyzed CMD-type C-H bond activation (**TS1**) generates  $\text{Ar}^1\text{Ag}$  which transmetalates to gold(I) via **TS2**, followed by PBX =  $\text{PhI}(\text{OCO})(\text{OPiv})$  oxidation to Au(III), which activates the indole C-H bond ( $\text{Ar}^2\text{H}$ ) (via **TS3**) prior to reductive  $\text{Ar}^1\text{-Ar}^2$  elimination. The silver-mediated CMD process is rate limiting.<sup>419</sup>

### Scheme 98. Double Arene C-H Activation and Coupling by an Au/Ag Bimetallic Catalyst



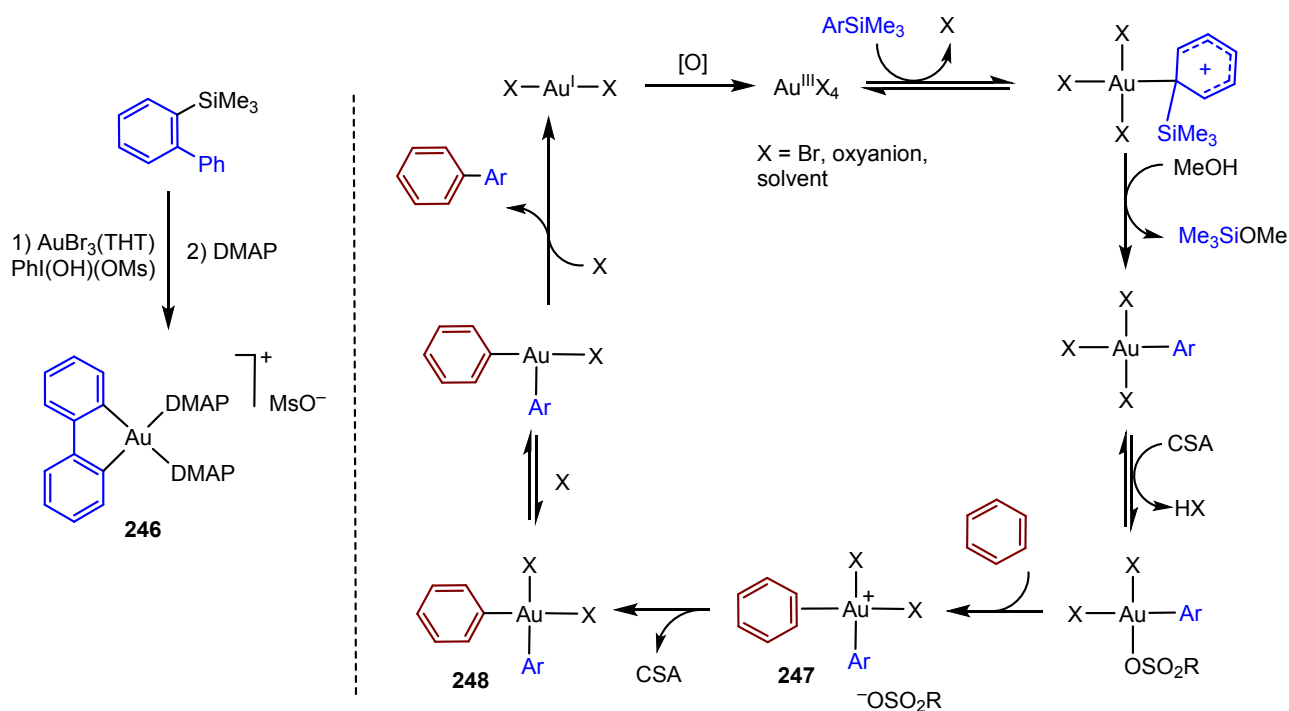
In addition to these reactions based on selective double C-H activations, C-C coupling was achieved by combining arene C-H activation with aryl anion equivalents, notably aryls of B, Si, Ge and Sn, as well as by reacting arenes with aryl halides. Based on the detection of arene homocoupling side-products in the heteroarylation of olefins with silylarene reagents,<sup>420</sup> Lloyd-Jones and co-workers developed a method for the selective oxidative cross-coupling of arenes with silylarenes using a  $\text{Ph}_3\text{PAuOTs}$  /  $\text{PhI}(\text{OAc})_2$  / camphorsulfonic acid (CSA) system (Scheme 99). A wide range of electron-donating and –withdrawing functional groups is tolerated, which makes this a valuable method for the synthesis of biaryl-based pharmaceuticals. Even bromo- and iodoarenes undergo C-H activation without affecting the C-hal bond.<sup>421</sup>

### Scheme 99. Selective Oxidative Cross-Coupling of Arenes with Silylarenes



Mechanistic studies showed that gold(I)  $\text{PPh}_3$  complexes as catalyst precursors suffered from long induction periods, commensurate with oxidative degradation of the phosphine. Consistent with this, there was no induction period with phosphine-free  $\text{AuBr}_3(\text{THT})$  which gave the best results. In the presence of  $\text{PhI}(\text{OAc})_2$  both  $\text{Ph}_3\text{PAuOTs}$  or  $\text{AuBr}_3$  are thought to lead to the same active species. Stoichiometric reactions between silylarenes and  $\text{AuBr}_3$  confirmed the aryl transmetalation to gold, e.g. by the isolation and crystallographic characterization of the arylation product **246** (Scheme 100). The reaction rate was first order in [arene] but independent of [silane]. Methanol was a co-solvent and silane scavenger but also had an inhibiting effect, and the turnover was suppressed by adventitious water. The results led to a catalytic cycle in which arene  $\pi$ -coordination to an Au(III) species **247** was rate limiting, followed by fast electrophilic arene activation and formation of a gold aryl **248** (Scheme 100).<sup>422</sup> This reaction was subsequently extended to the arylation of heterocycles<sup>423</sup> and intramolecular aryl-aryl coupling reactions to generate 5- to 9-membered rings.<sup>167</sup> The latter proved convenient systems for kinetic studies that showed a shift in the rate determining step, depending on the electronic and steric characteristics of the arenes. This ring formation by gold-catalyzed arylation has been used to generate the B ring in ( $\pm$ )-alcolchicine. Conversion of the  $\text{PhI}(\text{OAc}^F)_2$  oxidant into a diaryliodonium salt was found to have a powerful inhibiting effect.<sup>424</sup>

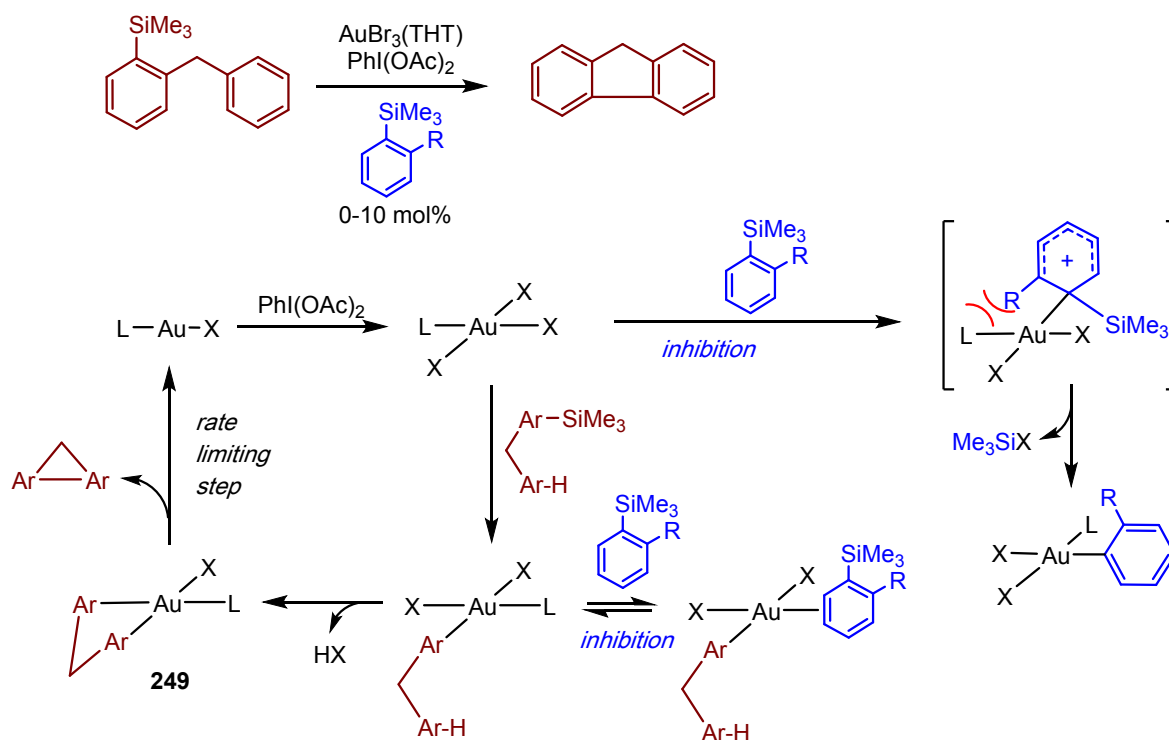
## Scheme 100. Mechanistic Proposal for Cross-Coupling of Arenes with Silylarenes



Coupling *ortho*-substituted arenes can be challenging. To address this problem, Robinson and Lloyd-Jones tested the influence of *o*-substituted silylarenes on the rate of cyclization of trimethylsilyl-2-benzylbenzene catalyzed by the AuBr<sub>3</sub>(THT) / PhI(OAc)<sub>2</sub> / CSA system, to give the intramolecular coupling product fluorene.<sup>425</sup> This reaction is zero order in arene, with the reductive elimination as rate limiting step. This is understandable considering that reductive elimination must be preceded by rotation of the aryl ligands into a conformation suitable for C-C bond formation, which is hindered in the bis(aryl) chelate **249** (Scheme 101). The rate of fluorene formation is retarded if the catalyst is partitioned between the productive cycle and the side-reaction with the *ortho*-silylarene, and this inhibition provides information about the relative rates of auration of *o*-silylarenes. The electrophilic Si/Au exchange was fastest for silylarenes with bulky *o*-substituents, with relative rates for R = H ( $k_{\text{rel}} < 0.05$ )  $\ll$  Ph (1.0) < Me (1.2) < Et (1.5) < *t*Bu (2.9), showing that auration is assisted by relief of steric compression.

The need for the arene to adopt an orientation co-planar with the square coordination sphere of the Au(III) catalyst is also shown by the rate acceleration observed when the silylarenes possess substituents that favor chelation, as in 2-R-C<sub>6</sub>H<sub>4</sub>SiMe<sub>3</sub> where R = (CH<sub>2</sub>)<sub>*n*</sub>OMe. Relative rates decreased with increasing chelate size,  $n = 1 > 2 \gg 3$ . This system also allowed the efficient coupling of *ortho*-substituted arenes with 2-bromothiophene and unactivated arenes.<sup>425</sup>



Scheme 101. Mechanism of Cross-Coupling of *o*-Substituted Silylarenes

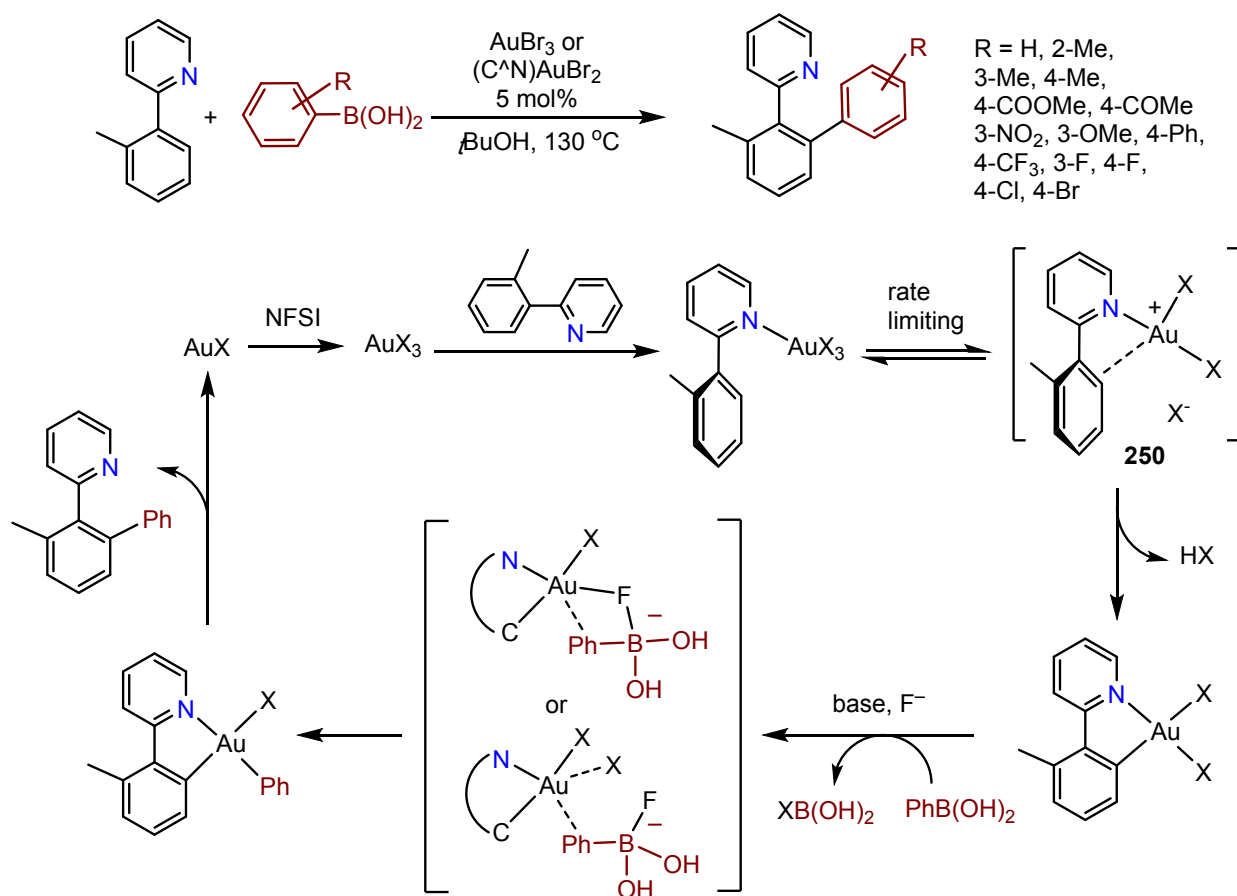
The C-E bond energy decreases within the series  $E = Si > Ge > Sn$  and the bond length increases. This means that the deformation energy required to reach the transition state in the  $S_{E}Ar$  step forming the gold(III) aryl from  $Ar-ER_3$  compounds diminishes in the same order. Taking advantage of this effect, Schoenebeck used germanium aryls in coupling reactions with both electron-rich and halogenated arenes, catalyzed by  $(Ph_3P)Au^I(OTs) / PhI(OAc)_2 /$  camphorsulfonic acid in  $CHCl_3/MeOH$  (50:1) or  $(Ph_3P)AuCl / Ag_2O /$  1-pivaloyloxy-1,2-benziodoxol-3(1H)-one (PBX). These systems maintain high regioselectivity under conditions where Pd / Cu coupling catalysts do not. A wide variety of functional groups was tolerated, including halides. Under the chosen conditions there was no reaction with  $ArSiMe_3$ .  $Me_3SiC_6H_4GeEt_3$  led to selective coupling via the Ge functionality only, so that the silyl substituent could be subjected to a series of post-coupling derivatizations.<sup>426,427</sup>

You and co-workers<sup>428</sup> developed a catalytic aryl-aryl coupling reaction based on the  $C^{\wedge}N$  chelating *o*-tolylpyridine ligand (Scheme 102). The oxidant used was *N*-fluorodi(benzenesulfon)-imide (NFSI); there was no reaction with  $PhI(OAc)_2$ . Stoichiometric reactions established various aspects of the catalytic cycle: (1) There was no reaction between  $(C^{\wedge}N)AuBr_2$  and  $PhB(OH)_2$  in *t*BuOH at 130 °C. (2) The coupling product was however formed in the presence of KF, KOH or  $KOtBu$ . KF acted as base, without evidence for Au-F bond formation. (3) Heating  $(C^{\wedge}N)Au(Ph)Br$  in *t*BuOH to 80 °C generated the reductive elimination product *py-tol-Ph*. However, since the formation of this product under catalytic conditions requires 130 °C and does not proceed at 80 °C,

reductive elimination could not be rate limiting. (4) C-H activation took place before aryl transfer from B to Au. (5) Aryl transfer from B to Au(I) before oxidation to Au(III) could be ruled out. (6) C-H activation leading to cyclometalation is irreversible. (7) The kinetic isotope effect of 0.96 suggested that C-H activation was not rate limiting. This suggested that the rate was limited by formation of the arene  $\pi$ -complex **250**, as also seen by Lloyd-Jones.<sup>422</sup>

This AuBr<sub>3</sub>-catalyzed reaction was used to prepare a wide range of *ortho*-arylated arenes with pyridine, quinoline and pyrimidine substituents.<sup>428</sup>

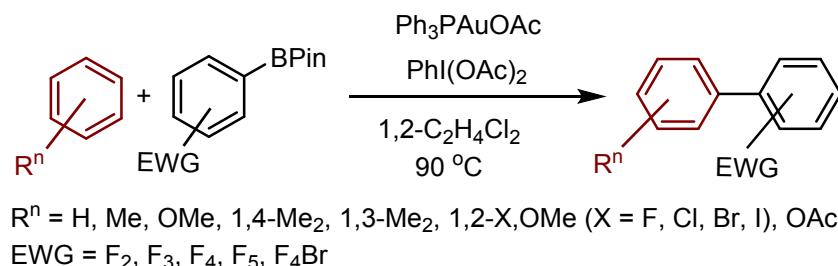
### Scheme 102. *o*-Tolpy / ArB(OH)<sub>2</sub> Cross-Coupling Reactions



In 2017 Hofer *et al.* described the Ar-Ar' coupling of arenes with electron-poor boronic esters using a Ph<sub>3</sub>PAuX catalyst combined with PhI(OAc)<sub>2</sub> as oxidant (Scheme 103). Acetate as base worked best. C<sub>6</sub>F<sub>5</sub>BPin was successful, whereas C<sub>6</sub>F<sub>5</sub>B(OH)<sub>2</sub> failed due to competitive protodeboronation. It was shown that the oxidation of Ph<sub>3</sub>PAuC<sub>6</sub>F<sub>5</sub> gives structurally characterized (Ph<sub>3</sub>P)Au(OAc)<sub>2</sub>(C<sub>6</sub>F<sub>5</sub>), which reacts with arenes stoichiometrically to give Ar-C<sub>6</sub>F<sub>5</sub> coupling products. The coupling of electron-deficient silanes ArSiMe<sub>3</sub> with electron-rich arenes was also achieved. The reaction was thought to involve transmetalation from B to Au(I), followed by oxidation and arene C-H activation. It remained unclear whether acetate or PPh<sub>3</sub> dissociates from

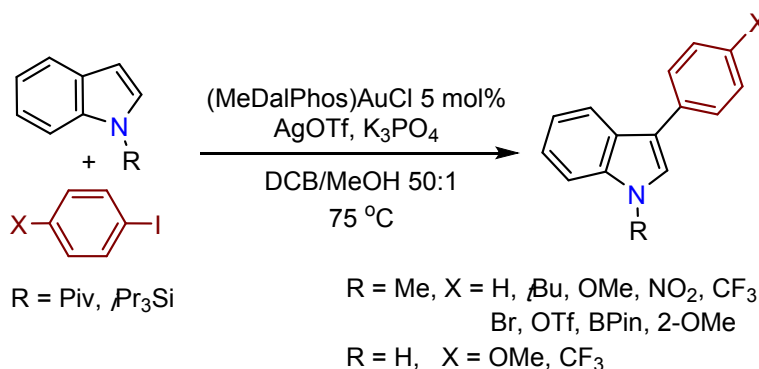
the Au(III) intermediate to enable coordination and activation of the arene prior to the coupling step. This catalytic method enabled the coupling of C<sub>6</sub>F<sub>5</sub> with ArH = benzene, toluene, xylenes, anisol, methylbenzoate esters and others but failed for ArH = pyridine or fluorobenzene.<sup>289</sup>

### Scheme 103. Coupling of Electron-Poor Arylboronic Esters with Arenes



The C-C formation of biaryls described in the previous sections all required an external oxidant. This is of course not required if one of the substrates acts as oxidant, as is the case with aryl halides. The coupling of aryl iodides with electron-rich arenes was explored by the group of Bourissou.<sup>310</sup> Taking advantage of the ability of the hemilabile MeDalPhos ligand to facilitate the oxidative addition of Ar-I to gold(I) (see Section 3.1.2, Scheme 41), the substituent influence of *p*-substituted iodoarenes on the rate of oxidative addition and coupling with trimethoxybenzene was explored. Contrary to palladium, oxidative addition to Au(I) is facilitated by increased electron density of the iodoarene. This effect can be understood as the result of the reduced back-donation in the Au(III) system: whereas back-donation is important for palladium and therefore favors the reaction with electron-poor substrates via an arene  $\pi$ -complex, the electrophilicity of Au(III) gold center favors reaction with electron-rich substrates via an Au-I-Ar  $\sigma$ -intermediate. Palladium and gold therefore constitute complementary systems for C-C coupling. The (MeDalPhos)AuCl / AgOTf / K<sub>3</sub>PO<sub>4</sub> catalyst mixture arylates indoles in 3-position (Scheme 104). Heterocyclic iodoarenes also work, as does the arylation of N-protected indoles.<sup>310</sup>

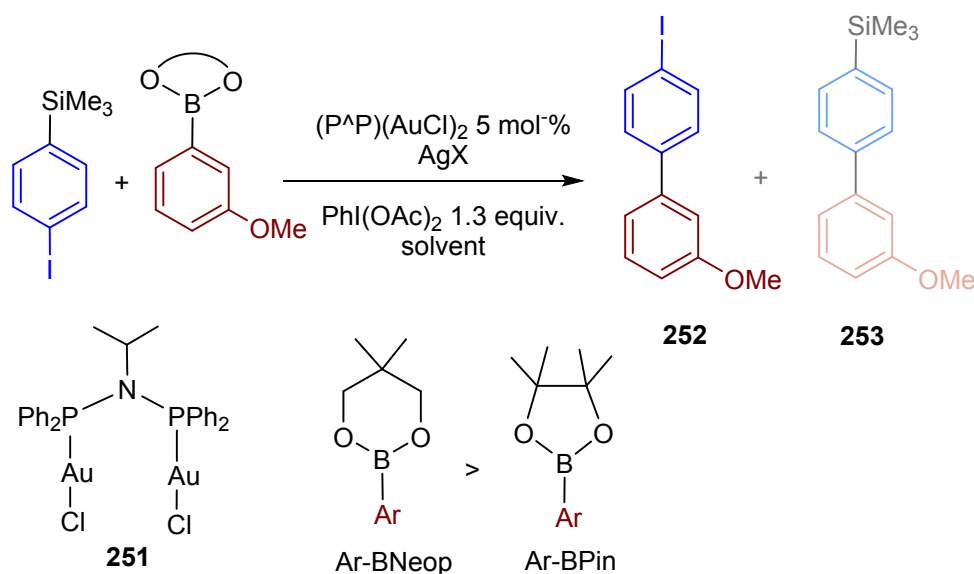
### Scheme 104. Catalytic Coupling of Iodoarenes with Electron-rich Arenes.



1  
2  
3  
4  
5 Tin organometallics as coupling partners were explored by Patil and co-workers, using R-  
6 SnBu<sub>3</sub> in combination with aryl diazonium salts [Ar-N<sub>2</sub>]<sup>+</sup>BF<sub>4</sub><sup>-</sup> and a Ph<sub>3</sub>PAuCl catalyst in MeCN at  
7 room temperature.<sup>429</sup> Although formation of the main product Ar-R was accompanied by some Ar-  
8 Ar and R-R homo-coupling byproducts, in most cases good yields of Ar-R could be obtained. As  
9 expected, there was excellent functional group tolerance on both R and Ar, and, as Schoenebeck  
10 had found in coupling reactions with trialkylgermyl compounds,<sup>426,427</sup> SiMe<sub>3</sub> substituents were left  
11 intact. The reaction proceeded with reasonably high yields even in the case of *ortho*-substituted Ar  
12 and with N-donor heterocycles such as Ar = quinolinyl. The range of tin reagents was extended to R  
13 = vinyl and alkynyl to give the corresponding Ar-vinyl and Ar-alkynyl cross-coupling products.  
14 Mechanistic studies supported the notion of R transfer to Au(I) before oxidation, as well as the  
15 formation of an Au(III)(R)(Ar) intermediate detected by HR-MS. <sup>31</sup>P NMR spectroscopy also  
16 allowed the identification of Ar-PPh<sub>3</sub><sup>+</sup> and R-PPh<sub>3</sub><sup>+</sup> as side-products of C-P reductive elimination,  
17 indicative of catalyst deactivation pathways.<sup>429</sup>

18  
19 The hetero-coupling of two different nucleophiles Ar<sup>1</sup>B(OR)<sub>2</sub> and Ar<sup>2</sup>SiMe<sub>3</sub> poses  
20 challenges since selective formation of the Ar<sup>1</sup>-Ar<sup>2</sup> product requires two kinetically distinct  
21 transmetalation events to the catalytic metal center, to avoid homo-coupling by-products. Xie and  
22 co-workers subjected this problem to a multi-parameter approach, testing various combinations of  
23 Au(I) precatalysts/ boron reagents / solvents / silver salts in the test reaction of 4-iodophenylsilane  
24 with 3-methoxyphenylboronic acid derivatives (Scheme 105).<sup>430</sup> Of the range of bisphosphine-  
25 bridged binuclear gold(I) complexes tested, dinuclear *i*PrN(Ph<sub>2</sub>PAuCl)<sub>2</sub> **251** gave the highest yields  
26 and best selectivity for the desired hetero-coupling product **252**. Cyclic voltammetry of **251**  
27 suggested two 1-electron oxidation steps to give an Au<sup>II</sup>-Au<sup>II</sup> intermediate, suggestive of Au(II)  
28 catalysis along the lines proposed by Toste (Scheme 94),<sup>412</sup> although disproportionation to Au<sup>I</sup>/Au<sup>III</sup>  
29 species could not be ruled out. While the boron reagent is able to transfer the aryl group to Au(I),  
30 the electrophilic activation of silylarenes requires Au(III). Of the silver additives, AgOTf and  
31 AgNTf<sub>2</sub> performed better than AgOTf. The sterically less demanding BNeop coupling partner  
32 proved to give higher yields than BPin, and 1,1,2-trichloroethane was the preferred solvent. The  
33 desired hetero-coupling products of type **252** were generated for a large variety of aryl-aryl  
34 combinations, essentially independent of electron-rich/poor character, in yields of about 40 – 85%,  
35 including *ortho*-substituted 2-TfOC<sub>6</sub>H<sub>4</sub>-C<sub>6</sub>H<sub>4</sub>-2'-Br (60% yield). Palladium catalysts, on the other  
36 hand, reacted only via oxidative addition of the Ar-I function to give **253**.<sup>430</sup>

### Scheme 105. Oxidative Aryl-Aryl Coupling of Two Different Nucleophiles



The synthesis of chiral biaryls through C-C coupling mediated by enantioselective catalysts was established for palladium some time ago<sup>431</sup> but has only recently attracted attention in gold catalysis. Using a hemilabile chiral P<sup>N</sup> ligand, Tabey *et al.* achieved the synthesis of axially chiral biaryls in stoichiometric reactions between Au(I) aryls and arenediazonium salts under blue light irradiation (see Section 4.1.3). Transmetalation to Au(I) prior to oxidation worked best and gave binaphthyls with up to 26 % e.e.<sup>432</sup> Subsequently Himmelstrup *et al.*<sup>433</sup> showed in another stoichiometric study that, with suitable ligand design, much higher yields and enantioselectivities could be achieved. Using binuclear precursors (P<sup>P\*</sup>)(AuCl)<sub>2</sub>, where P<sup>P\*</sup>= chiral bis(phosphine) ligands, CsF-assisted double transmetalation of naphthylboronic acids was achieved, followed by oxidation with PhICl<sub>2</sub> at -78 °C to generate the corresponding Au(III) complexes. Warming to room temperature led to reductive elimination of the binaphthyl products. It was speculated that this involved fast intramolecular aryl transfer in a di-gold Au(I)/Au(III) intermediate, as suggested by Toste,<sup>351</sup> to place both aryl ligands on the same Au(III) center.<sup>433</sup>

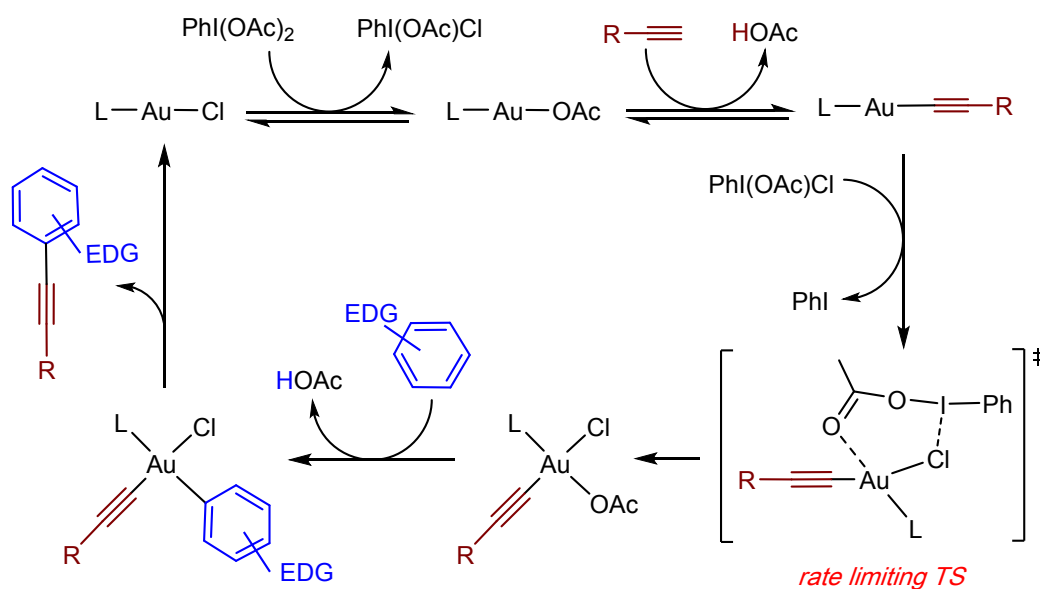
**Arene-Alkyne ( $C_{sp^2}$ - $C_{sp}$ ) Coupling.** The coupling between arenes and alkynes to give alkynyl-substituted arenes was first demonstrated in 2001 by Fuchita in stoichiometric reactions of gold(III) aryls.<sup>166</sup> Since then a number of catalytic methods have been developed and the synthetic scope has been widely explored. Many of these advances have been summarized in a 2013 review by Brand *et al.*<sup>434</sup>

The first example of the Sonogashira coupling to generate arylalkynes was reported by Qian and Zhang in 2011, using Ph<sub>3</sub>PAuCl in the presence of AgBF<sub>4</sub> with Selectfluor as oxidant. NEt<sub>3</sub> as base was also required. A plausible, standard Au(I)/Au(III) redox cycle was proposed.<sup>435</sup>

In 2010 de Haro and Nevado reported the coupling of alkynes to electron-rich arenes with a gold(I) catalyst in the presence of PhI(OAc)<sub>2</sub> as oxidant. Electron-rich aryl halides typically resist

oxidative addition with palladium catalysts and therefore C-C coupling reactions *via* this route are challenging. Of the various catalyst / activator combinations tried,  $\text{Ph}_3\text{PAuCl}$  (5 mol %) with  $\text{NaHCO}_3$  as base in 1,2-dichloroethane at 90 °C worked best.<sup>436</sup> Although the formation of a gold(I) alkynyl complex under these conditions was demonstrated in stoichiometric reactions, the initial investigation was unable to differentiate between an Au(I,III) redox cycle, or an Au(I)  $\pi$ -complex mechanism. A subsequent detailed experimental and computational study provided more insight. In particular, it demonstrated the importance of the *in-situ* generated asymmetric iodine(III) species  $\text{PhI}(\text{OAc})\text{Cl}$  which can oxidize the Au(I) acetylide intermediate  $\text{LAuC}\equiv\text{CR}$  with a much lower activation barrier than  $\text{PhI}(\text{OAc})_2$ . The process involved electrophilic attack on coordinated arene by an Au(III) species (Scheme 106).<sup>289</sup>

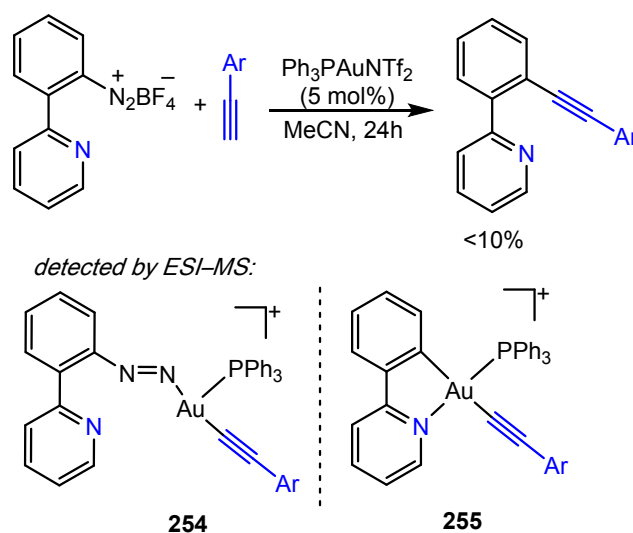
### Scheme 106. Role of $\text{PhI}(\text{OAc})\text{Cl}$ in Arene-Alkyne Coupling



In 2015 the Shi group demonstrated the catalytic coupling of terminal alkynes or boronic acids with arenediazonium salts, which was tested initially under dual gold/photoredox catalysis.<sup>437</sup> Optimization studies revealed that the outcome of these reactions was unaffected by the presence of the photocatalyst and that couplings were equally productive in the dark, particularly when donor ligands such as bipy were utilized. This would imply that a mechanistic alternative to photoactivation (whether photosensitized or not) is provided which efficiently leads to the oxidation of gold(I) by the diazonium salt. Spectroscopic studies revealed that while  $\text{Ph}_3\text{PAuNTf}_2$  and 4-fluorobenzenediazonium salts are unreactive for prolonged periods of time, the addition of bipy to the solution leads to the quantitative formation of arylphosphonium salts, as observed usually during photo-assisted reaction protocols (see Section 4.1.3). The same process was seen starting

from Au(I) acetylide complexes, where the reaction with arenediazonium salts and bipy leads to the formation of the C–C coupling product in high yield. Lower yields were observed without bipy. ESI-MS experiments performed using chelating diazonium salts suggested that the latter react with the Au(I) precursor affording aryldiazenido compounds **254** (Scheme 107). When bipy was used, the efficiency of N<sub>2</sub> extrusion increased and the Au(III) intermediate **255** was trapped.<sup>438</sup> Overall, these experiments suggested a base-assisted decomposition mechanism, where the oxidation of Au(I) to Au(III) occurs in a single step and does not involve Au<sup>II</sup> intermediates and, consequently, radical chains. In follow-up studies this method was shown to be broadly applicable to a range of organic substrates used in both dual/gold photoredox and photo-assisted gold catalysis, such as olefins, allenes and alkynes.<sup>439,440</sup>

### Scheme 107. Trapping Experiments in the Non-irradiative C–C Coupling of Arenediazonium Salts and Terminal Alkynes



Arenediazonium salts were also used in combination with nucleophiles to develop a broad range of heterocoupling reactions under thermal conditions. For example, in the coupling of aryls with bromide ions in a Sandmeyer-like reaction ESI-MS studies suggested the intermediacy of Au(III) dibromo aryl derivatives. In this case the addition of bipy was found not to be necessary, as the bromide itself can promote the decomposition of the diazonium salt. This methodology was extended to C–S coupling with thiols and C–P coupling with H-phosponates.<sup>441</sup>

A number of reactions have been reported where alkynyl-substituted iodine(III) reagents (ethynylbenziodoxol(on)es, EBXs) are used as coupling partners in arene and alkyne alkynylations. Scheme 108 shows some examples.<sup>442-446</sup> Various mechanistic possibilities have been proposed for these reactions, which either consider Au(I) as carbophilic Lewis acid forming alkyne  $\pi$ -complexes,

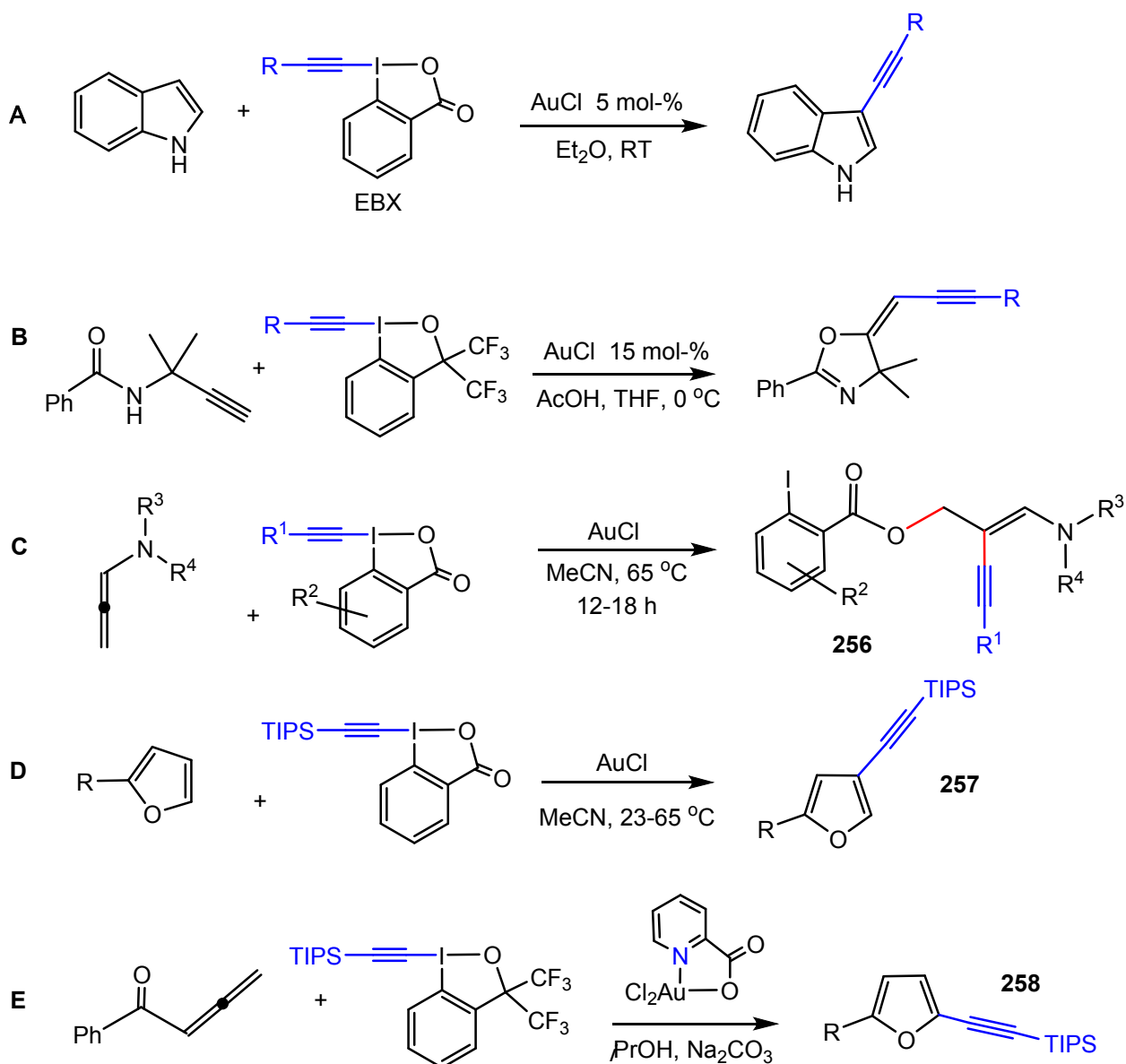
1  
2  
3 or assume Au(I, III) redox cycles.<sup>446</sup> The reaction was extended to the coupling of TIPS-EBX with  
4 thiophenes through an AuCl / trifluoroacetic acid “cooperative effect”, although the causes for this  
5 effect remained obscure.<sup>447</sup> N- allenamides react with EBX under AuCl catalysis in MeCN to give  
6 oxyalkynylation products **256** (Scheme 108 C). There was no catalysis with AuCl<sub>3</sub>. An Au(I, III)  
7 redox cycle was proposed.<sup>448</sup> Early in 2020 Patil and co-workers have critically reviewed the gold-  
8 EBX catalyst system, with particular emphasis on the various mechanistic alternatives, and this  
9 chemistry will therefore not be discussed here in detail.<sup>449</sup> The most active catalyst seems to be  
10 “ligand-free” AuCl. Given that AuCl is a coordination polymer that consists of chains held together  
11 by a network of aurophilic interactions, the precise nature of the catalyst under the reaction  
12 conditions must remain a matter of speculation.  
13  
14

15  
16  
17  
18  
19  
20 The reaction with TIPS-EBX was extended to the synthesis of 2- and 3-alkynylated furans  
21 **257** and **258**, using either an electrophilic C-H activation pathway with pre-formed furans, or an  
22 Au(III) catalyzed domino reaction starting from allenes (Scheme 108 D and E), although little  
23 mechanistic detail has been substantiated.<sup>450</sup>  
24  
25  
26  
27  
28

### 29 **Scheme 108. C-C formation Using EBX Reagents**

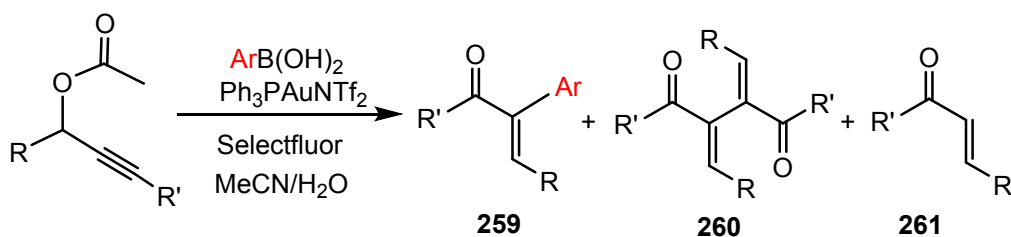
30  
31  
32  
33  
34  
35  
36  
37  
38  
39  
40  
41  
42  
43  
44  
45  
46  
47  
48  
49  
50  
51  
52  
53  
54  
55  
56  
57  
58  
59  
60





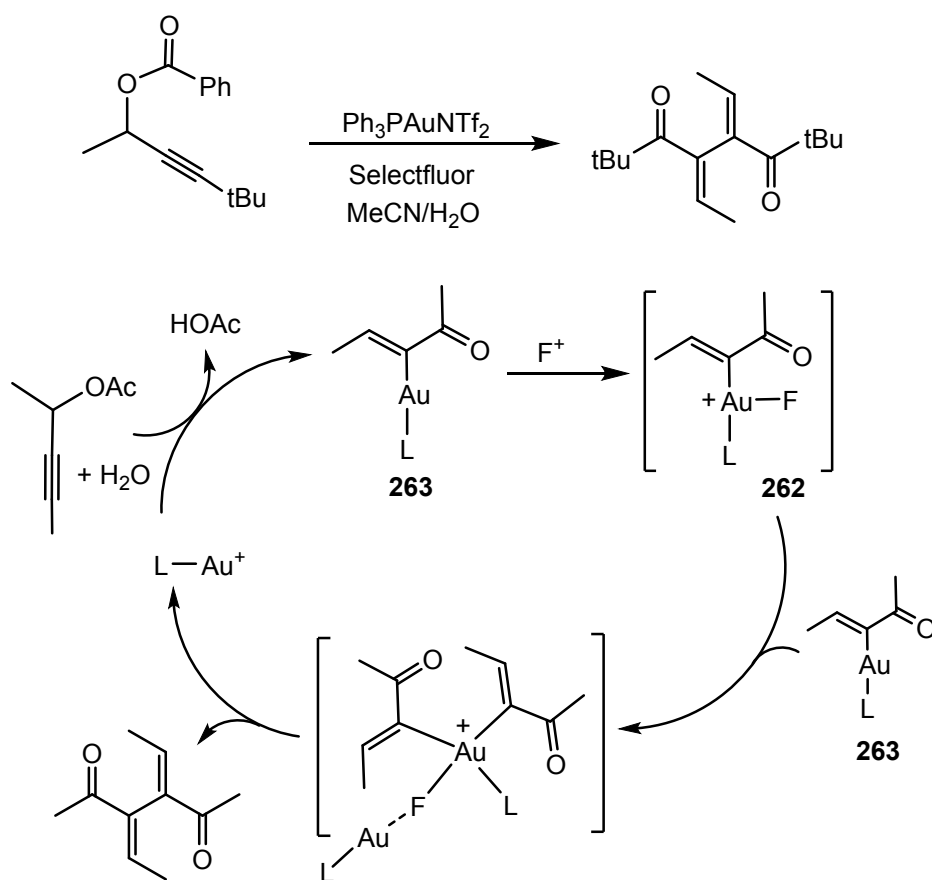
**Vinyl Coupling.** Zhang reported in 2009 that propargylic acetate can be coupled with phenylboronic acid to give **259**, alongside products of homocoupling **260** and protodeauration **261** (Scheme 109).<sup>404</sup> A mechanism involving oxidation to Au(III) followed by aryl transmetalation was proposed.  $K[PhBF_3]$  was too reactive as transmetalation agent and gave biphenyl as aryl-homocoupling product. The reaction mechanism was supported by detailed theoretical studies by Faza and López to explain the product distribution (Scheme 93).<sup>414</sup>

#### Scheme109. Aryl-Propargyl Coupling by Au(I)/Selectfluor



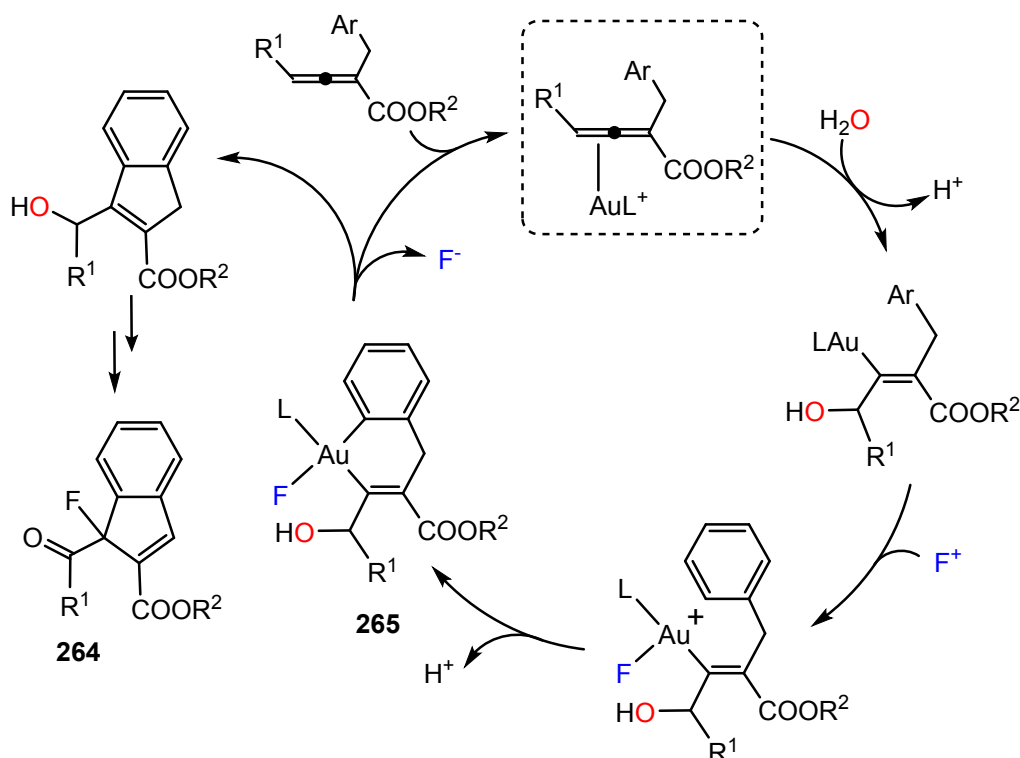
13 Mechanistically related are the reactions of propargylic derivatives, with formation of new  
14 C-C bonds and with or without the introduction of nucleophilic functional groups. For example, in  
15 the reaction of propargylic carboxylates in the presence of Au(I) catalysts and Selectfluor, Zhang  
16 discovered that with certain alkyne substrates the main product was due to vinyl-vinyl coupling.  
17 This could only have arisen by vinyl transfer to an Au(III)-vinyl intermediate **262**, presumably from  
18 an LAu(I)-vinyl precursor **263** (Scheme 110).<sup>451</sup> The same products were found as byproducts of  
19 the coupling reactions of propargylic esters with arylboronic acids.<sup>404</sup> Comprehensive DFT  
20 calculations support a mechanism of vinyl transmetalation from Au(I) to Au(III), followed by vinyl-  
21 vinyl reductive elimination,<sup>414</sup> which is known to be very facile.<sup>355</sup>

### 30 Scheme 110. Enone Homo-Coupling Catalyzed by the Au(I)/Selectfluor System



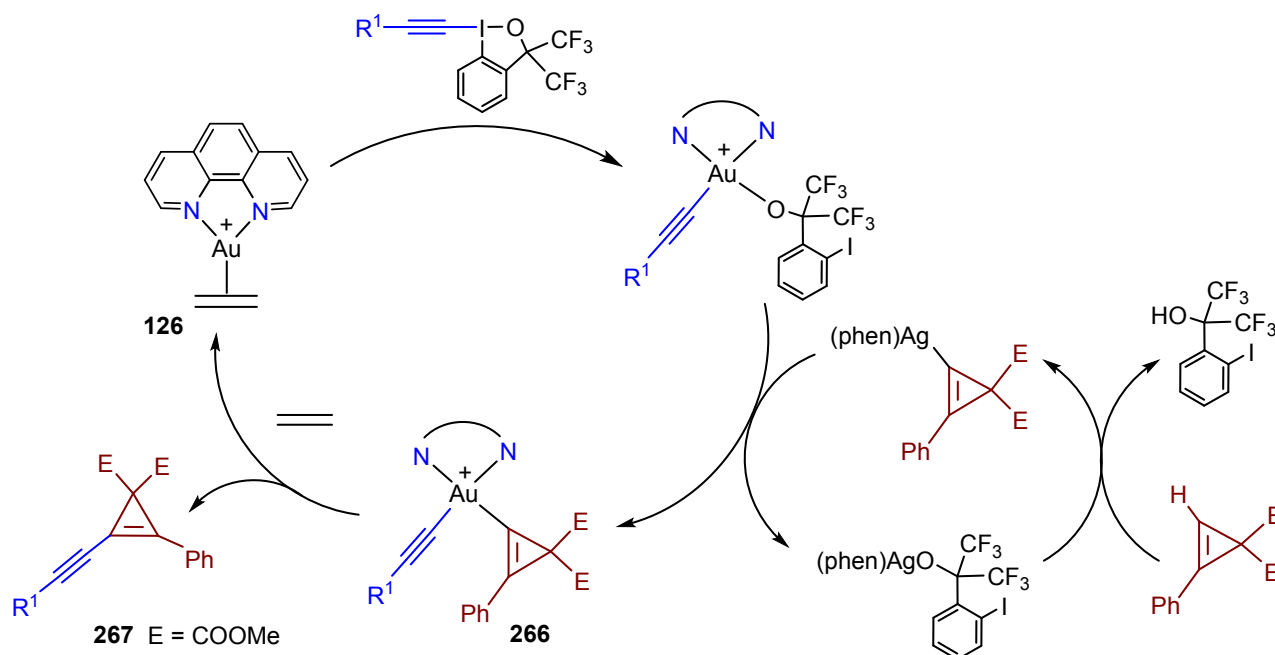
In 2012 Liu *et al.* reported a three-component tandem reaction between allene esters, Selectfluor, and water in the presence of Au(I) catalyst precursors, which gives fluorinated indene derivatives **264**. A plausible mechanism *via* Au(III) intermediates has been proposed (Scheme 111).  $^{18}\text{O}$  labelling established that the ketone-O was derived from water, and the kinetic isotope effect suggested that the cycloauration step to give **265** was rate-determining. The end product was formed by off-cycle oxidation/fluorination steps.<sup>452</sup>

### Scheme 111. Three-Component Allene Functionalization



In 2019 Hashmi and co-workers reported the coupling between terminal alkynes and cyclopropenes which was accomplished by a gold(I, III) catalyst cycle in the presence of silver salts. H/D exchange experiments on the cyclopropenes confirmed that it Ag<sup>+</sup> was responsible for C-H activation, followed by cyclopropenyl transfer from Ag(I) to Au(III), generating **266**, which on reductive elimination generates the alkynyl cyclopropene **267** (Scheme 112). The process was driven by (a) the presence of a phenanthroline ligand, which stabilizes both the silver and gold species, (b) the presence of a silver salt, and (c) by an atmosphere of ethylene, which assists the reductive elimination step by stabilizing the generated gold(I) species as the ethylene complex [(phen)Au(C<sub>2</sub>H<sub>4</sub>)]<sup>+</sup> **126**.<sup>306</sup>

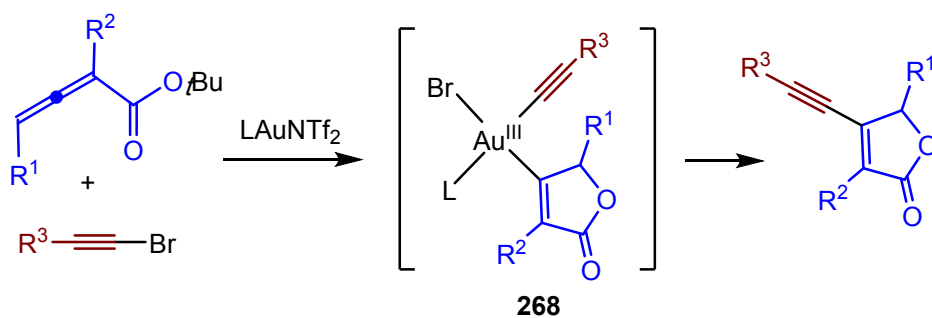
### Scheme 112. Dual Ag/Au Mediated Alkynylation of Cyclopropenes



26  
27  
28  
29  
30  
31  
32  
33  
34  
35  
36  
37  
38  
39  
40  
41  
42  
43  
44  
45  
46  
47  
48  
49  
50  
51  
52  
53  
54  
55  
56  
57  
58  
59  
60

The oxidative addition of 1-bromoalkynes has been used to couple alkynes with allenates for the synthesis of  $\beta$ -alkynyl- $\gamma$ -butenolides (Scheme 113), most probably via Au(III) alkynyl intermediates **268** followed by reductive C(sp<sup>2</sup>)-C(sp) coupling.<sup>453</sup> This contrasts with the coupling of tetrahydroisoquinolines and 1-bromoalkynes in the presence of [Au<sub>2</sub>( $\mu$ -dppm)<sub>2</sub>]Cl<sub>2</sub> under UVA LED light irradiation, for which a low-oxidation state radical quench pathway was proposed.<sup>454</sup>

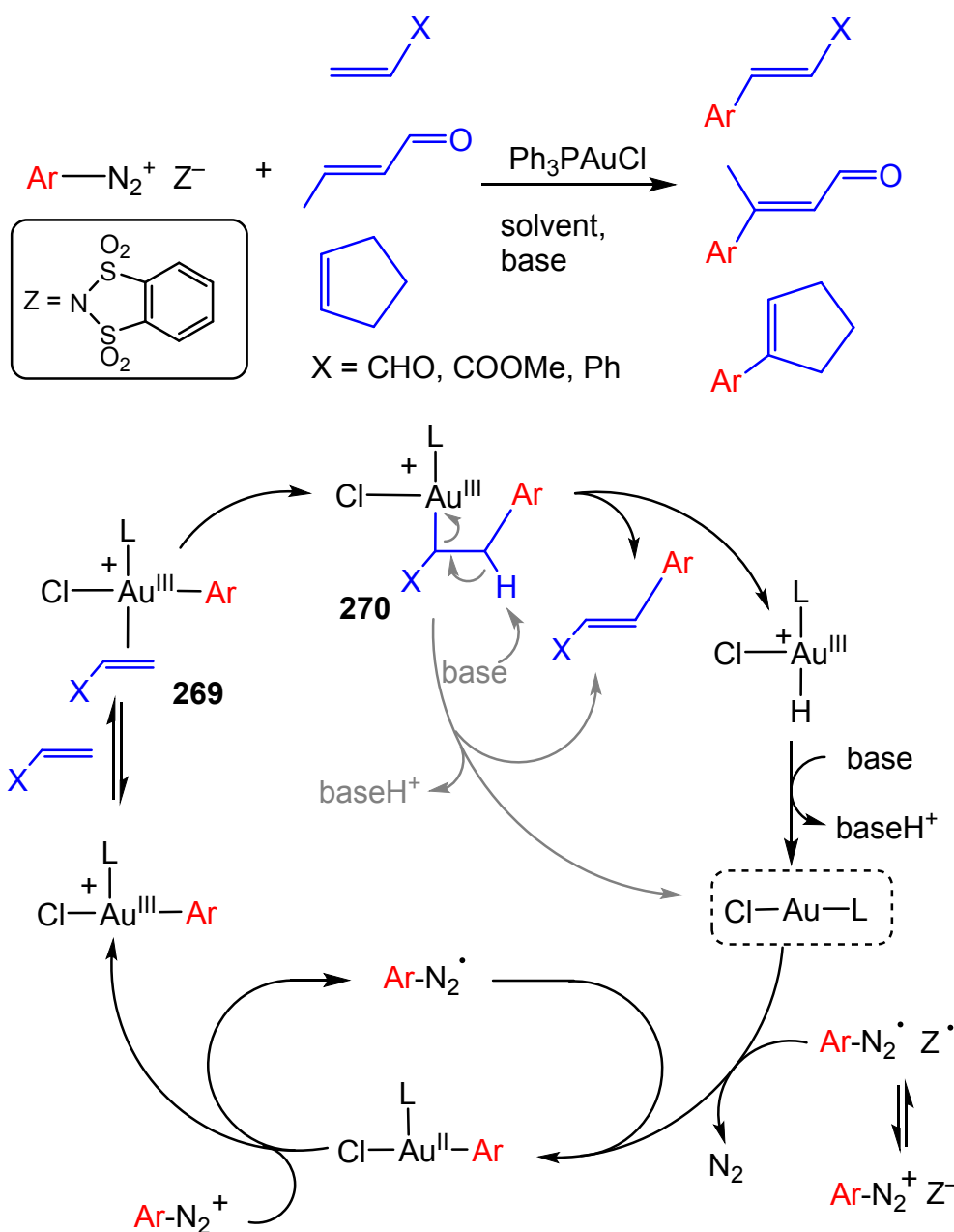
### Scheme 113. C-C Coupling via Oxidative Addition of 1-Bromoalkynes



The gold catalyzed Heck-coupling reactions of arenediazonium o-benzenedisulfonimides was described in 2018 by Barbero and Dughera.<sup>455</sup> Although originally conceived as photochemically assisted catalysis with [Ru(bipy)<sub>3</sub>]<sup>2+</sup> as photosensitizer, it became evident that these reactions proceeded very well in the dark, without sensitizers, using Ph<sub>3</sub>PAuCl in a variety of solvents of different polarity (toluene, THF, MeCN). Acetonitrile as solvent with CaCO<sub>3</sub> as base worked best. Unlike the usual BF<sub>4</sub><sup>-</sup> anion used in diazonium reagents, in this case the benzenedisulfonimide anion (Z<sup>-</sup>) assists in the generation of aryl radicals since it is redox active, a

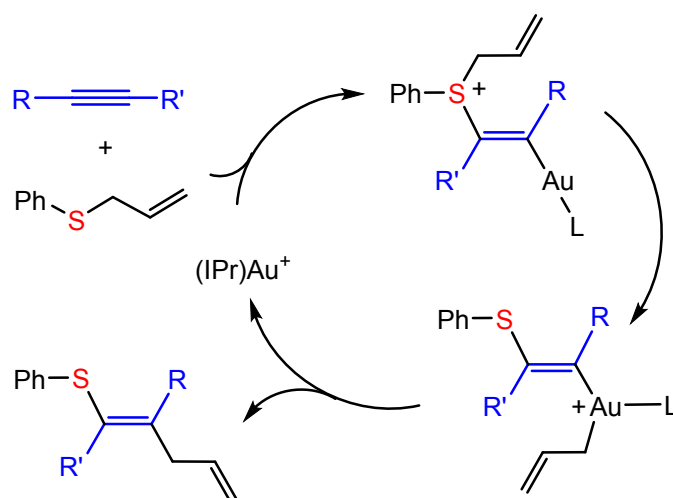
proposal supported by formation of Ar-Z as by-product, which seems to suggest that there is scope for anion engineering in order to increase the reactivity of diazonium reagents in the absence of photosensitizers. The system provided good to high yields of aryl-vinyl coupling products with vinylic halides and aldehydes, and with cyclopentene. A tentative mechanism was proposed (Scheme 114) based on close analogies with the Heck reaction, although some postulated reaction steps like alkene insertion into the Au-Ar bond of **269** and  $\beta$ -H elimination of a gold(III)-alkyl such as intermediate **270** would seem to warrant further scrutiny; the latter step might for example be replaced by a base-assisted reductive  $\beta$ -deprotonation sequence,<sup>160</sup> which would lead to the same product release.

### Scheme 114. Heck-type Coupling of Alkenes with Arenediazonium Benzenedisulfonimides



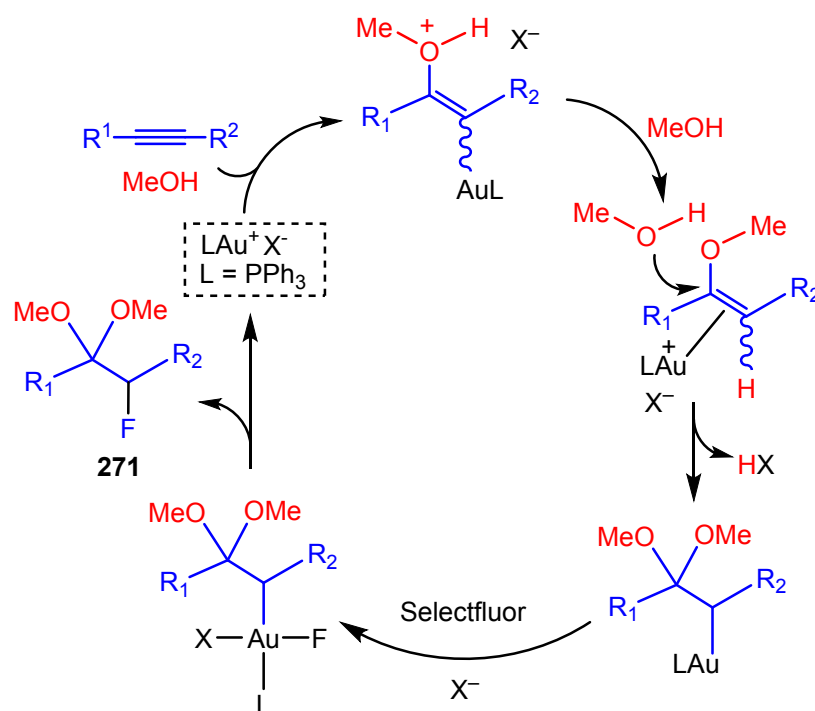
More recently, Shi and co-workers discovered that allyl thioethers can act as oxidants and lead to oxidative C-C forming reactions of disubstituted alkynes without the need for external oxidants (Scheme 115).<sup>456</sup> Although mechanistic information was restricted to mass spectrometry identification of Au(III) ions, a plausible pathway including the formal oxidative addition of RS-allyl to gold(I) most likely explains the product formation.

### Scheme 115. Catalytic Alkyne Thioallylation



If the reductive elimination step from a gold(III) intermediate involves the fluoride derived from Selectfluor, C-F products may be formed. This was demonstrated by the simultaneous addition of two MeO functions and alkyne fluorination to give **271**, following the reaction sequence of Scheme 116.<sup>457</sup> A similar mechanism has been proposed for the conversion of propargyl acetate derivatives with (IPr)AuNTf<sub>2</sub> / Selectfluor to give  $\alpha$ -fluoroenones.<sup>458</sup>

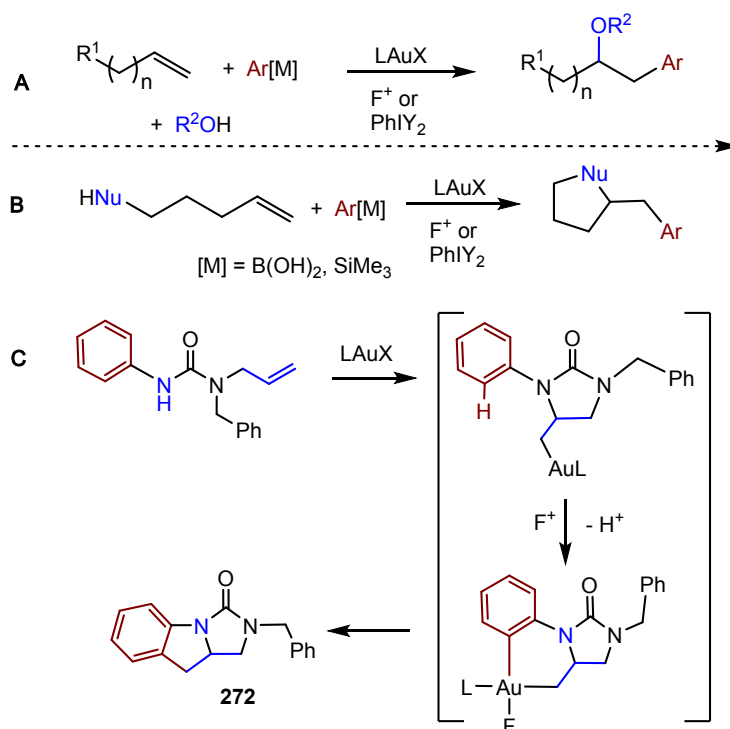
### Scheme 116. Proposed Alkyne Monofluorination Mechanism



**Arene-Alkene Coupling.** The functionalization of alkenes and alkynes in the presence of nucleophiles and external oxidants has been reviewed.<sup>98</sup> In 2010 Zhang reported that the nucleophilic approach to C=C and C-C bond formation occurs by anti-attack (Scheme 117; Nu = O or NH). The preferred catalyst was  $\text{Ph}_3\text{PAuCl}$  / Selectfluor in anhydrous MeCN.  $\text{PhI}(\text{OAc})_2$  as oxidant was ineffective. Nucleophilic attack precedes oxidation and transmetalation.<sup>459</sup> The system was extended to the intramolecular arene C-H activation in place of boronic acids, to generate tricyclic products **272** (Scheme 117 C).<sup>460</sup> The mechanism of this reaction was investigated by DFT calculations, which confirmed the sequence of Au(I) mediated N-attack on C=C, followed by oxidation by  $\text{F}^+$  in the rate determining step, followed by  $\text{C}(\text{sp}^2)\text{-C}(\text{sp}^3)$  reductive elimination. Water was found to reduce the activation barrier.<sup>461</sup>

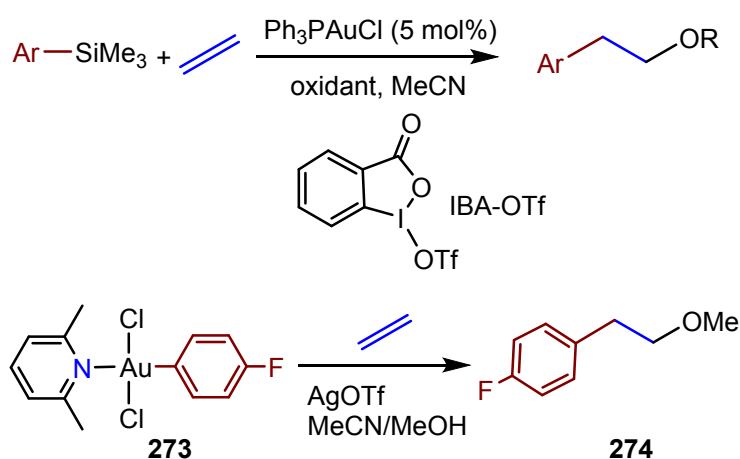
As reported by the Lloyd-Jones /Russell team<sup>420,462</sup> and the Toste group,<sup>412,463,464</sup> the oxidative coupling of olefins with main group aryls and alcohols or amines under oxidative conditions gives functionalized arylated alkanes. The reactions can be conducted with both intra- and intermolecular nucleophilic attack, using Selectfluor or iodine(III) oxidants, and either arylsilanes or arylboronic acids as transmetalating agents (Scheme 117B). Both B and Si reagents seem to perform about equally well, and both mononuclear and binuclear gold catalyst precursors have been used. For the latter, Toste has proposed a mechanism based on binuclear Au(II) species<sup>412</sup> (cf. Scheme 94).

**Scheme 117. Oxidative Oxyarylation of Alkenes**



More recently, the Russell group reported the direct 1,2-oxyarylation of ethylene (1 bar) (Scheme 118). The choice of the oxidant proved crucial, with IBA-OTf outperforming all other iodine(III) reagents. The proposed Au(I,III) redox cycle includes a C(sp<sup>2</sup>)-C(sp<sup>3</sup>) reductive elimination step and was supported by the stoichiometric reaction of (lutidine)AuCl<sub>2</sub>Ar **273**, which reacts with ethylene in the presence of methanol to give ArC<sub>2</sub>H<sub>4</sub>OMe **274**.<sup>465</sup>

### Scheme 118. Oxidative Oxyarylation of Ethylene



Taking advantage of the facile oxidative addition of aryl iodides to (MeDalPhos)Au(I) complexes,<sup>309</sup> Bourissou combined oxidative addition with oxyarylation to couple aryl iodides with functionalized alkenes.<sup>466</sup> The method allows alkene arylation independent of the electron-rich or

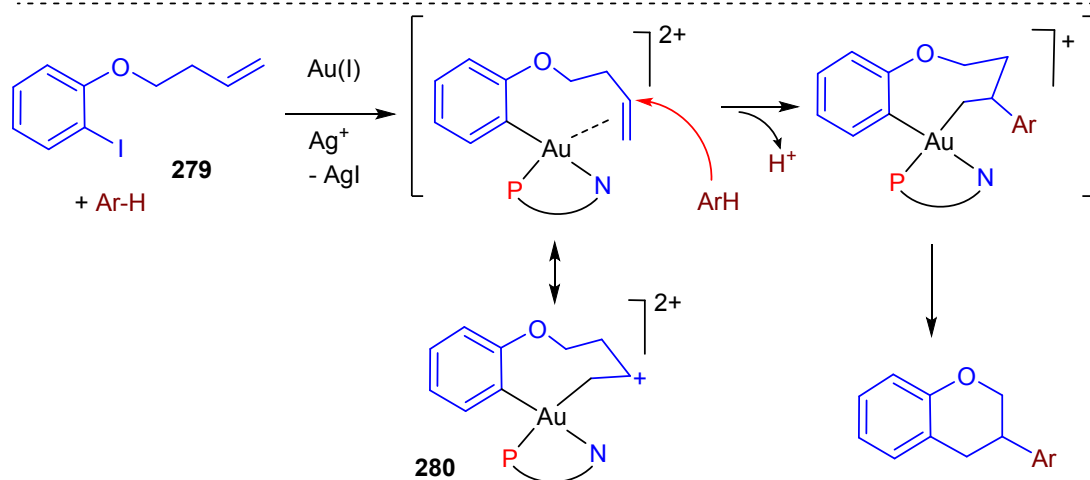
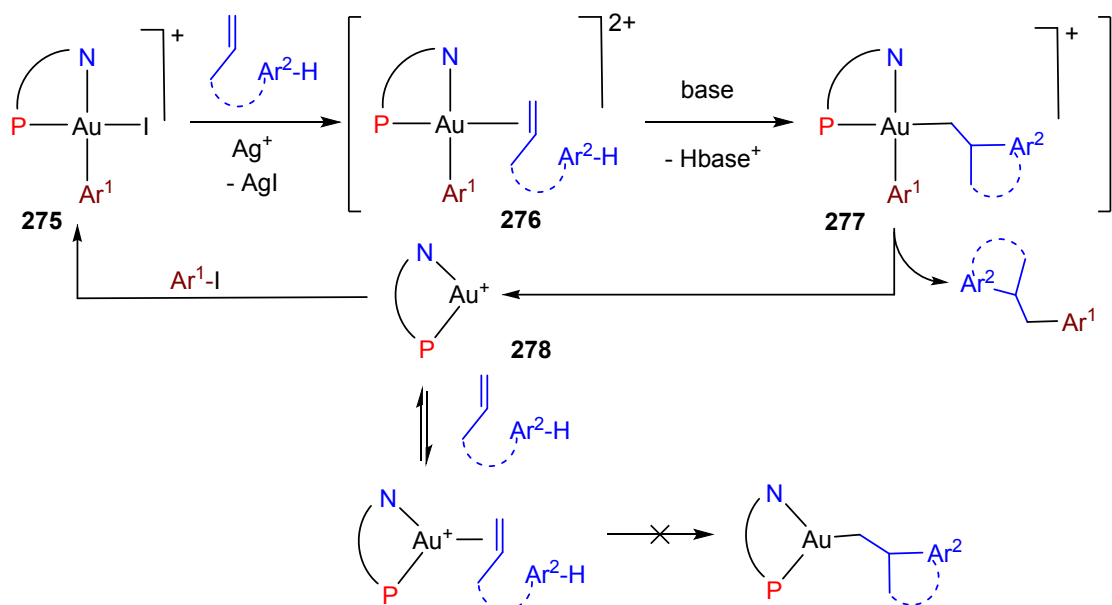
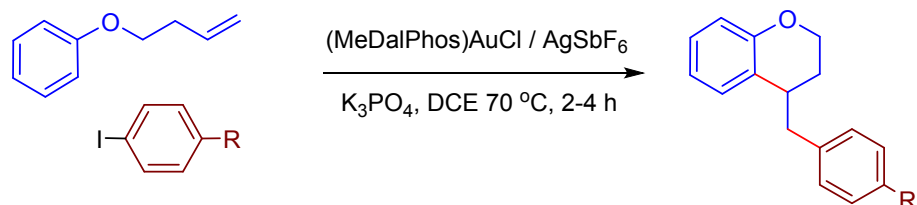
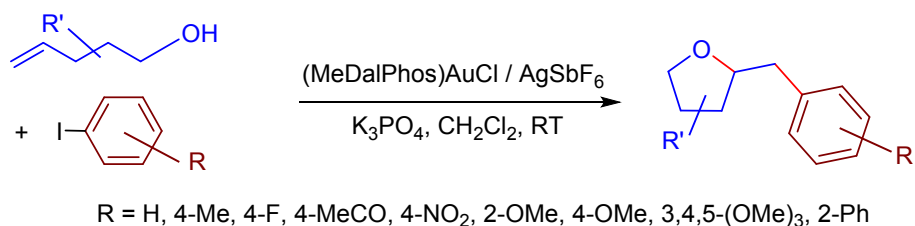


1  
2  
3 electron-poor characteristics of the aryl. Using a similar principle, in a simultaneous publication  
4 Patil reported a system for the 1,2-diarylation of arylalkenes (Scheme 119).<sup>467</sup> Here, too, a wide  
5 range of functional groups on both Ar<sup>1</sup> and Ar<sup>2</sup> was tolerated. Mechanistic studies showed that  
6 neither Au(I) nor Ag<sup>+</sup> were capable of arene-C-H activation, and a cycle was therefore formulated  
7 based on Ar<sup>2</sup>-I oxidative addition to give **275**, followed by halide removal by Ag<sup>+</sup> to give the  
8 dicationic Au(III) species **276**, which is thought to coordinate the alkene and provide sufficient  
9 electrophilic character to the C=C bond to facilitate attack on the tethered Ar<sup>1</sup> substituent (**277**). The  
10 alkene was found to significantly retard the rate of Ar-I oxidative addition, since alkene binding to  
11 [(P<sup>^</sup>N)Au]<sup>+</sup> (**278**) competes effectively with iodoarene binding to the same Au(I) cation prior to the  
12 oxidative addition step.  
13  
14  
15  
16  
17  
18  
19

20 It was also found possible to reverse the roles of Ar<sup>1</sup> and Ar<sup>2</sup>, and arylation of 2-iodophenyl-  
21 alkene **279** proved possible in case of electron-rich arenes like indoles. In this case electrophilic  
22 attack on an external arene is required, facilitated by the resonance structure **280** of the Au(III)  
23 alkene  $\pi$ -complex.<sup>467</sup> Alkene complexes of dicationic Au(III) species, where back-donation is  
24 expected to be minimal, are as yet unknown, and unfortunately no spectroscopic evidence for the  
25 formation of such species was obtained.  
26  
27  
28  
29  
30  
31

### 32 **Scheme 119. Au(III) Catalyzed 1,2-Arylation and Oxyarylation of Alkenes**

33  
34  
35  
36  
37  
38  
39  
40  
41  
42  
43  
44  
45  
46  
47  
48  
49  
50  
51  
52  
53  
54  
55  
56  
57  
58  
59  
60



55  
56  
57  
58  
59  
60

**Alkyne-Alkyne Coupling.** In 2012 Corma and co-workers reported the homo-coupling of terminal acetylenes, which was efficiently catalyzed by Ph<sub>3</sub>PAuCl or Ph<sub>3</sub>PAuNTf<sub>2</sub>, with Selectfluor as oxidant and Na<sub>2</sub>CO<sub>3</sub> as base in non-dried acetonitrile. Spectroscopic, cyclic voltammetry and kinetic investigations resulted in a mechanistic proposal where Au(I) forms an alkyne  $\pi$ -complex

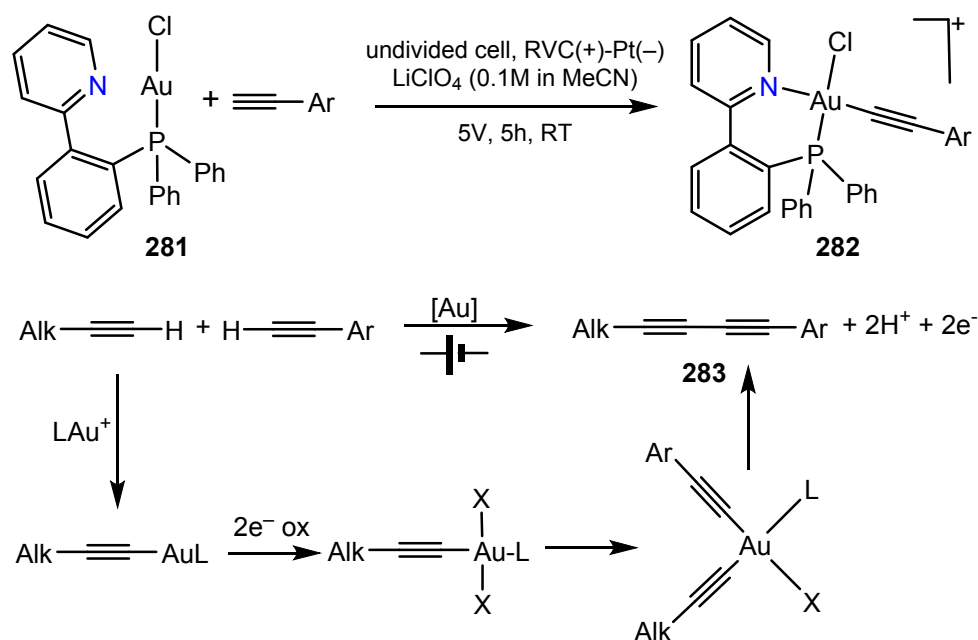
1  
2  
3 which is transformed into an acetylide  $\text{LAuC}\equiv\text{CR}$ , facilitated by proton removal by the base.  
4  
5 Oxidation generates a gold(III) monoacetylide species, which then reacts with further  $\text{LAuC}\equiv\text{CR}$  to  
6  
7 give a bis-acetylide intermediate. The cycle is closed by reductive alkynyl coupling. An Au(II)  
8  
9 pathway was thought not to operate under these conditions.<sup>468</sup> In the same year Zhu *et al.* reported  
10  
11 similar alkyne homo-couplings using a  $\text{Ph}_3\text{PAuCl} / \text{PhI}(\text{OAc})_2 / \text{K}_2\text{CO}_3$  system in 1,2-  
12  
13 dichloroethane at 60 °C. Possible mechanisms suggested include an Au(I,III) redox cycle or alkyne  
14  
15 insertion into an Au(I)-alkynyl bond.<sup>469</sup> Alkyne homo-coupling of longer-chain alkyl acetylenes  
16  
17 showed an unusual distal size selectivity: alkynes with 10 C-atoms in length undergo coupling  
18  
19 readily, while alkynes with 12 C-atoms are virtually unreactive. Incomplete oxidation by  
20  
21 Selectfluor generates Au(III) alkynyls in the presence of Au(I) alkynyls, which transfer the alkynyl  
22  
23 ligand to Au(III). The authors presented experimental evidence that the size selectivity effect can be  
24  
25 traced to the transmetalation step in an A-framed, mixed-valence digold (I, III) acetylide  
26  
27 intermediate. C(sp)-C(sp) reductive elimination from Au(III) was found to be extremely fast and  
28  
29 complete within <1 min at -78 °C (turnover frequency >0.016 s<sup>-1</sup>).<sup>360</sup>

30  
31 In 2014 the Shi group reported the oxidative cross-coupling of two different types of  
32  
33 alkynes to give asymmetric diynes  $\text{ArC}\equiv\text{C}-\text{C}\equiv\text{CAlk}$ . Screening of catalysts and ligands identified  
34  
35 the di-gold complex  $(\text{dppm})(\text{AuBr})_2$  as preferred catalyst, assisted by N^N ligands (bipy, phen)  
36  
37 which are thought to accelerate the reductive elimination step.  $\text{PhI}(\text{OAc})_2$  was the required oxidant,  
38  
39 whereas Selectfluor failed. The productivity of  $\text{AuCl}_3 / \text{phen}$  and of  $\text{LAuCl} / \text{phen}$  catalysts were  
40  
41 comparable but produced more homo-coupling products. The formation of gold(I) acetylides was  
42  
43 fast compared to oxidation, assisted by acetate as base. The reaction was thought to proceed *via* an  
44  
45 Au(III) bis-alkynyl intermediate.<sup>470</sup> The intramolecular coupling of two linked terminal alkynes to  
46  
47 give macrocyclic conjugated diynes with ring sizes of 13 to 28 atoms was achieved by an oxidative  
48  
49 Au(I) /  $\text{PhI}(\text{OAc})_2$  system, which gave faster reactions and better selectivities than a range of  
50  
51 alternative methods and metal complexes tested. Remarkably, the phosphine-free dichloroaurate  
52  
53 salt  $[\text{nBu}_4\text{N}][\text{AuCl}_2]$  was identified as preferred catalyst precursor, and the presence of phen was  
54  
55 found to be crucial. However, the nature of the species involved in this reaction and their effect on  
56  
57 selectivity for intramolecular coupling remain to be elucidated.<sup>471</sup> In 2017 Li *et al.*,<sup>472</sup> as well as  
58  
59 Banerjee and Patil,<sup>473</sup> showed that the combination of a terminal alkyne with alkynyl iodine(III)  
60  
oxidants in the presence of a gold(I) benzotriazolite catalyst precursor and phenanthroline afforded  
a large array of asymmetric 1,3-diynes, via an oxidative pathway and reductive elimination  
presumably from selectively formed  $[(\text{N}^{\wedge}\text{N})\text{Au}(\text{C}\equiv\text{CR}^1)(\text{C}\equiv\text{CR}^2)]^+$  intermediates.

A very intriguing development of oxidant-free gold catalysis is to use electrochemistry to  
facilitate the generation of electrophilic Au(III). Very recently, Ye *et al.* showed that Selectfluor or

PIDA as oxidants can be replaced by electrochemical oxidation. The hemilabile Au(I) precursor  $\text{Ph}_2(2\text{-py})\text{PAuCl}$  **281** in the presence of terminal alkynes can be oxidized to Au(III) acetylides in an electrochemical cell (Scheme 120).<sup>474</sup> Test reactions showed that the expected gold(III) complex  $(\text{P}^{\wedge}\text{N})\text{AuCl}(\text{C}\equiv\text{CAr})$  **282** was indeed formed and could be detected by HR-MS. An acidic medium was required to suppress gold metal deposition on the cathode due to reduction.  $\text{Ph}_3\text{PAuCl}$ , phen, MeCN:HOAc 4:1 under a 5mA current and 3-5 V generated a range of aryl-alkyl diynes **283** in excellent yields. The advantage of the method, apart from atom efficiency, is that the oxidation potential can be tailored to the catalyst. The method allows the synthesis of functionalized products that may be incompatible with the strong chemical oxidants.

**Scheme 120. Electrochemical Alkyne-Alkyne Redox Coupling**



#### 4.1.3 Photo-Assisted Coupling Reactions

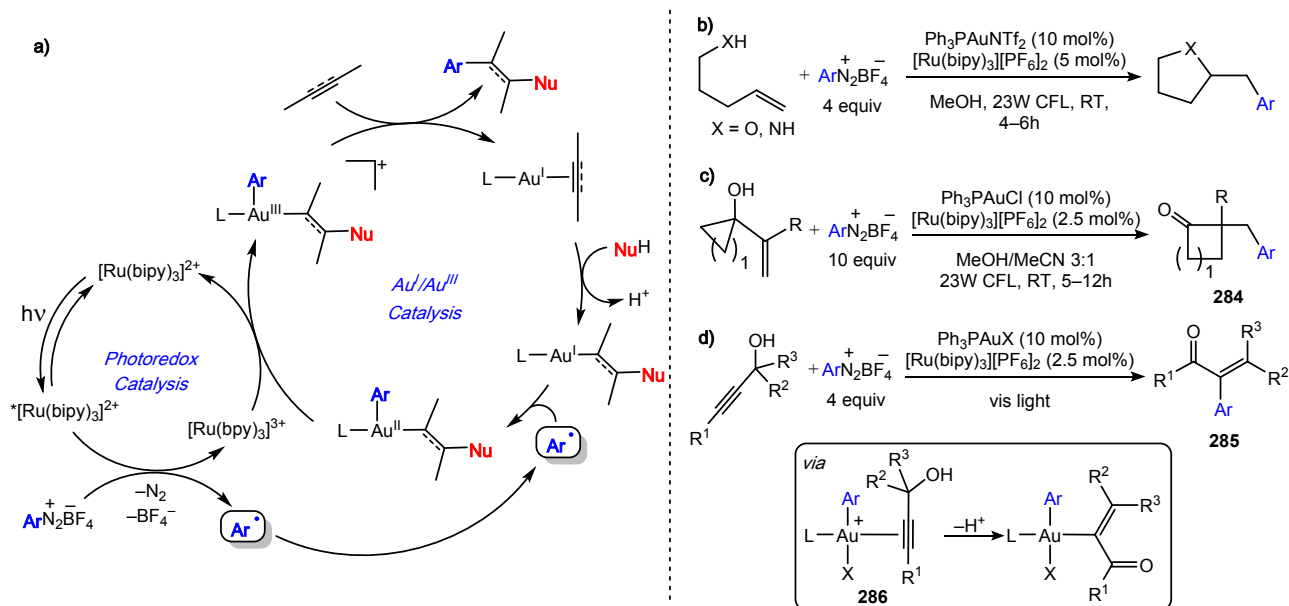
As shown above, species able to release aryl radicals, such as diazonium salts, have emerged recently as versatile reagents for Au redox catalysis as they can play the dual role of oxidizing agent and substrate in C–C and C–E cross-coupling reactions, thus offering a great advantage over sacrificial oxidants such as  $\text{PhIOAc}_2$  and Selectfluor. Aryl radicals generated under photochemical conditions engage in stepwise single-electron oxidations of gold in a  $+I \rightarrow +II \rightarrow +III$  cascade and can participate in radical chains. Since the first report by Glorius in 2013,<sup>475</sup> the area has been flourishing, with a large number of reports emerging in the literature. A description of the broad variety of organic products that are accessible through this methodology goes beyond the scope of this review and has been summarized recently by different authors.<sup>110,476</sup> In this section, we focus

1  
2  
3 on key concepts and mechanistic studies aimed at proving the importance of Au(III) intermediates  
4 in photo-assisted coupling reactions. Details about stoichiometric reactions of arenediazonium salts  
5 with Au(I) precursors are given in Section 3.  
6  
7

8 **Dual Gold/Photoredox Catalysis.** Based on the knowledge that aryl radicals can engage in  
9 single-electron oxidation of low-valent metal centers, Glorius and co-workers conceived the first  
10 dual gold/photoredox catalytic cycle (Scheme 121 a). Such a process exploits  $[\text{Ru}(\text{bipy})_3]^{2+}$  as  
11 photosensitizer for triggering the decomposition of an arenediazonium salt under irradiation to give  
12 an aryl radical. The aryl radical acts as a single-electron oxidant for the Au(I) intermediate that is  
13 obtained upon activation of an unsaturated substrate towards nucleophilic attack. This transient Au<sup>II</sup>  
14 intermediate is then further oxidized to a cationic Au(III) species by the oxidized form of the  
15 photosensitizer. Fast C–C reductive elimination forms the product and regenerates the Au<sup>I</sup> catalyst.  
16 Importantly, as the oxidation of Au and the formation of the metal-aryl bond occur at the same time,  
17 homo-coupling side-reactions are reduced to a minimum. This strategy was applied successfully to  
18 oxyarylations and aminoarylations (Scheme 121b). The method proved to be tolerant of functional  
19 groups and works under mild conditions.  
20  
21

22 While the oxidative addition of diazonium salts to Au(I) has been demonstrated  
23 experimentally immediately after the first catalytic discoveries, the other steps of this mechanism  
24 have remained rather obscure. Zhang *et al.* investigated the dual oxyarylation catalytic cycle by  
25 means of DFT calculations and proposed an “oxidation-first” type mechanism, where Au(III) is  
26 involved also in promoting nucleophilic attack, as a consequence of its higher electrophilicity  
27 compared to Au(II) and Au(I).<sup>477</sup>  
28  
29

30  
31  
32  
33  
34  
35  
36  
37  
38  
39  
40  
41 **Scheme 121. (a) Dual Gold/Photoredox Catalytic Cycle; (b) Oxyarylation and Aminoarylation of**  
42 **Alkenes; (c) Ring Expansion of Alkenyl Cycloalkanols; (d) Arylative Meyer–Schuster**  
43 **Rearrangements.**  
44  
45  
46  
47  
48  
49  
50  
51  
52  
53  
54  
55  
56  
57  
58  
59  
60



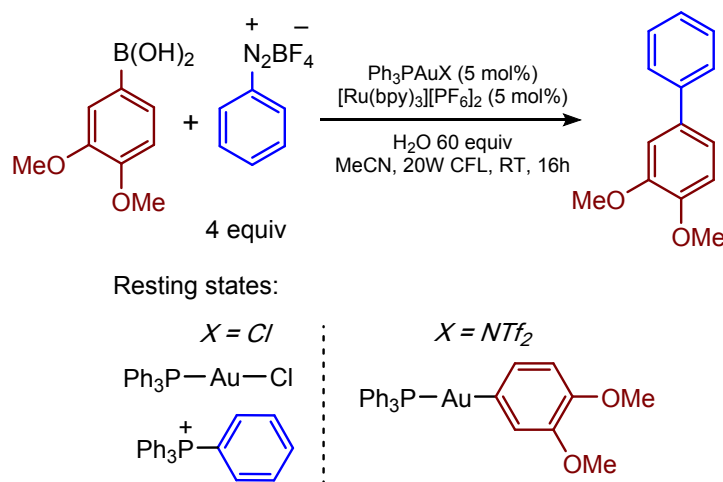
Soon after Glorius' report, Frei, Toste and co-workers described a dual gold/photoredox catalyzed arylation ring expansion of alkenyl and allenyl cycloalkanols to give products of type **284** (Scheme 121c).<sup>478</sup> The mechanism of this reaction was probed by FT-IR spectroscopy and deuterium labeling experiments. In analogy to the proposal by Yu and co-workers<sup>477</sup> for the oxyarylation catalysis, oxidative addition was suggested to precede substrate activation, so the alkenyl cycloalkanol was most likely activated by the Au(III) intermediate rather than the Au(I) precursor.

The importance of Au(III) intermediates in both electrophilic activation and coupling steps has been underlined in a number of following reports dealing with the arylation Meyer-Schuster rearrangements of alkynols to enones **285** (Scheme 121d). Independently, Glorius,<sup>479</sup> Shin<sup>480</sup> and Alcaide and Almendros<sup>481</sup> have suggested that the formal rearrangement leading from alkynol to enone is promoted by the Au(III) intermediate **286** formed after oxidation under photoredox conditions. In none of these cases was there experimental evidence provided for the formation of Au(III)  $\pi$ -intermediates, and reaction mechanisms have been mostly formulated based on speculations on previous results. This is not totally unexpected, considering the fleeting nature of such Au(III)  $\pi$ -complex intermediates (see Section 2).

Over the past few years the scope of dual gold/photoredox catalysis has been extended to a number of arylation reactions involving carbon-carbon and carbon-heteroatom bond formations, using substrates such as H-phosphonates,<sup>482</sup> boronic acids,<sup>483</sup> silanes,<sup>484–486</sup> and amino- and hydroxyalkynes.<sup>487,488</sup> With the development of a larger number of protocols, further experimental details aimed at elucidating the reaction mechanisms have been provided.

It is rather intriguing that mechanistic aspects of these reactions strongly depend on the catalytic system, which makes it difficult to sketch out a unified catalytic cycle for all these transformations. For example, while it is accepted that alkyne substrates usually follow an “oxidation first”-type mechanism, other coupling reactions seem to follow a “transmetalation first” route. This was shown by Gauchot and Lee who investigated the mechanism of dual gold/photoredox catalyzed aryl–aryl cross coupling between arenediazonium salts and arylboronic acids in the presence of  $\text{Ph}_3\text{PAuX}$ .<sup>489</sup> Monitoring the catalytic runs by  $^{31}\text{P}$  NMR spectroscopy, they were able to show that the nature of the resting state of the catalyst depended on X. With  $\text{X} = \text{Cl}$ ,  $\text{PPh}_4^+$  salts formed along with the starting precatalyst, thus suggesting the intermediacy of monoaryl  $\text{Au}^{\text{III}}$  species in an “oxidation first” mechanism. By contrast, for  $\text{X} = \text{NTf}_2$  the transmetalated  $\text{Au}(\text{I})$  aryl was observed as the main species, suggesting a “transmetalation first” type mechanism (Scheme 122).

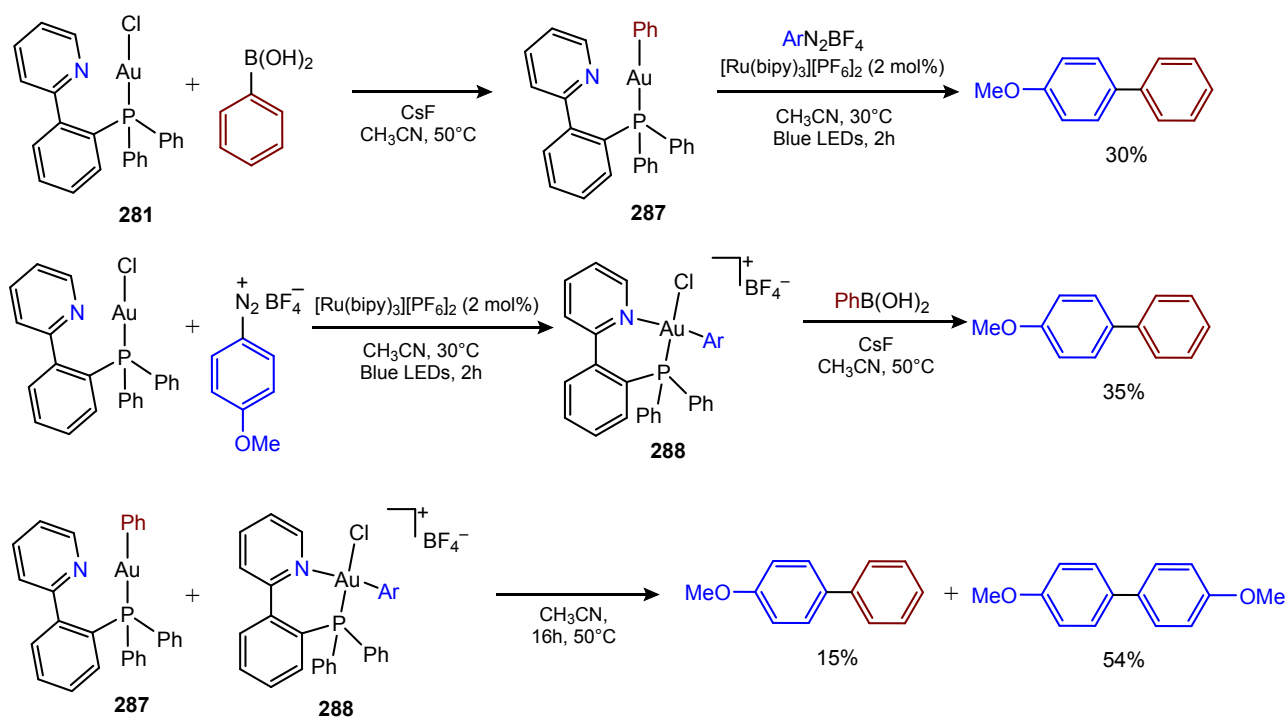
### Scheme 122. $\text{C}(\text{sp}^2)\text{--C}(\text{sp}^2)$ Coupling Under Dual Gold/Photoredox Catalysis



On the other hand, Fouquet and Hermange<sup>483</sup> hypothesized in a parallel study that  $\text{Ph}_3\text{PAuCl}$  may undergo transmetalation before oxidation. In follow-up work these authors used the hemilabile (2-pyridylphenyl- $\text{PPh}_2$ ) $\text{AuCl}$  complex **281** in stoichiometric experiments with boronic acids and arenediazonium salts (Scheme 123).<sup>432</sup> Initially,  $\text{Au}(\text{I})$  aryls **287** obtained upon transmetalation with boronic acids were found to undergo C–C coupling with the arenediazonium salt under photoredox conditions, thus confirming the viability of the “transmetalation first” pathway. However, if the  $\text{Au}(\text{I})$  chloride was reacted with the arenediazonium salt first, the well-defined  $\text{Au}(\text{III})$  aryl complex **288** formed in high yield, in agreement with similar results by Hashmi and co-workers.<sup>325</sup> This complex is then able to undergo transmetalation with the boronic acid and give C–C coupling, indicating that the “oxidation-first” pathway is also viable. Moreover, **287** and **288** were shown to

engage in transmetalation with each other, illustrating that other unforeseen reactions can further complicate speculated reaction mechanisms. These findings underline, once again, the fundamental difference in behavior between gold and palladium, for which oxidative addition always occurs before transmetalation in cross-coupling catalysis.

### Scheme 123. Stoichiometric Studies on C(sp<sup>2</sup>)-C(sp<sup>2</sup>) Coupling by Fouquet and Hermange



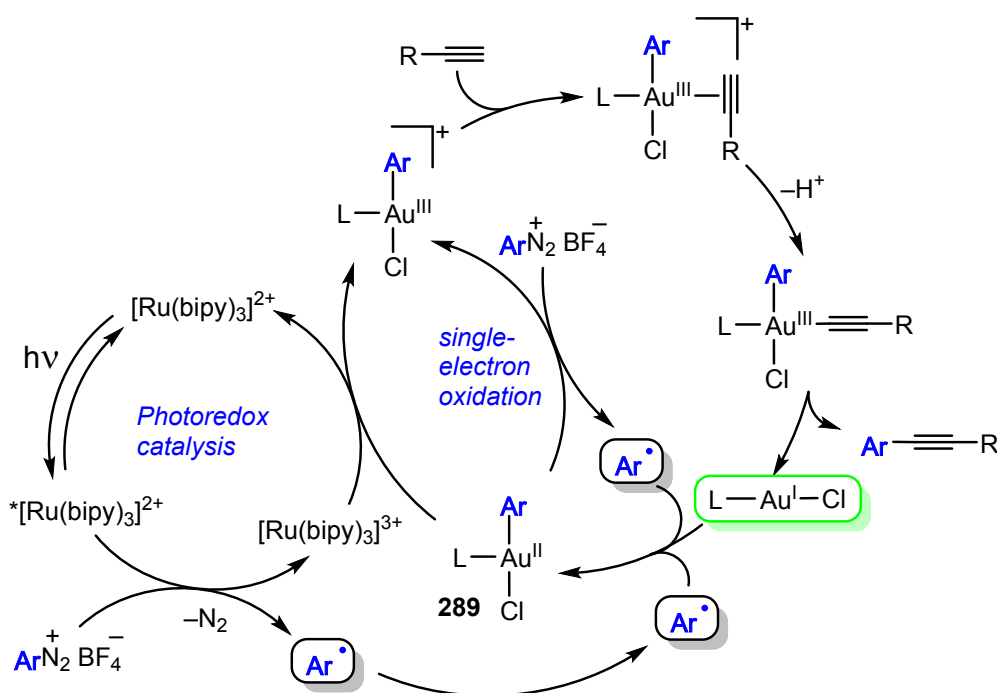
Patil and co-workers reported a catalytic cross-coupling between arenediazonium salts and allylsilanes.<sup>484</sup> Mass spectrometric and <sup>31</sup>P NMR spectroscopic studies indicated the formation of arylphosphonium salts, thus suggesting the intermediacy of Au(III) aryl complexes that undergo reductive decomposition if no excess substrate is present (see Section 3). Also, no formation of allyl complexes was observed when Ph<sub>3</sub>PAuCl was reacted with allylsilanes under photocatalytic conditions. This ruled out substrate activation by Au(I), as previously proposed for alkynes. The formation of arylphosphonium salts has been invoked as proof for the intermediacy of Au(III) in other similar catalytic cycles.<sup>484,485,490</sup>

One intriguing aspect that brings more complexity to the initial mechanistic scenario proposed in Scheme 121a is the possible participation of radical chains. In 2016 Glorius investigated the C-H arylation of terminal alkynes under dual gold/photoredox catalysis (Scheme 124) and measured the quantum yields of the reaction by chemical actinometry.<sup>491</sup> A value of  $\Phi = 3.6$  was obtained, which suggested that more than one molecule of product was produced per



photon absorbed. This implied the involvement of a radical chain, which originates most likely by the reaction of the Au<sup>II</sup> intermediate **289** with further diazonium salt, rather than with the oxidized state of the photocatalyst. Under this scenario, the photocatalyst acts as radical initiator, thus envisioning that it may be replaced with other efficient radical chain initiators.

### Scheme 124. Proposed Dual/Gold Photoredox Catalytic Cycle for Alkyne C–H Arylation



This seems to agree with earlier reports by Shin *et al.* and other groups, who indicated that some of the transformations carried out under dual gold/photoredox catalysis were also working in the dark in the absence of a photocatalyst and followed a different reaction mechanism where radical chains were likely involved.<sup>492</sup> It is worth noting that many other protocols were found to be inactive in the absence of light/photocatalyst.<sup>482,484,486</sup>

**Monometallic Light-Assisted Catalysis.** Investigating the dual gold/photoredox 1,2-oxoarylation of alkynes, Hashmi and co-workers discovered that using a photocatalyst is not a necessary requirement for these reactions to occur. Optimization studies showed higher yields when simple Au complexes such as Ph<sub>3</sub>PAuCl were reacted with diazonium salts and alkynes in wet methanol under blue LED irradiation, without a [Ru(bipy)<sub>3</sub>]<sup>2+</sup> photosensitizer.<sup>493</sup> No reactivity was observed in the dark, therefore a photoactivated step must be part of the mechanism. The method was further expanded to other 1,2-difunctionalizations and Suzuki-type coupling reactions,<sup>494</sup> showing high robustness and tolerance to different functional groups. Mechanistically, the low absorbance of the precatalyst in the blue region led initially to the conclusion that the Au(I)

1  
2  
3 complex itself did not act as a photosensitizer. Light on/off experiments suggested the absence of  
4 radical chain reactions. Moreover, chelating diazonium salts were shown to oxidatively add to Au(I)  
5 affording well-defined Au(III) aryls under the same experimental conditions (see Section 3).  
6  
7 Together, these findings seemed to suggest that arenediazonium salts can be degraded in the  
8 presence of the gold precursor and blue light, oxidatively add to Au(I) and generate catalytically  
9 active Au(III) electrophiles.  
10  
11

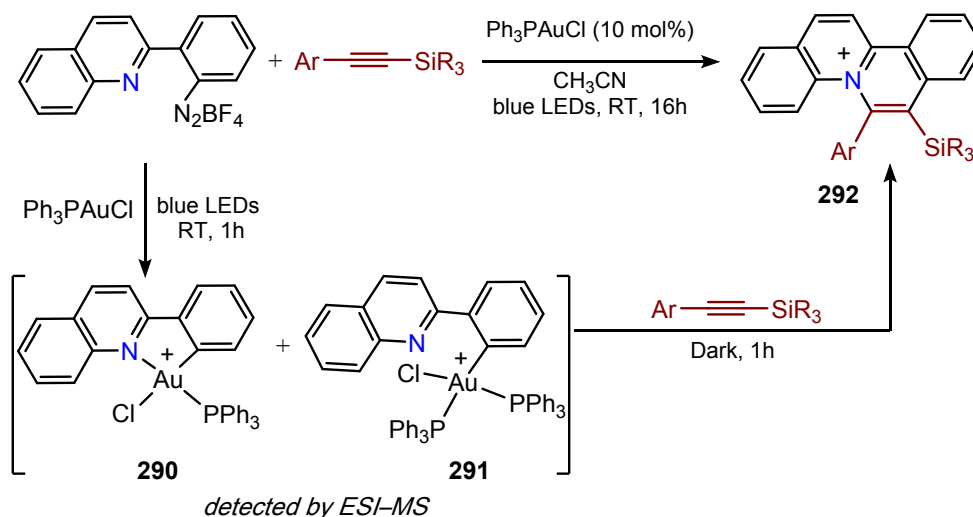
12  
13 Similarly, using arylazosulfones as coupling reagents and taking advantage of the visible  
14 light absorption of the labile  $-N_2SO_2R$  moiety, Bandini and co-workers discovered that Suzuki  
15 coupling with boronic acids could be achieved driven by blue LED light in the absence of a  
16 photocatalyst.<sup>495</sup>  
17  
18

19  
20 An extensive DFT study by Liu *et al.*<sup>496</sup> suggested the that key step of this reactivity is the  
21 formation of a charge transfer complex between the gold catalyst and the diazonium salt, which is  
22 capable of absorbing visible light to give a charge-transfer exciplex. This exciplex then generates an  
23 Au<sup>II</sup> species and a diazoarene radical upon quenching. The latter liberates the aryl radical that can  
24 start the catalytic cycle by adding either to the starting Au<sup>I</sup> complex or the Au<sup>II</sup> intermediate.  
25  
26

27  
28 Wong and co-workers used quinolone-substituted arenediazonium salts to promote the  
29 regioselective *cis*-difunctionalization of alkynyl silanes under photosensitizer-free conditions and  
30 provided considerable insights into the mechanism (Scheme 125).<sup>497</sup> Spectroscopic studies were  
31 performed stepwise by <sup>31</sup>P NMR spectroscopy and electrospray mass spectrometry and showed the  
32 formation of the oxidative addition products **290** and **291** under irradiation of Ph<sub>3</sub>PAuCl and the  
33 diazonium salt at room temperature. The further reaction in the dark generated the quinolizilium  
34 product **292**, suggesting that the photoactivated step is the oxidation of Au(I) to Au(III). Ph<sub>3</sub>PAuCl  
35 was found to quench the fluorescence of the diazonium salt, indicating that electron transfer from  
36 the gold complex may indeed occur, thus validating the theoretical proposal by Liu *et al.*  
37  
38  
39  
40  
41  
42  
43  
44  
45

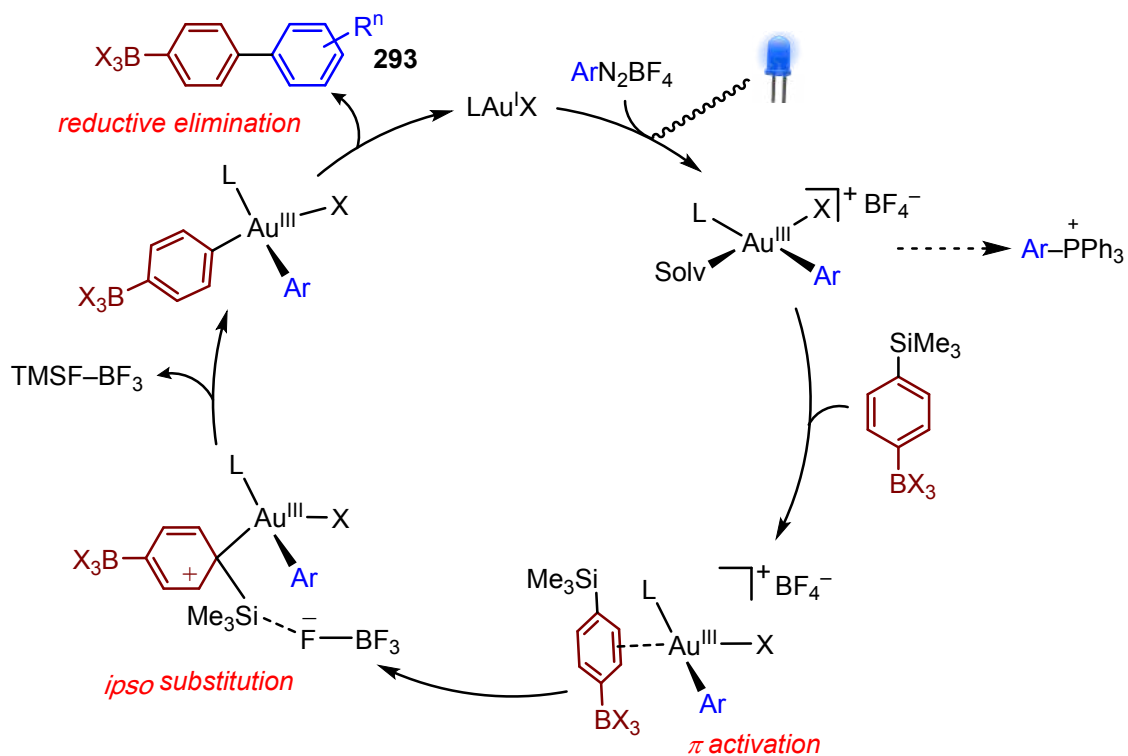
#### 46 **Scheme 125. Photoassisted *cis*-Difunctionalization of Alkynyl Silanes**

47  
48  
49  
50  
51  
52  
53  
54  
55  
56  
57  
58  
59  
60



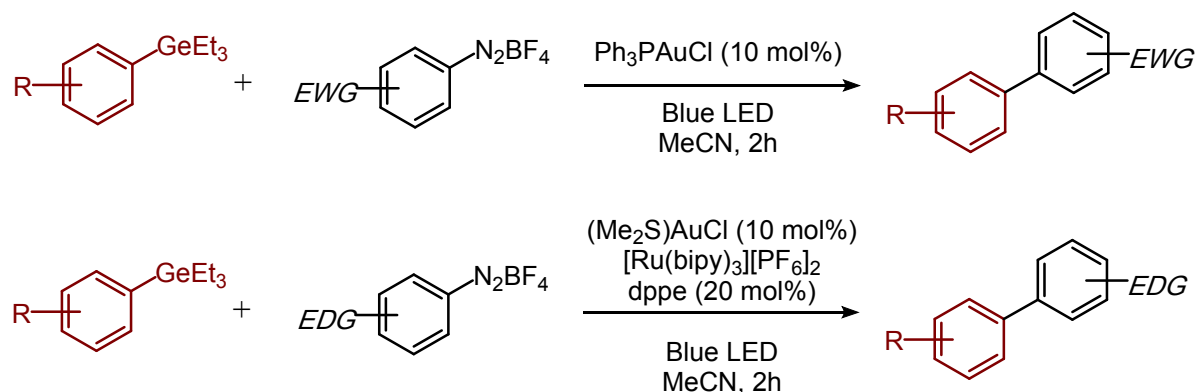
Hashmi and co-workers reported a photoassisted gold-catalyzed Hiyama coupling of silyl-substituted aryl boronates with arenediazonium salts to obtain biphenyl boronates **293** (Scheme 126).<sup>498</sup> The superior selectivity of this method allowed the use of substrates with functional groups that are usually not tolerated by Pd catalysts under similar conditions. Kinetic studies on the catalytic cycle revealed that initial rates of arylation are first-order in both catalyst and boronate, while they are zero-order in diazonium salt. This would suggest that the oxidation of Au(I) is fast and the activation of the C–Si bond by the oxidized Au(III) is the rate limiting step. Moreover, the formation of arylphosphonium salts was observed by <sup>31</sup>P NMR spectroscopy, thus confirming that Au(III) intermediates are quite reasonably involved in the mechanism. As a last piece of evidence, the precatalyst Ph<sub>3</sub>PAuNTf<sub>2</sub> was found to be unable to transmetalate the silyl arylboronate, while transient Au(III) complexes obtained by oxidation *in-situ* with Selectfluor are able to activate the C–Si bond. These mechanistic studies allowed the formation of a reasonable mechanism which underlines the superior reactivity of Au(III) transients in activating bonds that Au(I) precatalyst are unable to cleave.

### Scheme 126. Proposed Cycle for the Photosensitized Gold Catalyzed Hiyama Coupling



Very recently, Schoenebeck and co-workers have used aryl-germanes as coupling partners in photo-activated C–C coupling with aryldiazonium salts (Scheme 127).<sup>499</sup> By using  $Ph_3PAuCl$  under blue LED irradiation, a broad range of biaryl derivatives was obtained under mild conditions. Notably, arylgermanes were found to be more reactive than arylsilanes and arylboronic esters and chemoselective coupling of aryls containing BPin and  $SiEt_3$  substituents was achieved. However, as previously observed by Hashmi with arylsilanes, the C–C coupling was effective only when electron-poor arenediazonium salts were used. With the aid of DFT calculations the authors showed that the productive addition of an aryl radical to Au has a low barrier only in the case of electron deficient substrates, while for electron-rich ones unproductive side reactions became more favourable. In order to extend the methodology to electron-rich systems,  $[Ru(bipy)_3][PF_6]_2$  was used as photosensitizer in combination with  $(Me_2S)AuCl/dppe$  as catalyst. Under dual gold/photoredox catalysis, electron-rich diazonium salt containing *p*-*t*Bu and *p*-OMe groups were efficiently coupled with arylgermanes.

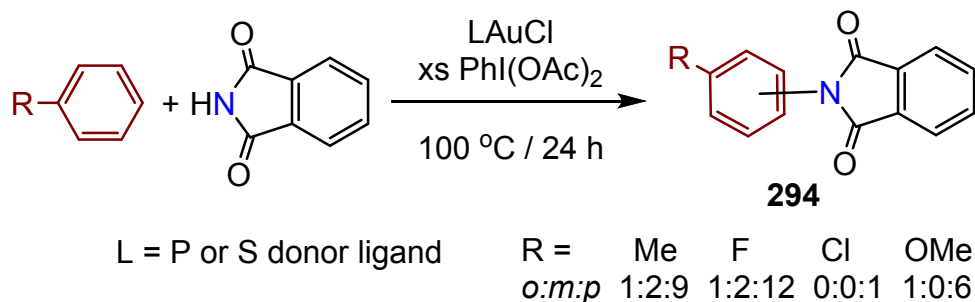
### Scheme 127. Photoassisted Coupling of Arylgermanes with Electron-Rich and Electron-Poor Arenediazonium Salts



**4.1.4 C-E Coupling Reactions (E = Non-Carbon Element).** Methods of C-E bond formation (E = O, S, N, P, B, halogen including F) catalyzed by homogeneous and heterogeneous gold catalysts have been comprehensively reviewed up to 2011.<sup>104</sup> As described for C-C couplings, C-E bond formation involves either the oxidative addition of an aryl halide to Au(I), or the combination of an arene with an Au(I) precatalyst and an external oxidant. Both stoichiometric and catalytic coupling reactions of C with heteroatoms have been explored.

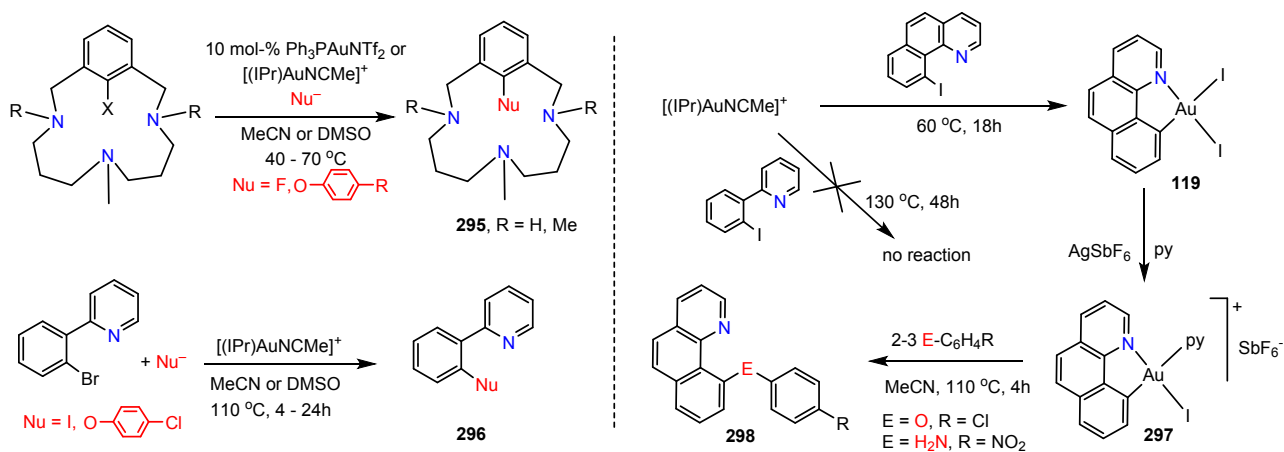
In a catalytic variant of this arene activation, DeBoef and co-workers used a mixture of LAuCl (10 mol-%) and PhI(OAc)<sub>2</sub> to couple variously substituted arenes with phthalimides to give substituted phthalimides **294** (Scheme 128).<sup>500</sup> Unlike the metal-free reaction which involves radicals, catalysis by gold gives very good *para*-selectivity, much higher than palladium catalysts, although the presence of by-products suggested that the radical pathway was not entirely suppressed. The reaction worked best for electron-rich arenes. The nature of L = phosphine was unimportant; both triaryl and trialkyl phosphines (PPh<sub>3</sub>, PCy<sub>3</sub>, P*i*Pr<sub>3</sub>) gave near-identical conversion and product distribution. However, high conversion was only achieved with an excess of the oxidizing agent, with 4 equiv of PhI(OAc)<sub>2</sub> being the optimum; this, together with the insensitivity of the reaction to the electronic and steric properties of L, would seem to suggest that some of the excess oxidant is needed to remove L by oxidation. Since PhI(OAc)<sub>2</sub> reacts with phthalimide to give PhI(OAc)(phth) and PhI(phth)<sub>2</sub>, it was suggested that this *in-situ* generated reagent was responsible for the transfer of phthalimide to the Au(III) intermediate. The kinetic isotope effect (KIE) of 1.04 demonstrated that the rate-limiting step does not involve C-H bond activation. The authors therefore favored an electrophilic aromatic metalation (EAM) process<sup>500</sup> over the concerted metalation-deprotonation (CMD) pathway proposed for palladium.<sup>171</sup>

#### Scheme 128. Gold Catalyzed C-N Coupling Reactions



The oxidative addition of macrocyclic aryl halides to Au(I) precatalysts, followed by halide substitution by a suitable nucleophile and reductive elimination, allowed the so-called “oxidant-free” synthesis of aryl derivatives **295**. Mechanistic investigations were however unable to detect the Au(III) aryl intermediate. Only chelating substrates were successful, such as arenes carrying an *ortho*-pyridyl substituent, to give the coupling products **296** (Scheme 129). The oxidative addition requires forcing conditions (110 °C, 4 – 24 h), and there is a strong solvent dependence.<sup>501</sup> On the other hand, simple potentially chelating substrates like 2-pyridyl-1-iodobenzene failed to oxidatively add to typical gold(I) precatalysts like [(IPr)AuNCMe]<sup>+</sup>, even at 110 °C, and the starting materials were recovered. However, the more rigid 10-iodobenzo[*h*]quinolone reacted with Au(I) at 60 °C to give the crystallographically characterized oxidative addition product **119** (see Section 3). Substitution of one of the iodo ligands by pyridine to give **297** followed by treatment with phenolate or anilines as nucleophiles generated the expected coupling products **298**, thereby supporting the previously suggested mechanism. Carrying the same reactions out with 10 mol-% Au(I) catalyst in the presence of excess IPr showed that the coupling reaction could be made catalytic.<sup>299</sup>

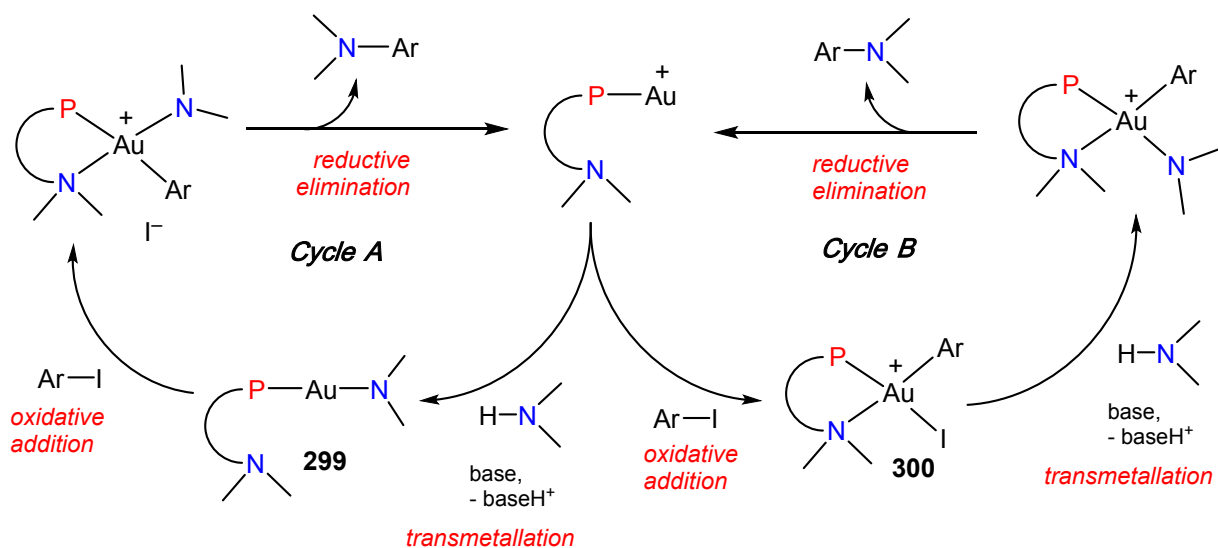
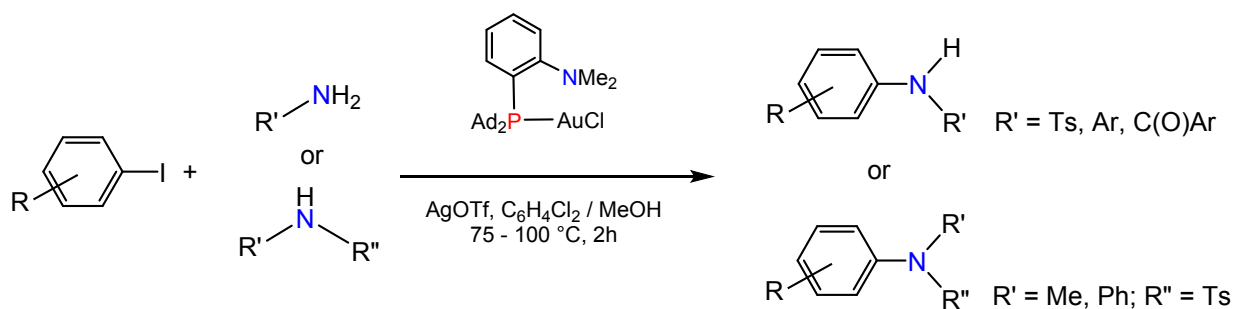
### Scheme 129. Gold Catalyzed C-Heteroatom Coupling Reactions



1  
2  
3 In 2019/2020 the groups of Bourissou<sup>502</sup> and Patil<sup>503</sup> showed that the coupling of aryl  
4 iodides with amines is catalyzed by (MeDalphos)AuCl in the presence of AgOTf or AgSbF<sub>6</sub> to give  
5 the corresponding aryl amines and amides, mostly in good yield (Scheme 130). In Bourissou's  
6 system the choice of base proved critical, with 2,6-di-*t*-butylpyridine (DTBP) giving best results.  
7 The reaction of *p*-tolyl iodide with aniline itself or with *p*-methoxyaniline gave no or poor yields,  
8 while anilines with electron-withdrawing *p*-substituents worked well. On the other hand, the  
9 coupling of *p*-methylbenzamide with aryl iodides was found to be insensitive to the electronic  
10 characteristics of the aryl and works equally well for aryl iodides I-C<sub>6</sub>H<sub>4</sub>R with electron donating or  
11 withdrawing substituents (R = *o*-OMe, *p*-OMe, *p*-NO<sub>2</sub>, *p*-Br, *p*-OTf, *p*-BPin) to give the coupling  
12 products in near-quantitative yields. Coupling was also achieved with secondary amides Ts-NHR  
13 (R = Me, Ph) in 94-98% yield.<sup>502</sup> Patil showed that a wide range of substituents on the aryl and the  
14 aniline building blocks was tolerated and that the method could be extended to the synthesis of  
15 indolinones and carbazoles.<sup>503</sup>

16  
17 As discussed before, in principle two catalytic cycles may be envisaged for this reaction:  
18 cycle A, where transmetalation takes place prior to oxidative addition, and cycle B, where these two  
19 steps are reversed (Scheme 130). This was tested by <sup>15</sup>N and <sup>31</sup>P NMR spectroscopic investigations  
20 and by preparing intermediates **299** and **300** separately. However, stoichiometric reactions showed  
21 that while **299** failed to undergo oxidative addition with aryl iodides, the aryl iodo complex **300**  
22 reacted with amides slowly to give the expected reductive elimination product. These reactions also  
23 showed that more basic amines such as aniline and *p*-anisidine retarded the reaction; since the  
24 oxidative addition must be initiated by a gold(I)-iodoarene adduct [LAu···I-Ar]<sup>+</sup>, it is clear that  
25 more basic amines compete with the iodoarene for coordination to the metal center and will retard  
26 the oxidative addition step. The evidence therefore supports the mechanism shown in cycle B.<sup>502</sup>

### 27 28 29 30 31 32 33 34 35 36 37 38 39 40 41 42 43 44 45 **Scheme 130. Catalyzed Coupling of Aryl Iodides with Amines and Amides**



#### 4.2 Lewis Acid Catalysis by Gold(III)

As early as 1976 Thomas and co-workers showed that HAuCl<sub>4</sub> can catalyze the hydration of alkynes to give ketones in water/methanol mixtures, revealing the potential of Au(III) in Lewis-acid catalyzed reactions.<sup>504</sup> With the advent of modern gold catalysis, Au(III) halides and well-defined complexes have been tested broadly in the catalytic activation of unsaturated substrates along with the typical Au(I) salts, albeit with contrasting results. As pointed out by Schmidbaur and Schier,<sup>116</sup> the reductive decomposition of gold(III) halides makes it difficult to ascertain the real nature of the catalyst in these processes, or even the actual phase where the reaction is taking place. The same may be true for systems with ancillary ligands that are supposed to increase stability, as suggested by some recent examples. This was illustrated by Fairlamb and co-workers who showed that well-defined Au(III) complexes such as (NHC)AuBr<sub>3</sub> or (NHC)AuBr<sub>2</sub>(N-imidate) (N-imidate = tetrafluorosuccinimide or phthalimide) as catalysts for the cycloisomerization of 1,5 enynes undergo facile reduction to Au(I) by release of bromine.<sup>505</sup> Similar conclusions were drawn by Kumar *et al.*, who synthesized expanded ring carbene complexes (NHC)Au(III)Br<sub>3</sub> and used them to catalyze the addition of amines to phenylacetylene.<sup>13</sup> C NMR studies indicated that activation of these species with silver salts led immediately to reduction to (NHC)Au(I) salts, thus questioning the real importance of Au(III) in this specific catalytic reaction.<sup>506</sup>



1  
2  
3 As mentioned before, the use of cyclometalated or pincer ligands can reduce the tendency of  
4 Au(III) to undergo reductive decomposition but it can also lead to a complete deactivation of its  
5 catalytic properties,<sup>507</sup> so a fine balance between stability and reactivity has to be struck. Pioneering  
6 work by Hashmi *et al.* showed that the introduction of bidentate N<sup>^</sup>O ligands increased activity,  
7 selectivity and durability of Au(III) catalysts for cyclization of furan-yne systems to give  
8 phenols.<sup>508</sup>

9  
10  
11  
12  
13 The literature of Lewis acid catalysis by Au(III), notably AuCl<sub>3</sub>, has been covered in a 2012  
14 review by Schmidbaur and Schier.<sup>116</sup> However, the past decade witnessed a major drive in  
15 developing well defined Au(III) complexes and mechanistic concepts for unleashing the potential of  
16 high-valent gold in Lewis acid catalysis. This section will focus on the latest advancements in the  
17 application of Au(III) complexes in two main areas: (i) catalytic functionalization of CC multiple  
18 bonds through  $\pi$ -complexation and (ii) Lewis acid catalysis through coordination to oxygen. In  
19 particular, we will show how the development of stable systems based on high-valent gold allows  
20 the unlocking of novel reactivity that is inaccessible to Au(I) and provide information about the  
21 hitherto unknown mechanistic details of these reactions.

22  
23  
24  
25  
26  
27  
28  
29 **4.2.1 Au(III) as a Carbophilic Lewis Acid.** The past few years have witnessed a  
30 spectacular rise in the application of Lewis acidic Au(III) species as catalysts for the  
31 functionalization of unsaturated and polyunsaturated substrates through  $\pi$ -activation.<sup>509,510</sup> Notable  
32 examples include hydration,<sup>511-513</sup> hydroamination,<sup>514</sup> hydroarylation,<sup>515</sup> cycloaddition /  
33 isomerization<sup>74,516-518</sup> and multi-component reactions, such as the alkyne-amine-aldehyde (A<sup>3</sup>)  
34 coupling.<sup>519-521</sup> Alkyne hydration by HAuCl<sub>4</sub> showed potential also for educational purposes.<sup>513</sup>

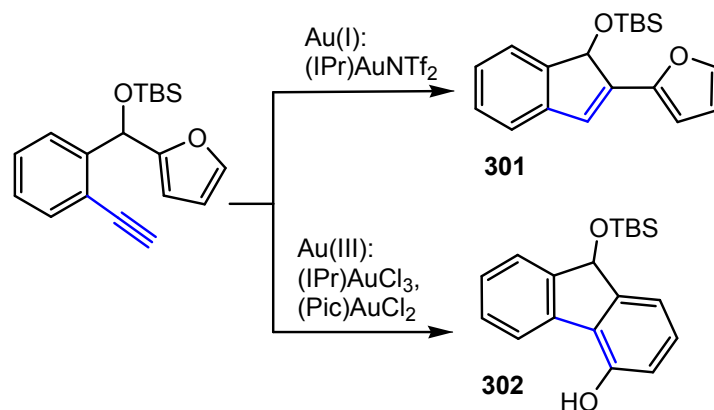
35  
36  
37  
38  
39  
40  
41  
42  
43  
44  
45  
46  
47  
48  
49  
50  
51  
52  
53 The fate of gold during most of these processes remained obscure and mechanisms are  
54 mainly probed computationally.<sup>522-524</sup> However, a growing body of evidence seems to indicate that  
55 Au(III) has different catalytic properties compared to Au(I) in terms of both activity and selectivity,  
56 and this pushed the development of comparative studies and more thorough mechanistic  
57 investigations. The specificity of Au(III) catalysis was exemplified by Ying and Pu, who showed  
58 that NaAuCl<sub>4</sub> is a competent catalyst for the regiospecific hydration of N-(diphenylphosphinoyl)-  
59 propargyl amines to the correspondent  $\beta$ -amino ketones, while Au(I) phosphine complexes, as well  
60 as other metal catalysts including Cu, Hg and Pt salts, are inactive.<sup>525</sup>

61  
62  
63  
64  
65  
66  
67  
68  
69  
70  
71  
72  
73  
74  
75  
76  
77  
78  
79  
80  
81  
82  
83  
84  
85  
86  
87  
88  
89  
90  
91  
92  
93  
94  
95  
96  
97  
98  
99  
100  
101  
102  
103  
104  
105  
106  
107  
108  
109  
110  
111  
112  
113  
114  
115  
116  
117  
118  
119  
120  
121  
122  
123  
124  
125  
126  
127  
128  
129  
130  
131  
132  
133  
134  
135  
136  
137  
138  
139  
140  
141  
142  
143  
144  
145  
146  
147  
148  
149  
150  
151  
152  
153  
154  
155  
156  
157  
158  
159  
160  
161  
162  
163  
164  
165  
166  
167  
168  
169  
170  
171  
172  
173  
174  
175  
176  
177  
178  
179  
180  
181  
182  
183  
184  
185  
186  
187  
188  
189  
190  
191  
192  
193  
194  
195  
196  
197  
198  
199  
200  
201  
202  
203  
204  
205  
206  
207  
208  
209  
210  
211  
212  
213  
214  
215  
216  
217  
218  
219  
220  
221  
222  
223  
224  
225  
226  
227  
228  
229  
230  
231  
232  
233  
234  
235  
236  
237  
238  
239  
240  
241  
242  
243  
244  
245  
246  
247  
248  
249  
250  
251  
252  
253  
254  
255  
256  
257  
258  
259  
260  
261  
262  
263  
264  
265  
266  
267  
268  
269  
270  
271  
272  
273  
274  
275  
276  
277  
278  
279  
280  
281  
282  
283  
284  
285  
286  
287  
288  
289  
290  
291  
292  
293  
294  
295  
296  
297  
298  
299  
300  
301  
302  
303  
304  
305  
306  
307  
308  
309  
310  
311  
312  
313  
314  
315  
316  
317  
318  
319  
320  
321  
322  
323  
324  
325  
326  
327  
328  
329  
330  
331  
332  
333  
334  
335  
336  
337  
338  
339  
340  
341  
342  
343  
344  
345  
346  
347  
348  
349  
350  
351  
352  
353  
354  
355  
356  
357  
358  
359  
360  
361  
362  
363  
364  
365  
366  
367  
368  
369  
370  
371  
372  
373  
374  
375  
376  
377  
378  
379  
380  
381  
382  
383  
384  
385  
386  
387  
388  
389  
390  
391  
392  
393  
394  
395  
396  
397  
398  
399  
400  
401  
402  
403  
404  
405  
406  
407  
408  
409  
410  
411  
412  
413  
414  
415  
416  
417  
418  
419  
420  
421  
422  
423  
424  
425  
426  
427  
428  
429  
430  
431  
432  
433  
434  
435  
436  
437  
438  
439  
440  
441  
442  
443  
444  
445  
446  
447  
448  
449  
450  
451  
452  
453  
454  
455  
456  
457  
458  
459  
460  
461  
462  
463  
464  
465  
466  
467  
468  
469  
470  
471  
472  
473  
474  
475  
476  
477  
478  
479  
480  
481  
482  
483  
484  
485  
486  
487  
488  
489  
490  
491  
492  
493  
494  
495  
496  
497  
498  
499  
500  
501  
502  
503  
504  
505  
506  
507  
508  
509  
510  
511  
512  
513  
514  
515  
516  
517  
518  
519  
520  
521  
522  
523  
524  
525  
526  
527  
528  
529  
530  
531  
532  
533  
534  
535  
536  
537  
538  
539  
540  
541  
542  
543  
544  
545  
546  
547  
548  
549  
550  
551  
552  
553  
554  
555  
556  
557  
558  
559  
560  
561  
562  
563  
564  
565  
566  
567  
568  
569  
570  
571  
572  
573  
574  
575  
576  
577  
578  
579  
580  
581  
582  
583  
584  
585  
586  
587  
588  
589  
590  
591  
592  
593  
594  
595  
596  
597  
598  
599  
600  
601  
602  
603  
604  
605  
606  
607  
608  
609  
610  
611  
612  
613  
614  
615  
616  
617  
618  
619  
620  
621  
622  
623  
624  
625  
626  
627  
628  
629  
630  
631  
632  
633  
634  
635  
636  
637  
638  
639  
640  
641  
642  
643  
644  
645  
646  
647  
648  
649  
650  
651  
652  
653  
654  
655  
656  
657  
658  
659  
660  
661  
662  
663  
664  
665  
666  
667  
668  
669  
670  
671  
672  
673  
674  
675  
676  
677  
678  
679  
680  
681  
682  
683  
684  
685  
686  
687  
688  
689  
690  
691  
692  
693  
694  
695  
696  
697  
698  
699  
700  
701  
702  
703  
704  
705  
706  
707  
708  
709  
710  
711  
712  
713  
714  
715  
716  
717  
718  
719  
720  
721  
722  
723  
724  
725  
726  
727  
728  
729  
730  
731  
732  
733  
734  
735  
736  
737  
738  
739  
740  
741  
742  
743  
744  
745  
746  
747  
748  
749  
750  
751  
752  
753  
754  
755  
756  
757  
758  
759  
760  
761  
762  
763  
764  
765  
766  
767  
768  
769  
770  
771  
772  
773  
774  
775  
776  
777  
778  
779  
780  
781  
782  
783  
784  
785  
786  
787  
788  
789  
790  
791  
792  
793  
794  
795  
796  
797  
798  
799  
800  
801  
802  
803  
804  
805  
806  
807  
808  
809  
810  
811  
812  
813  
814  
815  
816  
817  
818  
819  
820  
821  
822  
823  
824  
825  
826  
827  
828  
829  
830  
831  
832  
833  
834  
835  
836  
837  
838  
839  
840  
841  
842  
843  
844  
845  
846  
847  
848  
849  
850  
851  
852  
853  
854  
855  
856  
857  
858  
859  
860  
861  
862  
863  
864  
865  
866  
867  
868  
869  
870  
871  
872  
873  
874  
875  
876  
877  
878  
879  
880  
881  
882  
883  
884  
885  
886  
887  
888  
889  
890  
891  
892  
893  
894  
895  
896  
897  
898  
899  
900  
901  
902  
903  
904  
905  
906  
907  
908  
909  
910  
911  
912  
913  
914  
915  
916  
917  
918  
919  
920  
921  
922  
923  
924  
925  
926  
927  
928  
929  
930  
931  
932  
933  
934  
935  
936  
937  
938  
939  
940  
941  
942  
943  
944  
945  
946  
947  
948  
949  
950  
951  
952  
953  
954  
955  
956  
957  
958  
959  
960  
961  
962  
963  
964  
965  
966  
967  
968  
969  
970  
971  
972  
973  
974  
975  
976  
977  
978  
979  
980  
981  
982  
983  
984  
985  
986  
987  
988  
989  
990  
991  
992  
993  
994  
995  
996  
997  
998  
999  
1000

In 2013, Hashmi and co-workers reported a gold catalyzed cyclization of furan-yne systems with aromatic tethers, which showed an oxidation-state dependent chemoselectivity (Scheme 131).<sup>526</sup> Indeed, while (IPr)AuNTf<sub>2</sub> selectively afforded indene derivatives **301**, Au(III) complexes such as (IPr)AuCl<sub>3</sub> and (pyridine-2-carboxylate)AuCl<sub>2</sub> led to fluorene products **302**. The origin of the selectivity was ascribed to the different charge-donating abilities of Au(I) and Au(III), which

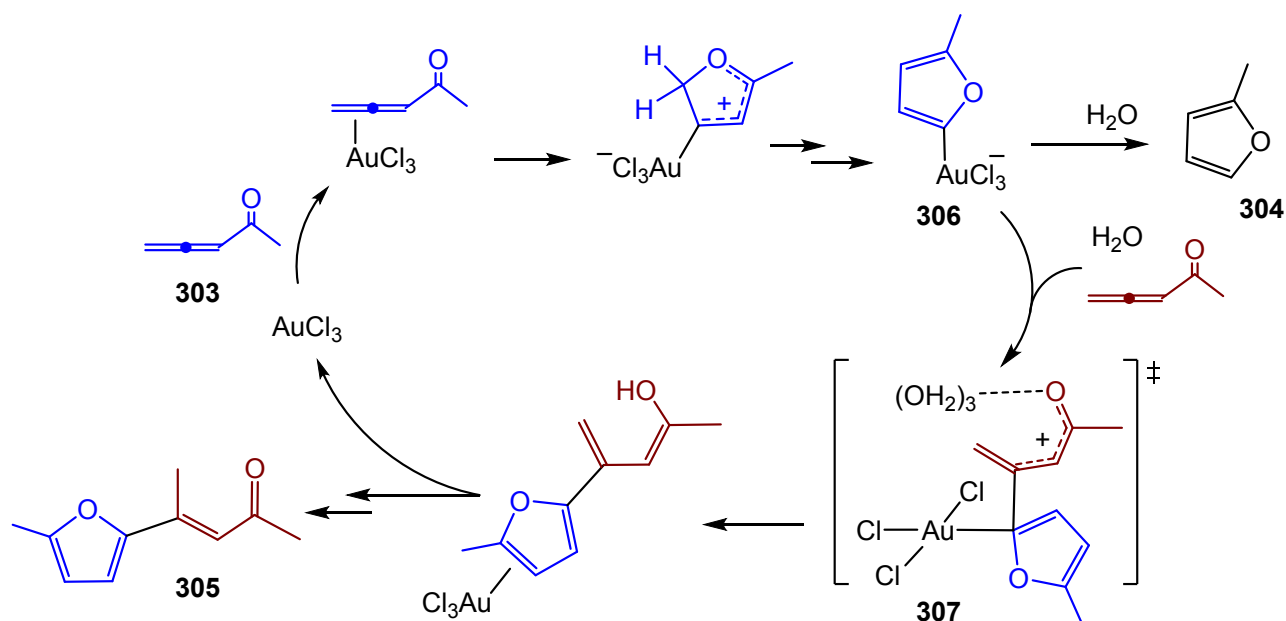
lead to different intermediates; however, mechanistic details remained mostly speculative. AuCl was shown to give the same product as Au(III), and disproportionation of Au(I) into Au(0) and Au(III) was invoked to reconcile the mechanistic conundrum.

### Scheme 131. Cyclization of Furan-yne Catalyzed by Au(I) and Au(III)



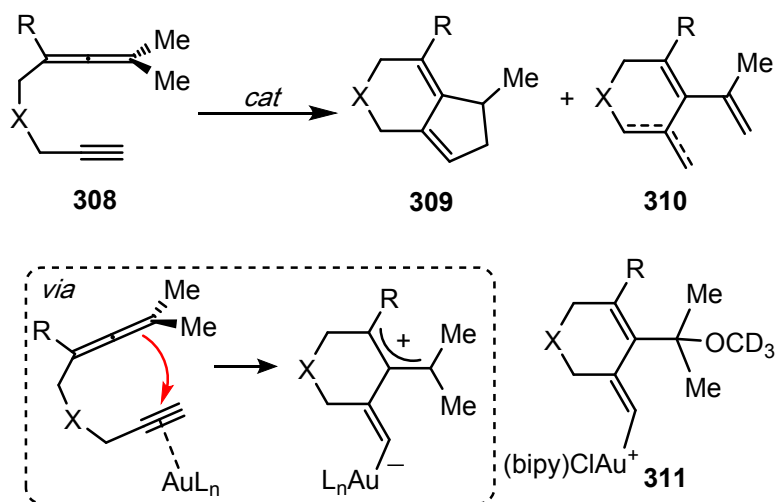
The complexity of AuCl<sub>3</sub>-catalyzed reactions was illustrated in a computational mechanistic investigation of the hydroarylation of allenyl ketones **303**, which gives furans **304** alongside furyl-substituted vinyl ketones **305**.<sup>527</sup> At least three catalytic cycles were found possible and which may be in competition with each other and in which a gold(III)  $\alpha$ -furyl species serves as nucleophile. The results were rationalized in terms of a new mechanism termed “concerted electrophilic ipso-substitution” (CEIS), in which the gold(III)-furyl  $\sigma$ -bond **306** produced by furan auration acts as a nucleophile and attacks the protonated allenyl ketone via a transition state of type **307** by an outer-sphere mechanism. Water and hydrogen bonding are important in this process. A simplified outline is depicted in Scheme 132.

### Scheme 132. Simplified Outline of the AuCl<sub>3</sub>-Catalyzed Hydroarylation of Allenyl Ketones



It is worth noting that regiodivergent reactivity might not necessarily arise from just a difference in Lewis acidity determined by the oxidation state, but most likely from a combination of effects. Jaroschik *et al.* investigated the gold-catalyzed cycloisomerization of 1,6-allen-yne and found that the outcome of this reaction was influenced by changes in the steric bulk of the ligands, the nature of the counterion, and the substrates themselves.<sup>528</sup> For instance,  $\text{AuCl}_3$  catalyzed the cycloisomerization of allen-yne **308** (Scheme 133,  $\text{X} = \text{C}(\text{CO}_2\text{Me})_2$ ,  $\text{R} = \text{Me}$ ) to hydrindiene **309**, while  $\text{Ph}_3\text{PAuNTf}_2$  led exclusively to the Alder-ene product **310**. However, when  $\text{X} = \text{C}(\text{CO}_2\text{Et})_2$  and  $\text{R} = \text{H}$ ,  $\text{AuCl}_3$  catalyzed selectively the formation of **310**, in analogy to what is observed with other Au(I) salts. A large screening study revealed that, in general, metal halide salts and cations with bulky ligands (NHC or encumbered phosphines) favor the formation of the hydrindiene **309**, while less bulky systems lead to the Alder-ene **310**. Ligand effects can be overridden by using triflate counterions, which always led to the formation of **310**. Mechanistically, **309** and **310** are thought to originate from a common vinyl intermediate formed upon  $\pi$ -activation of the triple bond by the metal (Scheme 133). By using  $[(\text{bipy})\text{AuCl}_2]\text{Cl}$  and  $\text{CD}_3\text{OD}$ , intermediate **311** was trapped and observed by ESI-MS, suggesting that protodeauration of these species is slow. The competition between protodeauration and different proton and hydride shifts from the common intermediate was suggested to account for the regiodivergent reactivity.<sup>528</sup>

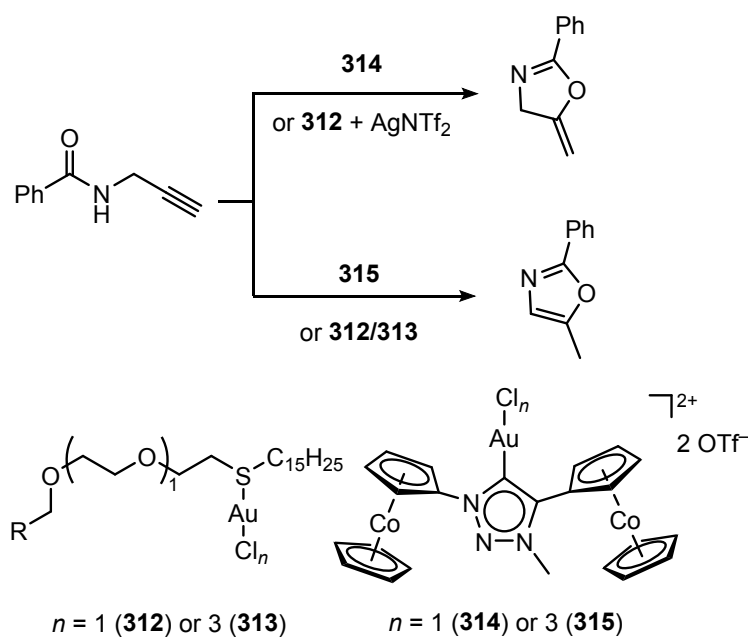
### Scheme 133. Cycloisomerization of 1,6 Allen-yne and Proposed Intermediates



21  
22  
23  
24  
25  
26  
27  
28  
29  
30  
31  
32  
33  
34  
35  
36  
37  
38  
39

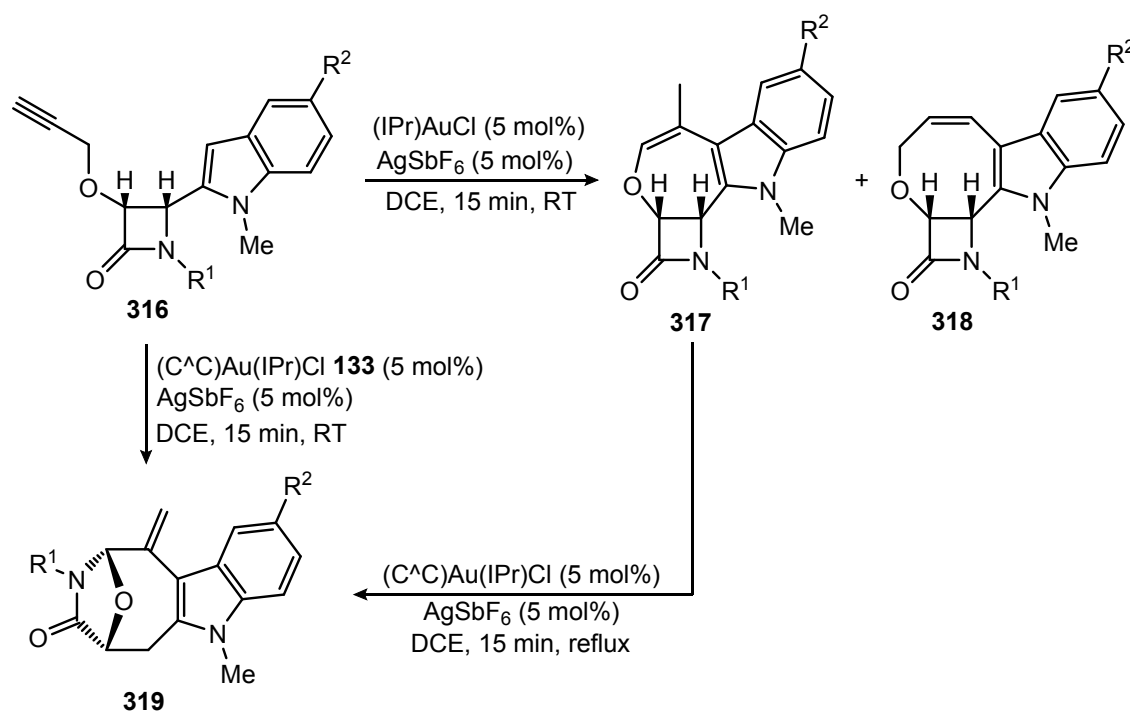
Bibal and co-workers reported that the thioether Au(III) trichloro complexes **313** catalyze the cycloisomerization of propargylamides into 1,3-disubstituted oxazoles,<sup>46</sup> matching earlier results by Hashmi and co-workers.<sup>529</sup> The same result was obtained with the Au(I) species **312** obtained upon photoreduction of **313**. On the other hand, cationic Au(I) species such as Ph<sub>3</sub>PAuNTf<sub>2</sub> catalyze the formation of dihydrooxazoles (Scheme 134). Vanicek *et al.* reported the synthesis of the mesoionic dicobaltoceniumyl carbene complex **315**, which was obtained straightforwardly upon oxidation of its Au(I) congener **314** in aqua regia.<sup>530</sup> As observed before for **313**, compound **315** catalyzed the formation of the oxazole, while the Au(I) complex **314** led to the formation of the methylene oxazoline (Scheme 134).

#### Scheme 134. Divergent Reactivity of Propargylamides with Au(I) and Au(III) Catalysts



Another striking case was reported by Alcaide *et al.*, who investigated the reactivity of alkyne-tethered lactams **316** in the presence of well-defined Au(I) and Au(III) catalysts.<sup>531</sup> Here, while (IPr)Au(I) salts afforded mixture of 7- and 8-membered carbocyclization products **317** and **318**, the biphenyldiyl chelate (C<sup>^</sup>C)Au(IPr)Cl **133** led to the exclusive formation of a bridged oxazabicyclo[4.2.1]nonenone **319** (Scheme 135). Mechanistic studies revealed that the Au(III) catalyst formed selectively **317** as an intermediate and catalyzed a further rearrangement to the bridged product **319**. This oxidation-state dependent reactivity was ascribed to the higher Lewis acidity of Au(III), as anticipated by Hashmi.<sup>526</sup>

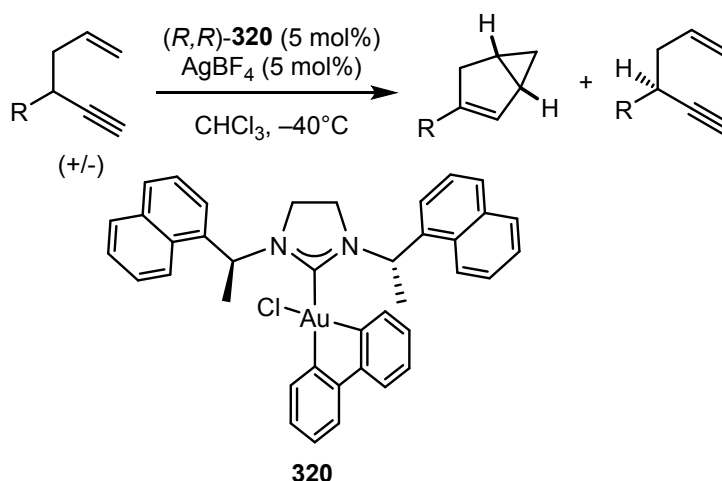
**Scheme 135. Regiodivergent Reactivity of Alkyne-Tethered Lactams in the Presence of Au(I) and Au(III) Catalysts**



As a consequence of its square-planar coordination environment, Au(III) is much more responsive to ligand effects and these can be used to induce asymmetric catalysis in a way that is not possible with linear Au(I).<sup>111</sup> Bohan and Toste have shown that (C<sup>^</sup>C)Au(III) chelates are very robust, reduction-resistant catalysts for enantioselective enyne activation.<sup>532</sup> Using the chiral NHC complex **320** they developed an enantioconvergent kinetic resolution affording enantioenriched 1,5-enynes and bicyclo[3.1.0]hexenes (Scheme 136). While efficient Au(I)-catalyzed asymmetric cyclopropanation protocols relying on chiral diphosphine ligands have been successfully developed for substrates such as propargyl esters or substituted enynes<sup>63,50</sup>, the 1,5-enyne cycloisomerization remained challenging for low-valent gold. The key for the success of this particular reaction is the

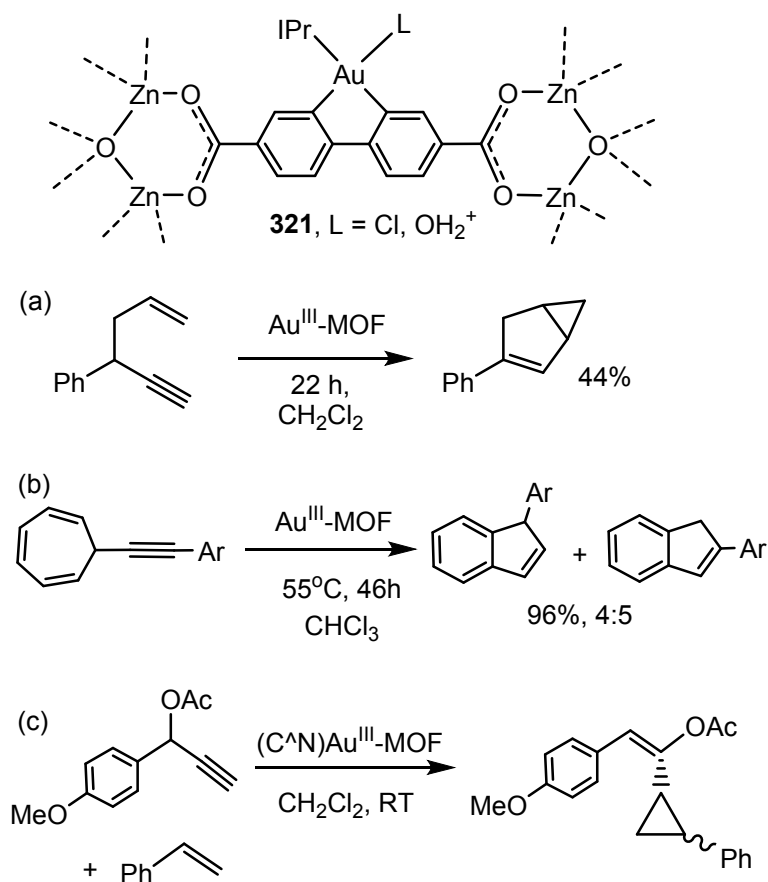
ability of the chiral Au(III) catalyst to override the inherent chirality transfer from the substrate and induce the two different enantiomers to converge to the same product. A detailed analysis and modeling of *ee* data *versus* conversion showed that, in striking contrast with standard kinetic resolution, satisfying enantio-enrichment can be achieved at synthetically useful conversions.

**Scheme 136. Enantioconvergent Kinetic Resolution of 1,5 Enynes with Chiral Au(III) Chelates**



The biphenyl scaffolds showed also interesting applications in supported catalysis. The incorporation of (C<sup>^</sup>C)Au(IPr) cations into metalorganic frameworks (MOFs) by using a carboxylate-derivatized biphenyl skeleton generated catalysts **321** with increased thermal stability and resistance to reduction compared to homogeneous analogues. Removal of chloride by AgSbF<sub>6</sub> was essential for the generation of active catalysts which could be recycled several times, although the formation of AgCl within the MOF framework proved somewhat limiting. The activity of the catalyst was tested in 1,5 enyne and alkynyl-cycloheptatriene cycloisomerization reactions (Scheme 137a, b), illustrating a promising future for well-defined supported Au(III) catalysis.<sup>533</sup> A similar approach was employed by Tilset and co-workers who incorporated C<sup>^</sup>N chelated Au(III) catalysts for the cyclopropanation reaction of propargylic esters with styrene (Scheme 137c). Au-functionalized UiO-67 MOFs were synthesized by exchanging linkers of UiO-67 MOF with Au{ppy(COOH)<sub>2</sub>}Cl<sub>2</sub>, to generate MOFs containing (N<sup>^</sup>C)-bound Au(III) as catalytic centers.<sup>534</sup>

**Scheme 137. MOF-Stabilized (C<sup>^</sup>C)Au(III) Catalysts and Test Reactions**

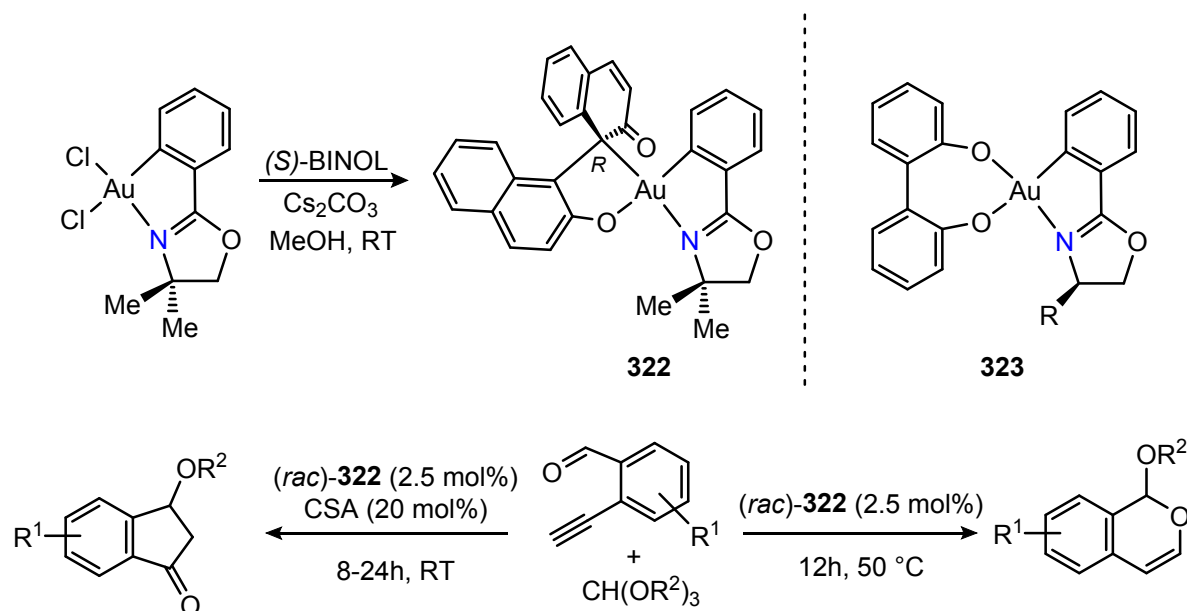


Wong and co-workers produced a large library of oxazolyne or pyridine-based (C<sup>^</sup>N)Au(III) BINOL complexes showing an unusual C, O rather than the expected O, O coordination of the BINOL ligand (Scheme 138).<sup>535</sup> These complexes are chiral as a consequence of an axial-to-central chirality transfer; their structures were confirmed by X-Ray crystallography and circular dichroism. Complex **322** was successfully used in the catalytic cycloisomerization/acetallization of 2-alkynylbenzaldehydes to give 6-membered acetals (Scheme 138). Remarkably, the introduction of D-(+)-camphorsulfonic acid (CSA) in the reaction mixture switched the selectivity of the reaction and afforded carboalkoxylation products. Other mononuclear Au(I) and simple cyclometalated Au(III) complexes proved to be inactive.<sup>536</sup> Preliminary results on enantioselective carboalkoxylation catalysis were obtained by using enantiopure Au(III) catalysts, albeit with moderate *ee* values of 40–50%.

In a follow-up study,<sup>537</sup> the authors tested O<sup>^</sup>O chelates of chiral oxazolines of the type **323** (Scheme 138) in asymmetric carboalkoxylation catalysis and found that the performance in enantioselectivity was dictated by the steric bulk of the substituent in *alpha* position to the nitrogen. By using bulky substituents such as mesityl, high *ee* values approaching 90% were observed. ESI-MS measurements suggested that the active species may originate from the protonation of one of the two Au–O bonds in **323**, to give a 3-coordinate, Lewis acidic Au(III) cation. The chirality of the

oxazoline ligand creates a chiral pocket which affects the geometry of the carboalkoxylation transition state and dictates the enantioselectivity.

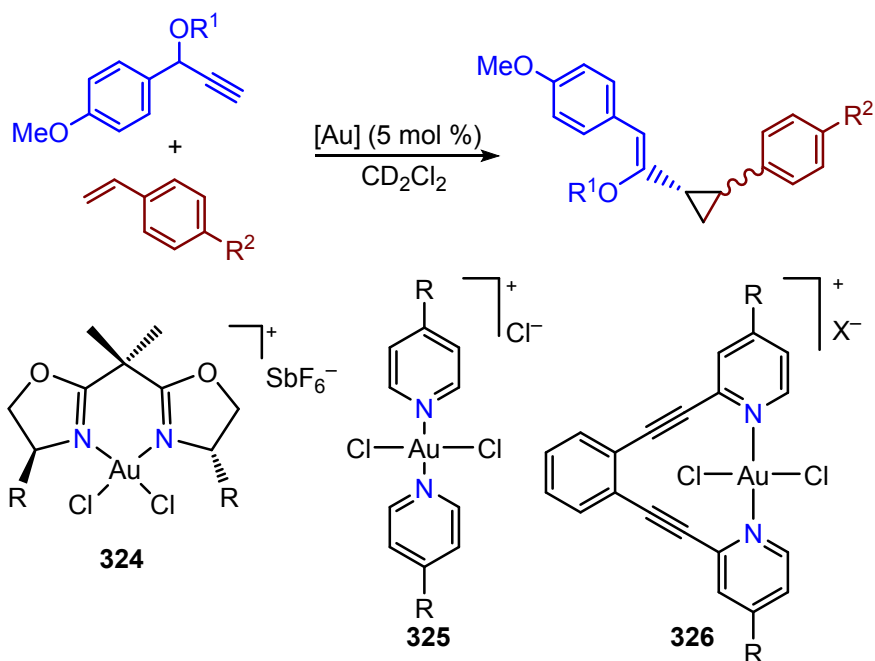
### Scheme 138. Synthesis of Chiral Au(III) C<sup>∞</sup>O BINOL Complexes and Catalytic Applications



Fiksdahl and co-workers have tested the cyclopropanation of propargyl esters with different gold complexes (Scheme 139).<sup>538</sup> The Au(III) bis-oxazoline complex **324** shows activities comparable with the benchmark Johnphos Au(I) complex and, more importantly, higher than other Au(III) species based on pyridine ligands or AuCl<sub>3</sub>, suggesting that the structure of the ligand plays an important role. Interestingly, **324** triggered a very efficient *cis/trans* isomerization of the formed vinylcyclopropanes, with rates higher than those of all the other Au(III) and Au(I) complexes studied. This allowed the selective formation of *trans* cyclopropanation products. Later on, *trans* bis-pyridine complexes **325** and **326** were tested in the same reaction and the role of the ligand was probed experimentally and theoretically.<sup>539</sup> It was found that unrestrained pyridine complexes **325** were generally more active than the restrained **326**, even though the substituent on the pyridine ligands played a pivotal role. Electron-withdrawing ligands were significantly more active than electron-donating ones, suggesting that one pyridine needs to dissociate to generate the active species.<sup>540</sup> <sup>15</sup>N NMR data strongly correlated with this finding, and DFT modeling showed that the energy of the key transition state was dependent on the electron density on the nitrogen atom in the pyridine ligand.

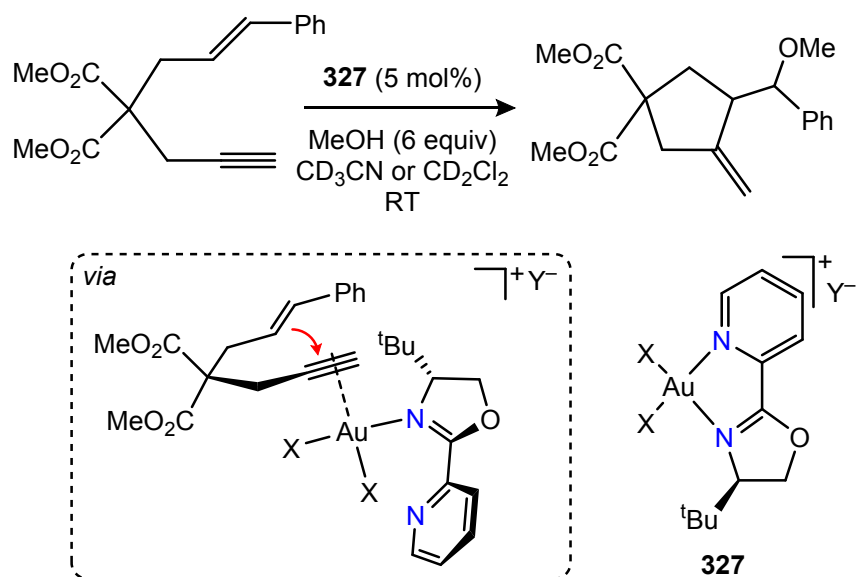
### Scheme 139. Au(III) Catalyzed Cyclopropanation of Propargyl Ethers with Styrenes





A similar conclusion was drawn for the alkoxyacylation of 1,6-enynes catalyzed by the pyridine-oxazoline Au(III) complex **327** (Scheme 140).<sup>541</sup> Catalytic experiments revealed a strong ligand effect on the productivity of the system; under identical experimental conditions the catalyst with X = Cl gave twice the conversion of the X = Br analogue. A considerable ion pair effect was also observed; e.g. more coordinating Y<sup>-</sup> = OTf<sup>-</sup> showed increased reactivity in more polar solvents, whereas this was not the case for less coordinating anions such as BF<sub>4</sub><sup>-</sup> and PF<sub>6</sub><sup>-</sup>. As (Me<sub>2</sub>S)AuCl was found to be inactive in combination with the oxazoline ligand in CH<sub>3</sub>CN, the authors concluded that the active species must be Au(III). The catalyst is thought to be activated by pyridine displacement, which allows alkyne coordination and cyclization, followed by MeOH attack and protodeauration. <sup>15</sup>N NMR experiments confirmed that the pyridine fragment is released under catalytic conditions, while the oxazoline remains coordinated. This mechanism was corroborated by DFT calculations, which indicated that the substrate coordination upon pyridine displacement is actually the rate limiting step of the reaction.

**Scheme 140. Alkoxyacylation of 1,6 Enynes with MeOH Catalyzed by Complex 327.**

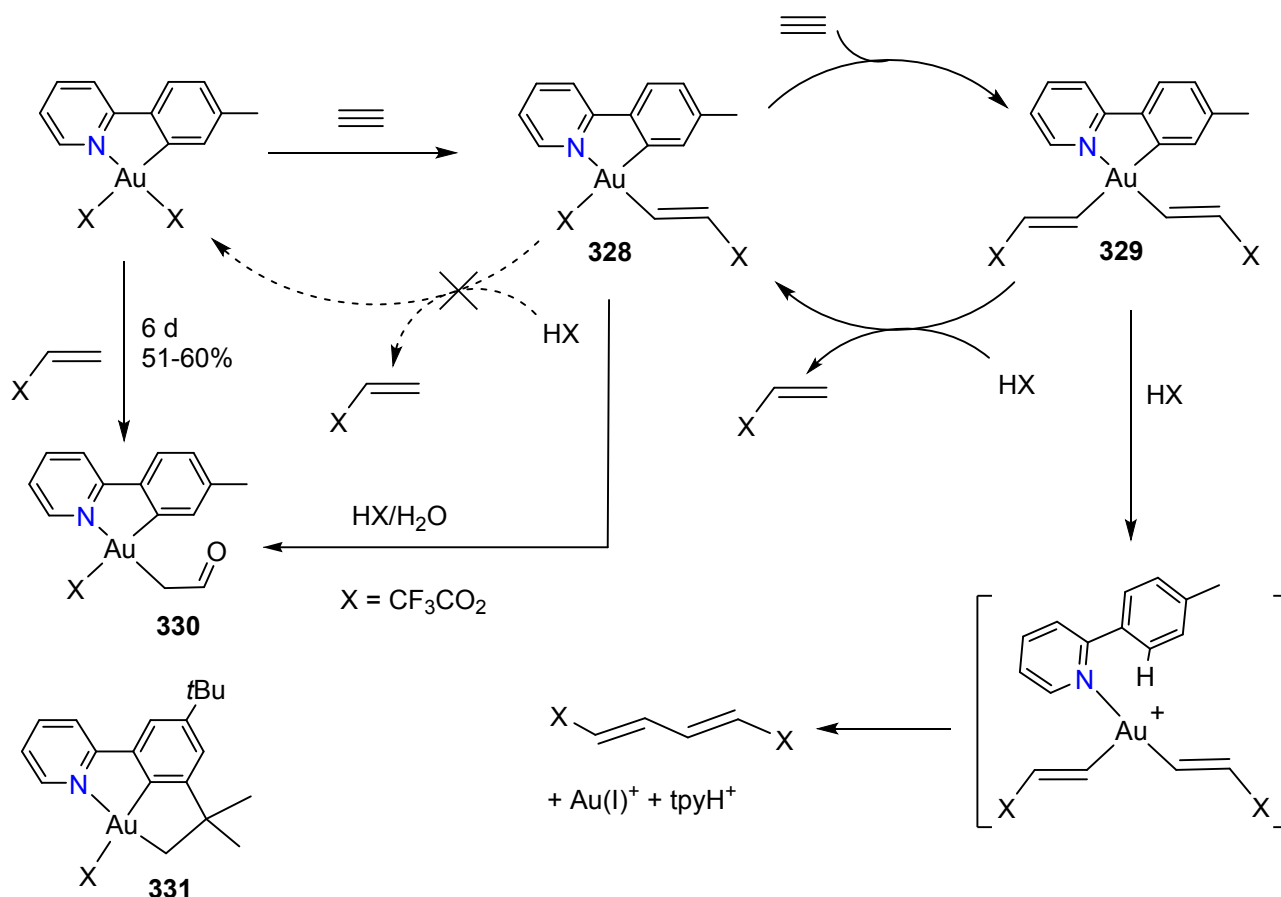


Tilset and co-workers showed that the Au(III) mediated nucleophilic functionalization of unsaturated substrates in the (C<sup>N</sup>)AuX<sub>2</sub> system described in Section 3.3 for stoichiometric alkene reactions (Scheme 70) become catalytic if alkynes are used. The reaction of (C<sup>N</sup>)Au(OAc<sup>F</sup>)<sub>2</sub> with acetylene in dichloromethane / trifluoroacetic acid (6:1) gives the structurally characterized gold vinyl complex **328** (Scheme 141).<sup>135</sup> Although a catalytic cycle based on formation and protodeauration of **328** might be expected, this vinyl complex proved to be resistant to Au-C bond cleavage under these conditions and did not generate vinyl trifluoroacetate. Instead, it was found that **328** reacts with a second equivalent of acetylene to give the bis(vinyl) complex **329**. In this compound the vinyl ligand *trans* to C is selectively protodeaured to generate vinyl acetate (11-12 TON / 24 h). Entering the catalytic cycle with (C<sup>N</sup>)Au(OAc<sup>F</sup>)(CD=CDOAc<sup>F</sup>), only Ac<sup>F</sup>OCH=CH<sub>2</sub> was formed, proving that the vinyl ligand *trans* to N is not liberated in this reaction. On prolonged reactions, formation of C<sub>2</sub>HD and C<sub>2</sub>H<sub>2</sub> was also seen, due to H/D exchange with HOAc<sup>F</sup>. There was also evidence for the formation of a reductive elimination product, the diene XCH=CH-CD=CDX (X = trifluoroacetate), accompanied by protonated tpy ligand, an indication of catalyst deactivation following Au-C(tolyl) protonolysis. Over time, the slow formation of the structurally characterized enolate complex **330** was seen, most probably due to hydrolysis of **328**.

DFT calculations showed that although formation of the intermediate gold-acetylene  $\pi$ -complex *trans* to C has a slightly lower barrier than *trans* to N, the subsequent insertion and formation of the vinyl product *trans* to N is thermodynamically more favorable. The second insertion and protonolysis *trans* to C also have lower barriers than *trans* to N, a reflection once again of the importance of the *trans*-influence in Au(III) catalysis.<sup>135</sup>

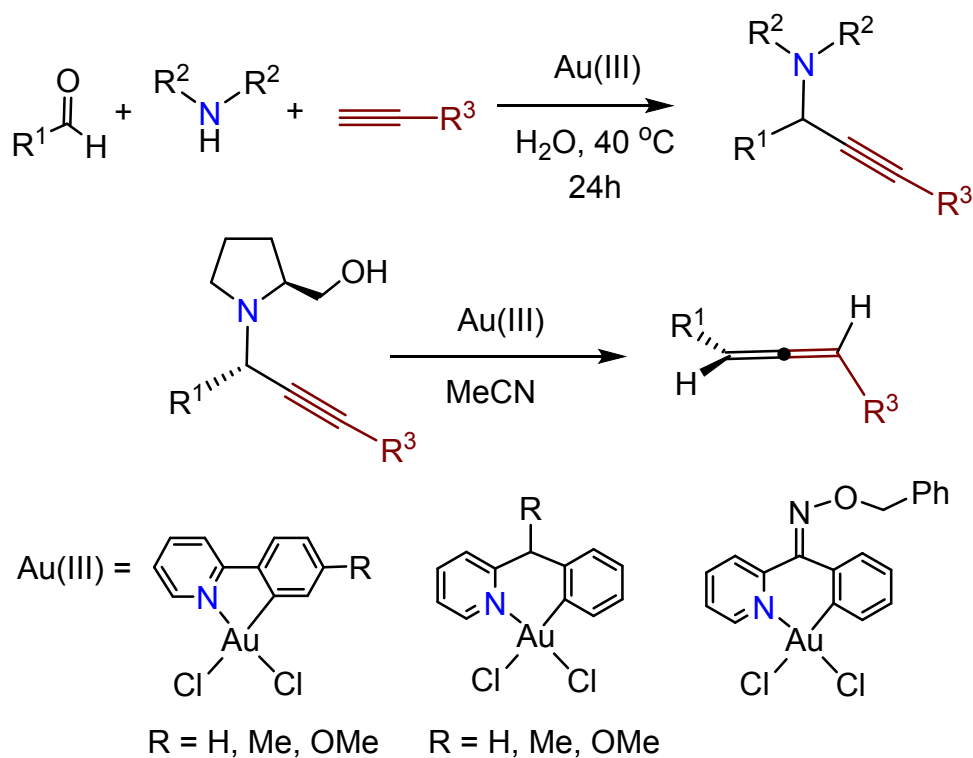
In order to improve the stability of the catalysts against protolytic decomposition, the C<sup>∧</sup>C<sup>∧</sup>N pincer complex **331** was developed. It shows significantly improved barriers towards Au-C bond protolytic cleavage and gives higher turnovers than the system based on **328**.<sup>542</sup>

**Scheme 141. Gold(III) Catalyzed Formation of Vinyl Acetate via a Double Insertion Pathway**



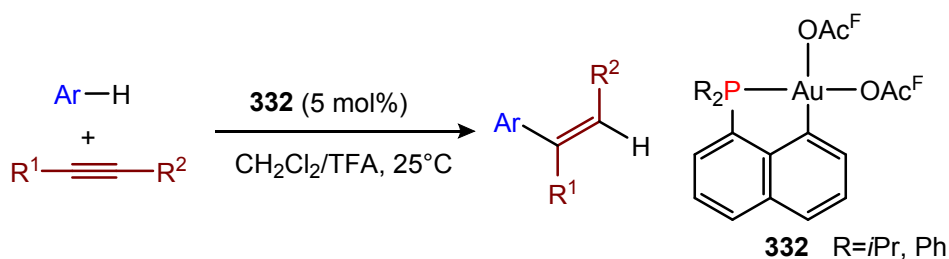
Gold(III) C<sup>∧</sup>N chelates also act as potent Lewis acid catalysts for the three-component condensation of aldehydes, amines and terminal alkynes (Scheme 142). Chiral propargylic amine products can be converted into allenes with enantioselectivities of up to 98%. Six-membered ring cyclometallated gold(III) complexes showed higher catalytic activities than five-membered analogues.<sup>543</sup>

**Scheme 142. (C<sup>∧</sup>N)AuCl<sub>2</sub> Catalyzed Condensation Reactions and Allene Synthesis**



Well-defined, stable (P<sup>∧</sup>C) gold chelates have been reported by Amgoune, Bourissou *et al.* as competent catalyst for the hydroarylation of internal alkynes with electron-rich arenes to give *trans*-styrene derivatives (Scheme 143).<sup>544</sup> The bis-trifluoroacetate Au(III) complex **332** showed good catalytic activities and high regio- and stereoselectivity in CH<sub>2</sub>Cl<sub>2</sub>/trifluoroacetic acid mixtures. No reactivity was observed in the absence of the acid. Interestingly, the catalytic performance of **332** proved superior to other cyclometalated Au(III) bis-trifluoroacetate complexes based on (C<sup>∧</sup>N) or (P<sup>∧</sup>C<sup>∧</sup>P) ligands. Unfortunately attempts to investigate the mechanism of the reaction by NMR spectroscopy showed no evidence for intermediates, so no unequivocal mechanistic information could be obtained. However, the *trans*-stereoselectivity of the hydroarylation suggests that the reaction is initiated by the formation of a cationic π-alkyne complex, which is capable of electrophilic attack on electron-rich arenes.

**Scheme 143. Hydroarylation of Internal Alkynes Catalyzed by Well-Defined (P<sup>∧</sup>C) Gold(III) Chelates.**



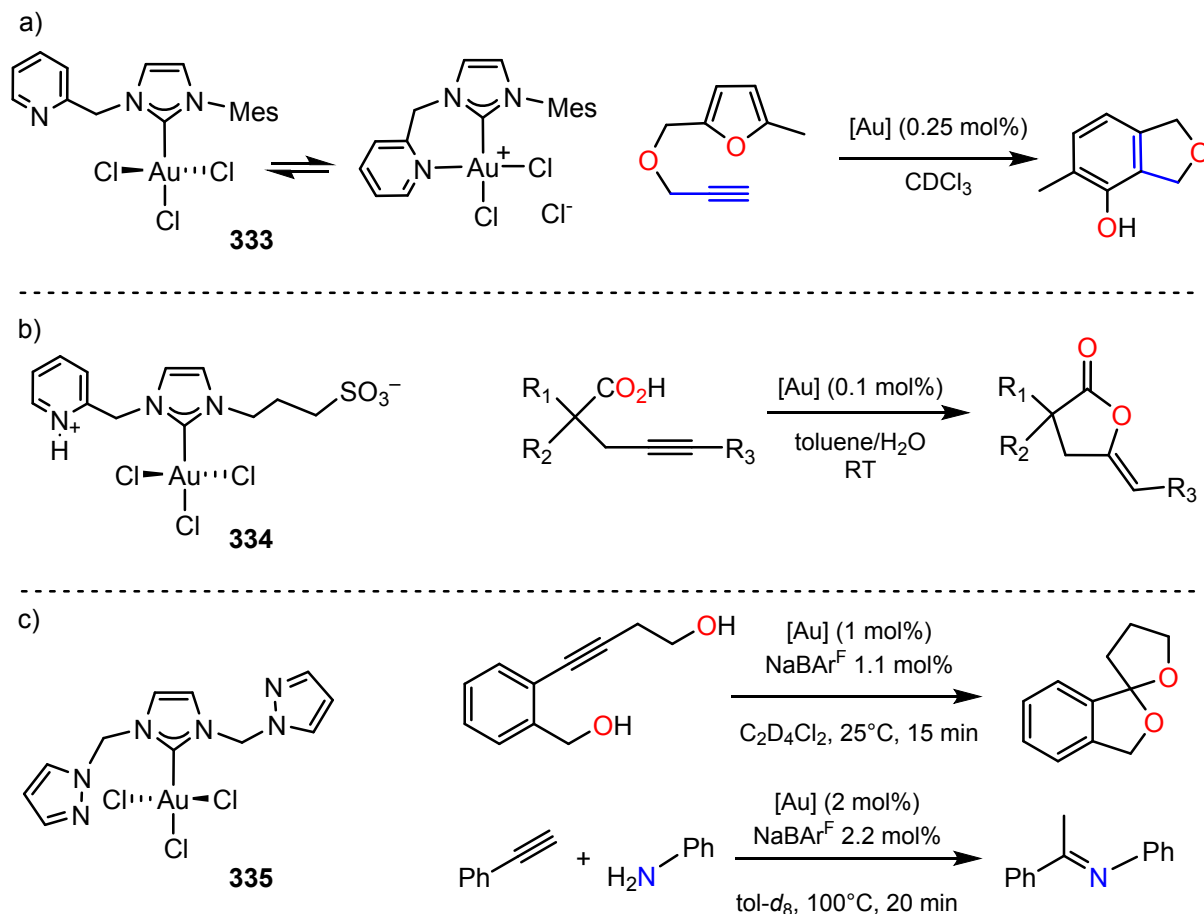
1  
2  
3  
4  
5 Another strategy for developing Au(III)-based alkyne activation catalysts with improved  
6 stability is to use potentially hemilabile ligands. This has been explored in particular for NHCs.  
7 Helaja and co-workers reinvestigated the catalytic activity of the carbene complex **333**,<sup>545</sup> which  
8 had previously been reported by Hashmi and Limbach<sup>291</sup> as catalyst for the cycloisomerization of  
9  $\omega$ -alkynylfurans upon activation with silver salts. The authors showed that **333** is moderately active  
10 also under silver-free conditions (Scheme 144), while its analogue with a phenyl ring in the place of  
11 pyridine is not active at all. This was ascribed to the presence of an ionization equilibrium due to  
12 reversible chloride displacement by the pyridine arm.  
13  
14  
15  
16  
17  
18

19 Similar carbenes have been used by Michelet, Cadierno *et al.* to generate water soluble  
20 Au(III) complexes **334** for the cycloisomerization of  $\gamma$ -alkynoic acids (Scheme 144).<sup>546</sup> These  
21 complexes undergo an ionization equilibrium similar to **333**. However, NMR studies and X-  
22 crystallography showed that the preferred form in water was the bidentate one, most likely because  
23 the extrusion of HCl is highly favorable. It is worth noting that the complex with a C<sub>2</sub> spacer  
24 between the pyridine and the imidazole scaffold preferred the non-chelated form. In any case, no  
25 significant catalytic advantage was found due to the chelation potential of these carbenes, even  
26 though Au(III) catalysts showed a higher recyclability with respect to the Au(I) analogues.  
27  
28  
29  
30  
31  
32

33 Messerle and co-workers have investigated the application of potentially tridentate carbenes  
34 by testing the bis-pyrazole complex **335** in the intramolecular dihydroalkoxylation of alkynyl diols  
35 and hydroamination of phenylacetylene (Scheme 144).<sup>547</sup> By reacting **335** with NaBAR<sup>F</sup>, very  
36 efficient catalytic systems with TONs of 1000 for the alkoxylation reaction were obtained. Kinetic  
37 studies revealed that the turnover frequency was dependent on the added amounts of NaBAR<sup>F</sup> (BAR<sup>F</sup>  
38 = B{C<sub>6</sub>H<sub>3</sub>(CF<sub>3</sub>)<sub>2</sub>-3,5}<sub>4</sub>), most likely as a consequence of the progressive abstraction of the chloride  
39 anions by the sodium salt. NMR experiments suggested the coordination of the pyrazole side arms  
40 upon cationization of the complex. Further control experiments showed no reduction to Au(I),  
41 suggesting that the coordination of the side arms of the ligands contribute to the overall stability of  
42 the catalytic system.  
43  
44  
45  
46  
47  
48  
49  
50

#### 51 **Scheme 144. Examples of Potentially-Hemilabile NHC Ligands for Au(III) Catalysis**

52  
53  
54  
55  
56  
57  
58  
59  
60

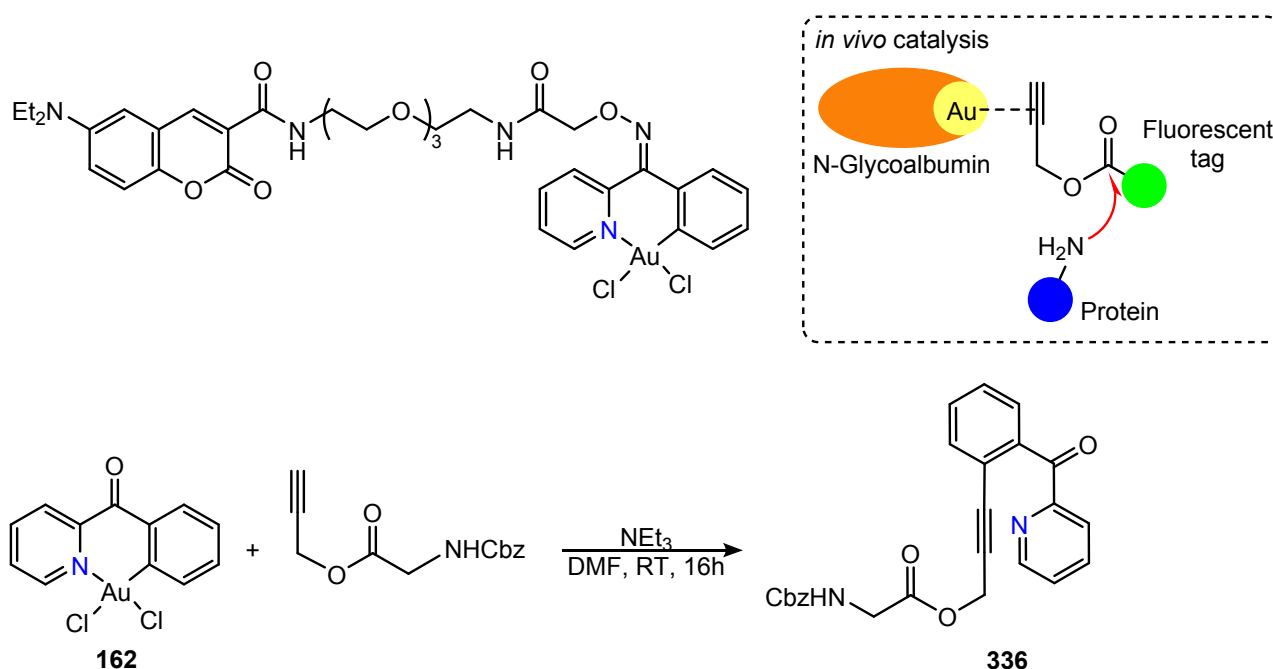


Au(III) catalysts have lately found interesting applications in biological chemistry for achieving chemical transformations in living environments. Tanaka and co-workers developed a cyclometalated Au(III) complex bearing a coumarin-tagged ligand, which is able to bind to glycoproteins such as N-glycoalbumin.<sup>548</sup> Upon injection in live mice, the latter accumulate selectively in organs such as liver or intestine, leading to a localized deposition of the metal. Such bioaccumulated Au(III) catalyzed the amidation of propargylic esters by proteic amine residues present on the surfaces of the organs. Tagging the propargylic esters with fluorescent groups indicated that the imaging reagent reacted selectively in the organs targeted by the N-glycoalbumin gold complexes (Scheme 145).

The mechanism of gold-mediated protein labeling was investigated in a second study by Tanaka, using 2-benzoylpyridine Au(III) salts lacking in the coumarin tags.<sup>549</sup> The latter showed similar activity in protein labeling, suggesting that the pre-immobilization of the gold reagent onto the protein is actually not necessary to achieve an efficient amidation reaction. In control studies, the (C<sup>N</sup>)AuCl<sub>2</sub> complex **162** was reacted with an N-protected propargyl ester for 16h in DMF in the presence of a base. After this time, the C(sp<sup>2</sup>)-C(sp) reductive elimination product **336** was isolated in 52% yield. Compound **273** was found to react with N-acyl aminoesters in the presence of

Au(I) precursors to give the model labeled aminoesters, indicating that an alternative way to protein labeling may be active through an “activated ester” approach. Only trace reactivity was observed when  $\text{NaAuCl}_4$  was used as the gold source, indicating that the presence of the cyclometalated ligand is key to achieving this reactivity.

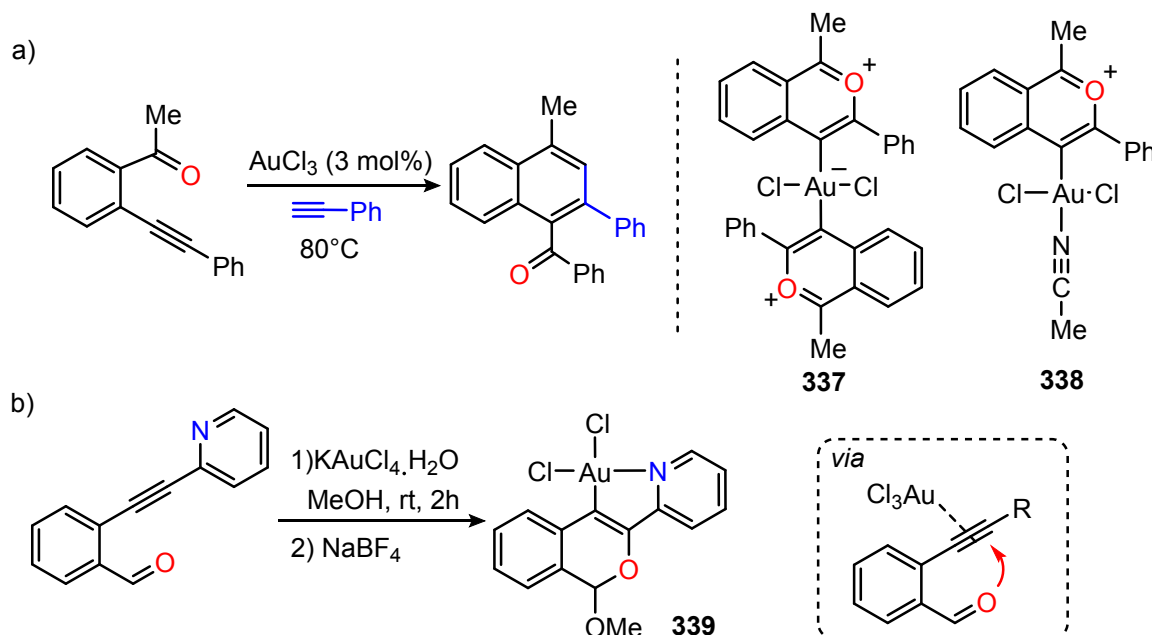
### Scheme 145. Coumarin-Tagged Au(III) Cyclometalated Complex for *In Vivo* Catalysis



Further experimental studies have also demonstrated the intermediacy of Au(III) vinyl species in catalytic alkyne activation reactions. Nguyen *et al.* studied the mechanism of benzannulation of 2-carbonylphenylalkynes catalyzed by AuCl<sub>3</sub> by extended X-ray absorption fine structure (EXAFS), NMR spectroscopy, and mass spectrometry.<sup>550</sup> By reacting the gold halide with 2-alkynyl acetophenone, the authors showed that Au(III) mono- and bis-flavylium intermediates **337** and **338** form as the most abundant species in solution before the reaction with the second alkyne molecule (Scheme 146). The diminished tendency of AuCl<sub>3</sub> to undergo reduction under catalytic conditions seemed to suggest that Au(III) was the actual catalyst of this reaction.

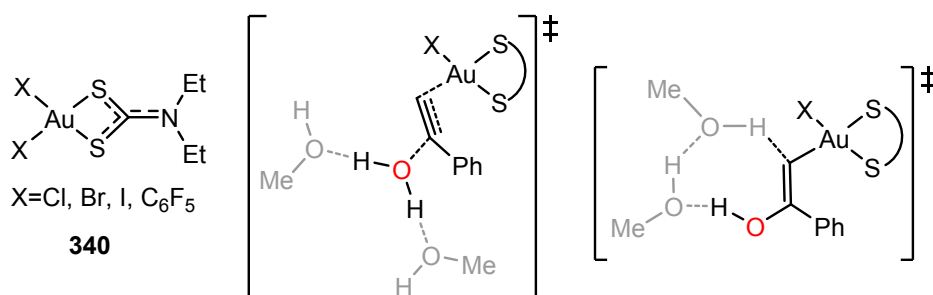
Starck, Michelet and co-workers have used 2-(pyridin-2-ylethynyl)benzaldehyde as a chelating substrate for trapping reaction intermediates of the gold-catalyzed cyclization-reduction of carbonylphenylalkynes to give isochromenes.<sup>551</sup> By using this substrate in combination with KAuCl<sub>4</sub> in MeOH, the authors isolated the Au(III) vinyl species **339**, which was crystallographically characterized (Scheme 146). Protodemetalation of **339** in the presence of reducing agents affords the organic product and liberates the metal.

**Scheme 146. (a) Benzannulation of 2-Acylphenylalkynes and Relevant Intermediates; (b) Trapping of Au(I) Vinyl Species Using Chelating Alkynyl Benzaldehydes**



López-de-Luzuriaga and co-workers investigated the mechanism of alkyne hydration using dithiocarbamate Au(III) complexes **340** (Scheme 147).<sup>369</sup> Catalytic studies showed that the dichloro and dibromo derivatives were moderately active for the hydration of phenylacetylene in refluxing aqueous MeOH, while the diiodo and bis- $\text{C}_6\text{F}_5$  derivatives were completely inactive. This was explained with the lower electronegativity of the iodide leading to decomposition, and the high stability of Au- $\text{C}_6\text{F}_5$  compounds. In addition, a protic solvent proved essential for the reaction to occur, and the addition of  $\text{HBF}_4$  doubled the conversion. On the basis of DFT studies a solvent-assisted mechanism was proposed, where methanol lowers the overall energy required for proton transfer, in analogy to that proposed earlier<sup>552</sup> for Au(I) catalysts.

**Scheme 147. Au(III) Dithiocarbamate Complexes and Solvent-Assisted Transition States for Phenylacetylene Hydration**



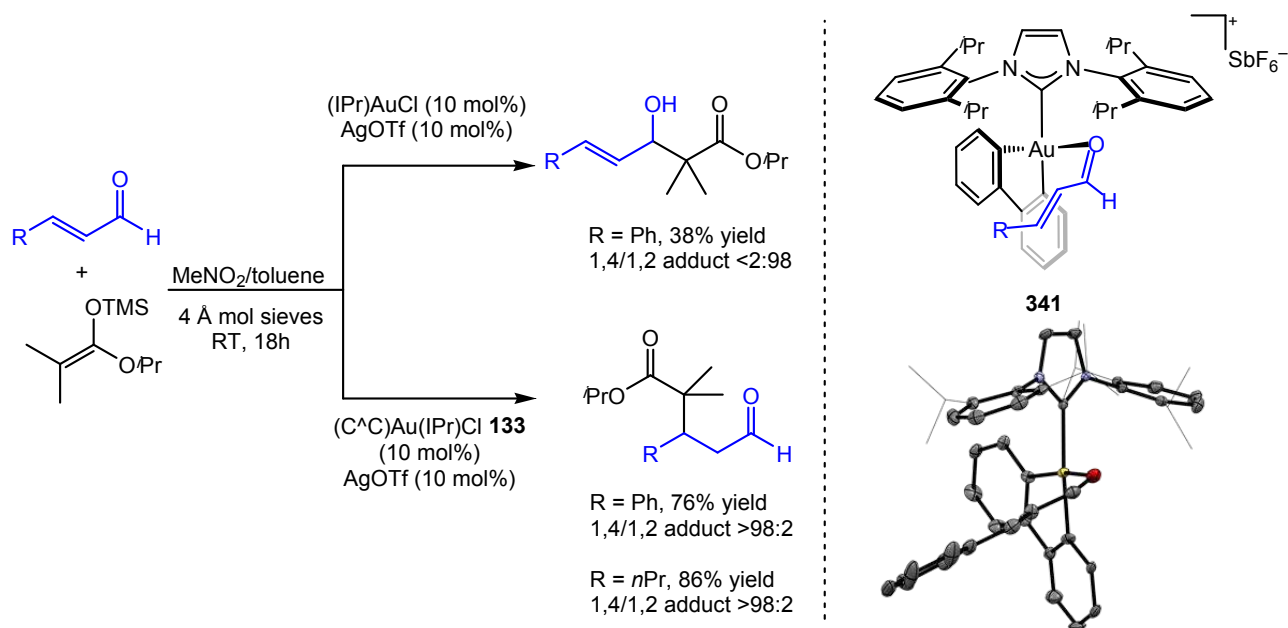


1  
2  
3  
4  
5  
6  
7 **4.2.2 Au(III) as Oxophilic Lewis Acid.** The hard character of Au(III) Lewis acids enables  
8 catalysis through coordination to the oxygen atom of carbonyl compounds or alcohols to promote  
9 reactivity such as aldol or Diels-Alder-type reactions. However, the number of examples is much  
10 more limited in comparison with  $\pi$ -complexation. In some cases Au(III) can offer improved  
11 performance with respect to other more usual Lewis acids; for instance, AuCl<sub>3</sub> can catalyze  
12 intramolecular oxa-Michael additions with higher activity and selectivity than stoichiometric  
13 BF<sub>3</sub>•OEt<sub>2</sub><sup>553</sup>.  
14  
15  
16  
17  
18

19 Toste and co-workers used (C<sup>^</sup>C)Au(III) chelates obtained upon oxidative addition of  
20 biphenylene to (NHC)Au(I) salts as selective Lewis acids for the Mukaiyama-Michael addition of  
21 ketene silyl acetals to  $\alpha,\beta$ -unsaturated aldehydes such as cinnamaldehyde (Scheme 148).<sup>308</sup>  
22 Typically, these reactions follow a 1,2-regiochemistry with the vast majority of Lewis acids and  
23 substrates. This was also the case of (IPr)AuCl, which afforded a 1,2 addition product in 38% yield  
24 when activated with AgOTf. On the other hand, the Au(III) species catalyzed selectively the  
25 formation of the 1,4 adducts with rather high yields. This was explained on the basis of the structure  
26 of the Au(III) catalyst, where the combination of the square-planar geometry and the steric bulk of  
27 the carbene ligand creates a reactive pocket that makes 1,2 addition unfavorable. This conclusion  
28 was further corroborated by the isolation of the cinnamaldehyde complex **341**, which was  
29 crystallographically characterized and showed how the carbonyl unit was hindered by the Dipp  
30 substituents of the IPr ligand.  
31  
32  
33  
34  
35  
36  
37  
38

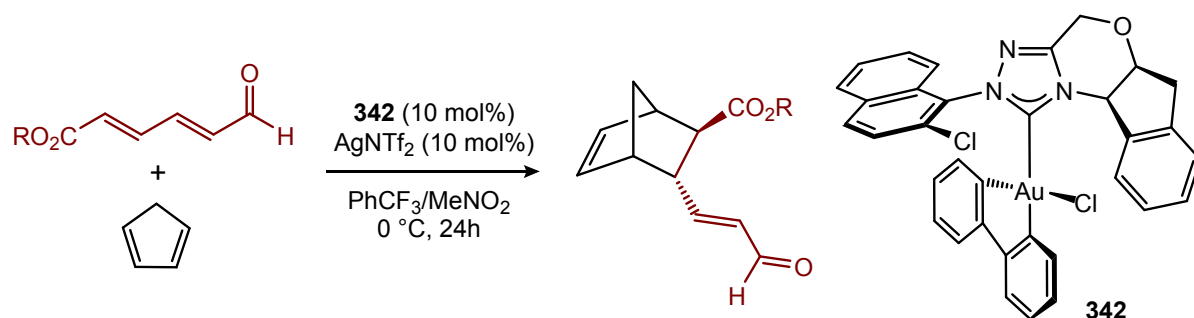
39 The high selectivity observed in the Mukaiyama-Michael reaction was also obtained in other  
40 reactions such as nitronate Michael addition, thiol addition, Hantzsch ester reductions, Diels-Alder  
41 and [2+2] cycloaddition, showing the superior properties of ligand-based stable Au(III) catalysts  
42 over the usually unselective AuCl<sub>3</sub> or Au(I) catalysts.  
43  
44  
45  
46  
47

48 **Scheme 148. Left: Mukaiyama-Michael Addition of Ketene Silyl Acetals to  $\alpha,\beta$  Unsaturated**  
49 **Aldehydes, and Crystal Structure of the Isolated Complex 341**  
50  
51  
52  
53  
54  
55  
56  
57  
58  
59  
60



This strategy was further developed to design chiral catalysts for the enantioselective  $\gamma,\delta$  Diels-Alder addition of cyclopentadiene to dienals (Scheme 149).<sup>554</sup> A thorough experimental and computational investigation revealed that a number of non-covalent interactions cooperate in the enantioselectivity control of this process, in a way that is not possible with Au(I). By performing a transition state and multivariate linear regression (MLR) analysis on the molecular descriptors that affect activity and selectivity, complex **342** emerged as an optimal catalyst, showing good productivity (60% yield) and enantioselectivity (82%).

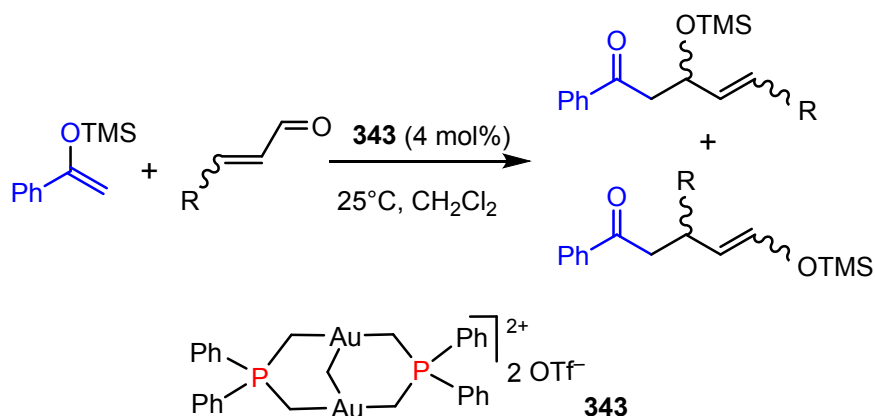
#### Scheme 149. Enantioselective $\gamma,\delta$ Diels-Alder Coupling of Cyclopentadiene and Dienals Catalyzed by Au(III)



The gold-catalyzed Mukaiyama addition of silyl enol ethers to  $\alpha,\beta$  unsaturated aldehydes was also achieved by Wade and co-workers with the dimeric phosphorus ylide complex **343**.<sup>555</sup> Compound **343** led to the formation of a mixture of 1,2 and 1,4 adducts in a 73:27 ratio in the case

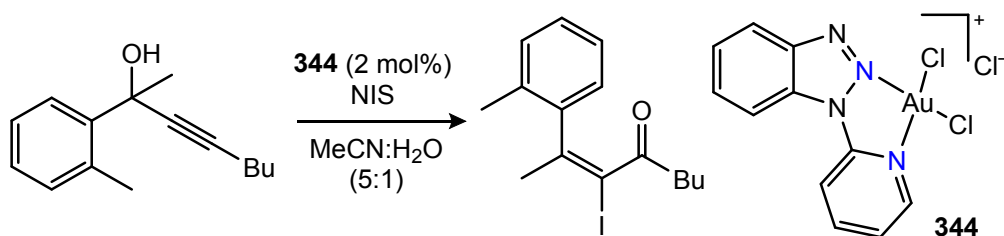
of crotonaldehyde, while only the 1,4 adduct was obtained in the case of cyclohexanone (Scheme 150). The catalytic performance of **343** was however found to be inferior to the corresponding Au<sup>II</sup> dimer with a direct Au–Au bond. This was tentatively ascribed to a lower rate of exchange between coordinated and uncoordinated ketones in the Au<sup>III</sup> complex. However, no clear difference in Lewis acidity between the two species was observed by the Gutmann-Beckett method. These species also showed carbophilic Lewis acidity and catalyzed the hydroamination of phenylacetylene.

### Scheme 150. Mukaiyama-Michael Addition Catalyzed by Au(III) Phosphorus Ylides



Shi and co-workers used well-defined Au(III) systems based on pyridine-substituted triazole ligands **344** to catalyze the synthesis of vinyl halides from propargyl alcohols and N-halosuccinimides (Scheme 151).<sup>556</sup> The reaction is assumed to involve an Au(III) catalyzed Meyer-Schuster rearrangement of the propargyl alcohol,<sup>557</sup> affording an allene intermediate that in turn reacts with the halogenating agent to give the final product. Complex **344** as well as (Pic)AuCl<sub>2</sub> produced high yields and showed good selectivity, while AuCl<sub>3</sub> and KAuCl<sub>4</sub> gave poor results.

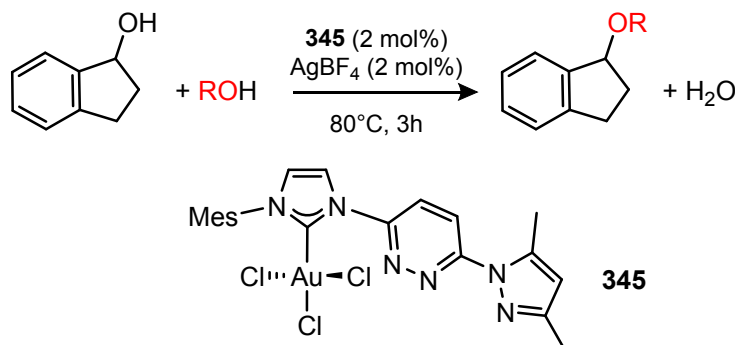
### Scheme 151. Well-Defined Au(III) Triazole Complexes for the Synthesis of Vinyl Halides



Au(III) complexes with hemilabile carbenes were shown to be moderately active also in etherification catalysis by Meyer and co-workers.<sup>558</sup> The trichloro complex **345** was obtained upon oxidation of the corresponding Au(I) complex with PhICl<sub>2</sub> and used to catalyze the etherification of

indanol to produce asymmetric ethers with good productivity, which proved to be higher than that of the Au(I) congener (Scheme 152).

### Scheme 152. Hemilabile NHC Au(III) Catalyst **345** for Etherification of Indanol



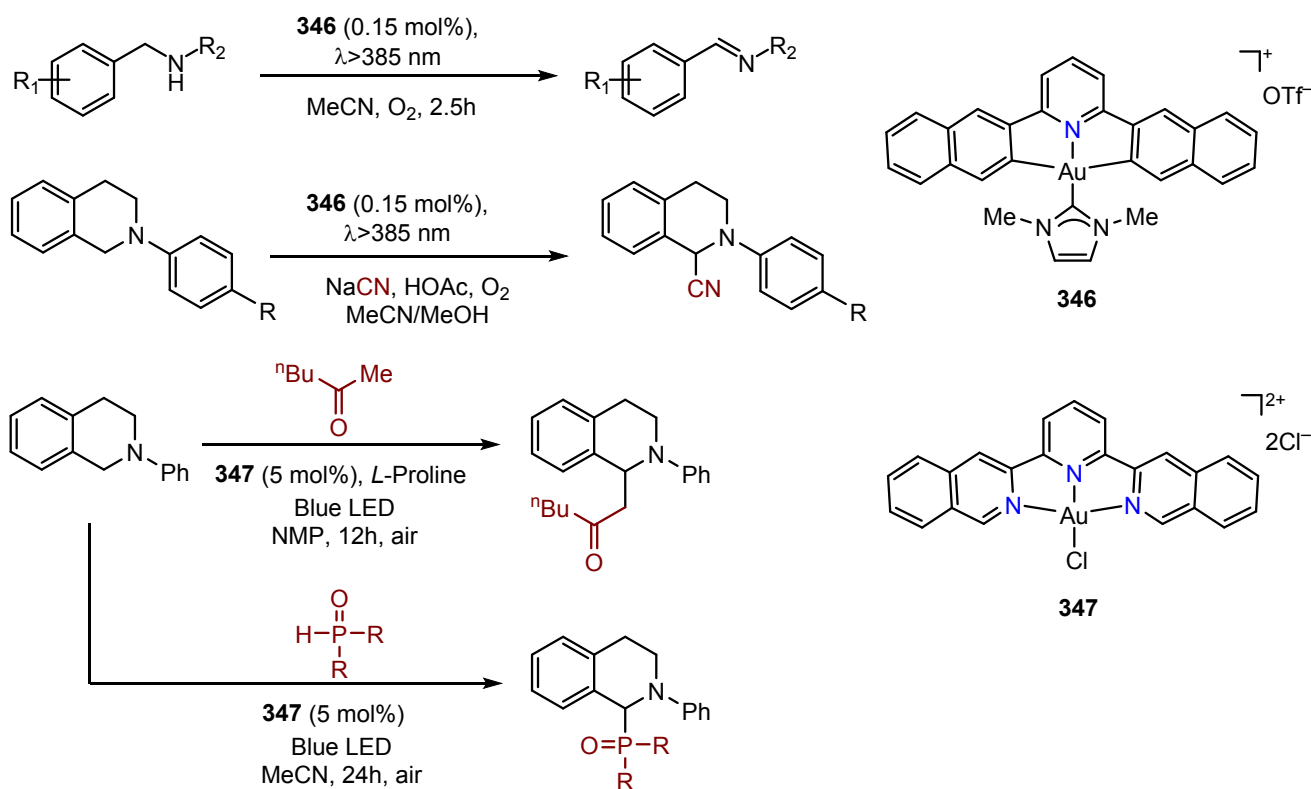
Over the past few years, gold catalyst found application also in glycosylation catalysis for the synthesis of carbohydrates.<sup>559</sup> Although it lags behind Au(I) in this area, AuCl<sub>3</sub> has found some specific applications, such as in the synthesis of furanosides.<sup>560</sup> This area is still in its infancy and under methodological development, so mechanistic details about these reactions are mostly speculative.

### 4.3 Au(III) as Photosensitizer

Well-defined Au(III) complexes showed potential as photocatalysts in oxidation reactions. Che and co-workers showed in 2012 that the cationic pincer carbene complexes **346** shows long-lived emissive states (282 and 506 μs) arising from the radiative decay of intraligand triplet states. These excited states were harnessed to catalyze the oxidation of secondary amines to imines and the cyanation of tertiary amines in high yields (Scheme 153). These reactions are thought to occur through the gold-sensitized generation of singlet-oxygen, which acts as oxidant in both transformations. Complex **346** also showed good activity in the photocatalytic H<sub>2</sub> generation in a three-component system consisting of a cobalt diglyoximate complex [Co(dmgh)<sub>2</sub>(Py)Cl], triethanolamine and degassed acetonitrile/water.<sup>561</sup>

Later on, Zhu and co-workers showed that cationic bidentate (N<sup>^</sup>N) and pincer (N<sup>^</sup>N<sup>^</sup>N) complexes can also act as efficient photocatalyst for the oxidative coupling of amines. As an example, complex **347** was used for the selective coupling of N-phenyl tetrahydroisoquinoline with ketones, malonates, phosphine oxides and phosphites under blue LED irradiation and with aerobic oxidation.<sup>562</sup>

### Scheme 153. Photocatalytic Au(III) Mediated Oxidations with Dioxygen



## 5. CONCLUSIONS

33 Over the last decade the coordination and organometallic chemistry of gold(III) has seen  
 34 major step-changes. As outlined in this review, a number of key complex types which had long  
 35 been postulated as being involved in catalytic cycles have finally been synthesized and  
 36 characterized, thus providing tools for either validation or dismissal of postulated mechanisms.  
 37 These new compound classes include the long-sought after gold(III) alkene, alkyne, CO and  
 38 hydride complexes, as well as peroxides and highly reactive species with weak  $\pi$ - and  $\sigma$ -  
 39 interactions. These synthetic advances have enabled the interrogation of the bonding characteristics  
 40 of gold and have illustrated the fundamental differences that exist between Au(III) and its  
 41 isoelectronic neighbor in the Periodic Table, platinum(II). It has become very evident that  
 42 mechanistic pathways that are observed for the Group 10 metal triad are not necessarily valid for  
 43 gold, and mechanistic analogies must be treated with caution. Nevertheless, a whole new body of  
 44 knowledge about rates and mechanisms e.g. of C-C and C-E reductive elimination mediated by  
 45 gold(III) has been gathered, which has allowed a very broad spectrum of homo- and hetero-  
 46 coupling reactions to be discovered and gold redox catalysis to be placed under the spotlight of the  
 47 synthetic community. In addition the electrophilic character of Au(III) has attracted much attention  
 48 in Lewis acid catalysis. Here, the high stability and tunability of Au(III) chelates allows a full  
 49  
 50  
 51  
 52  
 53  
 54  
 55  
 56  
 57  
 58  
 59

1  
2  
3 exploitation of ligand effects and the development of very efficient chemo-, regio- and enantio-  
4 selective reactions of double and triple bonds.  
5

6 On the other hand, while important reaction pathways that usually compose catalytic cycles  
7 have certainly been identified, such as oxidative addition of C–X bonds, alkene insertions into Au-  
8 C / Au-H bonds and  $\beta$ -H elimination, it is also true that these were mostly established for a rather  
9 narrow range of compound types supported by a limited range of “privileged” ligands, and/or apply  
10 only to a limited range of substrates. For instance, although a fair spectrum of gold(I) and gold(III)  
11 hydrides is now known, none of these exhibit the same high activity as heterogeneous gold  
12 hydrogenation catalysts. There is clearly much ligand development work to be done if gold  
13 complexes are to be “trained” to compete with homogeneous Group 9 and 10 hydrogenation,  
14 hydrosilylation or hydroboration catalysts.  
15  
16

17 Some intermediates and reaction pathways that are common for other late-transition metals,  
18 still remain unknown for gold(III). Notable examples are reactive gold(III) carbenes<sup>563</sup>  $\text{Au} \leftarrow \text{CR}_2 \leftrightarrow$   
19  $\text{Au-C}^{(+)}\text{R}_2$  and carbene insertion catalysis, whose potential remains to be tapped. Non-reductive  
20 product release from the metal remains challenging as well. This is typified by  $\beta$ -H elimination,  
21 which proved facile for very specific chelate-supported cationic 14-electron gold(III) alkyls but  
22 remains a high-barrier process in most cases.  
23

24 In spite of such limitations, quite new possibilities have arisen that take the story forward  
25 beyond classical catalysis based on even-electron species. There is mounting evidence of the  
26 importance of gold(II) as reaction intermediates, and of the involvement of electronically excited  
27 open-shell species which circumvent the coordinative limitations imposed on gold(III) compounds  
28 in the ground state. Routes to the selective generation of open-shell gold reagents are only now  
29 beginning to emerge, and new synthetic protocols, including stereo- and enantioselective processes  
30 based on mononuclear  $d^9$  and triplet intermediates remain to be developed. Similarly, the ability to  
31 fine-tune oxidation events by replacing strong chemical oxidants by electrochemical oxidation  
32 promises improvements in reaction scope, selectivity and atom-efficiency.  
33

34 Overall, this review shows how the fundamental discoveries in the chemistry of gold(III)  
35 unlocked a toolbox of reactivities that was unthinkable even 10 years ago. These advances expand  
36 the scope of gold catalysis and provide the foundation for more breakthroughs in the near future.  
37  
38  
39  
40  
41  
42  
43  
44  
45  
46  
47

## 48 AUTHOR INFORMATION

### 49 Corresponding Authors

50  
51  
52  
53  
54  
55  
56  
57  
58  
59  
60

1  
2  
3 **Luca Rocchigiani**, *School of Chemistry, University of East Anglia, Norwich Research Park,*  
4 *Norwich, NR47TJ, United Kingdom. ORCID:* <https://orcid.org/0000-0002-2679-8407>; Email:  
5 [L.Rocchigiani@uea.ac.uk](mailto:L.Rocchigiani@uea.ac.uk).  
6  
7

8 **Manfred Bochmann**, *School of Chemistry, University of East Anglia, Norwich Research Park,*  
9 *Norwich, NR47TJ, United Kingdom. ORCID:* <https://orcid.org/0000-0001-7736-5428>; Email:  
10 [M.Bochmann@uea.ac.uk](mailto:M.Bochmann@uea.ac.uk).  
11  
12  
13  
14

## 15 Notes

16 The authors declare no competing financial interest.  
17  
18  
19

## 20 Biographies

21 Luca Rocchigiani was an undergraduate at the University of Perugia where in 2011 he obtained his  
22 Ph.D. under the supervision of Prof. Alceo Macchioni. After a postdoctoral position in partnership  
23 with the Dutch Polymer Institute in 2015 he moved to University of East Anglia (UEA) to join the  
24 group of Prof. Manfred Bochmann. In 2019 he was appointed Lecturer in Inorganic Chemistry at  
25 the School of Chemistry at UEA. His research interests focus on mechanistic aspects of transition  
26 organometallic chemistry for small molecule activation and catalysis and, in particular, on the  
27 application of NMR spectroscopic techniques for the investigation of supramolecular  
28 organometallic aggregates and trapping of reactive intermediates.  
29  
30  
31  
32  
33  
34  
35  
36

37 Manfred Bochmann studied at the universities of Dortmund and Marburg and obtained his PhD  
38 from Imperial College London under the supervision of Prof. Sir Geoffrey Wilkinson. He started  
39 his professional career as a group leader in the chemical industry, working on areas of catalysis.  
40 From 1995-2000 he was Head of Inorganic and Structural Chemistry at the University of Leeds and  
41 since 2000 is Professor of Inorganic Chemistry at the University of East Anglia. From 2006 – 2011  
42 he was Head of the School of Chemical Sciences and Pharmacy. He is the author of several  
43 inorganic and organometallic textbooks. His research covers fundamental aspects of homogeneous  
44 catalysis and was mainly concerned with metallocene-based olefin polymerization before, more  
45 recently, exploring the organometallic chemistry of gold(III).  
46  
47  
48  
49  
50  
51  
52  
53  
54

## 55 ACKNOWLEDGEMENTS

56 Dedicated to the memory of Professor Malcolm L. H. Green (1936 - 2020), a giant of chemistry.  
57 Our work on gold(III) chemistry was supported by the University of East Anglia and the European  
58 Research Council. M. B. is an ERC Advanced Investigator Award holder (grant no. 338944-  
59  
60

GOCAT). We are particularly grateful to the talented co-workers without whom nothing could have been achieved and whose names appear as coauthors in the papers cited in this Review.

### Abbreviations

bipy	2,2'-bipyridyl	NBE	norbornene
CAAC	cyclic (alkyl)(amino)carbene	NFSI	<i>N</i> -fluorodi(benzenesulfon)imide
C <sup>^</sup> C	4,4'-di- <i>tert</i> -butylbiphenyl-2,2'-diyl	NHC	N-heterocyclic carbene
CDA	Charge decomposition analysis	NPA	natural population analysis
CMD	concerted metalation-deprotonation	OAc <sup>F</sup>	trifluoroacetate
COD	1,5-cyclooctadiene	OPiv	pivaloate, Me <sub>3</sub> CCO <sub>2</sub> <sup>-</sup>
CSA	camphorsulfonic acid	PBX	1-pivaloyloxy-1,2-benziodoxol-3(1H)-one, PhI(OCO)(OPiv)
Dipp	2,6-diisopropylphenyl	phen	1,10-phenanthroline
DMAD	dimethylacetylene dicarboxylate	pic	picolinate
DMAP	<i>N,N</i> -dimethylaminopyridine	PIDA	PhI(OAc) <sub>2</sub>
DTBMP	2,6-di- <i>tert</i> -butyl-4-methylpyridine	ppy	2-phenyl-2'-ylpyridine
EBX	ethynylbenziodoxol(on)e	RDS	rate determining step
ESI-MS	electrospray-ionization mass spectrometry	SIPr	1,3-bis(2,6-diisopropylphenyl)-imidazolin-2-ylidene
IPr	1,3-bis(2,6-diisopropylphenyl)-imidazole-2-ylidene	TIPS	triisopropylsilyl
NBD	norbornadiene	tpyH	2-( <i>p</i> -tolyl)pyridine

### REFERENCES

- (1) Raubenheimer, H. G.; Schmidbaur, H. The Late Start and Amazing Upswing in Gold Chemistry. *J. Chem. Educ.* **2014**, *91*, 2024–2036.
- (2) Hashmi, A. S. K. Gold-Catalyzed Organic Reactions, *Chem. Rev.* **2007**, *107*, 3180–3211.
- (3) Pyykkö, P. Theoretical Chemistry of Gold. *Angew. Chem. Int. Ed.* **2004**, *43*, 4412–4456.
- (4) Pyykkö, P. Theoretical Chemistry of Gold. II. *Inorg. Chim. Acta*, **2005**, *358*, 4113–4130.
- (5) Pyykkö, P. Theoretical Chemistry of Gold. III. *Chem. Soc. Rev.* **2008**, *37*, 1967–1997.
- (6) Schmidbaur, H.; Schier, A. A Briefing on Auophilicity. *Chem. Soc. Rev.* **2008**, *37*, 1931–1951.
- (7) Schmidbaur, H.; Schier, A. Auophilic Interactions as a Subject of Current Research: an Up-Date. *Chem. Soc. Rev.* **2012**, *41*, 370–412.



(8) Weber, D.; Gagné, M. R. Auophilicity in Gold Catalysis: Better or Worse? *Top. Curr. Chem.* **2015**, *357*, 167-211.

(9) Covalent radii for 2-coordinate cations  $[M(\text{PMes}_3)_2]^+$ : M = Cu 1.13, Ag 1.33, Au 1.25 Å: Bayler, A.; Schier, A.; Bowmaker, G. A.; Schmidbaur, H. Gold Is Smaller than Silver. Crystal Structures of [Bis(trimesitylphosphine)gold(I)] and [Bis(trimesitylphosphine)silver(I)] Tetrafluoroborate. *J. Am. Chem. Soc.* **1996**, *118*, 29, 7006-7007.

(10) Very similar radii were determined for compounds with linear N-M-N coordination: Omary, M. A.; Rawashdeh-Omary, M. A.; Gonser, M. W. A.; Elbjeirami, O.; Grimes, T.; Cundari, T. R. Metal Effect on the Supramolecular Structure, Photophysics, and Acid-Base Character of Trinuclear Pyrazolato Coinage Metal Complexes. *Inorg. Chem.* **2005**, *44*, 8200-8210.

(11) Tetra-coordinate  $M^I$  ions show the same trend (Cu 1.29, Ag 1.46, Au 1.37 Å): Tripathi, U. M.; Bauer, A.; Schmidbaur, H. Covalent Radii of Four-co-ordinate Copper(I), Silver(I) and Gold(I): Crystal Structures of  $[\text{Ag}(\text{AsPh}_3)_4]\text{BF}_4$  and  $[\text{Au}(\text{AsPh}_3)_4]\text{BF}_4$ . *J. Chem. Soc., Dalton Trans.* **1997**, 2865-2868.

(12) Pérez-Bitrián, A.; Baya, M.; Casas, J. M.; Martín, A.; Menjón, B.; Orduna, J. An Organogold(III) Difluoride with a *trans* Arrangement. *Angew. Chem. Int. Ed.* **2018**, *57*, 6517-6521.

(13) Schwerdtfeger, P.; Boyd, P. D. W.; Brienne, S.; Burrell, A. K. Relativistic Effects in Gold Chemistry 4. Gold(III) and Gold(V). *Inorg. Chem.* **1992**, *31*, 3411-3422.

(14) Harrach, G.; Valicsek, Z.; Horvath, O. Water-soluble Silver(II) and Gold(III) Porphyrins: The Effect of Structural Distortion on the Photophysical and Photochemical Behavior. *Inorg. Chem. Commun.* **2011**, *14*, 1756-1761.

(15) Lu, W.; Chan, K. T.; Wu, S.-X.; Chen, Y.; Che, C.-M. Quest for an Intermolecular Au(III)/Au(III) Interaction Between Cyclometalated Gold(III) Cations. *Chem. Sci.* **2012**, *3*, 752-755.

(16) Chernyshev, A.N.; Chernysheva, M. V.; Hirva, P.; Kukushkin, V. Y.; Haukka, M. Weak Auophilic Interactions in a Series of Au(III) Double Salts. *Dalton Trans.* **2015**, *44*, 14523-14531.

(17) for Au(III)-Au(I) interactions in the solid state see: Cao, L.; Jennings, M. C.; Puddephatt, R. J. Amine-Amide Equilibrium in Gold(III) Complexes and a Gold(III)-Gold(I) Auophilic Bond. *Inorg. Chem.* **2007**, *46*, 1361-1368, and cited refs.

(18) Roşca, D.-A.; Wright, J. A.; Bochmann, M. An Element Through the Looking Glass: Exploring the Au-C, Au-H and Au-O Energy Landscape. *Dalton Trans.* **2015**, *44*, 20785-20807.

(19) Gaillard, S.; Slawin, A. M. Z.; Nolan, S. P. An N-Heterocyclic Carbene Gold Hydroxide Complex: a Golden Synthone. *Chem. Commun.* **2010**, *46*, 2742-2744.

- 1  
2  
3 (20) For a report on OH-bridged gold(I) phosphine complexes see Yang, Y.; Sharp, P. R. New  
4 Gold Clusters  $[\text{Au}_8\text{L}_6](\text{BF}_4)_2$  and  $[(\text{AuL})_4](\text{BF}_4)_2$  (L = P(mesityl)<sub>3</sub>). *J. Am. Chem. Soc.* **1994**, *116*,  
5 6983-6984.  
6  
7  
8 (21) Nelson, D. J.; Nolan, S. P. Hydroxide Complexes of the Late Transition Metals:  
9 Organometallic Chemistry and Catalysis. *Coord. Chem. Rev.* **2017**, *353*, 278-294.  
10  
11 (22) Laitar, D. S.; Müller, P.; Gray, T. G.; Sadighi, J. P. A Carbene-Stabilized Gold(I) Fluoride:  
12 Synthesis and Theory. *Organometallics* **2005**, *24*, 4503-4505.  
13  
14 (23) Jander G.; Krien, G. Über Salze der Goldsäure. *Z. Anorg. Allg. Chem.* **1960**, *304*, 164-175.  
15  
16 (24) Jones, P. G.; Sheldrick, G. M. Digold Strontium Hydroxide,  $\text{Au}_2\text{Sr}(\text{OH})_8$ . *Acta*  
17 *Crystallogr. Section C*, **1984**, *C40*, 1776-1777.  
18  
19 (25) Jones, P. G.; Schelbach, R.; Schwarzmann, E. Hydroxy Complexes of Gold 2. Calcium  
20 Aurates. *Z. Naturforsch. B*, **1987**, *42*, 522-524.  
21  
22 (26) Einstein, F. W. B.; Rao, P. R.; Trotter, J.; Bartlett, N. The Crystal Structure of Gold  
23 Trifluoride. *J. Chem. Soc. (A)*, **1967**, 478-482.  
24  
25 (27) Edwards, A. J.; Jones, G. R. Fluoride Crystal Structures. VIII. Neutron Diffraction  
26 Studies of Potassium Tetrafluorobromate(III) and Potassium Tetrafluoroaurate(III). *J. Chem. Soc.*  
27 *A: Inorg. Phys. Theor.* **1969**, 1936-1938.  
28  
29 (28) Hector, A. L.; Levason, W.; Weller, M. T.; Hope, E. G. UV-Vis Spectroscopic Studies of  
30 Fluorides and Fluoro Anions of Silver(III) and Gold(III) and (V). *J. Fluor. Chem.* **1997**, *86*, 105-  
31 108.  
32  
33 (29) Réffy, B.; Kolonits, M.; Schulz, A.; Klapötke, T. M.; Hargittai, M. Intriguing Gold  
34 Trifluoride - Molecular Structure of Monomers and Dimers: An Electron Diffraction and Quantum  
35 Chemical Study. *J. Am. Chem. Soc.* **2000**, *122*, 3127-3134.  
36  
37 (30) Fürstner, A.; Davies, P. W. Catalytic Carbophilic Activation: Catalysis by Platinum and  
38 Gold  $\pi$ -Acids. *Angew. Chem. Int. Ed.* **2007**, *46*, 3410 – 3449.  
39  
40 (31) Fürstner, A. Gold and Platinum Catalysis—a Convenient Tool for Generating Molecular  
41 Complexity. *Chem. Soc. Rev.* **2009**, *38*, 3208–3221.  
42  
43 (32) Fürstner, A. From Understanding to Prediction: Gold- and Platinum-Based  $\pi$ -Acid  
44 Catalysis for Target Oriented Synthesis. *Acc. Chem. Res.* **2014**, *47*, 925-938.  
45  
46 (33) Leya-Perez, A.; Corma, A. Similarities and Differences between the “Relativistic” Triad  
47 Gold, Platinum, and Mercury in Catalysis. *Angew. Chem. Int. Ed.* **2012**, *51*, 614 – 635.  
48  
49 (34) Adcock, H. V.; Davies, P. W.  $\pi$ -Acid Mediated Insertion of Alkynes into Carbon-  
50 Heteroatom Bonds. *Synthesis* **2012**, *44*, 3401-3420.  
51  
52  
53  
54  
55  
56  
57  
58  
59  
60

(35) For a comparison of the catalytic aspects of Au(I) and Pd see: Nunes dos Santos Comprido, L.; Hashmi, A. S. K. Catalytic Oxidative Cyclisation Reactions of 1,6-Enynes: A Critical Comparison Between Gold and Palladium. *Isr. J. Chem.* **2013**, *53*, 883-891.

(36) Bratsch, S. G. Standard Electrode Potentials and Temperature Coefficients in Water at 298.15 K. *J. Phys. Chem. Ref. Data* **1989**, *18*, 1-22.

(37) Đurović, M. D.; Puchta, R.; Bugarčić, Ž. D.; van Eldik, R. Studies on the Reactions of  $[\text{AuCl}_4]^-$  with Different Nucleophiles in Aqueous Solution. *Dalton Trans.* **2014**, *43*, 8620–8632.

(38) Henderson, W. The Chemistry of Cyclometallated Gold(III) Complexes with C,N-Donor Ligands. In: *Adv. Organomet. Chem.*, West, R.; Hill A. F. (eds), Academic Press, 2006, Vol. 54, pp. 207-265.

(39) Bertrand, B.; Bochmann, M.; Fernandez-Cestau, J.; Rocchigiani, L. Pincer Complexes of Gold: An Overview of Synthesis, Reactivity, Photoluminescence and Biological Applications. In: Morales-Morales, D. (ed.): *Pincer Compounds – Chemistry and Applications*, Elsevier, Amsterdam 2018, p. 673-699. ISBN: 978-0-12-812931-9.

(40) Kumar, R.; Nevado, C. Cyclometalated Gold(III) Complexes: Synthesis, Reactivity, and Physicochemical Properties. *Angew. Chem. Int. Ed.* **2017**, *56*, 1994-2015.

(41) Langseth, E.; Görbitz, C. H.; Heyn, R. H.; Tilset, M. Versatile Methods for Preparation of New Cyclometalated Gold(III) Complexes. *Organometallics* **2012**, *31*, 6567-6571.

(42) Zou, T.; Lum, C. T.; Chui, S. S.-Y.; Che, C.-M. Gold(III) Complexes Containing N-Heterocyclic Carbene Ligands: Thiol “Switch-on” Fluorescent Probes and Anti-Cancer Agents. *Angew. Chem. Int. Ed.* **2013**, *52*, 2930–2933.

(43) Sánchez Delgado, G. Y.; Paschoal, D.; Dos Santos, H. F. Reactivity of the  $[\text{Au}(\text{C}^{\wedge}\text{N}^{\wedge}\text{C})\text{Cl}]$  Complex in the Presence of  $\text{H}_2\text{O}$  and N-, S- and Se-Containing Nucleophiles: A DFT Study. *J. Biol. Inorg. Chem.* **2018**, *23*, 1283-1293.

(44) Teets, T. S.; Nocera, D. G. Halogen Photoreductive Elimination from Gold(III) Centers. *J. Am. Chem. Soc.* **2009**, *131*, 7411-7420.

(45) Hirtenlehner, C.; Krims, C.; Hölbling, J.; List, M.; Zabel, M.; Fleck, M.; Berger, R. J. F.; Schoefberger, W.; Monkowius, U. Syntheses, Crystal Structures, Reactivity, and Photochemistry of Gold(III) Bromides Bearing N-Heterocyclic Carbenes. *Dalton Trans.* **2011**, *40*, 9899-9910.

(46) Cao, Z.; Bassani, D. M.; Bibal, B. Photoreduction of Thioether Gold(III) Complexes: Mechanistic Insight and Homogeneous Catalysis. *Chem. Eur. J.* **2018**, *24*, 18779-18787.

(47) Romanov, A. S.; Bochmann, M. Gold(I) and Gold(III) Complexes of Cyclic (Alkyl)(amino)carbenes. *Organometallics* **2015**, *34*, 2439-2454.

- 1  
2  
3 (48) Schützenberger, P. Sur un Nouveau Composé de Platine. *Compt. Rendus* **1868**, *66*, 666-  
4 668.  
5  
6 (49) Schützenberger, P. Sur Quelques Réactions Donnant Lieu à la Formation de l'Oxychlorure  
7 de Carbone et sur un Nouveau Composé Volatil de Platine. *Ann. Chim. Phys.* **1868**, *15*, 100-106.  
8  
9 (50) Donau, J. Über eine rote, mittels Kohlenoxyd erhaltene kolloidale Goldlösung. *Monatsh.*  
10 *Chem.* **1905**, *26*, 525-530.  
11  
12 (51) Hashmi, A. S. K.; Toste, F. D. (eds.): *Modern Gold-Catalyzed Synthesis*, Wiley-VCH,  
13 Weinheim, 2012, ISBN 978-3-527-31952-7.  
14  
15 (52) Toste, F. D.; Michelet, V. (eds): *Gold Catalysis – a Homogeneous Approach*, Imperial  
16 College Press, London, 2014, ISBN 978-1-84816-852-7.  
17  
18 (53) Slaughter, L. M. (ed.): *Homogeneous Gold Catalysis*, Springer, Heidelberg, 2015, ISBN  
19 978-3-319-13721-6.  
20  
21 (54) Hashmi, A. S. K. Homogeneous Catalysis by Gold. *Gold Bull.* **2004**, *37*, 51-65.  
22  
23 (55) Braun, I.; Asiri, A. M.; Hashmi, A. S. K. Gold Catalysis 2.0. *ACS Catal.* **2013**, *3*, 1902-  
24 1907.  
25  
26 (56) Yang, W.; Hashmi, A. S. K. Mechanistic Insights into the Gold Chemistry of Allenes.  
27 *Chem. Soc. Rev.* **2014**, *43*, 2941-2955.  
28  
29 (57) Pflästerer, D.; Hashmi, A. S. K. Gold Catalysis in Total Synthesis – Recent Achievements.  
30 *Chem. Soc. Rev.* **2016**, *45*, 1331-1367.  
31  
32 (58) Arndt, S.; Rudolph, M.; Hashmi, A. S. K. Gold-Based Frustrated Lewis Acid/Base Pairs  
33 (FLPs). *Gold Bull.* **2017**, *50*, 267-282.  
34  
35 (59) Jia, M.-Q.; Bandini, M. Counterion Effects in Homogeneous Gold Catalysis. *ACS Catal.*  
36 **2015**, *5*, 1638-1652.  
37  
38 (60) Zuccaccia, D.; Del Zotto, A.; Baratta, W. The Pivotal Role of the Counterion in Gold  
39 Catalyzed Hydration and Alkoxylation of Alkynes. *Coord. Chem. Rev.* **2019**, *396*, 103-116.  
40  
41 (61) Shapiro, N. D.; Toste, F. D. Reactivity-Driven Approach to the Discovery and  
42 Development of Gold-Catalyzed Organic Reactions. *Synlett.* **2010**, 675-691.  
43  
44 (62) Krause, N.; Winter, C. Gold-Catalyzed Nucleophilic Cyclization of Functionalized  
45 Allenes: A Powerful Access to Carbo- and Heterocycles. *Chem. Rev.* **2011**, *111*, 1994-2009.  
46  
47 (63) Alcaide, B.; Almendros, P. Gold-Catalyzed Cyclization Reactions of Allenol and Alkynol  
48 Derivatives. *Acc. Chem. Res.* **2014**, *47*, 939-952.  
49  
50 (64) Dorel, R.; Echavarren, A. M. Gold(I)-Catalyzed Activation of Alkynes for the  
51 Construction of Molecular Complexity, *Chem. Rev.* **2015**, *115*, 9028-9072.  
52  
53  
54  
55  
56  
57  
58  
59  
60

- (65) Wei, F.; Song, C.-L.; Ma, Y.; Zhou, L.; Tung, C.-H.; Xu, Z.-H. Gold Carbene Chemistry from Diazo Compounds. *Sci. Bull.* **2015**, *60*, 1479-1492.
- (66) Wang, Y.; Muratore, M. E.; Echavarren, A. M. Gold Carbene or Carbenoid: Is There a Difference? *Chem. Eur. J.* **2015**, *21*, 7332-7339.
- (67) Day, D. P.; Chan, P. W. H. Gold-Catalyzed Cycloisomerizations of 1,n-Diyne Carbonates and Esters. *Adv. Synth. Catal.* **2016**, *358*, 1368-1384.
- (68) Miró, J.; del Pozo, C. Fluorine and Gold: A Fruitful Partnership. *Chem. Rev.* **2016**, *116*, 11924-11966.
- (69) Halliday, C. J. V.; Lynam, J. M. Gold-Alkynyls in Catalysis: Alkyne Activation, Gold Cumulenes and Nuclearity. *Dalton Trans.* **2016**, *45*, 12611-12626.
- (70) Quach, R.; Furkert, D. P.; Brimble, M. A. Gold Catalysis: Synthesis of Spiro, Bridged, and Fused Ketal Natural Products. *Org. Biomol. Chem.* **2017**, *15*, 3098-3104.
- (71) Visbal, R.; Graus, S.; Herrera, R. P.; Gimeno, M. C. Gold Catalyzed Multicomponent Reactions Beyond A3 Coupling. *Molecules* **2018**, *23*, 2255.
- (72) Brill, M.; Nolan, S. P. Chiral Carbophilic Gold Lewis Acid Complexes in Enantioselective Catalysis Chiral Lewis Acids. *Top. Organomet. Chem.* **2018**, *62*, 51-90.
- (73) Praveen, C. Carbophilic Activation of  $\pi$ -Systems via Gold Coordination: Towards Regioselective Access of Intermolecular Addition Products. *Coord. Chem. Rev.* **2019**, *392*, 1-34.
- (74) Marín-Luna, M.; Nieto Faza, O.; López, C. S. Gold-Catalyzed Homogeneous (Cyclo)Isomerization Reactions. *Front. Chem.* **2019**, *7*, 296.
- (75) Gagosz, F. Gold Vinylidenes as Useful Intermediates in Synthetic Organic Chemistry. *Synthesis* **2019**, *51*, 1087-1099.
- (76) Jans, A. C. H.; Caumes, X.; Reek, J. N. H. Gold Catalysis in (Supra)Molecular Cages to Control Reactivity and Selectivity. *ChemCatChem* **2019**, *11*, 287-297.
- (77) Huang, B.; Hu, M.; Toste, F. D. Homogeneous Gold Redox Chemistry: Organometallics, Catalysis and Beyond. *Trends Chem.* **2020**, *2*, 707-720.
- (78) *Chem. Rev.* **2008**, *108* (8) Themed issue: Coinage Metals in Organic Synthesis, p. 2793-3442.
- (79) Arcadi, A. Alternative Synthetic Methods through New Developments in Catalysis by Gold. *Chem. Rev.* **2008**, *108*, 3266-3325.
- (80) Li, Z.-G.; Brouwer, C.; He, C. Gold-Catalyzed Organic Transformations. *Chem. Rev.* **2008**, *108*, 3239-3265.
- (81) Jiménez-Núñez, E.; Echavarren, A. M. Gold-Catalyzed Cycloisomerizations of Enynes: A Mechanistic Perspective. *Chem. Rev.* **2008**, *108*, 3326-3350.

1  
2  
3  
4  
5  
6  
7  
8  
9  
10  
11  
12  
13  
14  
15  
16  
17  
18  
19  
20  
21  
22  
23  
24  
25  
26  
27  
28  
29  
30  
31  
32  
33  
34  
35  
36  
37  
38  
39  
40  
41  
42  
43  
44  
45  
46  
47  
48  
49  
50  
51  
52  
53  
54  
55  
56  
57  
58  
59  
60

(82) Gorin, D. J.; Sherry, B. D.; Toste, F. D. Ligand Effects in Homogeneous Au Catalysis. *Chem. Rev.* **2008**, *108*, 3351-3378.

(83) *Chem. Soc. Rev.* **2008**, *45*, 1759-2134 Themed issue: Gold: Chemistry, Materials and Catalysis.

(84) Rudolph, M.; Hashmi, A. S. K. Gold Catalysis in Total Synthesis—an Update. *Chem. Soc. Rev.* **2008**, *37*, 1766-1775.

(85) Hashmi, A. S. K. (ed.), Themed issue: Gold Catalysis: New Perspectives for Homogeneous Catalysis. *J. Organomet. Chem.* **2009**, *694* (4), 481-598.

(86) Toste, F. D. (ed). Thematic series: Gold Catalysis for Organic Synthesis. *Beilstein J. Org. Chem.* **2011**, *7*.

(87) Hashmi, A. S. K. (ed). Special issue: Homogeneous Gold Catalysis. *Isr. J. Chem.* **2013**, *53*, 841-931.

(88) *Acc. Chem. Res.* **2014**, *47* (3), Themed issue: Gold Catalysis.

(89) Hashmi, A. S. K. Dual Gold Catalysis. *Acc. Chem. Res.* **2014**, *47*, 864-876.

(90) Zhang, L. M. A Non-Diazo Approach to  $\alpha$ -Oxo Gold Carbenes via Gold-Catalyzed Alkyne Oxidation. *Acc. Chem. Res.* **2014**, *47*, 877-888.

(91) Wang, Y.-M.; Lackner, A. D.; Toste, F. D. Development of Catalysts and Ligands for Enantioselective Gold Catalysis. *Acc. Chem. Res.* **2014**, *47*, 889-901.

(92) Obradors, C.; Echavarren, A. M. Gold-Catalyzed Rearrangements and Beyond. *Acc. Chem. Res.* **2014**, *47*, 902-912.

(93) Fensterbank, L.; Malacria, M. Molecular Complexity from Polyunsaturated Substrates: The Gold Catalysis Approach. *Acc. Chem. Res.* **2014**, *47*, 953-965.

(94) *Chem. Soc. Rev.* **2016**, *45* (16), 4445-4627 Themed issue: Coinage Metals in Organic Synthesis.

(95) Zi, W.-W.; Toste, F. D. Recent Advances in Enantioselective Gold Catalysis. *Chem. Soc. Rev.* **2016**, *45*, 4567-4589.

(96) Harris, R. J.; Widenhofer, R. A. Gold Carbenes, Gold-stabilized Carbocations, and Cationic Intermediates Relevant to Gold-Catalysed Enyne Cycloaddition. *Chem. Soc. Rev.* **2016**, *45*, 4533-4551.

(97) Asiri, A. M.; Hashmi, A. S. K. Gold-Catalysed Reactions of Dienes. *Chem. Soc. Rev.* **2016**, *45*, 4471-4503.

(98) Zheng, Z.-T.; Wang, Z.-X.; Wang Y.-L.; Zhang, L.-M. Au-Catalysed Oxidative Cyclisation, *Chem. Soc. Rev.* **2016**, *45*, 4448-4458.

(99) *Adv. Synth. Catal.* **2016**, *358*, 1345-1545 Special issue: Gold Catalysis, Quo Vadis?.

1  
2  
3 (100) Echavarren, A. M.; Hashmi, A. S. K.; Toste, F. D. Gold Catalysis – Steadily Increasing  
4 in Importance. *Adv. Synth. Catal.* **2016**, *358*, 1347.

5  
6 (101) Huple, D. B.; Ghorpade, S.; Liu, R.-S. Recent Advances in Gold-Catalyzed N- and O-  
7 Functionalizations of Alkynes with Nitrones, Nitroso, Nitro and Nitroxy Species. *Adv. Synth. Catal.*  
8 **2016**, *358*, 1348-1367.

9  
10 (102) Gassman, P. G.; Meyer, G. R.; Williams, F. J. Transition Metal Complex Promoted  
11 Rearrangements. The Effect of the Metal and of the Attached Ligands on the Mode of Cleavage of  
12 Methylated Bicyclo[1.1.0]butanes. *J. Am. Chem. Soc.* **1972**, *94*, 7741-7748.

13  
14 (103) Hashmi, A. S. K.; Hutchings, G. J. Gold Catalysis, *Angew. Chem. Int. Ed.* **2006**, *45*,  
15 7896-7936.

16  
17 (104) Corma, A.; Leyva-Pérez, A.; Sabater, M. J. Gold-Catalyzed Carbon-Heteroatom Bond-  
18 Forming Reactions. *Chem. Rev.* **2011**, *111*, 1657–1712.

19  
20 (105) Hopkinson, M. N.; Gee, A. D.; Gouverneur, V. Au(I)/Au(III) Catalysis: An Alternative  
21 Approach for C–C Oxidative Coupling. *Chem. Eur. J.* **2011**, *17*, 8248-8262.

22  
23 (106) Boorman, T. C.; Larrosa, I. Gold-mediated C–H Bond Functionalization. *Chem. Soc.*  
24 *Rev.* **2011**, *40*, 1910–1925.

25  
26 (107) Garayalde, D.; Nevado, C. Gold-Containing and Gold-Generated 1,n-Dipoles as Useful  
27 Platforms toward Cycloadditions and Cyclizations. *ACS Catal.* **2012**, *2*, 1462–1479.

28 (108) Merino, E.; Nevado, C. On Gold Catalysis and Beyond. *Chimia* **2013**, *67*, 663-668.

29 (109) Ranieri, B.; Escofet, I.; Echavarren, A. M. Anatomy of Gold Catalysts: Facts and Myths.  
30 *Org. Biomol. Chem.* **2015**, *13*, 7103-7118.

31 (110) Hopkinson, M. N.; Tlahuext-Aca, A.; Glorius, F. Merging Visible Light Photoredox and  
32 Gold Catalysis. *Acc. Chem. Res.* **2016**, *49*, 2261-2272.

33 (111) Rodriguez, J.; Bourissou, D. Well-Defined Chiral Gold(III) Complexes: New  
34 Opportunities in Asymmetric Catalysis. *Angew. Chem. Int. Ed.* **2018**, *57*, 386-388.

35 (112) Hashmi, A. S. K. Homogeneous Gold Catalysis Beyond Assumptions and Proposals –  
36 Characterized Intermediates. *Angew. Chem. Int. Ed.* **2010**, *49*, 5232-5241.

37 (113) Lauterbach, T.; Asiri, A. M.; Hashmi, A. S. K. Organometallic Intermediates of Gold  
38 Catalysis. *Adv. Organomet. Chem.* **2014**, *62*, 261-297.

39 (114) Liu, L.-P.; Hammond, G. B. Recent Advances in the Isolation and Reactivity of  
40 Organogold Complexes. *Chem. Soc. Rev.* **2012**, *41*, 3129-3139.

41 (115) Joost, M.; Amgoune, A.; Bourissou, D. Reactivity of Gold Complexes towards  
42 Elementary Organometallic Reactions. *Angew. Chem. Int. Ed.* **2015**, *54*, 15022-15045.

(116) Schmidbaur, H.; Schier, A. Gold(III) Compounds for Homogeneous Catalysis: Preparation, Reaction Conditions, and Scope of Application. *Arab. J. Sci. Eng.* **2012**, *37*, 1187-1225.

(117) V. W.-W. Yam; A. S.-Y. Law. Luminescent d<sup>8</sup> Metal Complexes of Platinum(II) and Gold(III): From Photophysics to Photofunctional Materials and Probes. *Coord. Chem. Rev.* **2020**, *414*, 213298.

(118) Zhou, D.; To, W.-P.; Kwak, Y.; Cho, Y.; Cheng, G.; So G.; Tong, M.; Che, C.-M. Thermally Stable Donor–Acceptor Type (Alkynyl)Gold(III) TADF Emitters Achieved EQEs and Luminance of up to 23.4% and 70 300 cd m<sup>-2</sup> in Vacuum-Deposited OLEDs. *Adv. Sci.* **2019**, 1802297, and cited refs.

(119) Bertrand, B.; Williams, M. R. M.; Bochmann, M. Gold(III) Complexes for Antitumor Applications: An Overview. *Chem. Eur. J.* **2018**, *24*, 11840-11851, and cited refs.

(120) Ahmed, E.; Clark, R. J. H.; Tobe, M. L.; Cattalini, L. The *trans* Effect in Gold(III) Complexes. Kinetics of Substitution Reactions of the Trichloro(phenyl)aurate(III) Anion in Methanol. *J. Chem. Soc., Dalton Trans.* **1990**, 2701-2706.

(121) Jones, P. G.; Williams, A. F. Structure and Bonding in Gold(I) Compounds, Part 1. The *trans* Influence in Linear Complexes. *J. Chem. Soc., Dalton Trans.* **1977**, 1430-1434.

(122) Sokolov, A. Y.; Sizova, O. V. Quantum-Chemical Study of *trans* Influence in Gold(I) Linear Complexes. *Russ. J. Gen. Chem.* **2010**, *80*, 1223-1231.

(123) Marchione, D.; Izquierdo, M. A.; Bistoni, G.; Havenith, R. W. A.; Macchioni, A.; Zuccaccia, D.; Tarantelli, F.; Belpassi, L. <sup>13</sup>C NMR Spectroscopy of N-Heterocyclic Carbenes Can Selectively Probe σ-Donation in Gold(I) Complexes. *Chem. Eur. J.* **2017**, *23*, 2722-2728.

(124) Greif, A. H.; Hrobárik, P.; Kaupp, M. Insights into *trans*-Ligand and Spin-Orbit Effects on Electronic Structure and Ligand NMR Shifts in Transition-Metal Complexes. *Chem. Eur. J.* **2017**, *23*, 9790-9803.

(125) Moreno-Alcántar, G.; Hernández-Toledo, H.; Guevara-Vela, J. M.; Rocha-Rinza, T.; Pendás, Á. M.; Flores-Álamo, M.; Torrens, H. Stability and *trans* Influence in Fluorinated Gold(I) Coordination Compounds. *Eur. J. Inorg. Chem.* **2018**, 4413-4420.

(126) Yang, Y.; Eberle, L.; Mulks, F. F.; Wunsch, J. F.; Zimmer, M.; Rominger, F.; Rudolph, M.; Hashmi, A. S. K. *Trans* Influence of Ligands on the Oxidation of Gold(I) Complexes. *J. Am. Chem. Soc.* **2019**, *141*, 17414–17420.

(127) Bandoli, G.; Clemente, D. A.; Marangon, G.; Cattalini, L. Ground-State *trans*-Effect and Molecular Structure of Trichloro(triphenylphosphine)gold(III). *J. Chem. Soc., Dalton Trans* **1973**, 886-889.



1  
2  
3 (128) *Compounds 1 and 2*: Fan, D.; Yang, C.-T.; Ranford, J. D.; Lee, P. F.; Vittal, J. J.  
4 Chemical and Biological Studies of the Dichloro(2-phenylpyridine)gold(III) Complex and its  
5 Derivatives. *Dalton Trans.* **2003**, 2680-2685.  
6  
7

8 (129) *Compound 3*: Venugopal, A.; Shaw, A. P.; Törnroos, K. W.; Heyn, R. H.; Tilset, M.  
9 Synthesis of a Coordinatively Labile Gold(III) Methyl Complex. *Organometallics* **2011**, *30*, 3250-  
10 3253.  
11  
12

13 (130) *Compound 4*: Smith, D. A.; Roşca, D.-A.; Bochmann, M. Selective Au–C Cleavage in  
14 (C<sup>N</sup>C)Au(III) Aryl and Alkyl Pincer Complexes. *Organometallics* **2012**, *31*, 5998-6000.  
15  
16

17 (131) *Compound 5*: Bachmann, M.; Blacque, O.; Venkatesan, K. Harnessing White-Light  
18 Luminescence via Tunable Singlet-and Triplet-Derived Emissions Based on Gold (III) Complexes.  
19 *Chem. Eur. J.* **2017**, *23*, 9451-9456.  
20  
21

22 (132) Langseth, E.; Nova, A.; Tråseth, E. A.; Rise, F.; Øien, S.; Heyn, R. H.; Tilset, M. A Gold  
23 Exchange: A Mechanistic Study of a Reversible, Formal Ethylene Insertion into a Gold (III)–  
24 Oxygen Bond. *J. Am. Chem. Soc.* **2014**, *136*, 10104-10115.  
25  
26

27 (133) Holmsen, M. S. M.; Nova, A.; Balcells, D.; Langseth, E.; Øien-Ødegaard, S.; Tråseth, E.  
28 A.; Heyn, R. H.; Tilset, M. Small-Molecule Activation at Au (III): Metallacycle Construction from  
29 Ethylene, Water, and Acetonitrile. *Dalton Trans.* **2016**, *45*, 14719–14724.  
30  
31

32 (134) Balcells, D.; Eisenstein, O.; Tilset, M.; Nova, A. Coordination and Insertion of Alkenes  
33 and Alkynes in Au<sup>III</sup> Complexes: Nature of the Intermediates from a Computational Perspective.  
34 *Dalton Trans.* **2016**, *45*, 5504-5513.  
35  
36

37 (135) Holmsen, M. S. M.; Nova, A.; Balcells, D.; Langseth, E.; ØienØdegaard, S.; Heyn, R. H.;  
38 Tilset, M.; Laurenczy, G. *Trans*-Mutation at Gold(III): A Mechanistic Study of a Catalytic  
39 Acetylene Functionalization via a Double Insertion Pathway. *ACS Catal.* **2017**, *7*, 5023-5034.  
40  
41

42 (136) Chambrier, I.; Hughes, D. L.; Jeans, R. J.; Welch, A. J.; Budzelaar, P. H. M.; Bochmann,  
43 M. Do Gold(III) Complexes Form Hydrogen Bonds? An Exploration of Au<sup>III</sup> Dicarboranyl  
44 Chemistry. *Chem. Eur. J.* **2020**, *26*, 939-947.  
45  
46

47 (137) Chambrier, I.; Rocchigiani, L.; Hughes, D. L.; Budzelaar, P. M. H.; Bochmann, M.  
48 Thermally Stable Gold(III) Alkene and Alkyne Complexes: Synthesis, Structures, and Assessment  
49 of the *trans*-Influence on Gold-Ligand Bond Enthalpies. *Chem. Eur. J.* **2018**, *24*, 11467-11474.  
50  
51

52 (138) Roşca, D.-A.; Fernandez-Cestau, J.; Morris, J.; Wright, J. A.; Bochmann, M. Gold(III)-  
53 CO and Gold(III)-CO<sub>2</sub> Complexes and Their Role in the Water-Gas Shift Reaction. *Sci. Adv.* **2015**,  
54 *1*, e1500761.  
55  
56  
57  
58  
59  
60

(139) Grünert, W.; Großmann, D.; Noei, H.; Pohl, M.-M.; Sinev, I.; De Toni, A.; Wang, Y.; Muhler, M. Low-Temperature Oxidation of Carbon Monoxide with Gold(III) Ions Supported on Titanium Oxide. *Angew. Chem. Int. Ed.* **2014**, *53*, 3245-3249.

(140) Willner, H.; Schaebs, J.; Hwang, G.; Mistry, F.; Jones, R.; Trotter, J.; Aubke, F. Bis(carbonyl)gold(I) Undecafluorodiantimonate(V), [Au(CO)<sub>2</sub>][Sb<sub>2</sub>F<sub>11</sub>]: Synthesis, Vibrational, and Carbon-13 NMR Study and the Molecular Structure of Bis(acetonitrile)gold(I) Hexafluoroantimonate(V), [Au(NCCH<sub>3</sub>)<sub>2</sub>][SbF<sub>6</sub>]. *J. Am. Chem. Soc.* **1992**, *114*, 8972–8980.

(141) Lai, S.-W.; Lam, H.-W.; Lu, W.; Cheung, K.-K.; Che, C.-M. Observation of Low-Energy Metal–Metal-to-Ligand Charge Transfer Absorption and Emission: Electronic Spectroscopy of Cyclometalated Platinum(II) Complexes with Isocyanide Ligands. *Organometallics* **2002**, *21*, 226-234.

(142) For (C<sup>N</sup>C)Pt-CO complexes see: Cave, G. W. V.; Fanizzi, F. P.; Deeth, R. J.; Errington, W.; Rourke, J. P. C-H Activation Induced by Water. Monocyclometalated to Dicyclopentametallated: C<sup>N</sup>C Tridentate Platinum Complexes. *Organometallics* **2000**, *19*, 1355-1364.

(143) See ref. 136. Geometry optimization at PCM(C1Bz)/B3LYP/SVP, then single point calculations at PCM(C1Bz)/TPSSH/cc-pVTZ+DFTD3 gave, after scaling for free CO = 2143 cm<sup>-1</sup>, [(C<sup>N</sup>C)AuCO]<sup>+</sup> 2174 cm<sup>-1</sup> and [(C<sup>N</sup>N)PtCO]<sup>+</sup> 2087 cm<sup>-1</sup>.

(144) Gaggioli, C. A.; Belpassi, L.; Tarantelli, F.; Belanzoni, P. The Gold(III)–CO Bond: a Missing Piece in the Gold Carbonyl Complex Landscape. *Chem. Commun.* **2017**, *53*, 1603-1606.

(145) Sorbelli, D.; Belpassi, L.; Tarantelli, F.; Belanzoni, P. Ligand Effect on Bonding in Gold(III) Carbonyl Complexes. *Inorg. Chem.* **2018**, *57*, 6161-6175.

(146) Schmidbaur, H.; Schier, A. Gold η<sup>2</sup>-Coordination to Unsaturated and Aromatic Hydrocarbons: The Key Step in Gold-Catalyzed Organic Transformations. *Organometallics* **2010**, *29*, 2–23.

(147) Zeise, W. C. Eine Besondere Platinverbindung. *Pogg. Ann. Phys. Chem.* **1827**, *9*, 632.

(148) Zeise, W. C. Von der Wirkung zwischen Platinchlorid und Alcohol, und den dabei Entstehenden Neuen Substanzen. *Pogg. Ann. Phys. Chem.* **1831**, *21*, 497-541.

(149) Zeise, W. C. Gekohlenwasserstofftes Chlorplatin-Ammoniak. *Pogg. Ann. Phys. Chem.* **1831**, *21*, 542-549.

(150) Blons, C.; Amgoune, A.; Bourissou, D. Gold(III) π Complexes. *Dalton Trans.* **2018**, *47*, 10388–10393.

(151) Savjani, N.; Roşca, D.-A.; Schormann, M.; Bochmann, M. Gold(III) Olefin Complexes. *Angew. Chem. Int. Ed.* **2013**, *52*, 874–877.

1  
2  
3 (152) For a recent discussion of structure and bonding in gold(I) alkene complexes see:  
4 Navarro, M.; Toledo, A.; Mallet-Ladeira, S.; Sosa Carrizo, E. D.; Miqueu, K.; Bourissou, D.  
5 Versatility and Adaptive Behaviour of the P<sup>N</sup> Chelating Ligand MeDalpos Within Gold(I)  $\pi$ -  
6 Complexes. *Chem. Sci.* **2020**, *11*, 2750-2758.  
7  
8

9  
10 (153) Navarro, M.; Toledo, A.; Joost, M.; Amgoune, A.; Mallet-Ladeira, S.; Bourissou, D.  $\pi$ -  
11 Complexes of P<sup>P</sup> and P<sup>N</sup> Chelated Gold(I). *Chem. Commun.* **2019**, *55*, 7974-7977.  
12

13 (154) Rekhroukh, F.; Estevez, L.; Bijani, C.; Miqueu, K.; Amgoune, A.; Bourissou, D.  
14 Coordination–Insertion of Norbornene at Gold: A Mechanistic Study. *Organometallics* **2016**, *35*,  
15 995–1001.  
16  
17

18 (155) Langseth, E.; Scheuermann, M. L.; Balcells, D.; Kaminsky, W.; Goldberg, K. I.;  
19 Eisenstein, O.; Heyn, R. H.; Tilset, M. Generation and Structural Characterization of a Gold(III)  
20 Alkene Complex. *Angew. Chem. Int. Ed.* **2013**, *52*, 1660–1663.  
21  
22

23 (156) Alyabyev, S. B.; Beletskaya, I. P. Gold as a Catalyst. Part II. Alkynes in the Reactions of  
24 Carbon-Carbon Bond Formation. *Russ. Chem. Rev.* **2018**, *87*, 984-1047.  
25  
26

27 (157) Chatt, J.; Duncanson, L. A.; Guy, R. G. Structure of  $\alpha$ -Hydroxyacetylene Complexes of  
28 Platinum(II). *Nature* **1959**, *184*, 526-527.  
29

30 (158) Brown, T. J.; Widenhoefer, R. A. Synthesis and Equilibrium Binding Studies of Cationic,  
31 Two-Coordinate Gold(I)  $\pi$ -Alkyne Complexes. *J. Organomet. Chem.* **2011**, *696*, 1216-1220.  
32  
33

34 (159) Casado, R.; Contel, M.; Laguna, M.; Romero, P.; Sanz, S. Organometallic Gold(III)  
35 Compounds as Catalysts for the Addition of Water and Methanol to Terminal Alkynes. *J. Am.*  
36 *Chem. Soc.* **2003**, *125*, 11925-11935.  
37  
38

39 (160) Rocchigiani, L.; Fernandez-Cestau, J.; Agonigi, G.; Chambrier, I.; Budzelaar, P. H. M.;  
40 Bochmann, M. Gold(III) Alkyne Complexes: Bonding and Reaction Pathways. *Angew. Chem. Int.*  
41 *Ed.* **2017**, *56*, 13861-13865.  
42  
43

44 (161) Zuccaccia, D.; Belpassi, L.; Rocchigiani, L.; Tarantelli, F.; Macchioni, A. A Phosphine  
45 Gold(I)  $\pi$ -Alkyne Complex: Tuning the Metal-Alkyne Bond Character and Counterion Position by  
46 the Choice of the Ancillary Ligand. *Inorg. Chem.* **2010**, *49*, 3080-3082.  
47  
48

49 (162) Hooper, T. N.; Green, M.; Russell, C. A. Cationic Au(I) Alkyne Complexes: Synthesis,  
50 Structure and Reactivity. *Chem. Commun.* **2010**, *46*, 2313-2315.  
51  
52

53 (163) Gregori, L.; Sorbelli, D.; Belpassi, L.; Tarantelli, F.; Belanzoni, P. Alkyne Activation  
54 with Gold(III) Complexes: A Quantitative Assessment of the Ligand Effect by Charge-  
55 Displacement Analysis. *Inorg. Chem.* **2019**, *58*, 3115-3129.  
56  
57  
58  
59  
60

1  
2  
3 (164) Pernpointner, M.; Hashmi, A. S. K. Fully Relativistic, Comparative Investigation of Gold  
4 and Platinum Alkyne Complexes of Relevance for the Catalysis of Nucleophilic Additions to  
5 Alkynes. *J. Chem. Theory Comput.* **2009**, *5*, 2717-2725.

6  
7  
8 (165) Kharasch, M. S.; Isbell, H. S. The Chemistry of Organic Gold Compounds. III. Direct  
9 Introduction of Gold into the Aromatic Nucleus. *J. Am. Chem. Soc.* **1931**, *53*, 3053-3059.

10  
11 (166) Fuchita, Y.; Utsunomiya, Y.; Yasutake, M. Synthesis and Reactivity of Arylgold(III)  
12 Complexes from Aromatic Hydrocarbons via C–H Bond Activation. *J. Chem. Soc., Dalton Trans.*  
13 **2001**, 2330-2334.

14  
15  
16 (167) Corrie, T. J. A.; Ball, L. T.; Russell C. A.; Lloyd-Jones, G. C. Au-Catalyzed Biaryl  
17 Coupling To Generate 5- to 9-Membered Rings: Turnover-Limiting Reductive Elimination versus  
18  $\pi$ -Complexation. *J. Am. Chem. Soc.* **2017**, *139*, 245-254.

19  
20 (168) Ghosh, M. K.; Tilset, M.; Venugopal, A.; Heyn, R. H.; Swang, O. Ping-Pong at Gold:  
21 Proton Jump Between Coordinated Phenyl and  $\eta^1$ -Benzene Ligands, A Computational Study. *J.*  
22 *Phys. Chem. A* **2010**, *114*, 8135–8141.

23  
24 (169) Rekhroukh, F.; Blons, C.; Estévez, L.; Mallet-Ladeira, S.; Miqueu, K.; Amgoune, A.;  
25 Bourissou, D. Gold(III)–Arene Complexes by Insertion of Olefins into Gold–Aryl Bonds. *Chem.*  
26 *Sci.* **2017**, *8*, 4539-4545.

27  
28 (170) Rocchigiani, L.; Fernandez-Cestau, J.; Budzelaar, P. H. M.; Bochmann, M. Arene C–H  
29 Activation by Gold(III): Solvent-Enabled Proton Shuttling, and Observation of a Pre-Metallation  
30 Au–Arene Intermediate. *Chem. Commun.* **2017**, *53*, 4358-4361.

31  
32 (171) Garcia-Cuadrado, D.; de Mendoza, P.; Braga, A. A. C.; Maseras, F.; Echavarren, A. M.  
33 Proton-Abstraction Mechanism in the Palladium-Catalyzed Intramolecular Arylation: Substituent  
34 Effects. *J. Am. Chem. Soc.* **2007**, *129*, 6880-6886.

35  
36 (172) Sanshiro, K.; Satoshi, O. Isolation of the First Allylic Gold(III) Complex Having a  
37 Triphenylphosphine Ligand. *Chem. Lett.* **1988**, *17*, 1431–1432.

38  
39 (173) Takuo, S.; Satoshi, O.; Noriko, K. C.; Atsushi, F.; Sanshiro, K. Synthesis, Structure, and  
40 Reactivities of *cis*-Dimethyl( $\eta^1$ -allyl)gold(III) Complex. Diastereoselective Allylation of Aromatic  
41 Aldehyde. *Bull. Chem. Soc. Jpn.* **1995**, *68*, 1523-1533.

42  
43 (174) Levin, M. D.; Chen, T. Q.; Neubig, M. E.; Hong, C. M.; Theulier, C. A.; Kobylanski, I.  
44 J.; Janabi, M.; O’Neil, J. P.; Toste, F. D. A Catalytic Fluoride-Rebound Mechanism for C(sp<sup>3</sup>)-CF<sub>3</sub>  
45 Bond Formation. *Science* **2017**, *356*, 1272–1276.

46  
47 (175) Rodriguez, J.; Szallki, G.; Sosa Carrizo, E. D.; Saffon-Merceron, N.; Miqueu, K.;  
48 Bourissou, D. Gold(III)  $\pi$ -Allyl Complexes. *Angew. Chem. Int. Ed.* **2020**, *59*, 1511-1515.

- (176) Martinsen Holmsen, M. S.; Nova, A.; Øien-Ødegaard, S.; Heyn, R. H.; Tilset, M. A. Highly Asymmetric Gold(III)  $\eta^3$ -Allyl Complex. *Angew. Chem. Int. Ed.* **2020**, *59*, 1516-1520.
- (177) Johnson, A.; Laguna, A.; Gimeno, M. C. Axially Chiral Allenyl Gold Complexes. *J. Am. Chem. Soc.* **2014**, *136*, 12812-12815.
- (178) Schmidbaur, H.; Raubenheimer, H. G.; Dobrzańska, L. The Gold–Hydrogen Bond, Au–H, and the Hydrogen Bond to Gold, Au $\cdots$ H–X. *Chem. Soc. Rev.* **2014**, *43*, 345-380.
- (179) Wang, X. F.; Andrews, L. Gold Hydrides AuH and (H<sub>2</sub>)AuH and the AuH<sub>3</sub> Transition State Stabilized in (H<sub>2</sub>)AuH<sub>3</sub>: Infrared Spectra and DFT Calculations. *J. Am. Chem. Soc.* **2001**, *123*, 12899-12900.
- (180) Wang, X. F.; Andrews, L. Infrared Spectra and DFT Calculations for the Gold Hydrides AuH, (H<sub>2</sub>)AuH, and the AuH<sub>3</sub> Transition State Stabilized in (H<sub>2</sub>)AuH<sub>3</sub>. *J. Phys. Chem. A* **2002**, *106*, 3744-3748.
- (181) Andrews, L.; Wang, X. F. Infrared Spectra and Structures of the Stable CuH<sub>2</sub><sup>-</sup>, AgH<sub>2</sub><sup>-</sup>, AuH<sub>2</sub><sup>-</sup>, and AuH<sub>4</sub><sup>-</sup> Anions and the AuH<sub>2</sub> Molecule. *J. Am. Chem. Soc.* **2003**, *125*, 11751-11760.
- (182) Wang, X. F.; Andrews, L.; Manceron, L.; Marsden, C. Infrared Spectra and DFT Calculations for the Coinage Metal Hydrides MH, (H<sub>2</sub>)MH, MH<sub>2</sub>, M<sub>2</sub>H, M<sub>2</sub>H<sup>-</sup>, and (H<sub>2</sub>)CuHCu in Solid Argon, Neon, and Hydrogen. *J. Phys. Chem. A*, **2003**, *107*, 8492-8505.
- (183) Wang, X. F.; Andrews, L. Gold Is Noble but Gold Hydride Anions Are Stable. *Angew. Chem. Int. Ed.* **2003**, *42*, 5201-5206.
- (184) Andrews, L.; Wang, X. F.; Manceron, L.; Balasubramanian, K. The Gold Dihydride Molecule, AuH<sub>2</sub>: Calculations of Structure, Stability, and Frequencies, and the Infrared Spectrum in Solid Hydrogen. *J. Phys. Chem. A*, **2004**, *108*, 2936-2940.
- (185) Khairallah, N.; O’Hair, R. A. J.; Bruce, M. I. Gas-phase Synthesis and Reactivity of Binuclear Gold Hydride Cations, (R<sub>3</sub>PAu)<sub>2</sub>H<sup>+</sup> (R = Me and Ph). *Dalton Trans.* **2006**, 3699-3707.
- (186) Comas-Vives, A.; González-Arellano, C.; Corma, A.; Iglesias, M.; Sánchez, F.; Ujaque, G. Single-Site Homogeneous and Heterogenized Gold(III) Hydrogenation Catalysts: Mechanistic Implications. *J. Am. Chem. Soc.* **2006**, *128*, 4756-4765.
- (187) Alcaide, B.; Almendros, P.; Martínez del Campo, T.; Fernández, I. Fascinating Reactivity in Gold Catalysis: Synthesis of Oxetenes through Rare 4-*exo-dig* Allene Cyclization and Infrequent  $\beta$ -Hydride Elimination. *Chem. Commun.* **2011**, *47*, 9054-9056.
- (188) Xie, J.; Li, H.; Zhou, J.; Cheng, Y.; Zhu, C. A Highly Efficient Gold-Catalyzed Oxidative C-C Coupling from C-H Bonds using Air as Oxidant. *Angew. Chem. Int. Ed. Engl.* **2012**, *51*, 1252-1255.

- 1  
2  
3 (189) Tsui, E. Y.; Müller, P.; Sadighi, J. P. Reactions of a Stable Monomeric Gold(I) Hydride  
4 Complex. *Angew. Chem. Int. Ed.* **2008**, *47*, 8937-8940.
- 5  
6 (190) Roşca, D.-A.; Smith, D. A.; Hughes, D. L.; Bochmann, M. A Thermally Stable Gold(III)  
7 Hydride: Synthesis, Reactivity, and Reductive Condensation as a Route to Au<sup>II</sup> Complexes. *Angew.*  
8 *Chem. Int. Ed.* **2012**, *51*, 10643-10646.
- 9  
10 (191) Hashmi, A. S. K. Fire and Ice: A Gold(III) Monohydride. *Angew. Chem. Int. Ed.* **2012**,  
11 *51*, 12935-12936.
- 12  
13 (192) Pintus, A.; Rocchigiani, L.; Fernandez-Cestau, J.; Budzelaar, P. H. M.; Bochmann, M.  
14 Stereo- and Regioselective Alkyne Hydrometallation with Gold(III) Hydrides. *Angew. Chem. Int.*  
15 *Ed.* **2016**, *55*, 12321-12324.
- 16  
17 (193) Roşca, D.-A.; Fernandez-Cestau, J.; Hughes, D. L.; Bochmann, M. Reactivity of Gold  
18 Hydrides: O<sub>2</sub> Insertion into the Au-H Bond. *Organometallics* **2015**, *34*, 2098-2101.
- 19  
20 (194) Roşca, D.-A.; Bochmann, M. Photochemical Disproportionation of an Au<sup>II</sup> Pincer  
21 Complex: Synthesis and Structure of an Au<sup>I</sup><sub>4</sub>Au<sup>III</sup><sub>4</sub> Macrocycle. *Organometallics* **2016**, *35*, 27-31.
- 22  
23 (195) Dann, T.; Roşca, D.-A.; Wildgoose, G. G.; Wright, J. A.; Bochmann, M.  
24 Electrochemistry of Au<sup>II</sup> and Au<sup>III</sup> Pincer Complexes: Determination of the Au<sup>II</sup>-Au<sup>II</sup> Bond Energy.  
25 *Chem. Commun.* **2013**, *49*, 10169-10171.
- 26  
27 (196) Roşca, D.-A.; Wright, J. A.; Hughes, D. L.; Bochmann, M. Gold Peroxide Complexes  
28 and the Conversion of Hydroperoxides into Gold Hydrides by Successive Oxygen-Transfer  
29 Reactions. *Nat. Commun.* **2013**, *4*, 2167.
- 30  
31 (197) Chambrier, I.; Roşca, D.-A.; Fernandez-Cestau, J.; Hughes, D. L.; Budzelaar, P. H. M.;  
32 Bochmann, M. Formation of Gold(III) Alkyls from Gold Alkoxide Complexes. *Organometallics*  
33 **2017**, *36*, 1358-1364.
- 34  
35 (198) Fernandez-Cestau, J.; Bertrand, B.; Pintus, A.; Bochmann, M. Synthesis, Structures, and  
36 Properties of Luminescent (C<sup>N</sup>C)gold(III) Alkyl Complexes: Correlation between Photoemission  
37 Energies and C-H Acidity. *Organometallics* **2017**, *36*, 3304-3312.
- 38  
39 (199) Luo, H.; Cao, B.; Chan, A. S. C.; Sun, R. W.-Y.; Zou, T. Cyclometalated Gold(III)-  
40 Hydride Complexes Exhibit Visible Light-Induced Thiol Reactivity and Act as Potent Photo-  
41 Activated Anti-Cancer Agents. *Angew. Chem. Int. Ed.* **2020**, *59*, 11046-11052.
- 42  
43 (200) Kleinhans, G.; Hansmann, M. M.; Guisado-Barrios, G.; Liles, D. C.; Bertrand, G.;  
44 Bezuidenhout, D. I. Nucleophilic T-Shaped (LXL)Au(I)-Pincer Complexes: Protonation and  
45 Alkylation. *J. Am. Chem. Soc.* **2016**, *138*, 15873-15876.
- 46  
47 (201) Rocchigiani, L.; Fernandez-Cestau, J.; Chambrier, I.; Hrobarik, P.; Bochmann, M.  
48 Unlocking Structural Diversity in Gold(III) Hydrides: Unexpected Interplay of *cis* / *trans*-Influence  
49  
50  
51  
52  
53  
54  
55  
56  
57  
58  
59  
60

1  
2  
3 on Stability, Insertion Chemistry and NMR Chemical Shifts. *J. Am. Chem. Soc.* **2018**, *140*, 8287-  
4 8302.

5  
6 (202) Kumar, R.; Krieger, J.-P.; Gómez-Bengoa, E.; Fox, T.; Linden, A.; Nevado, C. The First  
7 Gold(III) Formate: Evidence for  $\beta$ -Hydride Elimination. *Angew. Chem. Int. Ed.* **2017**, *56*, 12862-  
8 12865.

9  
10 (203) Nijamudheen, A.; Karmakar, S.; Datta, A. Understanding the Mechanisms of Unusually  
11 Fast H-H, C-H, and C-C Bond Reductive Eliminations from Gold(III) Complexes. *Chem. Eur. J.*  
12 **2014**, *20*, 14650-14658.

13  
14 (204) Boronat, M.; Leyva-Pérez, A.; Corma, A. Theoretical and Experimental Insights into the  
15 Origin of the Catalytic Activity of Subnanometric Gold Clusters: Attempts to Predict Reactivity  
16 with Clusters and Nanoparticles of Gold. *Acc. Chem. Res.* **2014**, *47*, 834-844.

17  
18 (205) Pan, M.; Brush, A. J.; Pozun, Z. D.; Ham, H. C.; Yu, W.-Y.; Henkelman, G.; Hwang, G.  
19 S.; Mullins, C. B. Model Studies of Heterogeneous Catalytic Hydrogenation Reactions with Gold.  
20 *Chem. Soc. Rev.* **2013**, *42*, 5002-5013.

21  
22 (206) Malta, G.; Kondrat, S. A.; Freakley, S. J.; Davies, C. J.; Lu, L.; Dawson, S.; Thetford, A.;  
23 Gibson, E. K.; Morgan, D. J.; Jones, W.; Wells, P. P.; Johnston, P.; Catlow, C. R. A.; Kiely, C. J.;  
24 Hutchings, G. J. Identification of Single-Site Gold Catalysis in Acetylene Hydrochlorination.  
25 *Science* **2017**, *355*, 1399-1403.

26  
27 (207) Klatt, G.; Xu, R.; Pernpointner, M.; Molinari, L.; Hung, T. Q.; Rominger, F.; Hashmi, A.  
28 S. K.; Köppel, H. Are  $\beta$ -H-Eliminations or Alkene Insertions Feasible Elementary Steps in  
29 Catalytic Cycles Involving Gold(I) Alkyl Species or Gold(I) Hydrides? *Chem. Eur. J.* **2013**, *19*,  
30 3954-3961.

31  
32 (208) Pope, W. J.; Gibson, C. S. The Alkyl Compounds of Gold. *J. Chem. Soc.* **1907**, *91*, 2061-  
33 2066.

34  
35 (209) Gibson, C. S.; Simonsen, J. L. The Organic Compounds of Gold. Part I. Diethylgold  
36 Bromide and Some Derivatives. *J. Chem. Soc.* **1930**, 2531-2536.

37  
38 (210) Castiñeira Reis, M.; López, C. S.; Kraka, E.; Cremer, D.; Faza, O. N. Rational Design in  
39 Catalysis: A Mechanistic Study of  $\beta$ -Hydride Eliminations in Gold(I) and Gold(III) Complexes  
40 Based on Features of the Reaction Valley. *Inorg. Chem.* **2016**, *55*, 8636-8645.

41  
42 (211) Kraus, F.; Schmidbaur, H.; Al-Juaid, S. S. Tracing Hydrogen Bonding Au $\cdots$ H-C at Gold  
43 Atoms: A Case Study. *Inorg. Chem.* **2013**, *52*, 9669-9674.

44  
45 (212) Rekhroukh, F.; Estévez, L.; Bijani, C.; Miqueu, K.; Amgoune, A.; Bourissou, D.  
46 Experimental and Theoretical Evidence for an Agostic Interaction in a Gold(III) Complex. *Angew.*  
47 *Chem. Int. Ed.* **2016**, *55*, 3414-3418.

(213) Rocchigiani, L.; Budzelaar, P. H. M.; Bochmann, M. Heterolytic Bond Activation at Gold: Evidence for Gold(III) H-B, H-Si Complexes, H-H and H-C Cleavage. *Chem. Sci.* **2019**, *10*, 2633-2642.

(214) Joost, M.; Mallet-Ladeira, S.; Miqueu, K.; Amgoune, A.; Bourissou, D.  $\sigma$ -SiH Complexes of Copper: Experimental Evidence and Computational Analysis. *Organometallics* **2013**, *32*, 898-902.

(215) Martinho Simões, J. A.; Beauchamp, J. L. Transition Metal-Hydrogen and Metal-Carbon Bond Strengths: The Keys to Catalysis. *Chem. Rev.* **1990**, *90*, 629-688.

(216) Rocchigiani, L.; Klooster, W. T.; Coles, S. J.; Hughes, D. L.; Hrobárik, P.; Bochmann, M. Hydride Transfer to Gold: Yes or No? Exploring the Unexpected Versatility of Au $\cdots$ H-M Bonding in Heterobimetallic Dihydrides. *Chem. Eur. J.* **2020**, *26*, 8267-8280.

(217) Groenewald, F.; Dillen, J.; Raubenheimer, H. G.; Esterhuysen, C. Preparing Gold(I) for Interactions with Proton Donors: The Elusive [Au] $\cdots$ HO Hydrogen Bond. *Angew. Chem. Int. Ed.* **2016**, *55*, 1694-1698.

(218) Groenewald, F.; Raubenheimer, H. G.; Dillen, J.; Esterhuysen, C. Gold Setting the “Gold Standard” among Transition Metals as a Hydrogen Bond Acceptor – A Theoretical Investigation. *Dalton Trans.* **2017**, *46*, 4960-4967.

(219) Berger, R. J. F.; Schoiber, J.; Monkowius, U. A Relativity Enhanced, Medium-Strong Au(I) $\cdots$ H-N Hydrogen Bond in a Protonated Phenylpyridine-Gold(I) Thiolate. *Inorg. Chem.* **2017**, *56*, 956-961.

(220) Rigoulet, M.; Massou, S.; Sosa Carrizo, E. D.; Mallet-Ladeira, S.; Amgoune, A.; Miqueu, K.; Bourissou, D. Evidence for Genuine Hydrogen Bonding in Gold(I) Complexes. *Proc. Natl. Acad. Sci. USA* **2019**, *116*, 46-51.

(221) Straka, M.; Andris, E.; Vícha, J.; Růžička, A.; Roithová, J.; Rulíšek, L. Spectroscopic and Computational Evidence of Intramolecular Au<sup>I</sup> $\cdots$ H<sup>+</sup>-N Hydrogen Bonding. *Angew. Chem. Int. Ed.* **2019**, *58*, 2011-2016.

(222) Schmidbaur, H. Proof of Concept for Hydrogen Bonding to Gold, Au $\cdots$ H-X. *Angew. Chem. Int. Ed.* **2019**, *58*, 5806– 5809.

(223) Brammer, L. Metals and Hydrogen Bonds. *Dalton Trans.* **2003**, 3145-3157.

(224) Riddlestone, I. M.; Kraft, A.; Schaefer, J.; Krossing, I. Taming the Cationic Beast: Novel Developments in the Synthesis and Application of Weakly Coordinating Anions. *Angew. Chem. Int. Ed.* **2018**, *57*, 13982-14024.

(225) Bochmann, M. The Chemistry of Catalyst Activation: The Case of Group 4 Polymerization Catalysts. *Organometallics* **2010**, *29*, 4711-4740.



(226) Chen, E. Y.-X.; Marks, T. J. Cocatalysts for Metal-Catalyzed Olefin Polymerization: Activators, Activation Processes, and Structure-Activity Relationships. *Chem. Rev.* **2000**, *100*, 1391-1434.

(227) Macchioni, A. Ion Pairing in Transition-Metal Organometallic Chemistry. *Chem Rev.* **2005**, *105*, 6, 2039–2074.

(228) Schiebl, J.; Schulmeister, J.; Doppiu, A.; Wörner, E.; Rudolph, M.; Karch, R.; Hashmi, A. S. K. An Industrial Perspective on Counter Anions in Gold Catalysis: Underestimated with Respect to “Ligand Effects”. *Adv. Synth. Catal.* **2018**, *360*, 2493-2502.

(229) Schiebl, J.; Schulmeister, J.; Doppiu, A.; Wörner, E.; Rudolph, M.; Karch, R.; Hashmi, A. S. K. An Industrial Perspective on Counter Anions in Gold Catalysis: On Alternative Counter Anions. *Adv. Synth. Catal.* **2018**, *360*, 3949-3959.

(230) Roesky, H. W.; Singh, S.; Yusuff, K. K. M.; Maguire, J. A.; Hosmane, N. S. Organometallic Hydroxides of Transition Elements. *Chem. Rev.* **2006**, *106*, 3813-3843.

(231) Harris, S. J.; Tobias, R. S. Inorganic Condensation Reactions. The Hydrolysis of Dimethylgold(III) and the Growth of Tetrakis(dimethylgold hydroxide). *Inorg. Chem.* **1969**, *8*, 2259-2264.

(232) Vicente, J.; Bermúdez, M. D.; Carrión, F. J.; Jones, P. G. Synthesis of some  $\mu$ -Hydroxo, Phenoxo and O,O-Acetylacetonato-Arylgold(III) Complexes. Crystal Structure of  $[\text{Au}(\text{C}_6\text{H}_4\text{NO}_2-2)_2(\mu\text{-OH})_2 \cdot 2\text{Et}_2\text{O}]$ . *J. Organomet. Chem.* **1996**, *508*, 53-57.

(233) Cinellu, M. A.; Minghetti, G.; Pinna, M. V.; Stoccoro, S.; Zucca, A.; Manassero, M. Gold(III) Derivatives with Anionic Oxygen Ligands: Mononuclear Hydroxo, Alkoxo and Acetato Complexes. Crystal Structure of  $[\text{Au}(\text{bpy})(\text{OMe})_2][\text{PF}_6]$ . *J. Chem. Soc., Dalton Trans.* **2000**, 1261-1265.

(234) Corbo, R.; Ryan, G. F.; Haghghatbin, M. A.; Hogan, C. F.; Wilson, D. J. D.; Hulett, M.D.; Barnard, P. J.; Dutton, J. L. Access to the Parent Tetrakis(pyridine)gold(III) Trication, Facile Formation of Rare Au(III) Terminal Hydroxides, and Preliminary Studies of Biological Properties. *Inorg. Chem.* **2016**, *55*, 2830-2839.

(235) Corbo, R.; Albayer, M.; Hall, N. B.; Dutton, J. L. Direct Formation of Au(III) Acetyl, Alkoxyl and Alkynyl Functionalities via Halide Free Tricationic Au(III) Precursors. *Dalton Trans.* **2018**, *47*, 4228-4235.

(236) Roşca, D.-A.; Smith, D. A.; Bochmann, M. Cyclometallated Gold(III) Hydroxides as Versatile Synthons for Au–N, Au–C Complexes and Luminescent Compounds. *Chem. Commun.* **2012**, *48*, 7247-7249.

1  
2  
3 (237) Roşca, D.-A. Synthesis and Reactivity of Gold(III) Complexes with Pincer Ligands.  
4 Ph.D. Thesis, University of East Anglia, February 2014.

5  
6 (238) Wong, K.-H.; Cheung, K.-K.; Chan, M. C.-W.; Che, C.-M. Application of 2,6-  
7 Diphenylpyridine as a Tridentate [C<sup>N</sup>C] Dianionic Ligand in Organogold(III) Chemistry.  
8 Structural and Spectroscopic Properties of Mono- and Binuclear Transmetalated Gold(III)  
9 Complexes. *Organometallics* **1998**, *17*, 3505-3511.

10  
11 (239) For an alternative synthesis see: Eppel, D.; Rudolph, M.; Rominger, F.; Hashmi, A. S. K.  
12 Mercury-Free Synthesis of Pincer [C<sup>N</sup>C]Au<sup>III</sup> Complexes by an Oxidative Addition/CH  
13 Activation Cascade. *ChemSusChem* **2020**, *13*, 1986-1990.

14  
15 (240) Hofer, M.; Gomez-Bengoa, E.; Nevado, C. A Neutral Gold(III)-Boron Transmetalation.  
16 *Organometallics* **2014**, *33*, 1328-1332.

17  
18 (241) Maity, A.; Sulicz, A. N.; Deligonul, N.; Zeller, M.; Hunter, A. D.; Gray, T. G. Suzuki-  
19 Miyaura Coupling of Arylboronic Acids to Gold(III). *Chem. Sci.* **2015**, *6*, 981-986.

20  
21 (242) Browne, A. R.; Deligonul, N.; Anderson, B. L.; Zeller, M.; Hunter, A. D.; Gray, T. G.  
22 Cyclometalated (boroxinato)gold(III) Complexes from Arrested Transmetalation. *Chem. Commun.*  
23 **2015**, *51*, 15800-15803.

24  
25 (243) Ayoub, N. A.; Browne, A. R.; Anderson, B. L.; Gray, T. G. Cyclometalated Gold(III)  
26 Trioxadiborin Complexes: Studies of the Bonding and Excited States. *Dalton Trans.* **2016**, *45*,  
27 3820-3830.

28  
29 (244) Diaz-Morales, O.; Calle-Vallejo, F.; de Munck, C.; Koper, M. T. M. Electrochemical  
30 Water Splitting by Gold: Evidence for an Oxide Decomposition Mechanism. *Chem. Sci.* **2013**, *4*,  
31 2334-2343.

32  
33 (245) Weiher, N.; Beesley, A. M.; Tsapatsaris, N.; Delannoy, L.; Louis, C.; van Bokhoven, J.  
34 A.; Schroeder, S. L. M. Activation of Oxygen by Metallic Gold in Au/TiO<sub>2</sub> Catalysis. *J. Am. Chem.*  
35 *Soc.* **2007**, *129*, 2240-2241.

36  
37 (246) Woodham, A. P.; Meijer, G.; Fielicke, A. Activation of Molecular Oxygen by Anionic  
38 Gold Clusters. *Angew. Chem. Int. Ed.* **2012**, *51*, 4444-4447.

39  
40 (247) Woodham, A. P.; Meijer, G.; Fielicke, A. Charge Separation Promoted Activation of  
41 Molecular Oxygen by Neutral Gold Clusters. *J. Am. Chem. Soc.* **2013**, *135*, 1727-1730.

42  
43 (248) O'Halloran, K. P.; Zhao, C.; Ando, N. S.; Schultz, A. J.; Koetzle, T. F.; Piccoli, P. M. B.;  
44 Hedman, B.; Hodgson, K. O.; Bobyr, E.; Kirk, M. L.; Knottenbelt, S.; Depperman, E. C.; Stein, B.;  
45 Anderson, T. M.; Cao, R.; Geletii, Y. V.; Hardcastle, K. I.; Musaev, D. G.; Neiwert, W. A.; Fang,  
46 X.; Morokuma, K.; Wu, S.; Kögerler, P.; Hill, C. L. Revisiting the Polyoxometalate-Based Late-  
47 Transition-Metal-Oxo Complexes: The "Oxo Wall" Stands. *Inorg. Chem.* **2012**, *51*, 7025-7031.  
48  
49  
50  
51  
52  
53  
54  
55  
56  
57  
58  
59  
60

1  
2  
3 (249) Mankad, N. P.; Toste, F. D. C-C Coupling Reactivity of an Alkylgold(III) Fluoride  
4 Complex with Arylboronic Acids. *J. Am. Chem. Soc.* **2010**, *132*, 12859-12861.

5  
6 (250) Scott, V. J.; Labinger, J. A.; Bercaw, J. E. Mechanism of Reductive Elimination of  
7 Methyl Iodide from a Novel Gold(III)-Monomethyl Complex. *Organometallics* **2010**, *29*, 4090-  
8 4096.

9  
10 (251) Mankad, N. P.; Toste, F. D. C(sp<sup>3</sup>)-F Reductive Elimination from Alkylgold(III)  
11 Fluoride Complexes. *Chem. Sci.* **2012**, *3*, 72-76.

12  
13 (252) Bernhardt, E.; Finze, M.; Willner, H. Synthesis and NMR Spectroscopic Investigation of  
14 Salts Containing the Novel [Au(CF<sub>3</sub>)<sub>n</sub>X<sub>4-n</sub>]<sup>-</sup> (n = 4-1, X = F, CN, Cl) Anions. *J. Fluorine Chem.*  
15 **2004**, *125*, 967-973.

16  
17 (253) Ellwanger, M. A.; Steinhauer, S.; Golz, P.; Beckers, H.; Wiesner, A.; Braun-Cula, B.;  
18 Braun, T.; Riedel, S. Taming the High Reactivity of Gold(III) Fluoride: Fluorido Gold(III)  
19 Complexes with N-Based Ligands. *Chem. Eur. J.* **2017**, *23*, 13501-13509.

20  
21 (254) Albayer, M.; Corbo, R.; Dutton, J. L. Well Defined Difluorogold(III) Complexes  
22 Supported by N-ligands. *Chem. Commun.* **2018**, *54*, 6832-6834.

23  
24 (255) Albayer, M.; Sharp-Bucknall, L.; Withanage, N.; Armendariz-Vidales, G.; Hogan, C. F.;  
25 Dutton, J. L. Metathesis Reactions between Heavy d-8 Fluorides and I(III)-Pyridine Complexes.  
26 *Inorg. Chem.* **2020**, *59*, 2765-2770.

27  
28 (256) Ellwanger, M. A.; Steinhauer, S.; Golz, P.; Braun, T.; Riedel, S. Stabilization of Lewis  
29 Acidic AuF<sub>3</sub> as an N-Heterocyclic Carbene Complex: Preparation and Characterization of  
30 [AuF<sub>3</sub>(SIMes)]. *Angew. Chem. Int. Ed.* **2018**, *57*, 7210-7214.

31  
32 (257) Ellwanger, M. A.; von Randow, C.; Steinhauer, S.; Zhou, Y.; Wiesner, A.; Beckers, H.;  
33 Braun, T.; Riedel, S. Tuning the Lewis Acidity of Difluorido Gold(III) Complexes: The Synthesis  
34 of [AuClF<sub>2</sub>(SIMes)] and [AuF<sub>2</sub>(OTeF<sub>5</sub>)(SIMes)]. *Chem. Commun.* **2018**, *54*, 9301-9304.

35  
36 (258) Pérez-Bitrián, A.; Martínez-Salvador, S.; Baya, M.; Casas, J. M.; Martín, A.; Menjón, B.;  
37 Orduna, J. Anionic Derivatives of Perfluorinated Trimethylgold. *Chem. Eur. J.* **2017**, *23*, 6919-  
38 6929.

39  
40 (259) Kumar, R.; Linden, A.; Nevado, C. Evidence for Direct Transmetalation of Au<sup>III</sup>-F with  
41 Boronic Acids. *J. Am. Chem. Soc.* **2016**, *138*, 13790-13793.

42  
43 (260) Kumar, R.; Linden, A.; Nevado, C. Luminescent (N<sup>^</sup>C<sup>^</sup>C)-Gold(III) Complexes:  
44 Stabilized Gold(III) Fluorides. *Angew. Chem. Int. Ed.* **2015**, *54*, 14287-14290.

45  
46 (261) Kleinhans, G.; Chan, A. K.-W.; Leung, M.-Y.; Liles, D. C.; Fernandes, M. A.; Yam, V.  
47 W. W.; Fernández, I.; Bezuidenhout, D. I. Synthesis and Photophysical Properties of T-shaped  
48 Coinage Metal Complexes. *Chem. Eur. J.* **2020**, *26*, 6993-6998.

1  
2  
3 (262) Hartwig, J. F. *Organotransition Metal Chemistry: From Bonding to Catalysis*. University  
4 Science Books, Sausalito, 2009; ISBN 978-1891389535.

5  
6 (263) Bochmann, M. *Organometallics and Catalysis: An Introduction*. Oxford University  
7 Press, Oxford, 2014; ISBN 978-0199668212.

8  
9  
10 (264) Crabtree, R. H. *The Organometallic Chemistry of the Transition Metals*, 7th Ed., Wiley-  
11 Blackwell, Hoboken, New Jersey, 2019. ISBN 978-1119465881.

12  
13 (265) Shiotani, A.; Schmidbaur, H. Organogold-Chemie IX. Versuche zur Oxydativen Addition  
14 an Organogold-Komplexe. *J. Organomet. Chem.* **1972**, *37*, C24–C26.

15  
16 (266) Tamaki, A.; Kochi, J. K. Catalytic Mechanism Involving Oxidative Addition in the  
17 Coupling of Alkylgold(I) with Alkyl Halides. *J. Organomet. Chem.* **1972**, *40*, C81-C84.

18  
19 (267) Tamaki, A.; Kochi, J. K. Reactions of Dialkylaurate(I) with Electrophiles: Synthesis of  
20 Trialkylgold(III) Compounds. *J. Chem. Soc, Dalton Trans.* **1973**, 2620-2626.

21  
22 (268) Johnson, A.; Puddephatt, R. J. Oxidative Addition Reactions of Methylgold(I)  
23 Compounds. *Inorg. Nucl. Chem. Lett.* **1973**, *9*, 1175-1177.

24  
25 (269) Usón, R.; Laguna, A.; Vicente, J.; Garcia, J. Preparation of Organogold(III) Complexes  
26 by Oxidizing Dichloro- or Bis(pentafluorophenyl)- $\mu$ -bis(diphenylphosphino)ethanedigold(I). *J.*  
27 *Organomet. Chem.* **1976**, *104*, 401-406.

28  
29 (270) Minghetti, G.; Bonati, F.; Banditelli, G. Carbene Complexes of Au(III) and Reactions of  
30 the Coordinated Ligand. *Inorg. Chem.* **1976**, *15*, 1718-1720.

31  
32 (271) Parks, J. E.; Balch, A. L. Gold Carbene Complexes: Preparation, Oxidation and Ligand  
33 Displacement. *J. Organomet. Chem.* **1974**, *71*, 453-463.

34  
35 (272) Raubenheimer, H. G.; Olivier, P. J.; Lindeque, L.; Desmet, M.; Hrusak, J.; Kruger, G. J.  
36 Oxidative Addition of Mono and Bis(carbene) Complexes Derived from Imidazolyl and Thiazolyl  
37 Gold(I) Compounds. *J. Organomet. Chem.* **1997**, *544*, 91-100.

38  
39 (273) Schneider, D.; Schier, A.; Schmidbaur, H. Governing the Oxidative Addition of Iodine to  
40 Gold(I) Complexes by Ligand Tuning. *Dalton Trans.* **2004**, 1995-2005.

41  
42 (274) Schneider, D.; Schuster, O.; Schmidbaur, H. Bromination of (Phosphine)gold(I) Bromide  
43 Complexes: Stoichiometry and Structure of Products. *Dalton Trans.* **2005**, 1940-1947.

44  
45 (275) Schneider, D.; Schuster, O.; Schmidbaur, H. Attempted Oxidative Addition of Halogens  
46 to (Isocyanide)gold(I) Complexes. *Organometallics*, **2005**, *24*, 3547-3551.

47  
48 (276) de Frémont, P.; Singh, R.; Stevens, E. D.; Petersen, J. L.; Nolan, S. P. Synthesis,  
49 Characterization and Reactivity of N-Heterocyclic Carbene Gold(III) Complexes. *Organometallics*,  
50 **2007**, *26*, 1376-1385.

1  
2  
3 (277) Gaillard, S.; Slawin, A. M. Z.; Bonura, A. T. Stevens, E. D.; Nolan, S. P. Synthetic and  
4 Structural Studies of [AuCl<sub>3</sub>NHC] Complexes. *Organometallics* **2010**, *29*, 394-402.

5  
6 (278) Methyl-substituted NHC Au complexes undergo similar reactivity, even though the  
7 carbene backbone reacts with Cl<sub>2</sub> as well, see: Gaillard, S.; Bantreil, X.; Slawin, A. M. Z.; Nolan, S.  
8 P. Synthesis and Characterization of IPr<sup>Me</sup>-containing Silver(I), Gold(I) and Gold(III) Complexes.  
9 *Dalton Trans.* **2009**, 6967-6971.

10  
11 (279) Canovese, L.; Visentin, F.; Levi, C.; Santo, C. Reactivity of Cationic Gold(I) Carbene  
12 Complexes toward Oxidative Addition of Bromine. *Inorg. Chim. Acta* **2012**, *391*, 141-149.

13  
14 (280) Jothibas, R.; Huynh, H. V.; Koh, L. L. Au(I) and Au(III) Complexes of a Sterically  
15 Bulky Benzimidazole-Derived N-Heterocyclic Carbene. *J. Organomet. Chem.* **2008**, *693*, 374-380.

16  
17 (281) Baron, M.; Tubaro, C.; Basato, M.; Isse, A. A.; Gennaro, A.; Cavallo, L.; Graiff, C.;  
18 Dolmella, A.; Falivene, L.; Caporaso, L. Insights into the Halogen Oxidative Addition Reaction to  
19 Dinuclear Gold(I) Di(NHC) Complexes. *Chem. Eur. J.* **2016**, *22*, 10211-10224.

20  
21 (282) Kriechbaum, M.; Otte, D.; List, M.; Monkowius, U. Facile Oxidation of NHC-Au(I) to  
22 NHC-Au(III) Complexes by CsBr<sub>3</sub>. *Dalton Trans.* **2014**, *43*, 8781-8791.

23  
24 (283) Martínez-Salvador, S.; Falvello, L. R.; Martín, A.; Menjón, B. Gold(I) and Gold(III)  
25 Trifluoromethyl Derivatives. *Chem. Eur. J.* **2013**, *19*, 14540-14552.

26  
27 (284) Kar, A.; Mangu, N.; Kaiser, H. M.; Beller, M.; Tse, M. K. A. General Gold-Catalyzed  
28 Direct Oxidative Coupling of Non-activated Arenes. *Chem. Commun.* **2008**, 386-388.

29  
30 (285) Kar, A.; Mangu, N.; Kaiser, H. M.; Tse, M. K. Gold-Catalyzed Direct Oxidative  
31 Coupling Reactions of Non-activated Arenes. *J. Organomet. Chem.* **2009**, *694*, 524-537.

32  
33 (286) Iglesias, A.; Muñiz, K. Oxidative Interception of the Hydroamination Pathway: A Gold-  
34 Catalyzed Deamination of Alkenes. *Chem. Eur. J.* **2009**, *15*, 10563-10569.

35  
36 (287) Hofer, M.; Nevado, C. Unexpected Outcomes of the Oxidation of (Pentafluorophenyl)-  
37 triphenylphosphane-gold(I). *Eur. J. Inorg. Chem.* **2012**, 1338-1341.

38  
39 (288) Hofer, M.; Nevado, C. Cross-Coupling of Arene-Gold(III) Complexes. *Tetrahedron*,  
40 **2013**, *69*, 5751-5757.

41  
42 (289) Hofer, M.; Genoux, A.; Kumar, R.; Nevado, C. Gold-Catalyzed Direct Oxidative  
43 Arylation with Boron Coupling Partners. *Angew. Chem. Int. Ed.* **2017**, *56*, 1021-1025.

44  
45 (290) Hofer, M.; De Haro, T.; Gómez-Bengo, E.; Genoux, A.; Nevado, C. Oxidant Speciation  
46 and Anionic Ligand Effects in the Gold-Catalyzed Oxidative Coupling of Arenes and Alkynes.  
47 *Chem. Sci.* **2019**, *10*, 8411-8420.

48  
49 (291) Pazicky, M.; Loos, A.; Ferreira, M. J.; Serra, D.; Vinokurov, N.; Rominger, F.; Jäkel, C.;  
50 Hashmi, A. S. K.; Limbach, M. Synthesis, Reactivity and Electrochemical Studies of Gold(I) and  
51  
52  
53  
54  
55  
56  
57  
58  
59  
60

1  
2  
3 Gold(III) Complexes Supported by N-Heterocyclic Carbenes and their Application in Catalysis.  
4 *Organometallics* **2010**, *29*, 4448-4458.

5  
6 (292) Ghidui, M. J.; Pistner, A. J.; Yap, G. P. A.; Lutterman, D. A.; Rosenthal, J. Thermal  
7 versus Photochemical Reductive Elimination of Aryl Chlorides from NHC-Gold Complexes.  
8 *Organometallics*, **2013**, *32*, 5026-5029.

9  
10 (293) Orbisaglia, S.; Jacques, B.; Braunstein, P.; Hueber, D.; Pale, P.; Blanc, A.; de Frémont, P.  
11 Synthesis, Characterization and Catalytic Activity of Cationic NHC Gold(III) Pyridine Complexes.  
12 *Organometallics*, **2013**, *32*, 4153-4164.

13  
14 (294) Collado, A.; Bohnenberger, J.; Oliva-Madrid, M.-J.; Nun, P.; Cordes, D. B.; Slawin, A.  
15 M. Z.; Nolan, S. P. Synthesis of Au<sup>I</sup>- and Au<sup>III</sup>-bis(NHC) Complexes: Ligand Influence on  
16 Oxidative Addition to Au<sup>I</sup> species. *Eur. J. Inorg. Chem.* **2016**, 4111-4122.

17  
18 (295) Corbo, R.; Pell, T. P.; Stringer, B. D.; Hogan, C. F.; Wilson, D. J. D.; Barnard, P. J.;  
19 Dutton, J. L. Facile Formation of Homoleptic Au(III) Trications via Simultaneous Oxidation and  
20 Ligand Delivery from [PhI(pyridine)<sub>2</sub>]<sup>2+</sup>. *J. Am. Chem. Soc.* **2014**, *136*, 12415-12421.

21  
22 (296) Levin, M. D.; Toste, F. D. Gold-Catalyzed Allylation of Aryl Boronic Acids: Accessing  
23 Cross-Coupling Reactivity with Gold. *Angew. Chem. Int. Ed.* **2014**, *53*, 6211–6215.

24  
25 (297) Guenther, J.; Mallet-Ladeira, S.; Estevez, L.; Miqueu, K.; Amgoune, A.; Bourissou, D.  
26 Activation of Aryl Halides at Gold(I): Practical Synthesis of (P,C) Cyclometalated Gold(III)  
27 Complexes. *J. Am. Chem. Soc.* **2014**, *136*, 1778-1781.

28  
29 (298) Livendahl, M.; Goehry, C.; Maseras, F.; Echavarren, A. M. Rationale for the Sluggish  
30 Oxidative Addition of Aryl Halides to Au(I). *Chem. Commun.* **2014**, *50*, 1333-1336.

31  
32 (299) Serra, J.; Parella, T.; Ribas, X. Au(III)-Aryl Intermediates in Oxidant-Free C-N and C-O  
33 Cross-Coupling Catalysis. *Chem. Sci.* **2017**, *8*, 946-952.

34  
35 (300) Robinson, P. S. D.; Khairallah, G. N.; da Silva, D.; Lioe, H.; O'Hair, R. A. J. Gold-  
36 Mediated C–I Bond Activation of Iodobenzene. *Angew. Chem. Int. Ed.* **2012**, *51*, 3812-3817.

37  
38 (301) Fernández, I.; Wolters, L. P.; Bickelhaupt, F. M. Controlling the Oxidative Addition of  
39 Aryl Halides to Au(I). *J. Comput. Chem.* **2014**, *35*, 2140–2145.

40  
41 (302) Angels Carvajal, M.; Novoa, J. J.; Alvarez, S. Choice of Coordination Number in d<sup>10</sup>  
42 Complexes of Group 11 Metals. *J. Am. Chem. Soc.* **2004**, *126*, 1465-1477.

43  
44 (303) Joost, M.; Zeineddine, A.; Estévez, L.; Mallet-Ladeira, S.; Miqueu, K.; Amgoune, A.;  
45 Bourissou, D. Facile Oxidative Addition of Aryl Iodides to Gold(I) by Ligand Design: Bending  
46 Turns on Reactivity. *J. Am. Chem. Soc.* **2014**, *136*, 14654-14657.

47  
48 (304) Harper, M. J.; Arthur, C. J.; Crosby, J.; Emmett, E. J.; Falconer, R. L.; Fensham-Smith,  
49 A. J.; Gates, P. J.; Leman, T.; McGrady, J. E.; Bower, J. F.; Russell, C. A. Oxidative Addition,  
50  
51  
52  
53  
54  
55  
56  
57  
58  
59  
60

1  
2  
3 Transmetalation, and Reductive Elimination at a 2,2'-Bipyridyl-Ligated Gold Center. *J. Am. Chem.*  
4 *Soc.* **2018**, 140, 4440-4445.

5  
6 (305) Cadge, J. A.; Sparkes, H.A.; Bower, J.; Russell, C. A. Oxidative Addition of Alkenyl and  
7 Alkynyl Iodides to an Au<sup>I</sup> Complex. *Angew. Chem. Int. Ed.* **2020**, 59, 6617-6621.

8  
9 (306) Yang, Y.; Antoni, P.; Zimmer, M.; Sekine, K.; Mulks, F. F.; Hu, L.; Zhang, L.; Rudolph,  
10 M.; Rominger, F.; Hashmi, A. S. K. Dual Gold/Silver Catalysis Involving Alkynylgold(III)  
11 Intermediates Formed by Oxidative Addition and Silver-Catalyzed C–H Activation for the Direct  
12 Alkynylation of Cyclopropenes. *Angew. Chem. Int. Ed.* **2019**, 58, 5129-5133.

13  
14 (307) Joost, M.; Estévez, L.; Miqueu, K.; Amgoune, A.; Bourissou, D. Oxidative Addition of  
15 Carbon-Carbon Bonds to Gold. *Angew. Chem. Int. Ed.* **2015**, 54, 5236-5240.

16  
17 (308) Wu, C. Y.; Horibe, T.; Jacobsen, C. B.; Toste, F. D. Stable Gold(III) Catalysts by  
18 Oxidative Addition of a Carbon-Carbon Bond. *Nature* **2015**, 517, 449-454.

19  
20 (309) Zeineddine, A.; Estévez, L.; Mallet-Ladeira, S.; Miqueu, K.; Amgoune, A.; Bourissou, D.  
21 Rational Development of Catalytic Au(I)/Au(III) Arylation Involving Mild Oxidative Addition of  
22 Aryl Halides. *Nat. Commun.* **2017**, 8, 565.

23  
24 (310) Rodriguez, J.; Zeineddine, A.; Sosa Carrizo, E. D.; Miqueu, K.; Saffon-Merceron, N.;  
25 Amgoune, A.; Bourissou, D. Catalytic Au(I)/Au(III) Arylation with the Hemilabile MeDalphos  
26 Ligand: Unusual Selectivity for Electron-rich Iodoarenes and Efficient Application to Indoles.  
27 *Chem. Sci.* **2019**, 10, 7183-7192.

28  
29 (311) Chu, J.; Munz, D.; Jazzar, R.; Melaimi, M.; Bertrand, G. Synthesis of Hemilabile Cyclic  
30 (Alkyl)(amino)carbenes (CAACs) and Applications in Organometallic Chemistry. *J. Am. Chem.*  
31 *Soc.* **2016**, 138, 7884-7887.

32  
33 (312) Wilkins, L. C.; Kim, Y.; Litle, E. D.; Gabbaï, F. Stabilized Carbenium Ions as Latent,  
34 Z-type Ligands. *Angew. Chem. Int. Ed.* **2019**, 58, 18266-18270.

35  
36 (313) Bachman, R. E.; Bodolosky-Bettis, S. A.; Pyle, C. J.; Gray, M. A. Reversible Oxidative  
37 Addition and Reductive Elimination of Fluorinated Disulfides at Gold(I) Thiolate Complexes: A  
38 New Ligand Exchange Mechanism. *J. Am. Chem. Soc.* **2008**, 130, 14303-14310.

39  
40 (314) Gualco, P.; Ladeira, S.; Miqueu, K.; Amgoune, A.; Bourissou, D. Spontaneous Oxidative  
41 Addition of  $\sigma$ -Si-Si Bonds at Gold. *Angew. Chem. Int. Ed.* **2011**, 50, 8320-8324.

42  
43 (315) Gualco, P.; Ladeira, S.; Miqueu, K.; Amgoune, A.; Bourissou, D. Gold-Mediated  
44 Insertion of Oxygen into Silicon-Silicon Bond: An Original Au(I)/Au(III) Redox Sequence.  
45 *Organometallics* **2012**, 31, 6001-6004.

(316) Joost, M.; Gualco, P.; Coppel, Y.; Miqueu, K.; Kefalidis, C. E.; Maron, L.; Amgoune, A.; Bourissou, D. Direct Evidence for Intermolecular Oxidative Addition of  $\sigma(\text{Si-Si})$  Bonds to Gold. *Angew. Chem. Int. Ed.* **2014**, *53*, 747-751.

(317) Lassauque, N.; Gualco, P.; Mallet-Ladeira, S.; Miqueu, K.; Amgoune, A.; Bourissou, D. Activation of a  $\sigma\text{-Sn-Sn}$  bond at copper, followed by double addition to an alkyne. *J. Am. Chem. Soc.* **2013**, *135*, 13287-13834.

(318) Chahdoura, F.; Lassauque, N.; Bourissou, D.; Amgoune, A. Gold-Catalyzed Bis(stannylation) of Propiolates. *Org. Chem. Front.* **2016**, *3*, 856-860.

(319) Asomoza-Solís, E. O.; Rojas-Ocampo, J.; Toscano, R. A.; Porcel, S. Arenediazonium Salts as Electrophiles for the Oxidative Addition of Gold(I). *Chem. Commun.* **2016**, *52*, 7295-7298.

(320) Medina-Mercado, I.; Asomoza-Solís, E. O.; Martínez-González, E.; Ugalde-Saldívar, V. M.; Ledesma-Olvera, L. G.; Barquera-Lozada, J. E.; Gómez-Vidales, V.; Barroso-Flores, J.; Frontana-Uribe, B. A.; Porcel, S. Ascorbic Acid as an Aryl Radical Inducer in the Gold-Mediated Arylation of Indoles with Aryldiazonium Chlorides. *Chem. Eur. J.* **2020**, *26*, 634-642.

(321) Gil-Rubio, J.; Vicente, J. Gold Trifluoromethyl Complexes. *Dalton Trans.* **2015**, *44*, 19432-19442.

(322) Winston, M. S.; Wolf, W. J.; Toste, F. D. Photoinitiated Oxidative Addition of  $\text{CF}_3\text{I}$  to Gold(I) and Facile Aryl- $\text{CF}_3$  Reductive Elimination. *J. Am. Chem. Soc.* **2014**, *136*, 7777-7782.

(323) Portugués, A.; López-García, I.; Jiménez-Bernad, J.; Bautista, D.; Gil-Rubio, J. Photoinitiated Reactions of Haloperfluorocarbons with Gold(I) Organometallic Complexes: Perfluoroalkyl Gold(I) and Gold(III) Complexes. *Chem. Eur. J.* **2019**, *25*, 15535-15547.

(324) Tlahuext-Aca, A.; Hopkinson, M. N.; Daniliuc, C. G.; Glorius, F. Oxidative Addition to Gold(I) by Photoredox Catalysis: Straightforward Access to Diverse (C,N)-Cyclometalated Gold(III) Complexes. *Chem. Eur. J.* **2016**, *22*, 11587-11592.

(325) Huang, L.; Rominger, F.; Rudolph, M.; Hashmi, A. S. K. A General Access to Organogold(III) Complexes by Oxidative Addition of Diazonium Salts. *Chem. Commun.* **2016**, *52*, 6435-6438.

(326) Kim, S.; Toste, F. D. Mechanism of Photoredox-Initiated C-C and C-N Bond Formation by Arylation of  $\text{IPrAu(I)-CF}_3$  and  $\text{IPrAu(I)-Succinimide}$ . *J. Am. Chem. Soc.* **2019**, *141*, 4308-4315.

(327) Xia, Z.; Corcé, V.; Zhao, F.; Przybylski, C.; Espagne, A.; Jullien, L.; Le Saux, T.; Gimbert, Y.; Dossmann, H.; Mouriès-Mansuy, V.; Ollivier, C.; Fensterbank, L. Photosensitized Oxidative Addition to Gold(I) Enables Alkynylative Cyclization of *o*-Alkynylphenols with Iodoalkynes. *Nat. Chem.* **2019**, *11*, 797-805.



1  
2  
3 (328) Burowoy, A.; Gibson, C. S. The Organic Compounds of Gold. Part IV. n-Propyl  
4 Compounds. *J. Chem. Soc.* **1935**, 219-223.

5  
6 (329) Shaw, C. F. III; Lundeen, J. W.; Tobias, R. S. Complex Bis(tertiaryphosphine)-  
7 Dimethylgold(III) Cations: Phosphine Exchange and Reductive Elimination of Ethane. *J.*  
8 *Organomet. Chem.* **1973**, *51*, 365-374.

9  
10 (330) Tamaki, A.; Magennis, S. A.; Kochi, J. K. Catalysis by Gold. Alkyl Isomerization, *cis-*  
11 *trans* Rearrangement, and Reductive Elimination of Alkylgold(III) Complexes. *J. Am. Chem. Soc.*  
12 **1974**, *96*, 6140-6148.

13  
14 (331) Komiya, S.; Albright, T. A.; Hoffmann, R.; Kochi, J. K. Reductive Elimination and  
15 Isomerization of Organogold Complexes. Theoretical Studies of Trialkylgold Species as Reactive  
16 Intermediates. *J. Am. Chem. Soc.* **1976**, *98*, 7255-7265.

17  
18 (332) Komiya, S.; Ozaki, S.; Shibue, A. Leaving Group Selectivity in Reductive Elimination  
19 from Organogold(III) Complexes. *J. Chem. Soc. Chem. Commun.* **1986**, 1555-1556.

20  
21 (333) Aresta, M.; Vasapollo, G. Reactivity of Carbon-Metal Bonds in Organogold(I)  
22 Complexes Containing *o*-Vinylphenyl and *o*-Allylphenyl Ligands. *J. Organomet. Chem.* **1973**, *50*,  
23 C51-C53.

24  
25 (334) Blaya, M.; Bautista, D.; Gil-Rubio, J.; Vicente, J. Synthesis of Au(I) Trifluoromethyl  
26 Complexes. Oxidation to Au(III) and Reductive Elimination of Halotrifluoromethanes.  
27 *Organometallics* **2014**, *33*, 6358-6368.

28  
29 (335) Winston, M. S.; Wolf, W. J.; Toste, F. D. Halide-Dependent Mechanisms of Reductive  
30 Elimination from Gold(III). *J. Am. Chem. Soc.* **2015**, *137*, 7921-7928.

31  
32 (336) Bhattacharjee, R.; Nijamudheen, A.; Datta, A. Direct and Autocatalytic Reductive  
33 Elimination from Gold Complexes ( $[(\text{Ph}_3\text{P})\text{Au}(\text{Ar})(\text{CF}_3)(\text{X})]$ , X=F, Cl, Br, I): The Key Role of  
34 Halide Ligands. *Chem. Eur. J.* **2017**, *23*, 4169-4179.

35  
36 (337) Kawai, H.; Wolf, W. J.; DiPasquale, A. G.; Winston, M. S.; Toste, F. D. Phosphonium  
37 Formation by Facile Carbon-Phosphorus Reductive Elimination from Gold(III). *J. Am. Chem. Soc.*  
38 **2016**, *138*, 587-593.

39  
40 (338) Bonsignore, R.; Thomas, S. R.; Klooster, W. T.; Coles, S. J.; Jenkins, R. L.; Bourissou,  
41 D.; Barone, G.; Casini, A. Carbon-Phosphorus Coupling from C<sup>N</sup> Cyclometalated Au<sup>III</sup>  
42 Complexes. *Chem. Eur. J.* **2020**, *26*, 4226-4231.

43  
44 (339) Li, Z.; Capretto, D. A.; Rahaman, R. O.; He, C. Gold(III)-Catalyzed Nitrene Insertion  
45 into Aromatic and Benzylic C-H Groups. *J. Am. Chem. Soc.* **2007**, *129*, 12058-12059.

(340) Lavy, S.; Miller, J. J.; Pažický, M.; Rodrigues, A.-S.; Rominger, F.; Jäkel, C.; Serra, D.; Vinokurov, N.; Limbach, M. Stoichiometric Reductive CN Bond Formation of Arylgold(III) Complexes with N-Nucleophiles. *Adv. Synth. Catal.* **2010**, *352*, 2993-3000.

(341) Kim, J. H.; Mertens, R. T.; Agarwal, A.; Parkin, S.; Berger, G.; Awuah, S. G. Direct Intramolecular Carbon(sp<sup>2</sup>)-Nitrogen(sp<sup>2</sup>) Reductive Elimination from Gold(III). *Dalton Trans.* **2019**, *48*, 6273-6282.

(342) Kung, K. K.-Y.; Ko, H.-O.; Cui, J.-F.; Chong, H.-C. Leung, Y.-C.; Wong, M.-K. Cyclometalated Gold(III) Complexes for Chemoselective Cysteine Modification *via* Ligand Controlled C-S Bond-Forming Reductive Elimination. *Chem. Commun.* **2014**, *50*, 11899-11902.

(343) Currie, L.; Rocchigiani, L.; Hughes, D. L.; Bochmann, M. Carbon-Sulfur Bond Formation by Reductive Elimination of Gold(III) Thiolates. *Dalton Trans.* **2018**, *47*, 6333-6343.

(344) Currie, L.; Fernandez-Cestau, J.; Rocchigiani, L.; Bertrand, B.; Lancaster, S. J.; Hughes, D. L.; Duckworth, H.; Jones, S. T. E.; Credginton, D.; Penfold, T. J.; Bochmann, M. Luminescent Gold(III) Thiolates: Supramolecular Interactions Trigger and Control Switchable Photoemissions from Bimolecular Excited States. *Chem. Eur. J.* **2017**, *23*, 105-113.

(345) Messina, M.; Stauber, J. M.; Waddington, M. A.; Rheingold, A. L.; Maynard, H. D.; Spokoyny, A. M. Organometallic Gold(III) Reagents for Cysteine Arylation. *J. Am. Chem. Soc.* **2018**, *140*, 7065-7069.

(346) Zhang, S.-L.; Dong, J.-J. Mechanism and Chemoselectivity Origins of Bioconjugation of Cysteine with Au(III)-Aryl Reagents. *Org. Biomol. Chem.* **2019**, *17*, 1245-1253.

(347) Wenzel, M. N.; Bonsignore, R.; Thomas, S. R.; Bourissou, D.; Barone, G.; Casini, A. Cyclometalated Au<sup>III</sup> Complexes for Cysteine Arylation in Zinc Finger Protein Domains: Towards Controlled Reductive Elimination. *Chem. Eur. J.* **2019**, *25*, 7628-7634.

(348) Stauber, J. M.; Qian, E. A.; Han, Y.; Rheingold, A. L.; Král, P.; Fujita, D.; Spokoyny, A. M. An Organometallic Strategy for Assembling Atomically Precise Hybrid Nanomaterials. *J. Am. Chem. Soc.* **2020**, *142*, 327-334.

(349) Komiya, S.; Shibue, A. Steric and Electronic Effects of the Tertiary Phosphine Ligand on the Dissociative Reductive Elimination from *cis*-Aryldimethyl(triarylphosphine)gold(III). *Organometallics*, **1985**, *4*, 684-687.

(350) Vicente, J.; Bermudez, M. D.; Escribano, J.; Carrillo, M. P.; Jones, P. G. Synthesis of Intermediates in the C-H Activation of Acetone with 2-Phenylazophenylgold(III) Complexes and in the C-C Coupling of Aryl Groups from Diarylgold(III) Complexes. Crystal and Molecular Structures of [Au{C<sub>6</sub>H<sub>3</sub>(N=NC<sub>6</sub>H<sub>4</sub>Me-4')-2-Me-5}(acac-C)Cl] (acac = acetylacetonate), *cis*-

[Au(C<sub>6</sub>H<sub>4</sub>N=NPh-2)Cl<sub>2</sub>(PPh<sub>3</sub>)], and [Au(C<sub>6</sub>H<sub>4</sub>CH<sub>2</sub>NMe<sub>2</sub>-2)(C<sub>6</sub>F<sub>5</sub>)Cl]. *J. Chem. Soc. Dalton Trans.* **1990**, 3083-3089.

(351) Wolf, W. J.; Winston, M. S.; Toste, F. D. Exceptionally Fast Carbon-Carbon Bond Reductive Elimination from Gold(III). *Nat. Chem.* **2014**, *6*, 159-164.

(352) Kang, K.; Liu, S.; Xu, T.; Wang, D.; Leng, X.; Bai, R.; Lan, Y.; Shen, Q. C(sp<sup>2</sup>)-C(sp<sup>2</sup>) Reductive Elimination from Well-Defined Diarylgold(III) Complexes. *Organometallics*, **2017**, *36*, 4727-4740.

(353) Liu, S.; Kang, K.; Liu, S.; Wang, D.; Ping, W.; Lan, Y.; Shen, Q. The Difluoromethylated Organogold(III) Complex *cis*-[Au(PCy<sub>3</sub>)(4-FC<sub>6</sub>H<sub>4</sub>)(CF<sub>2</sub>H)(Cl)]: Preparation, Characterization, and its C(sp<sup>2</sup>)-CF<sub>2</sub>H Reductive Elimination. *Organometallics* **2018**, *37*, 3901-3908.

(354) Ko, H.-H.; Deng, J. -R.; Cui, J.-F.; Kung, K. K.-Y.; Leung, Y.-C.; Wong, M.-K. Selective Modification of Alkyne-linked Peptides and Proteins by Cyclometalated Gold(III) (C<sup>N</sup>) Complex-Mediated Alkynylation. *Bioorg. Med. Chem.* **2020**, *28*, 115375.

(355) Rocchigiani, L.; Fernandez-Cestau, J.; Budzelaar, P. H. M.; Bochmann, M. Reductive Elimination Leading to C-C Bond Formation in Gold(III) Complexes: A Mechanistic and Computational Study. *Chem. Eur. J.* **2018**, *24*, 8893-8903.

(356) Vicente, J.; Bermaez, M. D.; Escribano, J. Gold in Organic Synthesis. Preparation of Symmetrical and Unsymmetrical Biaryls via C-C Coupling from *cis*-Diarylgold(III) Complexes. *Organometallics* **1991**, *10*, 3380-3384.

(357) Vicente, J.; Bermúdez, M. D.; Carrión, F. J. Gold in Organic Synthesis Part 2. Preparation of Benzyl-alkyl and -arylketones via C-C Coupling. *Inorg. Chim. Acta* **1994**, *220*, 1-3.

(358) Genoux, A.; González, J. A.; Merino, E.; Nevado, C. Mechanistic Insights into C(sp<sup>2</sup>)-C(sp)N Reductive Elimination from Gold(III) Cyanide Complexes. *Angew. Chem. Int. Ed.* **2020**, *59*, accepted article. DOI: 10.1002/anie.202005731.

(359) Klinkenberg J. L.; Hartwig, J. F. Reductive Elimination from Arylpalladium Cyanide Complexes. *J. Am. Chem. Soc.* **2012**, *134*, 5758-5761.

(360) Leyva-Pérez, A.; Doménech-Carbó, A.; Corma, A. Unique Distal Size Selectivity with a Digold Catalyst During Alkyne Homocoupling. *Nat. Commun.* **2015**, *6*, 6703.

(361) Kaphan, D. M.; Levin, M. D.; Bergman, R. G.; Raymond, K. N.; Toste, F. D. A Supramolecular Microenvironment Strategy for Transition Metal Catalysis. *Science*, **2015**, *350*, 1235-1238.

(362) Levin, M. D.; Kaphan, D. M.; Hong, C. M.; Bergman, R. G.; Raymond, K. N.; Toste, F. D. Scope and Mechanism of Cooperativity at the Intersection of Organometallic and Supramolecular Catalysis. *J. Am. Chem. Soc.* **2016**, *138*, 9682-9693.

1  
2  
3 (363) Norjmaa, G.; Maréchal, J.-D.; Ujaque, G. Microsolvation and Encapsulation Effects on  
4 Supramolecular Catalysis: C–C Reductive Elimination inside  $[\text{Ga}_4\text{L}_6]^{12-}$  Metallo cage. *J. Am. Chem*  
5 *Soc.* **2019**, *141*, 13114-13123.

6  
7  
8 (364) Norjmaa, G.; Maréchal, J.-D.; Ujaque, G. Reaction Rate Inside the Cavity of  $[\text{Ga}_4\text{L}_6]^{12-}$   
9 Supramolecular Metallo cage is Regulated by the Encapsulated Solvent. *Chem. Eur. J.* **2020**, *26*,  
10 6988-6992.

11  
12  
13 (365) Vaissier Welborn, W.; Head-Gordon, T. Electrostatics Generated by a Supramolecular  
14 Capsule Stabilizes the Transition State for Carbon–Carbon Reductive Elimination from Gold(III)  
15 Complex. *J. Phys. Chem. Lett.* **2018**, *9*, 3814-3818.

16  
17  
18 (366) Vaissier Welborn, W.; Li, W.-L.; Head-Gordon, T. Interplay of Water and a  
19 Supramolecular Capsule for Catalysis of Reductive Elimination Reaction from Gold. *Nat. Commun.*  
20 **2020**, *11*, 415.

21  
22  
23 (367) Alyabyev, S. B.; Beletskaya, I. P. Gold as a Catalyst. Part I. Nucleophilic Addition to the  
24 Triple Bonds. *Russ. Chem. Rev.* **2017**, *86*, 689-749.

25  
26  
27 (368) Lein, M.; Rudolph, M.; Hashmi, A. S. K.; Schwerdtfeger, P. Homogeneous Gold  
28 Catalysis: Mechanism and Relativistic Effects of the Addition of Water to Propyne.  
29 *Organometallics* **2010**, *29*, 2206–2210.

30  
31  
32 (369) Cordon, J.; Jiménez-Osés, G.; López-de-Luzuriaga, J. M.; Monge, M.; Olmos, M. E.;  
33 Pascual, D. Experimental and Theoretical Study of Gold(III)-Catalyzed Hydration of Alkynes.  
34 *Organometallics* **2014**, *33*, 3823–3830.

35  
36  
37 (370) Rezsnyak, C. E.; Autschbach, J.; Atwood, J. D.; Moncho, S. Reactions of Gold(III)  
38 complexes with Alkenes in Aqueous Media: Generation of Bis-( $\beta$ -hydroxyalkyl)gold(III)  
39 Complexes. *J. Coord. Chem.* **2013**, *66*, 1153-1165.

40  
41  
42 (371) Martinsen Holmsen, M. S.; Ihlefeldt, F. S.; Øien-Ødegaard, S.; Langseth, E.; Wencke,  
43 Y.; Heyn, R. H.; Tilset, M. Markovnikov at Gold: Nucleophilic Addition to Alkenes at Au(III).  
44 *Organometallics* **2018**, *37*, 1937-1947.

45  
46  
47 (372) Levchenko, V. A.; Nova, A.; Øien-Ødegaard, S.; Balcells, D.; Tilset, M. Synthesis,  
48 Characterization, and Reactivity of Cyclometalated Gold(III) Dihalide Complexes in Aqua Regia.  
49 *Eur. J. Inorg. Chem.* **2020**, DOI: 10.1002/ejic.202000529.

50  
51  
52 (373) Egorova, O. A.; Seo, H.; Kim, Y.; Moon, D.; Rhee, Y. M.; Ahn, K. H. Characterization  
53 of Vinylgold Intermediates: Gold-Mediated Cyclization of Acetylenic Amides. *Angew. Chem. Int.*  
54 *Ed.* **2011**, *50*, 11446-11450.

1  
2  
3 (374) Melchionna, M.; Nieger, M.; Helaja, J. Isolation of a Zwitterionic Dienegold(III)  
4 Complex Intermediate in the Direct Conversion of Enyne–Amines to Cyclopentadienes. *Chem. Eur.*  
5 *J.* **2010**, *16*, 8262-8267.

6  
7  
8 (375) Ung, G.; Soleilhavoup, M.; Bertrand, G. Gold(III)- versus Gold(I)-Induced Cyclization:  
9 Synthesis of Six- Membered Mesoionic Carbene and Acyclic (Aryl)(Heteroaryl) Carbene  
10 Complexes. *Angew. Chem. Int. Ed.* **2013**, *52*, 758–761.

11  
12 (376) Haupt, H.–J.; Petters, D.; Flörke, U. First Examples of Acylgold(I) Complexes  
13 RCOAuPPh<sub>3</sub> (R = Me, n-Bu, t-Bu, Ph) Trapped as Oxygen Coordinated Ligands L at one of  
14 Rhenium Atoms in Re<sub>2</sub>(μ-PPh<sub>2</sub>)<sub>2</sub>(CO)<sub>7</sub>(ax-L). *J. Organomet. Chem.* **1998**, *553*, 497-501.

15  
16 (377) Raubenheimer, H. G.; Esterhuysen, M. W.; Esterhuysen, C. Gold Acyls and Imidoyls  
17 Prepared from Anionic Fischer-type Carbene Complexes. *Inorg. Chim. Acta* **2005**, *358*, 4217-4228.

18  
19 (378) The converse reaction, the extrusion of CO from a gold-acyl reaction intermediate, has  
20 been observed: Bucher, J.; Stößer, T.; Rudolph, M.; Rominger, F.; Hashmi, A. S. K. CO Extrusion  
21 in Homogeneous Gold Catalysis: Reactivity of Gold Acyl Species Generated through Water  
22 Addition to Gold Vinylidenes. *Angew. Chem. Int. Ed.* **2015**, *54*, 1666-1670.

23  
24 (379) Mitchell, C. M.; Stone, F. G. A. Reactions of Low-Valent Metal Complexes with  
25 Fluorocarbons. Part XXII. Tertiary Phosphine Gold Complexes. *J. Chem. Soc., Dalton Trans.* **1972**,  
26 102-107.

27  
28 (380) Johnson, A.; Puddephatt, R. J. Reactions of Methylgold Complexes with Unsaturated  
29 Reagents. *J. Chem. Soc., Dalton Trans.* **1977**, 1384-1388.

30  
31 (381) Rekhroukh, F.; Brousses, R.; Amgoune, A.; Bourissou, D. Cationic Gold(III) Alkyl  
32 Complexes: Generation, Trapping, and Insertion of Norbornene. *Angew. Chem. Int. Ed.* **2015**, *54*,  
33 1266-1269.

34  
35 (382) Serra, J.; Font, P.; Sosa Carrizo, E. D.; Mallet-Ladeira, S.; Massou, S.; Parella, T.;  
36 Miqueu, K.; Amgoune, A.; Ribas, X.; Bourissou, D. Cyclometalated gold(III) Complexes:  
37 Noticeable Differences between (N,C) and (P,C) Ligands in Migratory Insertion. *Chem. Sci.* **2018**,  
38 *9*, 3932–3940.

39  
40 (383) Zhukhovitskiy, A. V.; Kobylanski, I. J.; Wu, C.-Y.; Toste, F. D. Migratory Insertion of  
41 Carbenes into Au(III)–C Bonds. *J. Am. Chem. Soc.* **2018**, *140*, 466-474.

42  
43 (384) Ung, G.; Bertrand, G. β- and α-Hydride Abstraction in Gold(I) Alkyl Complexes. *Angew.*  
44 *Chem. Int. Ed.* **2013**, *52*, 11388-11391.

45  
46 (385) Rekhroukh, F.; Estevez, L.; Mallet-Ladeira, S.; Miqueu, K.; Amgoune, A.; Bourissou, D.  
47 β-Hydride Elimination at Low-Coordinate Gold(III) Centers. *J. Am. Chem. Soc.* **2016**, *138*, 11920-  
48 11929.

1  
2  
3 (386) Pintus, A.; Bochmann, M. Radical-initiated Alkene Hydroauration as a Route to  
4 Gold(III) Alkyls: An Experimental and Computational Study. *RSC Adv.* **2018**, *8*, 2795-2803.

5  
6 (387) Fernandez-Cestau, J.; Rocchigiani, L.; Pintus, A.; Rama, R. J.; Budzelaar, P. H. M.;  
7  
8 Bochmann, M. Isocyanide Insertion into Au-H Bonds: First Gold Iminoformyl Complexes. *Chem.*  
9 *Commun.* **2018**, *54*, 11447-11450.

10  
11 (388) Roşca, D.-A.; Fernandez-Cestau, J.; Romanov, A. S.; Bochmann, M. Synthesis, C-N  
12 Cleavage and Photoluminescence of Gold(III) Isocyanide Complexes. *J. Organomet. Chem.* **2015**,  
13 *792*, 117-122.

14  
15 (389) Matsuura, K.; Muto, H. Electronic Structure of Acetylene Radical Anion with a *trans*-  
16 Bent Form. *J. Phys. Chem.* **1993**, *97*, 8842-8844.

17  
18 (390) Huang, M.-B.; Liu, Y. The *trans*-Bent Structures of the Acetylene and Methylacetylene  
19 Radical Anions. *J. Phys. Chem. A* **2001**, *105*, 923-929.

20  
21 (391) Yang, M.; Li, S.; Wang, Y.; Herron, J. A.; Xu, Y.; Allard, L. F.; Lee, S.; Huang, J.;  
22 Mavrikakis, M.; Flytzani-Stephanopoulos, M. Catalytically Active Au-O(OH)<sub>x</sub> Species Stabilized  
23 by Alkali Ions on Zeolites and Mesoporous Oxides. *Science* **2014**, *346*, 1498-1501.

24  
25 (392) Komiya, S.; Ishikawa, M.; Ozaki, S. Isolation of *cis*-Dimethyl(methoxycarbonyl)-  
26 (triphenylphosphine)gold(III). *Organometallics* **1988**, *7*, 2238-2239.

27  
28 (393) Komiya, S.; Sone, T.; Ozaki, S.; Ishikawa, M.; Kasuga, N. Synthesis, Structure and  
29 Properties of Dimethyl(alkoxycarbonyl)gold(III) Complexes Having a Triphenylphosphine Ligand.  
30 *J. Organomet. Chem.* **1992**, *428*, 303-313.

31  
32 (394) Bond, G. Mechanisms of the Gold-Catalysed Water-Gas Shift. *Gold Bull.* **2009**, *42*, 337-  
33 342.

34  
35 (395) Beucher, H.; Merino, E.; Genoux, A.; Fox, T.; Nevado, C.  $\kappa^3$ -(N<sup>^</sup>C<sup>^</sup>C)gold(III)  
36 Carboxylates: Evidence for Decarbonylation Processes. *Angew. Chem. Int. Ed.* **2019**, *58*, 9064-  
37 9067.

38  
39 (396) Garcia, P.; Malacria, M.; Aubert, C.; Gandon, V.; Fensterbank, L. Gold-Catalyzed Cross-  
40 Couplings: New Opportunities for C-C Bond Formation. *ChemCatChem* **2010**, *2*, 493-497.

41  
42 (397) Wegner, H. A.; Auzias, M. Gold for C-C Coupling Reactions: A Swiss-Army-Knife  
43 Catalyst? *Angew. Chem. Int. Ed.* **2011**, *50*, 8236-8247.

44  
45 (398) Kramer, S. Recent Advances in Gold-Catalyzed Intermolecular Aryl C-H  
46 Functionalization. *Chem. Eur. J.* **2016**, *22*, 15584-15598.

47  
48 (399) Meera, G.; Rohit, K. R.; Treesa, G. S. S.; Anilkumar, G. Advances and Prospects in  
49 Gold-Catalyzed C-H Activation. *Asian J. Org. Chem.* **2020**, *9*, 144-161.

- 1  
2  
3 (400) Nijamudheen, A.; Datta, A. Gold-Catalyzed Cross-Coupling Reactions: An Overview of  
4 Design Strategies, Mechanistic Studies, and Applications. *Chem. Eur. J.* **2020**, *26*, 1442-1487.
- 5  
6 (401) Kramer, S. Homogeneous Gold-Catalyzed Aryl–Aryl Coupling Reactions. *Synthesis*  
7  
8 **2020**, *52*, 2017-2030.
- 9  
10 (402) Shiotani, A.; Itatni, H.; Inagaki, T. Selective Coupling of Dimethyl Phthalate with  
11 Palladium Catalysts at Atmospheric Pressure. *J. Mol. Catal.* **1986**, *34*, 57-66.
- 12  
13 (403) Stuart, D. R.; Fagnou, K. The Catalytic Cross-Coupling of Unactivated Arenes. *Science*  
14 **2007**, *316*, 1172-1175.
- 15  
16 (404) Zhang, G.; Peng, Y.; Cui, L.; Zhang, L. Gold-Catalyzed Homogeneous Oxidative  
17 Cross-Coupling Reactions. *Angew. Chem. Int. Ed.* **2009**, *48*, 3112-3115.
- 18  
19 (405) Lauterbach, T.; Livendahl, M.; Rosellon, A.; Espinet, P.; Echavarren, A. M. Unlikelihood  
20 of Pd-Free Gold(I)-Catalyzed Sonogashira Coupling Reactions. *Org. Lett.* **2010**, *12*, 3006-3009.
- 21  
22 (406) Livendahl, M.; Espinet, P.; Echavarren, A. M. Is Gold a Catalyst in Cross-Coupling  
23 Reactions in the Absence of Palladium? *Platinum Metals Rev.* **2011**, *55*, 212-214.
- 24  
25 (407) Corma, A.; Juárez, R.; Boronat, M.; Sánchez, F.; Iglesias, M.; García, H. Gold Catalyzes  
26 the Sonogashira Coupling Reaction Without the Requirement of Palladium Impurities. *Chem.*  
27 *Commun.* **2011**, *47*, 1446-1448.
- 28  
29 (408) Kyriakou, G.; Beaumont, S. K.; Humphrey, S. M.; Antonetti, C.; Lambert, R. M.  
30 Sonogashira Coupling Catalyzed by Gold Nanoparticles: Does Homogeneous or Heterogeneous  
31 Catalysis Dominate? *ChemCatChem* **2010**, *2*, 1444-1449.
- 32  
33 (409) Xu, Q.; Gu, P.; Wang, F.; Shi, M. Selectfluor Promoted NHC–oxazoline Gold(I)  
34 Complex Catalyzed Cycloaddition/Oxidation Reaction of Enynones with Alkenes. *Org. Chem.*  
35 *Front.* **2015**, *2*, 1475–1484.
- 36  
37 (410) Siah, H.-S. M.; Fiksdahl, A. Dual-Gold(I)-Generated Trifluoromethylation of Terminal  
38 Alkynes with Togni's Reagent. *J. Fluor. Chem.* **2017**, *197*, 24–33.
- 39  
40 (411) Geng, C.; Zhu, R.; Li, M.; Lu, T.; Wheeler, S. E.; Liu, C. Revised Role of Selectfluor in  
41 Homogeneous Au-Catalyzed Oxidative C-O Bond Formations. *Chem. Eur. J.* **2014**, *20*, 15833-  
42 15839.
- 43  
44 (412) Tkatchouk, E.; Mankad, N. P.; Benitez, D.; Goddard, III, W. A.; Toste, F. D. Two Metals  
45 Are Better Than One in the Gold Catalyzed Oxidative Heteroarylation of Alkenes. *J. Am. Chem.*  
46 *Soc.* **2011**, *133*, 14293–14300.
- 47  
48 (413) Brenzovich, W. E.; Benitez, D.; Lackner, A. D.; Shunatona, H. P.; Tkatchouk, E.;  
49 Goddard, W. A.; Toste, F. D. Gold-Catalyzed Intramolecular Aminoarylation of Alkenes: C-C  
50  
51  
52  
53  
54  
55  
56  
57  
58  
59  
60

1  
2  
3 Bond Formation through Bimolecular Reductive Elimination. *Angew. Chem. Int. Ed.* **2010**, *49*,  
4 5519–5522.

5  
6 (414) Faza, O. N.; López, C. S. Computational Study of Gold-Catalyzed Homo- and Cross-  
7  
8 Coupling Reactions. *J. Org. Chem.* **2013**, *78*, 4929-4939.

9  
10 (415) Lu, P.; Boorman, T. C.; Slawin, A. M. Z.; Larrosa, I. Gold(I)-Mediated C-H Activation  
11  
12 of Arenes. *J. Am. Chem. Soc.* **2010**, *132*, 5580-5581.

13  
14 (416) Cambeiro, X. C.; Boorman, T. C.; Lu, P.; Larrosa, I. Redox-Controlled Selectivity of CH  
15  
16 Activation in the Oxidative Cross-Coupling of Arenes. *Angew. Chem. Int. Ed.* **2013**, *52*, 1781-1784.

17  
18 (417) Cambeiro, X. C.; Ahlsten, N.; Larrosa, I. Au-Catalyzed Cross-Coupling of Arenes via  
19  
20 Double C–H Activation. *J. Am. Chem. Soc.* **2015**, *137*, 15636-15639.

21  
22 (418) Li, W.; Yuan, D.; Wang, G.; Zhao, Y.; Xie, J.; Li, S.; Zhu, C. Cooperative Au/Ag Dual-  
23  
24 Catalyzed Cross-Dehydrogenative Biaryl Coupling: Reaction Development and Mechanistic  
25  
26 Insight. *J. Am. Chem. Soc.* **2019**, *141*, 3187-3197.

27  
28 (419) Liu, J.-R.; Duan, Y.-Q.; Zhang, S.-Q.; Zhu, L.-J.; Jiang, Y.-Y.; Bi, S.; Hong, X. C–H  
29  
30 Acidity and Arene Nucleophilicity as Orthogonal Control of Chemoselectivity in Dual C–H Bond  
31  
32 Activation. *Org. Lett.* **2019**, *21*, 2360-2364.

33  
34 (420) Ball, L. T.; Green, M.; Lloyd-Jones, G. C.; Russell, C. A. Arylsilanes: Application to  
35  
36 Gold-Catalyzed Oxyarylation of Alkenes. *Org. Lett.* **2010**, *12*, 4724-4727.

37  
38 (421) Ball, L. T.; Lloyd-Jones, G. C.; Russell, C. A. Gold-Catalyzed Direct Arylation. *Science*  
39  
40 **2012**, *337*, 1644-1648.

41  
42 (422) Ball, L. T.; Lloyd-Jones, G. C.; Russell, C. A. Gold-Catalyzed Oxidative Coupling of  
43  
44 Arylsilanes and Arenes: Origin of Selectivity and Improved Precatalyst. *J. Am. Chem. Soc.* **2014**,  
45  
46 *136*, 254–264.

47  
48 (423) Cresswell, A. J.; Lloyd-Jones, G. C. Room-Temperature Gold-Catalysed Arylation of  
49  
50 Heteroarenes: Complementarity to Palladium Catalysis. *Chem. Eur. J.* **2016**, *22*, 12641-12645.

51  
52 (424) Corrie, T. J. A.; Lloyd-Jones, G. C. Formal Synthesis of (±)-Allocolchicine Via Gold-  
53  
54 Catalysed Direct Arylation: Implication of Aryl Iodine(III) Oxidant in Catalyst Deactivation  
55  
56 Pathways. *Top. Catal.* **2017**, *60*, 570-579.

57  
58 (425) Robinson, M. P.; Lloyd-Jones, G. C. Au-Catalyzed Oxidative Arylation: Chelation-  
59  
60 Induced Turnover of *ortho*-Substituted Arylsilanes. *ACS Catal.* **2018**, *8*, 7484-7488.

(426) Fricke, C.; Dahiya, A.; Reid, W. B.; Schoenebeck, F. Gold-Catalyzed C–H  
Functionalization with Aryl Germanes. *ACS Catal.* **2019**, *9*, 9231-9236.



1  
2  
3 (427) Dahiya, A.; Fricke, C.; Schoenebeck, F. Gold-Catalyzed Chemoselective Couplings of  
4 Polyfluoroarenes with Aryl Germanes and Downstream Diversification. *J. Am. Chem. Soc.* **2020**,  
5 *142*, 7754-7759.  
6  
7

8 (428) Wu, Q.; Du, C.; Huang, Y.; Liu, X.; Long, Z.; Song, F.; You, J. Stoichiometric to  
9 Catalytic Reactivity of the Aryl Cycloaurated Species with Arylboronic Acids: Insight into the  
10 Mechanism of Gold-Catalyzed Oxidative C(sp<sup>2</sup>)-H Arylation. *Chem. Sci.* **2015**, *6*, 288-293.  
11  
12

13 (429) Akram, M. O.; Shinde, P. S.; Chintawar, C. C.; Patil, N. T. Gold(I)-Catalyzed Cross-  
14 Coupling Reactions of Aryldiazonium Salts with Organostannanes. *Org. Biomol. Chem.* **2018**, *16*,  
15 2865-2869.  
16  
17

18 (430) Liu, K.; Li, N.; Ning, Y.; Zhu, C.; Xie, J. Gold-Catalyzed Oxidative Biaryl Cross-  
19 Coupling of Organometallics. *Chem* **2019**, *5*, 2718-2730.  
20  
21

22 (431) Cammidge A. N.; Crépy, K. V. L. The First Asymmetric Suzuki Cross-Coupling  
23 Reaction. *Chem. Commun.* **2000**, 1723-1724.  
24  
25

26 (432) Tabey, A.; Berlande, M.; Hermange, P.; Fouquet, P. Mechanistic and Asymmetric  
27 Investigations of the Au-Catalysed Cross-Coupling between Aryldiazonium Salts and Arylboronic  
28 Acids Using (P,N) Gold Complexes. *Chem. Commun.* **2018**, *54*, 12867-12870.  
29  
30

31 (433) Himmelstrup, J.; Buendia, M. B.; Sun, X.-W.; Kramer, S. Enantioselective Aryl-Aryl  
32 Coupling Facilitated by Chiral Binuclear Gold Complexes. *Chem. Commun.* **2019**, *55*, 12988-  
33 12991.  
34  
35

36 (434) Brand, J. P.; Li, Y.; Waser, J. Gold-Catalyzed Alkynylation: Acetylene-Transfer instead  
37 of Functionalization. *Isr. J. Chem.* **2013**, *53*, 901-910.  
38  
39

40 (435) Qian, D.; Zhang, J. Au(I)/Au(III)-Catalyzed Sonogashira-type Reactions of  
41 Functionalized Terminal Alkynes with Arylboronic Acids under Mild Conditions. *Beilstein J. Org.*  
42 *Chem.* **2011**, *7*, 808-812.  
43  
44

45 (436) de Haro, T.; Nevado, C. Gold-Catalyzed Ethynylation of Arenes. *J. Am. Chem. Soc.*  
46 **2010**, *132*, 1512-1513.  
47  
48

49 (437) Cai, R.; Lu, M.; Aguilera, E. Y.; Xi, Y.; Akhmedov, N. G.; Petersen, J. L.; Chen, H.; Shi,  
50 X. Ligand-Assisted Gold-Catalyzed Cross-Coupling with Aryldiazonium Salts: Redox Gold  
51 Catalysis without an External Oxidant. *Angew. Chem. Int. Ed.* **2015**, *54*, 8772-8776.  
52  
53

54 (438) Pyridine bases are thought to accelerate diazonium decomposition through nucleophilic  
55 attack, see: Sakakura, T.; Hara, M.; Tanaka, M.  $\alpha$ -Arylation of Ketones via the Reaction of Silyl  
56 Enol Ethers with Arenediazonium Salts. *J. Chem. Soc., Chem. Commun.* **1985**, 1545-1546.  
57  
58  
59  
60

(439) Dong, B.; Peng, H.; Motika, S. E.; Shi, X. Gold Redox Catalysis through Base-Initiated Diazonium Decomposition toward Alkene, Alkyne, and Allene Activation. *Chem. Eur. J.* **2017**, *23*, 11093–11099.

(440) Jimoh, A. A.; Hosseyni, S.; Ye, X.; Wojtas, L.; Hu, Y.; Shi, X. Gold Redox Catalysis for Cyclization/Arylation of Allylic Oximes: Synthesis of Isoxazoline Derivatives. *Chem. Commun.* **2019**, *55*, 8150–8153.

(441) Peng, H.; Cai, R.; Xu, C.; Chen, H.; Shi, X. Nucleophile Promoted Gold Redox Catalysis with Diazonium Salts: C–Br, C–S and C–P Bond Formation through Catalytic Sandmeyer Coupling. *Chem. Sci.* **2016**, *7*, 6190–6196.

(442) Brand, J. P.; Charpentier, J.; Waser, J. Direct Alkynylation of Indole and Pyrrole Heterocycles. *Angew. Chem. Int. Ed.* **2009**, *48*, 9346–9349.

(443) Brand, J. P.; Chevalley, C.; Waser, J. One-Pot Gold-Catalyzed Synthesis of 3-Silylethynyl Indoles from Unprotected *o*-Alkynylanilines. *Beilstein J. Org. Chem.* **2011**, *7*, 565–569.

(444) Brand, J. P.; Chevalley, C.; Scopelliti, R.; Waser, J. Ethynyl Benziiodoxolones for the Direct Alkynylation of Heterocycles: Structural Requirement, Improved Procedure for Pyrroles, and Insights into the Mechanism. *Chem. Eur. J.* **2012**, *18*, 5655–5666.

(445) Brand, J. P.; Waser, J. Para-Selective Gold-Catalyzed Direct Alkynylation of Anilines. *Org. Lett.* **2012**, *14*, 744–747.

(446) Zhao, X.; Tian, B.; Yang, Y.; Si, X.; Mulks, F. F.; Rudolph, M.; Rominger, F.; Hashmi, A. S. K. Gold-Catalyzed Stereoselective Domino Cyclization/Alkynylation of N-Propargyl-carboxamides with Benziiodoxole Reagents for the Synthesis of Alkynyloxazolines. *Adv. Synth. Catal.* **2019**, *361*, 3155–3162.

(447) Brand, J. P.; Waser, J. Direct Alkynylation of Thiophenes: Cooperative Activation of TIPS–EBX with Gold and Brønsted Acids. *Angew. Chem. Int. Ed.* **2010**, *49*, 7304–7307.

(448) Banerjee, S.; Senthilkumar, B.; Patil, N. T. Gold-Catalyzed 1,2-Oxyalkynylation of N-Allenamides with Ethynylbenziiodoxolones. *Org. Lett.* **2019**, *21*, 180–184.

(449) Banerjee, S.; Bhojare, V. W.; Patil, N. T. Gold and Hypervalent Iodine(III): Liaisons over a Decade for Electrophilic Functional Group Transfer Reactions. *Chem. Commun.* **2020**, *56*, 2677–2690.

(450) Li, Y.; Brand, J. P.; Waser, J. Gold-Catalyzed Regioselective Synthesis of 2- and 3-Alkynyl Furans. *Angew. Chem. Int. Ed.* **2013**, *52*, 6743–6747.

(451) Peng, Y.; Cui, L.; Zhang, G.; Zhang, L. Gold-Catalyzed Homogeneous Oxidative C-O Bond Formation: Efficient Synthesis of 1-Benzoxyvinyl Ketones. *J. Am. Chem. Soc.* **2009**, *131*, 5062-5063.

(452) Liu, Y.; Zhu, J.; Qian, J.; Xu, Z. Gold-Catalyzed Simultaneous Formation of C-C, C=O, and C-F bonds in the Presence of Selectfluor: A Synthesis of Fluoroindenes from Allene Esters. *J. Org. Chem.* **2012**, *77*, 5411-5417.

(453) Yang, Y.; Schiebl, J.; Zallouz, S.; Göker, V.; Gross, J.; Rudolph, M.; Rominger, F.; Hashmi, A. S. K. Gold-Catalyzed C(sp<sup>2</sup>)-C(sp) Coupling by Alkynylation through Oxidative Addition of Bromoalkynes. *Chem. Eur. J.* **2019**, *25*, 9624-9628.

(454) Zhao, Y.; Jin, J.; Chan, P. W. H. Gold Catalyzed Photoredox C1-Alkynylation of N-Alkyl-1,2,3,4-tetrahydroisoquinolines by 1-Bromoalkynes with UVA LED Light. *Adv. Synth. Catal.* **2019**, *361*, 1313-1321.

(455) Barbero, M.; Dughera, S. Gold Catalyzed Heck-Coupling of Arenediazonium *o*-benzenedisulfonimides. *Org. Biomol. Chem.* **2018**, *16*, 295-301.

(456) Wang, J.; Zhang, S.; Xu, C.; Wojtas, L.; Akhmedov, N. G.; Chen, H.; Shi, X. Highly Efficient and Stereoselective Thioallylation of Alkynes: Possible Gold Redox Catalysis with No Need for a Strong Oxidant. *Angew. Chem. Int. Ed.* **2018**, *57*, 6915-6920.

(457) de Haro, T.; Nevado, C. Gold-Catalyzed Synthesis of  $\alpha$ -Fluoro Acetals and  $\alpha$ -Fluoro Ketones from Alkynes. *Adv. Synth. Catal.* **2010**, *352*, 2767-2772.

(458) de Haro, T.; Nevado, C. Domino Gold-Catalyzed Rearrangement and Fluorination of Propargyl Acetates. *Chem. Commun.* **2011**, *47*, 248-249.

(459) Zhang, G.; Cui, L.; Wang, Y.; Zhang, L. Homogeneous Gold-Catalyzed Oxidative Carboheterofunctionalization of Alkenes. *J. Am. Chem. Soc.* **2010**, *132*, 1474-1475.

(460) Zhang, G.; Luo, Y.; Wang, Y.; Zhang, L. Combining Gold(I)/Gold(III) Catalysis and CH Functionalization: A Formal Intramolecular [3+2] Annulation towards Tricyclic Indolines and Mechanistic Studies. *Angew. Chem. Int. Ed.* **2011**, *50*, 4450-4454.

(461) Geng, C.; Zhang, S.; Duan, C.; Lu, T.; Zhu, R.; Liu, C. Theoretical Investigation of Gold-Catalyzed Oxidative C<sub>sp3</sub>-C<sub>sp2</sub> Bond Formation via Aromatic C-H activation. *RSC Adv.* **2015**, *5*, 80048-80056.

(462) Lloyd-Jones, G. C.; Russell, C. A. Gold-Catalysed Oxyarylation of Styrenes and Mono- and gem-Disubstituted Olefins Facilitated by an Iodine(III) Oxidant. *Chem. Eur. J.* **2012**, *18*, 2931-2937.

(463) Brenzovich, Jr.; W. E.; Brazeau, J.-F.; Toste, F. D. Gold-Catalyzed Oxidative Coupling Reactions with Aryltrimethylsilanes. *Org. Lett.* **2010**, *12*, 4728-4731.

- (464) Melhado, A. D.; Brenzovich, W. E.; Lackner, A. D.; Toste, F. D. Gold-Catalyzed Three-Component Coupling: Oxidative Oxyarylation of Alkenes. *J Am Chem Soc* **2010**, *132*, 8885-8887.
- (465) Harper, M. J.; Emmett, E. J.; Bower, J. F.; Russell, C. A. Oxidative 1,2-Difunctionalization of Ethylene via Gold-Catalyzed Oxyarylation. *J. Am. Chem. Soc.* **2017**, *139*, 12386-12389.
- (466) Rigoulet, M.; Thillaye du Boullay, O.; Amgoune, A.; Bourissou, D. Gold(I)/Gold(III) Catalysis Merging Oxidative Addition and  $\pi$ -Alkene Activation. *Angew. Chem. Int. Ed.* **2020**, *59*, ASAP. DOI: 10.1002/anie.202006074
- (467) Chintawar, C. C.; Yadav, A. K.; Patil, N. T. Gold-Catalyzed 1,2-Diarylation of Alkenes. *Angew. Chem. Int. Ed.* **2020**, *59*, 11808-11813.
- (468) Leyva-Pérez, A.; Doménech, A.; Al-Resayes, S. I.; Corma, A. Gold Redox Catalytic Cycles for the Oxidative Coupling of Alkynes. *ACS Catal.* **2012**, *2*, 121-126.
- (469) Zhu, M.; Ning, M.; Fu, W.; Xu, C.; Zou, G. Gold-Catalyzed Homocoupling Reaction of Terminal Alkynes to 1,3-Diynes. *Bull. Korean Chem. Soc.* **2012**, *33*, 1325-1328.
- (470) Peng, H.; Xi, Y.; Ronaghi, N.; Dong, B.; Akhmedov, N. G.; Shi, X. Gold-Catalyzed Oxidative Cross-Coupling of Terminal Alkynes: Selective Synthesis of Unsymmetrical 1,3-Diynes. *J. Am. Chem. Soc.* **2014**, *136*, 13174-13177.
- (471) Ye, X.; Peng, H.; Wei, C.; Yuan, T.; Wojtas, L.; Shi, X. Gold-Catalyzed Oxidative Coupling of Alkynes toward the Synthesis of Cyclic Conjugated Diynes. *Chem* **2018**, *4*, 1983-1993.
- (472) Li, X.; Xie, X.; Sun, N.; Liu, Y. Gold-Catalyzed Cadiot–Chodkiewicz-type Cross-Coupling of Terminal Alkynes with Alkynyl Hypervalent Iodine Reagents: Highly Selective Synthesis of Unsymmetrical 1,3-Diynes. *Angew. Chem. Int. Ed.* **2017**, *56*, 6994-6998.
- (473) Banerjee, S.; Patil, N. T. Exploiting the Dual Role of Ethynylbenziodoxolones in Gold-Catalyzed C(sp)–C(sp) Cross-Coupling Reactions. *Chem. Commun.* **2017**, *53*, 7937-7940.
- (474) Ye, X.; Zhao, P.; Zhang, S.; Zhang, Y.; Wang, Q.; Shan, C.; Wojtas, L.; Guo, H.; Chen, H.; Shi, X. Facilitating Gold Redox Catalysis with Electrochemistry: An Efficient Chemical-Oxidant-Free Approach. *Angew. Chem. Int. Ed.* **2019**, *58*, 17226–17230.
- (475) Sahoo, B.; Hopkinson, M. N.; Glorius, F. Combining Gold and Photoredox Catalysis: Visible Light-Mediated Oxy- and Aminoarylation of Alkenes. *J. Am. Chem. Soc.* **2013**, *135*, 5505–5508.
- (476) Akram, M. O.; Banerjee, S.; Saswade, S. S.; Bedi, V.; Patil, N. T. Oxidant-free Oxidative Gold Catalysis: The New Paradigm in Cross-Coupling Reactions. *Chem. Commun.* **2018**, *54*, 11069-11083.

- (477) Zhang, Q.; Zhang, Z.-Q.; Fu, Y.; Yu, H.-Z. Mechanism of the Visible Light-Mediated Gold-Catalyzed Oxyarylation Reaction of Alkenes. *ACS Catal.* **2016**, *6*, 798-808.
- (478) Shu, X.-Z.; Zhang, M.; He, Y.; Frei, H.; Toste, F. D. Dual Visible Light Photoredox and Gold-Catalyzed Arylative Ring Expansion. *J. Am. Chem. Soc.* **2014**, *136*, 5844–5847.
- (479) Tlahuext-Aca, A.; Hopkinson, M. N.; Garza-Sanchez, R. A.; Glorius, F. Alkyne Difunctionalization by Dual Gold/Photoredox Catalysis. *Chem. Eur. J.* **2016**, *22*, 5909–5913.
- (480) Um, J.; Yun, H.; Shin, S. Cross-Coupling of Meyer–Schuster Intermediates under Dual Gold-Photoredox Catalysis. *Org. Lett.* **2016**, *18*, 484–487.
- (481) Alcaide, D.; Almendros, P.; Busto, E.; Luna, A. Domino Meyer–Schuster/Arylation Reaction of Alkynols or Alkynyl Hydroperoxides with Diazonium Salts Promoted by Visible Light under Dual Gold and Ruthenium Catalysis. *Adv. Synth. Catal.* **2016**, *358*, 1526–1533.
- (482) He, Y.; Wu, H.; Toste, F. D. A Dual Catalytic Strategy for Carbon–Phosphorus Cross-Coupling via Gold and Photoredox Catalysis. *Chem. Sci.* **2015**, *6*, 1194-1198.
- (483) Cornilleau, T.; Hermange, P.; Fouquet, E. Gold-Catalysed Cross-Coupling between Aryldiazonium Salts and Arylboronic Acids: Probing the Usefulness of Photoredox Conditions. *Chem. Commun.* **2016**, *52*, 10040–10043.
- (484) Akram, M. O.; Mali, P. S.; Patil, N. T. Cross-Coupling Reactions of Aryldiazonium Salts with Allylsilanes under Merged Gold/Visible-Light Photoredox Catalysis. *Org. Lett.* **2017**, *19*, 3075–3078.
- (485) Chakrabarty, I.; Akram, M. O.; Biswas, S.; Patil, N. T. Visible Light Mediated Desilylative C(sp<sup>2</sup>)–C(sp<sup>2</sup>) Cross-Coupling Reactions of Arylsilanes with Aryldiazonium Salts under Au(I)/Au(III) Catalysis. *Chem. Commun.* **2018**, *54*, 7223–7226.
- (486) Kim, S.; Rojas-Martin, J.; Toste, F. D. Visible Light-mediated Gold-Catalyzed Carbon(sp<sup>2</sup>)–Carbon(sp) Cross-Coupling. *Chem. Sci.* **2016**, *7*, 85–88.
- (487) Xia, Z.; Khaled, O.; Mouriès–Mansuy, V.; Ollivier, C.; Fensterbank, L. Dual Photoredox/Gold Catalysis Arylative Cyclization of o-Alkynylphenols with Aryldiazonium Salts: A Flexible Synthesis of Benzofurans. *J. Org. Chem.* **2016**, *81*, 7182–7190.
- (488) Qu, C.; Zhang, S.; Du, H.; Zhu, C. Cascade Photoredox/Gold Catalysis: Access to Multisubstituted Indoles via Aminoarylation of Alkynes. *Chem. Commun.* **2016**, *52*, 14400–14403.
- (489) Gauchot, V.; Lee, A.-L. Dual Gold Photoredox C(sp<sup>2</sup>)–C(sp<sup>2</sup>) Cross Couplings – Development and Mechanistic Studies. *Chem. Commun.* **2016**, *52*, 10163–10166.
- (490) Gauchot, V.; Sutherland, D. R.; Lee, A. –L. Dual Gold and Photoredox Catalysed C–H Activation of Arenes for Aryl–Aryl Cross Couplings. *Chem. Sci.* **2017**, *8*, 2885–2889.

(491) Tlahuext-Aca, A.; Hopkinson, M. N.; Sahoo, B.; Glorius, F. Dual Gold/Photoredox-Catalyzed C(sp)-H Arylation of Terminal Alkynes with Diazonium Salts. *Chem. Sci.* **2016**, *7*, 89-93.

(492) Patil, D. V.; Yun, H.; Shin, S. Catalytic Cross-Coupling of Vinyl Golds with Diazonium Salts under Photoredox and Thermal Conditions. *Adv. Synth. Catal.* **2015**, *357*, 2622-2628.

(493) Huang, L.; Rudolph, M.; Rominger, F.; Hashmi, A. S. K. Photosensitizer-Free Visible-Light-Mediated Gold-Catalyzed 1,2-Difunctionalization of Alkynes. *Angew. Chem. Int. Ed.* **2016**, *55*, 4808-4813.

(494) Witzel, S.; Xie, J.; Rudolph, M.; Hashmi, A. S. K. Photosensitizer-Free, Gold-Catalyzed C-C Cross-Coupling of Boronic Acids and Diazonium Salts Enabled by Visible Light. *Adv. Synth. Catal.* **2017**, *359*, 1522-1528.

(495) Sauer, C.; Liu, Y.; De Nisi, A.; Protti, S.; Fagnoni, M.; Bandini, M. Photocatalyst-Free, Visible Light Driven, Gold Promoted Suzuki Synthesis of (Hetero)Biaryls. *ChemCatChem* **2017**, *9*, 4456-4459.

(496) Liu, Y.; Yang, Y.; Zhu, R.; Liu, C.; Zhang, D. The Dual Role of Gold(I) Complexes in Photosensitizer-Free Visible-Light-Mediated Gold-Catalyzed 1,2-Difunctionalization of Alkynes: A DFT Study. *Chem. Eur. J.* **2018**, *24*, 14119-14126.

(497) Deng, J. -R.; Chan, W. -C.; Lai, N. C. -H.; Yang, B.; Tsang, C. -S.; Ko, B. C. -B.; Chan, S. L. -F.; Wong, M. -K. Photosensitizer-Free Visible Light-mediated Gold Catalysed *cis*-Difunctionalization of Silyl-substituted Alkynes. *Chem. Sci.* **2017**, *8*, 7537-7544.

(498) Xie, J.; Sekine, K.; Witzel, S.; Krämer, P.; Rudolph, M.; Rominger, F.; Hashmi, A. S. K. Light-Induced Gold-Catalyzed Hiyama Arylation: A Coupling Access to Biarylboronates. *Angew. Chem. Int. Ed.* **2018**, *57*, 16648-16653.

(499) Sherborne, G. J.; Gevondian, A. G.; Funes-Ardoiz, I.; Dahiya, A.; Fricke, C.; Schoenebeck, F. Modular and Selective Arylation of Aryl Germanes (C-GeEt<sub>3</sub>) over C-Bpin, C-SiR<sub>3</sub> and Halogens enabled by Light-Activated Gold-Catalysis. *Angew. Chem. Int. Ed.* **2020**, *59*, 15543-15548.

(500) Marchetti, L.; Kantak, A.; Davis, R.; DeBoef, B. Regioselective Gold-Catalyzed Oxidative C-N Bond Formation. *Org. Lett.* **2015**, *17*, 358-361.

(501) Serra, J.; Whiteoak, C. J.; Acuña-Parés, F.; Font, M.; Luis, J. M.; Lloret-Fillol, J.; Ribas, X. Oxidant-Free Au(I)-Catalyzed Halide Exchange and C<sub>sp</sub><sup>2</sup>-O Bond Forming Reactions. *J. Am. Chem. Soc.* **2015**, *137*, 13389-13397.

(502) Rodriguez, J.; Adet, N.; Saffon-Merceron, N.; Bourissou, D. Au(I)/Au(III)-Catalyzed C-N Coupling. *Chem. Commun.* **2020**, *56*, 94-97.

(503) Akram, M. O.; Das, A.; Chakrabarty, I.; Patil, N. T. Ligand-Enabled Gold-Catalyzed C(sp<sup>2</sup>)-N Cross-Coupling Reactions of Aryl Iodides with Amines. *Org. Lett.* **2019**, *21*, 8101-8105.

(504) Norman, R. O. C.; Parr, W. J. E.; Thomas, C. B. The reactions of Alkynes, Cyclopropanes, and Benzene Derivatives with Gold(III). *J. Chem. Soc., Perkin Trans. 1* **1976**, 1983-1987.

(505) Reeds, J. P.; Healy, M. P.; Fairlamb, I. J. S. Mechanistic Examination of Au<sup>III</sup>-mediated 1,5-Enyne Cycloisomerization by AuBr<sub>2</sub>(N-imidate)(NHC)/AgX Precatalysts – Is the Active Catalyst Au<sup>III</sup> or Au<sup>I</sup>? *Catal. Sci. Technol.* **2014**, *4*, 3524-3533.

(506) Kumar, A.; Singh, C.; Tinnermann, H.; Huynh, H. V.; Gold(I) and Gold(III) Complexes of Expanded-Ring N-Heterocyclic Carbenes: Structure, Reactivity, and Catalytic Applications. *Organometallics*, **2020**, *39*, 172-181.

(507) Pincer complexes with electron donating groups are catalytically inactive, see: Johnson, M. W.; DiPasquale, A. G.; Bergman, R. G.; Toste, F. D. Synthesis of Stable Gold(III) Pincer Complexes with Anionic Heteroatom Donors. *Organometallics*, **2014**, *33*, 4169-4172.

(508) Hashmi, A. S. K.; Weyrauch, J. P.; Rudolph, M.; Kurpejović, E. Gold Catalysis: The Benefits of N and N,O ligands. *Angew. Chem. Int. Ed.* **2004**, *43*, 6545-6547.

(509) For examples of earlier applications of Au(III) see: Jiménez-Núñez, E.; Echavarren, A. M. Molecular Diversity through Gold Catalysis with Alkynes. *Chem. Commun.* **2007**, 333-346.

(510) Chiarucci, M.; Bandini, M. New Developments in Gold-Catalyzed Manipulation of Inactivated Alkenes. *Beilstein J. Org. Chem.* **2013**, *9*, 2586-2614.

(511) Chen, C.; Cai, C. Catalytic Hydration of Alkynes to Ketones by a Salen-Gold(III) Complex. *Catal. Commun.* **2015**, *65*, 102-104.

(512) Schaaf, P.; Gojic, V.; Bayer, T.; Rudroff, F.; Schnürch, M.; Mihovilovic, M. D. Easy Access to Enantiopure (S)- and (R)-Aryl Alkyl Alcohols by a Combination of Gold(III)-Catalyzed Alkyne Hydration and Enzymatic Reduction. *ChemCatChem* **2018**, *10*, 920-924.

(513) Leslie, J. M.; Tzeel, B. Gold(III)-Catalyzed Hydration of Phenylacetylene. *J. Chem. Educ.* **2016**, *93*, 1100-1102.

(514) O'Neill, J. A. T.; Rosair, G. M.; Lee, A.-L, Gold(III)-Oxo Complexes as Catalysts in Intramolecular Hydroamination. *Catal. Sci. Technol.* **2012**, *2*, 1818-1821.

(515) Tubaro, C.; Baron, M.; Biffis, A.; Basato, M. Alkyne Hydroarylation with Au N-Heterocyclic Carbene Catalysts. *Beilstein J. Org. Chem.* **2013**, *9*, 246-253.

(516) Li, D.; Rao, W.; Liang, G. L.; Ayers, B. J.; Chan, P. W. H. Gold-Catalyzed Cycloisomerization of 1,6-Diyne Esters to 1H-Cyclopenta[b]naphthalenes, *cis*-Cyclopenten-2-yl  $\delta$ -Diketones, and Bicyclo[3.2.0]hepta-1,5-dienes. *J. Org. Chem.* **2014**, *79*, 11301-11315.

(517) Li, J.; Xing, H.-W.; Yang, F.; Chen, Z.-S.; Ji, Kegong, Gold(III)-Catalyzed Regioselective Oxidation/Cycloisomerization of Diyines: An Approach to Fused Furan Derivatives. *Org. Lett.* **2018**, *20*, 4622–4626.

(518) Song, L.; Tian, X.; Rudolph, M.; Rominger, F.; Hashmi, A. S. K.; Gold(III)-Catalyzed Chemoselective Annulations of Anthranils with N-Allylnamides for the Synthesis of 3-Azabicyclo[3.1.0]hexan-2-imines. *Chem. Commun.* **2019**, *55*, 9007–9010.

(519) Li, J.; Rudolph, M.; Rominger, F.; Xie, J.; Hashmi, A. S. K. A Gold-Catalyzed A3 Coupling/Cyclization/Elimination Sequence as Versatile Tool for the Synthesis of Furfuryl Alcohol Derivatives from Glyceraldehyde and Alkynes. *Adv. Synth. Catal.* **2016**, *358*, 207–211.

(520) Ko, H.-M.; Kung, K. K. Y.; Cui, J.-F.; Wong, M.-K. Bis-Cyclometallated Gold(III) Complexes as Efficient Catalysts for Synthesis of Propargylamines and Alkylated Indoles. *Chem. Commun.* **2013**, *49*, 8869–8871.

(521) Villaverde, G.; Corma, A.; Iglesias, M.; Sánchez, F, Heterogenized Gold Complexes: Recoverable Catalysts for Multicomponent Reactions of Aldehydes, Terminal Alkynes, and Amines. *ACS Catal.* **2012**, *2*, 399–406.

(522) See for example: Hines, J. M.; Eason, J. J.; Siebert, M. R. One Lump or Two? A Plurality of Pathways in Gold(III)-Catalyzed Cyclization Transforming Propargyl Acetates to a Carene-like Bicyclo[4.1.0]heptane. *Organometallics* **2017**, *36*, 920–926.

(523) Li, Y.; Lin, Z. Gold(III)-Catalyzed Intramolecular Cyclization of  $\alpha$ -Pyrroles to Pyrrolopyridinones and Pyrroloazepinones: A DFT Study. *Organometallics* **2015**, *34*, 3538–3545.

(524) Wirtanen, T.; Muuronen, M.; Melchionna, M.; Patzsche, M.; Helaja, J. Gold(III)-Catalyzed Enynamine–Cyclopentadiene Cycloisomerization with Chirality Transfer: An Experimental and Theoretical Study Indicating Involvement of Dual Au(III) Push–Pull Assisted *cis–trans* Isomerism. *J. Org. Chem.* **2014**, *79*, 10269–10283.

(525) Ying, J.; Pu, L. Regiospecific Hydration of N-(Diphenylphosphinoyl)propargyl Amines: Synthesis of  $\beta$ -Amino Ketones by Au(III) Catalysis. *J. Org. Chem.* **2016**, *81*, 8135–8141.

(526) Hashmi, A. S. K.; Hofmann, J.; Shi, S.; Schütz, A.; Rudolph, M.; Lothschütz, C.; Wietek, M.; Bührle, M.; Wölflle, M.; Rominger, F. Gold Catalysis: Catalyst Oxidation State Dependent Dichotomy in the Cyclization of Furan–Yne Systems with Aromatic Tethers. *Chem. Eur. J.* **2013**, *19*, 382–389.

(527) A. H. Bagi, Y. Khaledi, H. Ghari, S. Arndt, A. S. K. Hashmi, B. F. Yates, A. Ariafard, A Mechanistic Investigation of the Gold(III)-Catalyzed Hydrofurylation of C–C Multiple Bonds. *J. Am. Chem. Soc.* **2016**, *138*, 14599–14608.



(528) Jaroschik, F.; Simonneau, A.; Lemièrre, G.; Cariou, K.; Agenet, N.; Amouri, H.; Aubert, C.; Goddard, J.-P.; Lesage, D.; Malacria, M.; Gimbert, Y.; Gandon, V.; Fensterbank, L. Assessing Ligand and Counterion Effects in the Noble Metal Catalyzed Cycloisomerization Reactions of 1,6-Allenynes: a Combined Experimental and Theoretical Approach. *ACS Catal.* **2016**, *6*, 5146–5160.

(529) Weyrauch, J. P.; Hashmi, A. S. K.; Schuster, A.; Hengst, T.; Schetter, S.; Littmann, A.; Rudolph, M.; Hamzic, M.; Visus, J.; Rominger, F.; Frey, W.; Bats, J. W. Cyclization of Propargylic Amides: Mild Access to Oxazole Derivatives. *Chem. Eur. J.* **2010**, *16*, 956–963.

(530) Vanicek, S.; Beerhues, J.; Bens, T.; Levchenko, V.; Wurst, K.; Bildstein, B.; Tilset, M.; Sarkar, B. Oxidative Access via Aqua Regia to an Electrophilic, Mesoionic Dicobaltoceniumyl-triazolylidene Gold(III) Catalyst. *Organometallics*, **2019**, *38*, 4383–4386.

(531) Alcaide, B.; Almendros, P.; Cembellín, S.; Fernández, I.; Martínez del Campo, T. Cationic Au<sup>III</sup> versus Au<sup>I</sup>: Catalyst-Controlled Divergent Reactivity of Alkyne-Tethered Lactams. *Chem. Eur. J.* **2017**, *23*, 3012–3015.

(532) Bohan, P. T.; Toste, F. D. Well-Defined Chiral Gold(III) Complex Catalyzed Direct Enantioconvergent Kinetic Resolution of 1,5-Enynes. *J. Am. Chem. Soc.* **2017**, *139*, 11016–11019.

(533) Lee, J. S.; Kapustin, E. A.; Pei, X.; Llopis, S.; Yaghi, O. M.; Toste, F. D. Architectural Stabilization of a Gold(III) Catalyst in Metal-Organic Frameworks. *Chem* **2020**, *6*, 142–152.

(534) Levchenko, V. A.; Siah, H.-S. M.; Øien-Ødegaard, S.; Kaur, G.; Fiksdahl, A.; Tilset, M. Catalytic studies of cyclometalated gold(III) complexes and their related UiO-67 MOF. *Mol. Catal.* **2020**, *492*, 111009.

(535) Cui, J.-F.; Ko, H.-M.; Shing, K.-P.; Deng, J.-R.; Lai, N. C.-H.; Wong, M.-K. C,O-Chelated BINOL/Gold(III) Complexes: Synthesis and Catalysis with Tunable Product Profiles. *Angew. Chem. Int. Ed.* **2017**, *56*, 3074-3079.

(536) A similar carboalkoxylation reactivity was observed with binuclear Au(I) complexes derived from biaryl-diphosphines, see: Zi, W.; Toste, F. D. Gold(I)-Catalyzed Enantioselective Carboalkoxylation of Alkynes. *J. Am. Chem. Soc.* **2013**, *135*, 12600–12603.

(537) Jiang, J.-J.; Cui, J.-F.; Yang, B.; Ning, Y.; Lai, N. C.-H.; Wong, M.-K. Chiral Cyclometalated Oxazoline Gold(III) Complex-Catalyzed Asymmetric Carboalkoxylation of Alkynes. *Org. Lett.* **2019**, *21*, 6289–6294.

(538) Reiersølmoen, A. C.; Østrem, E.; Fiksdahl, A. Gold(III)-Catalyzed *cis*-to-*trans* Cyclopropyl Isomerization. *Eur. J. Org. Chem.* **2018**, 3317–3325.

(539) Reiersølmoen, A. C.; Csókás, D.; Øien-Ødegaard, S.; Vanderkooy, A.; Gupta, A. K.; Carlsson, A.-C. C; Orthaber, A.; Fiksdahl, A.; Pápai, I; Erdélyi, M. Catalytic Activity of *trans*-Bis(pyridine)gold Complexes. *J. Am. Chem. Soc.* **2020**, *142*, 6439–6446.

1  
2  
3 (540) Reiersølmoen, A. C.; Fiksdahl, A. Pyridine- and Quinoline-Based Gold(III) Complexes:  
4 Synthesis, Characterization, and Application. *Eur. J. Org. Chem.* **2020**, 1–12.

5  
6 (541) Reiersølmoen, A. C.; Csókás, D.; Pápai, I.; Fiksdahl, A.; Erdélyi, M. Mechanism of  
7 Au(III)-Mediated Alkoxy cyclization of a 1,6-Enyne. *J. Am. Chem. Soc.* **2019**, *141*, 18221–18229.

8  
9 (542) Martinsen Holmsen, M. S.; Nova, A.; Hylland, K.; Wragg, D. S.; Øien-Ødegaard, S.;  
10 Heyn, R. H.; Tilset, M. Synthesis of a (N,C,C) Au(III) Pincer Complex via C<sub>sp</sub><sup>3</sup>-H Bond  
11 Activation: Increasing Catalyst Robustness by Rational Catalyst Design. *Chem. Commun.* **2018**, *54*,  
12 11104-11107.

13  
14 (543) Kung, K. K.-Y.; Lo, V. K.-Y.; Ko, H.-M.; Li, G.-L.; Chan, P.-Y.; Leung, K.-C.; Zhou,  
15 Z.; Wang, M.-Z.; Che, C.-M.; Wong, M.-K. Cyclometallated Gold(III) Complexes as Effective  
16 Catalysts for Synthesis of Propargylic Amines, Chiral Allenes and Isoxazoles. *Adv. Synth.*  
17 *Catal.* **2013**, *355*, 2055-2070.

18  
19 (544) Blons, C.; Mallet-Ladeira, S.; Amgoune, A.; Bourissou, D. (P,C) Cyclometalated  
20 Gold(III) Complexes: Highly Active Catalysts for the Hydroarylation of Alkynes. *Angew. Chem.*  
21 *Int. Ed.* **2018**, *57*, 11732–11736.

22  
23 (545) Muuronen, M.; Perea-Buceta, J. E.; Nieger, M.; Patzschke, M.; Helaja, J. Cationic Gold  
24 Catalysis with Pyridine-Tethered Au(III) NHC-Carbenes: An Experimental and DFT  
25 Computational Study. *Organometallics* **2012**, *31*, 4320–4330.

26  
27 (546) Tomás-Mendivil, E.; Toullec, P. Y.; Borge, J.; Conejero, S.; Michelet, V.; Cadierno, V.  
28 Water-Soluble Gold(I) and Gold(III) Complexes with Sulfonated *N*-Heterocyclic Carbene Ligands:  
29 Synthesis, Characterization, and Application in the Catalytic Cycloisomerization of  $\gamma$ -Alkynoic  
30 Acids into Enol-Lactones. *ACS Catal.* **2013**, *3*, 3086–3098.

31  
32 (547) Nair, A. G.; McBurney, R. T.; Gatus, M. R. D.; Binding, S. C.; Messerle, B. A. Gold(III)  
33 NHC Complexes for Catalyzing Dihydroalkoxylation and Hydroamination Reactions. *Inorg. Chem.*  
34 **2017**, *56*, 12067–12075.

35  
36 (548) Tsubokura, K.; Vong, K. K. H.; Pradipta, A. R.; Ogura, A.; Urano, S.; Tahara, T.;  
37 Nozaki, S.; Onoe, H.; Nakao, Y.; Sibgatullina, R.; Kurbangalieva, A.; Watanabe, Y.; Tanaka, K. In-  
38 Vivo Gold Complex Catalysis within Live Mice. *Angew. Chem. Int. Ed.* **2017**, *56*, 3579-3584.

39  
40 (549) Lin, Y.; Vong, K.; Koji, M.; Tanaka, K. 2-Benzoylpyridine Ligand Complexation with  
41 Gold Critical for Propargyl Ester-Based Protein Labeling. *Chem. Eur. J.* **2018**, *24*, 10595–10600.

42  
43 (550) Nguyen, B. N.; Adrio, L. A.; Barreiro, E. M.; Brazier, J. B.; Haycock, P.; Hii, K. K.;  
44 Nachtegaal, M.; Newton, M. A.; Szlachetko, J. Deconvolution of the Mechanism of Homogeneous  
45 Gold-Catalyzed Reactions. *Organometallics* **2012**, *31*, 2395–2402.

(551) Tomás-Mendevíl, E.; Heinrich, C. F.; Ortuno, J.-C.; Starck, J.; Michelet, V. Gold-Catalyzed Access to 1H-Isochromenes: Reaction Development and Mechanistic Insight. *ACS Catal.* **2017**, *7*, 380–387.

(552) Krauter, C. M.; A. S. K. Hashmi, Pernpointner, M. A New Insight into Gold(I)-Catalyzed Hydration of Alkynes: Proton Transfer. *ChemCatChem* **2010**, *2*, 1226–1230.

(553) Ciesielski, J.; Leboef, D.; Stern, H. A.; Frontier, A. J. Gold (III) Chloride-Catalyzed 6-*endo-trig* Oxa-Michael Addition Reactions for Diastereoselective Synthesis of Fused Tetrahydropyranones. *Adv. Synth. Catal.* **2013**, *355*, 2077–2082.

(554) Reid, J. P.; Hu, M.; Ito, S.; Huang, B.; Hong, C. M.; Xiang, H.; Sigman, M. S.; Toste, F. D. Strategies for Remote Enantiocontrol in Chiral Gold(III) Complexes Applied to Catalytic Enantioselective  $\gamma$ ,  $\delta$ -Diels–Alder Reactions. *Chem. Sci.* **2020**, *11*, 6450–6456.

(555) Reiner, B. R.; Bezpalko, M. W.; Foxman, B. M.; Wade, C. R. Lewis Acid Catalysis with Cationic Dinuclear Gold(II,II) and Gold(III,III) Phosphorus Ylide Complexes. *Organometallics* **2016**, *35*, 2830–2835.

(556) Yang, Y.; Hu, W.; Ye, X.; Wang, D.; Shi, X. Preparation of Triazole Gold(III) Complex as an Effective Catalyst for the Synthesis of *E*- $\alpha$ -Haloenones. *Adv. Synth. Catal.* **2016**, *358*, 2583–2588.

(557) Yang, Y.; Shen, Y.; Wang, X.; Zhang, Y.; Wang, D.; Shi, X. Triazole Acetyl Gold(III) Catalyzed Meyer–Schuster Rearrangement of Propargyl Alcohols. *Tetrahedron Lett.* **2016**, *57*, 2280–2282.

(558) Wimberg, J.; Meyer, S.; Dechert, S.; Meyer, F. Gold(I), Gold(III), and Heterometallic Gold(I)–Silver(I) and Gold(I)–Copper(I) Complexes of a Pyridazine-Bridged NHC/Pyrazole Hybrid Ligand and Their Initial Application in Catalysis. *Organometallics* **2012**, *31*, 5025–5033.

(559) Li, W.; Yu, B. Gold-Catalyzed Glycosylation in the Synthesis of Complex Carbohydrate-Containing Natural Products. *Chem. Soc. Rev.* **2018**, *47*, 7954–7984.

(560) Thadke, S. A.; Mishra, B.; Hotha, S. Gold(III)-Catalyzed Glycosidations for 1,2-*trans* and 1,2-*cis* Furanosides. *J. Org. Chem.* **2014**, *79*, 7358–7371.

(561) To, W.-P.; Tong, G. S.-M.; Lu, W.; Ma, C. Liu, J.; Chow, A. L.-F.; Che, C.-M. Luminescent Organogold(III) Complexes with Long-Lived Triplet Excited States for Light-Induced Oxidative C–H Bond Functionalization and Hydrogen Production. *Angew. Chem. Int. Ed.* **2012**, *51*, 2654–2657.

(562) Xue, Q.; Xie, J.; Jin, H.; Cheng, Y.; Zhu, C. Highly Efficient Visible-Light-Induced Aerobic Oxidative C–C, C–P Coupling from C–H Bonds Catalyzed by a Gold(III)-Complex. *Org. Biomol. Chem.* **2013**, *11*, 1606–1609.

1  
2  
3 (563) For an example of a specific non-NHC type Au(III) carbene complex see: Pujol, A.;  
4 Lafage, M.; Rekhroukh, F.; Saffon-Merceron, N.; Amgoune, A.; Bourissou, D.; Nebra, N.; Fustier-  
5 Boutignon, M.; Mézailles, N. A Nucleophilic Gold(III) Carbene Complex. *Angew. Chem. Int. Ed.*  
6 **2017**, *56*, 12264-12267.  
7  
8  
9  
10  
11  
12  
13  
14  
15  
16  
17  
18  
19  
20  
21  
22  
23  
24  
25  
26  
27  
28  
29  
30  
31  
32  
33  
34  
35  
36  
37  
38  
39  
40  
41  
42  
43  
44  
45  
46  
47  
48  
49  
50  
51  
52  
53  
54  
55  
56  
57  
58  
59  
60

## TOC Graphic

